

Université d'Ottawa • University of Ottawa

MODELLING AN SBR WASTE TREATMENT SYSTEM

by

Tianhua Sun

A thesis

submitted under the supervision of Dr. R. L. Droste

in partial fulfillment of the requirements for

the degree of Ph.D in Civil Engineering

Department of Civil Engineering

University of Ottawa

Ottawa, Canada, K1N 6N5

August, 1996

National Library
of Canada

Acquisitions and
Bibliographic Services

395 Wellington Street
Ottawa ON K1A 0N4
Canada

Bibliothèque nationale
du Canada

Acquisisitons et
services bibliographiques

395, rue Wellington
Ottawa ON K1A 0N4
Canada

Your file Votre référence
ISBN: 0-612-90012-6
Our file Notre référence
ISBN: 0-612-90012-6

The author has granted a non-exclusive licence allowing the National Library of Canada to reproduce, loan, distribute or sell copies of this thesis in microform, paper or electronic formats.

The author retains ownership of the copyright in this thesis. Neither the thesis nor substantial extracts from it may be printed or otherwise reproduced without the author's permission.

L'auteur a accordé une licence non exclusive permettant à la Bibliothèque nationale du Canada de reproduire, prêter, distribuer ou vendre des copies de cette thèse sous la forme de microfiche/film, de reproduction sur papier ou sur format électronique.

L'auteur conserve la propriété du droit d'auteur qui protège cette thèse. Ni la thèse ni des extraits substantiels de celle-ci ne doivent être imprimés ou aturement reproduits sans son autorisation.

In compliance with the Canadian Privacy Act some supporting forms may have been removed from this dissertation.

While these forms may be included in the document page count, their removal does not represent any loss of content from the dissertation.

Conformément à la loi canadienne sur la protection de la vie privée, quelques formulaires secondaires ont été enlevés de ce manuscrit.

Bien que ces formulaires aient inclus dans la pagination, il n'y aura aucun contenu manquant.

Canada

ACKNOWLEDGMENTS

The author expresses his most sincere appreciation to Dr. R. L. Droste for his academic guidance, patience, encouragement, friendship and financial support throughout the project.

Special thanks are given to Dr. L. Fernandes, Dr. K. J. Kennedy and Dr. R. Narbaitz for their help during the research.

Deep appreciation is felt for my family: Haiyan, Yangguang and my parents, for their love, understanding, encouragement and continued support.

ABSTRACT

The sequencing batch reactor (SBR), developed from batch reactor technology, has made significant progress in the past two decades with increasing use in wastewater treatment. However, there are still some important aspects of the system that need improvement. Modelling SBR system, developing lab methods for estimation of the model parameters, re-defining SBR design parameters and comparing SBR and continuous flow stirred tank reactor (CFSTR) systems were the four objectives of this thesis.

Previous SBR models cannot predict an entire SBR operation cycle because they have some obvious deficiencies. No consideration of soluble microbial products (SMP) by the models is one of the deficiencies. These deficiencies were carefully reviewed and discussed before beginning the modelling work.

A new mathematical model based on the standard Lawrence and McCarty model and IAWPRC model No. 1 has been developed for the SBR activated sludge system. In contrast with previous SBR models, the most important developments of the new model are involving expressions for SMP formed from substrate metabolism and released from activated sludge decay and classifying different basic chemical oxygen demand (COD) categories based on their biodegradabilities. In the new SBR model, total COD is divided into two parts: soluble and insoluble. The soluble part is further subdivided into easy-to-biodegrade substrate (EBS), difficult-to-biodegrade substrate (DBS) and biologically inert organic materials (IOM). The classification of COD makes it possible to describe the degradation process of organic substances more precisely.

Quantitative batch test methods for the classification of the substrate have been devised to aid in characterizing and developing the coefficient values of the new SBR model. The batch test techniques were employed for measuring the three different (EBS, DBS and IOM) soluble COD fractions in the influent as well as the formation or release of these three types of substances from metabolism and sludge decay. The kinetic constants of the new model can also be estimated by the techniques. It was found that EBS degradation followed Monod kinetics and DBS degradation followed first-order kinetics. It was also found that the soluble COD released from substrate metabolism is closely related to the type of substrate degraded while the soluble COD released from activated sludge decay is not. Experiments furthermore revealed that the major portion of soluble COD released from sludge decay is easily biodegradable which is different from expectation.

With a single set of experimentally measured kinetic constants and other coefficients, and supported by a computer program, the model successfully predicted the SBR performance over a wide range.

The third important contribution of the project is systematic development of design definitions and engineering parameters for SBR systems. Although SBR technology has been widely used in wastewater treatment, it is not as popular as continuous flow systems for many reasons. One of the major reasons is lack of widely accepted design standards. The parameters of an SBR system which are different from those in continuous flow systems and need to be redefined are effective reactor volume, true hydraulic retention time, true sludge age, total effective biomass, sludge decay rate constant, true sludge

loading rate and volumetric loading rate.

In an SBR system, the effective reactor volume is variable and depends on both the aeration time and fill time in an operational cycle. The true hydraulic retention time is a function mainly of the fill length after total and initial reactor volumes and cycle length are determined. The total effective biomass in an SBR reactor is significantly affected by the operational mode and the biokinetic parameters. The true sludge age is also affected by the operational mode. The true sludge loading rate is calculated based on the total effective biomass and the true volumetric loading rate based on the effective reactor volume.

The last major contribution is the completion of an overall experimental comparison between SBR and CFSTR systems. Systematic comparison of three SBR and three CFSTR reactors was conducted under equivalent HRT. The SBR system showed slightly improved kinetics over the CFSTR, while having more strict physical constraints than the latter. The major physical constraint is initial reactor volume at the beginning of each SBR cycle, which reduced reactor volume utilization rate and limited the quantity of sludge held in the reactor. As a result of the constraints, the advantages of SBR system compared to CFSTR system are seriously diminished. Based on equivalent HRT, the overall average COD removal efficiency by the SBR system was about one percent higher than that of the CFSTR system. Also at equivalent conditions, the SBR system possessed slightly higher volumetric loading and slightly higher specific substrate removal rates. Results of analysis of variance (ANOVA) for the two systems revealed that improved performance in the SBR is significant at $\alpha = 0.05$ but not significant at $\alpha = 0.01$. From the

comprehensive comparison of the two systems, it was concluded that an SBR will show no overwhelming advantages to a CFSTR system under the circumstances of low and comparatively stable feed concentration, easy-to-biodegrade organic components and stable influent flow rate. Only with high strength or refractory organic components, unstable flow rate, unstable concentration, theoretically, will an SBR system be expected to perform better than a CFSTR. These situations require a treatment system that can provide low F/M ratio, flexible HRT and sludge age to deal with various organic compounds and large capacity of withstanding hydraulic or organic shock. Further experimental verification is required to confirm these theoretical predictions.

TABLE OF CONTENTS

ACKNOWLEDGMENTS i

ABSTRACT ii

TABLE OF CONTENTS vi

LIST OF TABLES xi

LIST OF FIGURES xiii

NOMENCLATURE xvi

CHAPTER 1 INTRODUCTION 1

CHAPTER 2 THEORY AND LITERATURE REVIEW 4

2.1. SBR ACTIVATED SLUDGE SYSTEM 4

2.2 THEORETICAL ANALYSIS OF EFFECTIVE VOLUME FOR BATCH REACTOR, CFSTR AND PFR 7

2.3. THE ADVANTAGES OF SBR SYSTEM AND ITS APPLICATION 12

2.4. MODELS FOR A SBR SYSTEM 15

2.4.1. Lawrence & McCarty Model 16

2.4.2. Irvine and Ritcher ' s Model 17

2.4.3. Orhon's Model 18

2.4.4. Droste's Model 19

2.4.5. Silverstein and Schroeder's Model 21

2.4.6. Nakazawa and Tannaka's Model 22

2.4.7. Summary of Analysis of Earlier SBR Models 26

2.5. SOME IMPORTANT MODELS FOR ACTIVATED SLUDGE PROCESS 28

2.5.1. The IAWPRC Task Group Model No. 1 28

2.5.2. Application of IAWPRC Model No. 1 to SBR System 32

2.5.3. Models Concerning with the Soluble Microbial Products (SMP) 32

CHAPTER 3 EXPERIMENTAL APPROACH 35

3.1. EXPERIMENTAL DEVICES AND GENERAL CONDITIONS 35

3.2. OPERATIONAL PARAMETERS 36

3.3. FEED SELECTION 40

3.4. BATCH TEST FOR THE ESTIMATION OF STOICHIOMETRIC AND KINETIC COEFFICIENTS 43

3.5. ANALYSIS METHODS 43

PART I DYNAMIC MODELLING AN SBR SYSTEM 44

CHAPTER 4 A NEW MODEL FOR SEQUENCING BATCH REACTOR SYSTEM 45

4.1. SUBSTRATE CLASSIFICATIONS IN THE NEW MODEL 45

4.2. THE DEVELOPMENT OF THE NEW DYNAMIC MODEL FOR SBR SYSTEM 50

4.2.1. Assumptions for the New Model 50

4.2.2. The Development of the New SBR model 51

4.2.3. The Boundary Conditions of the New SBR Model 56

4.3. A NEW MODEL FOR CFSTR ACTIVATED SLUDGE SYSTEM 57

CHAPTER 5 ESTIMATION OF PARAMETERS IN THE NEW SBR MODEL 59

5.1 PRINCIPLE, ASSUMPTIONS AND PROCEDURE OF BATCH REACTOR TEST 60

5.1.1. Principle 60

5.1.2. Test Conditions 63

5.2. QUANTITATIVE TEST OF INFLUENT COD FRACTIONS 66

5.2.1. Measurement of f_1, f_2 and f_3 66

5.2.2. Measurement of f_{X_1}, f_{X_2} and f_{X_3} 76

5.2.3. Determination of γ_x and γ_s 80

5.3. THE EXPERIMENTAL VALIDATION OF SAP AND BAP EXPRESSIONS IN THE NEW SBR MODEL 80

5.3.1. Analysis Result of Remaining Amino Acids 82

5.3.2. Saccharose as a Sole Carbon Source for an SBR Run 85

5.4. EXPERIMENTAL DETERMINATION OF KINETIC CONSTANTS 89

5.4.1. Evaluation of k_1 and K_{S_1} 89

5.4.2. The Results of Experimental Testing k_1 and K_{S_1} 92

5.4.3. Estimation of k_2 and K_{S_2} 93

5.4.4. The Correction of Feedback Inhibition on k_2 95

5.4.5. Determination of k_e and Y Coefficients 98

5.4.6. The Results of Experimental Testing k_e and Y 102

5.4.7. Determination of switch function constant K_0 104

CHAPTER 6 DYNAMIC MODELING OF SBR SYSTEM WITH MEASURED KINETIC AND STOICHIOMITRIC PARAMETERS 105

6.1. NEW MODEL SIMULATION OF SBR PROCESS 105

6.2. PRELIMINARY STATISTICAL ANALYSIS FOR THE FIT OF THE NEW SBR MODEL 121

CHAPTER 7 CONCLUSION OF PART I: DYNAMIC MODELLING SBR SYSTEM 126

PART II AN OVERALL COMPARISON OF SBR AND CFSTR SYSTEMS 128

CHAPTER 8 THEORETICAL COMPARISON OF SBR AND CFSTR SYSTEM 129

8.1 THEORETICAL BASIS 130

8.2 DROSTE'S APPROACH FOR THE RELATIONSHIP OF SBR AND CFSTR AND FIRST ANALYSIS OF PHYSICAL CONSTRAINTS OF SBR OPERATION 131

8.3 THE EFFECTIVE VOLUME V_{ef} AND TRUE HYDRAULIC RETENTION TIME t_{tr} IN THE SBR SYSTEM 133

8.3.1. Defining the Effective Volume V_{ef} and the True HRT t_{tr} in an SBR System 134

8.3.2. Defining Volumetric Loading Rate of an SBR System 142

8.3.3. Sample Calculation of V_{ef}, t_{tr} and L_{vtr} 143

8.3.4. Defining Basic Biokinetics Parameters of SBR System 146

8.3.5. Another Derivation of True Specific Substrate Removal Rate R_{tr} in an SBR Reactor 146

8.3.6. Sludge Loading Rate, L_{xtr} of an SBR System 148

CHAPTER 9 EXPERIMENTAL COMPARISON OF SBR AND CFSTR SYSTEMS 150

9.1. COMPARISON OF SUBSTRATE REMOVAL EFFICIENCY 150

9.1.1. Comparison of COD Removal Efficiency Based on the Equivalent HRT 150

9.1.2. Comparison of COD Removal Efficiency Based on the Volumetric Loading 154

9.2. COMPARISON OF KINETIC COEFFICIENTS 156

9.2.1. Comparison of Overall Specific Substrate Removal rates 156

9.2.2. Comparison of Y and k_e 162

9.3. COMPARISON OF SLUDGE COMPACTIBILITY AND THE EFFECT OF V_i ON THE PERFORMANCE OF SBR 164

9.3.1. Comparison of Sludge Loading Rate 164

9.3.2. Comparison of SVI in the Two Systems 166

9.4. COMPARISON OF REACTOR VOLUME UTILIZATION EFFICIENCY 171

9.4.1. Comparison of Volumetric Loading 171

9.4.2. Comparison of Physical Volume Utilization Ratios of SBR and CFSTR 174

9.5. COMPARISON OF OPERATIONAL CONSTRAINTS OF THE TWO SYSTEMS 176

9.6. CHARACTERIZATIONS AND CONCLUSION OF THE SBR SYSTEM 180

CHAPTER 10 DESIGN PROCEDURES OF SBR SYSTEMS 182

10.1. TEST OF KINETIC RATE CONSTANTS 182

10.2. THE NUMBER OF REACTORS IN THE SYSTEM, n, THE CYCLE TIME t_c, THE NUMBER OF CYCLES EACH DAY, N_c 182

10.3. THE DETERMINATION OF INITIAL REACTOR VOLUME RATIO α, FILL TIME, REACT TIME, SETTLE TIME, DRAW TIME AND REACTIVE TIME RATIO φ 183

10.4. REACTOR VOLUME V_b, TOTAL SYSTEM VOLUME nV_b AND TRUE HYDRAULIC RETENTION TIME t_{tr} 185

10.5. THE VERIFICATION OF SPECIFIC SUBSTRATE REMOVAL RATE R_{tr} AND THE MODIFICATION OF nV_b 186

CHAPTER 11 CONCLUSION OF PART II: AN OVERALL COMPARISON OF SBR AND CFSTR SYSTEMS 187

REFERENCES 190

APPENDIX 198

LIST OF TABLES

Table 3-1	Summary of factors in the experiments	38
Table 3-2	Operational mode design and related parameter values of SBR experiments	39
Table 3-3	Operational mode design and related parameter values of CFSTR experiments	40
Table 3-4	The Components of the vegetable protein	42
Table 5-1	The measured f_1, f_2 and f_3 values from thirteen sets of batch reactor tests	74
Table 5-2	Statistics of measured f_1, f_2 , f_3 and $(f_{x1} + f_{x2})$ values from batch actor tests	75
Table 5-3	Measured amino acids, carbohydrates and COD for the batch reactor and other systems with the vegetable protein as feed	83
Table 5-4	Approximate estimation of the organic materials other than typical amino acids and carbohydrates for the various protein systems	85
Table 5-5	Measured amino acids, carbohydrates and COD for the batch test with saccharose as sole carbon source	87
Table 5-6	Kinetic rate constants measured from the batch reactor tests	92
Table 5-7	Statistical results of the adjusted $k_2'_{test}$ values	97
Table 5-8	Results of Y and k_e adjusted with φ in the SBR system	103
Table 5-9	Sstatistics for the measured Y and k_e in the SBR system	104
Table 6-1	Typical ranges of kinetic and stoichiometric parameters of the new SBR model	106
Table 6-2	Preliminary values of ANOVA calculation	123
Table 6-3	Final results of ANOVA for the new SBR model fit	123
Table 6-4	Regression results between the model prediction and the experimental measurements	123

Table 6-5	Results of the correlation of the two data sets	125
Table 8-1	Hydraulic characteristic comparison of the two system	143
Table 9-1	ANOVA results of soluble COD removal comparison between the two systems	152
Table 9-2a	ANOVA results of soluble COD removal efficiencies vs volumetric loadings between the two systems (S_0 = 250 mg/L)	155
Table 9-2b	ANOVA results of soluble COD removal efficiencies vs volumetric loadings between the two systems (S_0 = 500 mg/L)	156
Table 9-3	ANOVA results of specific substrate removal rates, R and R_{tr}, in the two systems	160
Table 9-4	ANOVA results of soluble COD removal efficiency vs specific substrate removal rate in the two systems	162
Table 9-5	Y and k_e forf the CFSTR system	163
Table 9-6	ANOVA of SVI in the two systems within specific substrate removal rate range of 0 to 0.8 g COD/g VSS/d	170
Table 9-7	Operational mode design and related parameter values of CFSTR experiments	175
Table 9-8	Comparison of successive operations in the two systems (S_0 = 250 mg/L)	179
Table 9-9	Comparison of successive operations in the two systems (S_0 = 500 mg/L)	179

LIST OF FIGURES

Figure 2-1	Typical five phases of an operational cycle in a single tank SBR system	4
Figure 2-2	Operating sequence of a three tank SBR system for a continuous flow	5
Figure 2-3	Effective volume comparison between BR and CFSTR	12
Figure 2-4	Comparison of earlier SBR models with experimental result	27
Figure 3-1	Schematic outline of the two experiment devices of SBR and CFSTR systems	36
Figure 4-1	Substrate classification and the new SBR model mechanisms	49
Figure 5-1	A flow chart for experimental estimations of the new SBR model parameters	66
Figure 5-2a	Soluble COD degradation curves from a batch test with three different initial concentrations	67
Figure 5-2b	Soluble COD degradation curves from a batch test with three different initial concentrations (with a y-axis range of 0-100 mg/L)	67
Figure 5-3	BAP_{nd} - time curve from the batch reactor test	68
Figure 5-4	Remaining soluble COD- time curves adjusted by BAP_{nd} from a batch reactor test	68
Figure 5-5a	dS/dt-S curve from a batch test with S_0 = 468 mg/L	69
Figure 5-5b	dS/dt-S curve from a batch test with S_0 = 216 mg/L	69
Figure 5-5c	dS/dt-S curve from a batch test with S_0 = 130 mg/L	70
Figure 5-6	BAP_T and BAP_{nd} vs time curves from a blank batch reactor test	76
Figure 5-7	The linear relationship of BAP_{nd} accumulation rate to COD_T from a blank batch reactor test	77
Figure 5-8	The linear relationship of BAP_T degradation rate to COD_T from a blank batch reactor test	77

Figure 5-9	The ratio of BAP_d/BAP_T showing most of BAP degradable	78
Figure 5-10	Plot of the differential method	90
Figure 5-11	A plot to determine k_1 and $K_{S\,1}$	91
Figure 5-12	The linear relation between S_0 and ln $k_2'_{tets}$	95
Figure 6-1	New model prediction of an SBR performance: Experimental set No. 2-250 series	111
Figure 6-2	New model prediction of an SBR performance: Experimental set No. 3-500 series	112
Figure 6-3	New model prediction of an SBR performance: Experimental set No. 5-250 series	113
Figure 6-4	New model prediction of an SBR performance: Experimental set No. 5-500 series	114
Figure 6-5	New model prediction of an SBR performance: Experimental set No. 6-250 series	115
Figure 6-6	New model prediction of an SBR performance: Experimental set No. 6-500 series	116
Figure 6-7	New model prediction of an SBR performance: Experimental set No. 7-250 series	117
Figure 6-8	New model prediction of an SBR performance: Experimental set No. 7-500 series	118
Figure 6-9	New model prediction of an SBR performance: Experimental set No. 8-250 series	119
Figure 6-10	New model prediction of an SBR performance: Experimental set No. 8-500 series	120
Figure 6-11	Fit of the model predicted results	124
Figure 6-12	Residuals of the observed results	124
Figure 8-1	Effective reactor volume change in an SBR operational cycle	137
Figure 8-2	Relationships of fill time to effective reactor volume, V_{ef}, true HRT, t_{tr} and volumetric loading rate, L_{vtr}	144
Figure 9-1	Comparison of COD removal efficiency η vs HRT in the two systems	151
Figure 9-2	COD removal efficiency η vs t_{tr} of the SBR system	153
Figure 9-3a	Comparison of COD removal efficiency η vs volumetric loading	

	in the two system (S_0 = 250 mg/L)	154
Figure 9-3b	Comparison of COD removal efficiency η vs volumetric loading in the two system (S_0 = 500 mg/L)	155
Figure 9-4	Specific substrate removal rate vs t_{dc} or t_{ed} in the two systems (S_0 = 250 mg/L runs)	158
Figure 9-5	Specific substrate removal rate vs t_{dc} or t_{ed} in the two systems (S_0 = 500 mg/L runs)	159
Figure 9-6	Relationship of COD removal efficiency η vs true specific substrate removal rate R_{tr} in the SBR system	161
Figure 9-7	Relationship of COD removal efficiency η vs specific substrate removal rate R in the CFSTR system	161
Figure 9-8	Relationship of true sludge loading R_{tr} vs t_{tr} in the SBR system	166
Figure 9-9	Relationship of sludge loading R vs t_{dc} in the CFSTR system	166
Figure 9-10	Relationship of true sludge loading, R_{tr}, and SVI in the SBR system	167
Figure 9-11	Relationship of true sludge age and SVI in the SBR system	167
Figure 9-12	Relationship of sludge loading and SVI in the CFSTR system	168
Figure 9-13	Relationship of true sludge age and SVI in the CFSTR system	169
Figure 9-14	Relationship of true sludge loading and SVI in the SBR system (L_{xtr} = 0 - 1 gCOD/gVSS/d range)	169
Figure 9-15	Comparison of volumetric loading, L_v or L_{vtr} vs HRT, t_{dc}, or t_{ed} between CFSTR and SBR systems, respectively (Average data from S_0 = 250 mg/L runs)	172
Figure 9-16	Comparison of volumetric loading, L_v or L_{vtr} vs t_{dc} or t_{tr}, between CFSTR and SBR systems respectively (Average data from S_0 = 250 mg/L runs)	172
Figure 9-17	Comparison of volumetric loading L_v or L_{vtr}, vs t_{dc} or t_{ed} between the two systems (Average data from S_0 = 500 mg/L runs)	173
Figure 9-18	Comparison of volumetric loading L_v or L_{vtr}, vs t_{dc} or t_{tr} between the two systems (Average data from S_0 = 500 mg/L runs)	174
Figure 9-19	The relationship of β (V_{ef}/V_b) and t_{tr} in the SBR system	175

NOMENCLATURE

Abbreviations

BAP	biomass-associated products
BR	batch reactor
CFS	continuous flow system
CM	completely mixed
CFSTR	continuous flow stirred tank reactor
DBS	difficult-to-biodegrade substrate
EBS	easy-to-biodegrade substrate
HRT	hydraulic retention time
IOM	biologically inert organic material
PF	plug flow
PFR	plug flow reactor
SBR	sequencing batch reactor
SMP	soluble microbial products
UAP	utilization-ssociated products

Glossary (Units)

A_s	constant to adjust the conversion coefficient of UAP to soluble COD
A_x	constant to adjust the conversion coefficient of decayed VSS to soluble COD
BOD	biological oxygen demand (mg/L)
BOD_L	ultimate biological oxygen demand (mg/L)
C	substrate concentration in a reactor (mg/L)
C_0	substrate concentration of influent (mg/L)
COD	chemical oxygen demand (mg/L)
COD_T	total COD including soluble and particulate (mg/L)
C_s	constant to adjust the conversion coefficient of UAP to soluble COD
C_x	constant to adjust the conversion coefficient of decayed VSS to soluble COD
d	day(s)
DO	dissolved oxygen concentration (mg/L)
f_1, f_2, f_3, and f_p	fractions of EBS, DBS, IOM and particulate substrate, respectively (%)
F/M	ratio of feed to microorganisms (mg COD/mg VSS)

h	hour(s)
[I]	inhibitor concentration (mg/L)
k	rate constant (d^{-1})
k_1 and k_2	rate constants for EBS and DBS degradation, respectively (d^{-1})
k_2'	ratio of k_2/K_{S2} (mg/Ld)
$k_{2'test}$	measured k_2' (mg/Ld)
$k_{2'adj}$	corrected k_2' (mg/Ld) with ratio of P_I/K_I
k_e	rate constant of endogenous decay (d^{-1})
f_{x1}, f_{x2}, f_{x3}	fractions of EBS, DBS and IOM released from sludge endogenous decay respectively (%)
K_{S_1} and K_{S_2}	half velocity constants for EBS and DBS degradation (mg/L)
K_0	constant for switch function to limit the degradation of DBS when EBS exists (mg/L)
K_I	inhibition constant (mg/L)
L_v	volumetric loading rate ($mg/L^{-2}/d$)
L_{vtr}	true volumetric loading rate in SBR system ($mg/L^{-2}/d$)
L_x	sludge loading rate ($mg/L^{-2}/d$)
L_{xtr}	true sludge loading rate in SBR system ($mg/L^{-2}/d$)
mg	microgram
min	minute(s)
M_x	total biomass in system (Mass)
$\overline{M}_X$	average total biomass in a non-steady-state system (Mass)
MLVSS	mixed liquid volatile suspended solids (mg/L)
n	reaction order (dimensionless) or number of reactors
N_c	SBR operation cycles per day (No./d)
p_s and p_p	fractions of soluble and particulate substrate from sludge endogenous decay (%)
OUR	oxygen utilization rate (mg/L/t)
P_I	percentage of inhibitor in the influent (%)
q	substrate removed rate (mass/time)
Q	influent flow rate (L/h)
Q_d	influent flow rate per day (L/d)
Q_w	waste sludge flow rate (L/d)
r_s	substrate degradation rate expression (mg/L/d)
r_{Xv}	biomass growth rate expression (mg/L/d)
r_{Xvd}	sludge decay rate expression (mg/L/d)
r_{Xs}	SMP formation rate expression (mg/L/d)

R	substrate removal rate based on unit VSS (d^{-1}) or correlation coefficient in statistics
R_{tr}	true substrate removal rate based on unit VSS in SBR system (d^{-1})
S	substrate concentration (mg/L)
$\overline{S}$	soluble average COD concentration (mg/L)
S''	limiting substrate concentration (mg/L)
S_0 and S_e	soluble COD concentration of influent and effluent, respectively (mg/L)
S_1, S_2 and S_3	concentrations of EBS, DBS and IOM in the new SBR model simulation, respectively.
S_{01}, S_{02} and S_{03}	three different soluble COD concentrations in the batch test (mg/L)
S_{1e}, S_{2e} and S_{3e}	effluent concentrations of EBS, DBS and IOM in the new model, respectively, (mg/L)
SVI	sludge volume index (mL/g)
t	time
t_c	cycle time of SBR system (h or d)
t_d	detention time (d)
t_{dc}	detention time in CFSTR (d)
t_{ed}	equivalent detention time in SBR system to HRT in CFSTR system (d)
t_f	fill time in SBR system (h or d)
t_r	reaction time in SBR system (h or d)
t_s	settle time in SBR system (h or d)
t_{sc}	detention time in the sedimentation basin of CFSTR system (d)
t_{sw}	settle and draw time in SBR system (h or d)
t_{tr}	true HRT in SBR system (h or d)
t_u	unproductive time (d)
t_w	draw time in SBR system (h or d)
TSS	total suspended solids (mg/L)
u	ratio of t_u to t_d (-)
V	reactor volume
v_s	settling velocity of sludge (M/min)
V_b	total volume of each SBR reactor (L^3)
V_c	volume of CFSTR (L^3)
V_{ef}	effective reactor volume of SBR system (L^3)
V_i	initial volume of SBR reactor in its cycle (L^3)
V_p	effective volume of PFR (L^3)
V_s	effective volume of BR (L^3)
V_{sc}	volume of sedimentation basin in CFSTR system (L^3)
VSS	volatile suspended solids mainly composed of microorganisms (mg/L)

X_a	concentration of active biomass (mg/L)
X_e	concentration of sludge washed out (mg/L)
X_i	initial sludge concentration in SBR system (mg/L)
X_v	concentration of volatile suspended solids (mg/L)
$\overline{X}$	average sludge concentration (mg/L)
$\overline{X}_v$	average VSS concentration (mg/L)
X_w	concentration of waste sludge (mg/L)
Y	true yield factor (mg biomass/mg COD)
y_u	vector of measured result for u'th run of SBR operation
α	ratio of initial volume to total volume of SBR reactor (%)
β	reactor volume utilization ratio (%) or dimensionless saturation constant
γ_x	conversion coefficient for soluble COD from decomposed VSS (mg/mg)
γ_s	conversion coefficient for soluble COD from UAP (mg/mg)
ε	dimensionless substrate concentration
ε_u	vector of error for u'th run in model simulation of SBR operation
η	substrate removal efficiency (%)
η_u	vector of the new SBR model simulation result for u'th run of SBR operation
θ_x	sludge age (d)
θ_{xob}	observed sludge age in SBR system (d)
μ_m	maximum specific growth rate (d^{-1})
ρ	ratio of P_I/K_I
τ	dimensionless time
φ	reaction or aeration time ratio in SBR system (%)
ϕ	variable kinetic parameter, dimensionless

Subscripts

d	degradable
e	effluent
ed	equivalent (detention) condition
ef	effective
nd	non-degradable
p	plug flow or particulate
s	settling or soluble
tr	true
T	total
x	VSS

CHAPTER 1 INTRODUCTION

Batch reactors have been widely used in chemical engineering for a long time. Batch reactors (BR) were used in seminal laboratory work performed to develop the activated sludge process for sewage treatment early in this century (Ardern and Lockett, 1914a, 1914b, 1915). However, continuous flow stirred tank reactors (CFSTR) were installed in the field because wastewater was continuously delivered from a city or a plant and the batch operating mode was difficult to implement at that time. In the past 20 years, with the development of computer technology and the improvement of other automated control devices such as level sensors and valves, engineers and researchers have been able to refine and develop sequencing batch reactor (SBR) technology to treat a continuous flow wastewater. Consequently, the process has been a focus of research in environmental engineering for more than two decades.

Mechanistic-based mathematical modelling of wastewater treatment can serve many purposes. First, modelling can offer an overall conceptual understanding to researchers and extend their knowledge. Second, it can provide designers with the tools to evaluate a wide range of system variables to find optimal designs in which the process objectives can be reached at the lowest cost. Third, modelling can serve operators of wastewater treatment plants by optimizing the operation or adjusting some operating parameters to realize the desired performance. Finally, modelling can be a tool for students with which they can learn more systematically and easily.

Unfortunately, the modelling of an SBR activated sludge process has not been as successful as that of a CFSTR system because a CFSTR system works under more constant conditions in which the changes of substrate and biomass concentrations in the reactors can commonly be neglected. This simplifies the process and benefits model building. In contrast, substrate removal in the SBR system is carried out under an unsteady state in which both the substrate and biomass concentrations in the system change significantly. This is a more complicated situation and, consequently, provides a greater challenge to environmental researchers to mathematically model the system.

In spite of many advantages, environmental engineers are sometimes reluctant to use mathematical models because some models are highly "mathematical" and mechanically unclear, or so complicated in their expressions that the parameters are difficult to estimate and, therefore, not easily employed in practice. Engineers prefer to use simple mechanistic models, for example, the Lawrence & McCarty (1970) model for the activated sludge processes, which was proposed in 1970 and has been widely accepted by environmental engineers and scientists because it is simple in formula and clear in mechanism. Attention should be paid to these practical concerns when developing a mathematical model.

More study with consequent development has been given to CFSTR systems compared to the SBR systems. A researcher or an engineer can summarize the advantages and disadvantages of a CFSTR system and this can be done for an SBR system too. But, it is still unclear what level of performance can be achieved and what biological and physical constraints will occur if an SBR system is applied to situations that a CFSTR system can

or cannot handle. In other words, there has been no comparison study for the two systems. Irvine and Ketchum (1989) stated in their summary report on SBRs that the relationships among sludge age, mass loading, hydraulic residence time (HRT), and tank sizing are not clear for an SBR because of the dramatic impact of aeration and mixing strategies on overall performance.

From the above analysis, the objectives of the thesis are as follows:

1. Derive a mechanistically-based mathematical model that can predict SBR performance over a wide range of operating conditions.
2. Develop a set of experimental methods to test the parameters of the new model.
3. Make an overall comparison between SBR and CFSTR systems based on experiment and model simulation.
4. Summarize operational constraints of SBR.
5. Develop the quantitative calculation methods for the effective reactor volume, true HRT, true sludge age, true sludge loading rate and true volumetric loading rate for an SBR system.
6. Propose procedures for SBR system design.

CHAPTER 2 THEORY AND LITERATURE REVIEW

2.1. THE SEQUENCING BATCH REACTOR ACTIVATED SLUDGE SYSTEM

Actually, an SBR is a batch system operated according to a designated time sequence. In its simplest form, the SBR system consists of a single vessel in which timed periods of filling, reacting, settling, drawing and idling sequentially take place. Figure 1 shows the five phases in one cycle of a single tank SBR. To provide batch treatment in a continuous flow situation, the system must have more than one tank (reactor). In a multi-tank SBR system, each reactor works independently but follows the same cycle although each tank is in a different phase of the cycle.

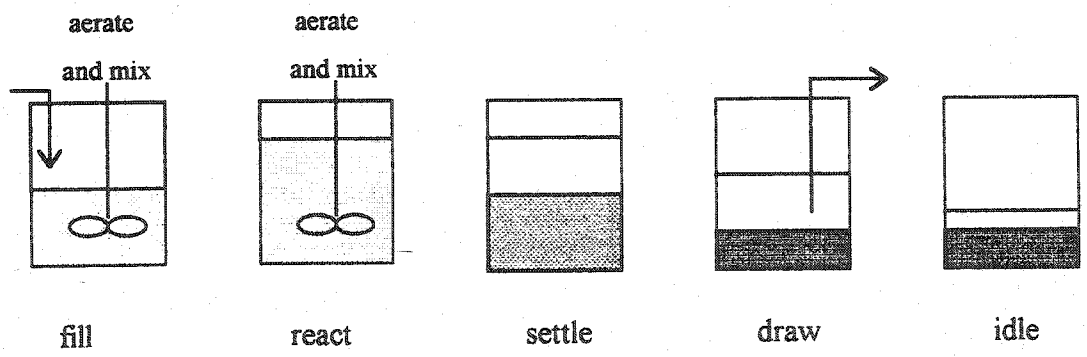


Figure 2-1. Typical five phases of an operational cycle in a single tank SBR system

For example, consider a three tank system where each tank is in an idle phase and they all contain a concentrated sludge occupying the bottom portion of the tank. At the beginning there is no flow coming into the system. When a constant continuous flow is initiated, the

first reactor begins to fill with wastewater and aeration is commenced. The first reactor fills to capacity and flow is directed to the second reactor which begins its fill period. The first reactor now enters the react phase. When the second reactor is full, flow is directed to the third reactor. Now the second reactor enters the react phase. The first reactor must complete the phases of react, settle, draw and idle during the fill periods of the second, and third reactors to have the available volume to receive influent when the third reactor is full. When the third reactor is full, the influent is directed back into the first reactor which then repeats the whole cycle as the second and third reactors go through the phases of react, settle, draw and idle to be able to accept influent at the appropriate time. Sludge produced during the cycle can be removed during the draw or idle phases. A pictorial representation of this operating sequence is shown in Fig. 2-2.

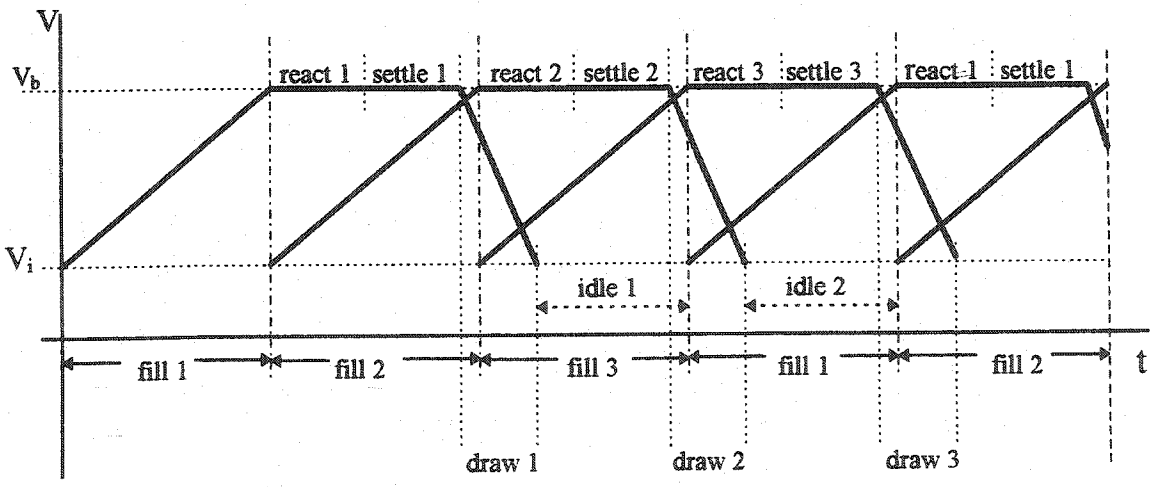


Figure 2-2. Operating sequence of a three tank SBR system for a continuous flow

In Fig. 2-2, the x axis represents time and the y axis the reactor volume. Each reactor has the same initial volume, V_i, full reactor volume, V_b, and cycle mode. There are no a priori

requirements on the duration of each phase of the cycle. The only mandatory requirement is that at least one reactor has available volume at any time to receive influent. In a steady flow situation, maximum treatment efficiency will be attained when each reactor has the same cycle as shown in Fig. 2-2. Idle time would not be incorporated into the cycle in a steady flow situation because it is wasted time and therefore wasted volume.

The phases do not normally have the same duration. For instance consider a wastewater which gives rise to a sludge that settles in 20 min. The designer uses a three tank system and sets the cycle time at 6 h for a steady flow. For maximum volume efficiency in this system the fill time will be 2 h, the react and draw periods will total 3 h and 40 min, respectively. How this time is split between the react and draw periods depends on the pumping capacity for withdrawing clarified effluent. If more reaction time is required, the designer can increase pumping capacity with due consideration to turbulence and concomitant disturbance of the settled sludge. Or the volume of the tanks can be increased which will increase the fill, react and cycle times. Obviously there are many routes to vary the relative duration of each phase of the cycle. These range from physical measures such as volume adjustments (which can also be additional tanks) to measures such as adding a chemical agent to improve settling or heat to increase the rate of reaction.

In a variable flow situation, optimum treatment will dictate that the durations of the phases are variable under the constraint that one reactor is always available to receive influent. When the flow rate is high the reactor receiving the influent will have a shorter fill period.

As flows decrease, the reactor receiving influent will have a longer fill period and the previously filled reactor(s) will have longer times for react, settle, draw and idle periods. Idle time will probably occur on a periodic basis. The degree of flow variability and the regularity of the flow pattern will determine the total system volume and cycle variability through time.

2.2 THEORETICAL ANALYSIS OF EFFECTIVE VOLUME FOR BATCH REACTOR, CONTINUOUS FLOW AND STIRRED TANK REACTOR AND PLUG FLOW REACTOR

In this section, three typical types of reactors, BR, CFSTR and PFR, will be compared based on the theoretical analysis of their effective reactor volume. SBR, as described before, is a BR operated according to a pre-set time sequence. Thus the BR can be used as a representative of SBR for a theoretical comparison. An assumption for a BR should be made before the theoretical comparison, that is, neglecting fill and draw time and considering a "pure" effective reactor volume for this system.

The effective volume is the basic factor to evaluate a reactor. The treatment efficiency, η, similar to the conversion efficiency in chemical engineering, and the substrate removal rate, q, are the two main factors for selecting an appropriate reactor for wastewater treatment. Reliability and simplicity of operation are also important considerations. The treatment efficiency and substrate removal rate are defined as

$$\eta = \frac{S_0 - S}{S_0} = 1 - \frac{S}{S_0} \qquad (2\text{-}1)$$

where S_0 and S are the substrate concentrations of influent and effluent respectively, and

$$q = \frac{VS_0\,\eta}{t_d} \tag{2-2}$$

where V is the effective volume of the reactor for BR, CFSTR and PFR systems and t_d in the effective reaction time or HRT.

Differentiating Eq. (2-1) with respect to time t results in

$$\frac{d\eta}{dt} = \frac{1}{S_0}\frac{dS}{dt} \tag{2-3}$$

The reaction in the BR can be assumed to be first-order and the reaction equation is

$$\frac{dS}{dt} = -kS$$

where k is the first-order rate constant. Applying this expression with Eq. (2-1) to Eq. (2-3) yields

$$\frac{d\eta}{dt} = -\frac{1}{S_0}kS = -k(1-\eta) \tag{2-4}$$

Integrating Eq. (2-4) gives

$$\int_0^{\eta} \frac{d(1-\eta)}{(1-\eta)} = \int_0^{t_d} k\,dt$$

which becomes

$$t_d = \frac{1}{k}\ln\left(\frac{1}{1-\eta}\right) \tag{2-5}$$

Applying Eq. (2-5) to Eq. (2-2) and rearranging it results in

$$\frac{kV_bS_0h}{q} = \ln\left(\frac{1}{1-\eta}\right) \qquad (2\text{-}6)$$

The subscript b refers to a BR. This equation is for a BR under the condition of a first-order reaction. Similarly, from the mass balance and at steady state, the treatment efficiency in a CFSTR with a first-order reaction can be determined:

$$QS_0 - QS - kSV = \frac{dS}{dt}V = 0$$

and

$$S_0 - S = \frac{kSV}{Q} = kSt_d.$$

Then

$$\eta = 1 - \frac{S}{S_0} = \frac{t_dk}{1+t_dk} \qquad (2\text{-}7)$$

and

$$t_d = \frac{\eta}{k(1-\eta)}$$

is obtained from Eq. (2-7). Applying this to Eq. (2-2) results in

$$\frac{kV_cS_0\eta}{q} = \frac{\eta}{1-\eta} \qquad (2\text{-}8)$$

The subscript c refers to a CFSTR.

For a PFR, the same equations and same derivation procedures as for a BR reactor are used. Hence, the same equation for t_d related to the treatment efficiency is applied:

$$t_d = \frac{1}{k}\ln\left(\frac{1}{1-\eta}\right) \tag{2-9}$$

After substituting Eq. (2-9) into Eq. (2-2), a result similar to the above equations is obtained,

$$\frac{kV_pS_0\eta}{q} = \ln\left(\frac{1}{1-\eta}\right) \tag{2-10}$$

The subscript p refers to a PFR.

The effective volumes of the three reactors may now be compared. When k, S_0, q and η have the same values in each system, the effective volume ratio of a BR to a CFSTR is

$$\frac{V_b}{V_c} = \frac{\ln[1/(1-\eta)]}{\eta/(1-\eta)} = \frac{(1-\eta)\ln[1/(1-\eta)]}{\eta} \tag{2-11}$$

and the effective volume ratio of a BR to a PFR is

$$\frac{V_b}{V_p} = \frac{\ln[1/(1-\eta)]}{\ln[1/(1-\eta)]} = 1 \tag{2-12}$$

Using the same method, the general equation for an nth-order reaction in a BR is

$$\frac{kV_bS_0{}^n\eta}{q} = \frac{1}{(n-1)}[(1-\eta)^{1-n}-1] \qquad (n \geq 0, \quad n \neq 1) \tag{2-13}$$

Also a general equation for a CFSTR is

$$\frac{kV_c S_0^{\,n}\eta}{q} = \frac{\eta}{(1-\eta)^n} \qquad (n \geq 0, \quad n \neq 1) \qquad (2\text{-}14)$$

and for a PFR:

$$\frac{kV_p S_0^{\,n}\eta}{q} = \frac{1}{(n-1)}[(1-\eta)^{1-n} - 1] \qquad (n \geq 0, \quad n \neq 1) \qquad (2\text{-}15)$$

Thereafter the effective volume ratios for general expressions are

$$\frac{V_b}{V_c} = \frac{(1-\eta)-(1-\eta)^n}{\eta(n-1)} \qquad (n \geq 0, \quad n \neq 1) \qquad (2\text{-}16)$$

and

$$\frac{V_b}{V_p} = 1 \qquad (n \geq 0, \quad n \neq 1) \qquad (2\text{-}17)$$

Assuming treatment efficiencies, η = 0.1, 0.2, 0.3, 0.4, 0.5, 0.6, 0.7, 0.8, 0.9, and 1, respectively, and considering reaction orders of n = 0, 0.5, 1.0, 1.5 and 2, a series of V_b/V_c curves were generated and are shown in Fig. 2-3.

These curves indicate that for higher order reactions and higher treatment efficiency, the BR requires less effective volume than a CFSTR if fill and draw times of a BR are neglected. From Eqs. (2-12) and (2-17), it is obvious that a BR always requires the same effective volume as a PFR.

Most of the biological reactions in wastewater treatment are considered as first-order

(Grady and Lim, 1980) except when the influent has a very high substrate concentration. In the latter situation, the reaction is zero-order because the reaction rate is not affected by substrate concentration, and a BR should not be the first choice (as shown in Fig. 2-3) unless other factors are important.

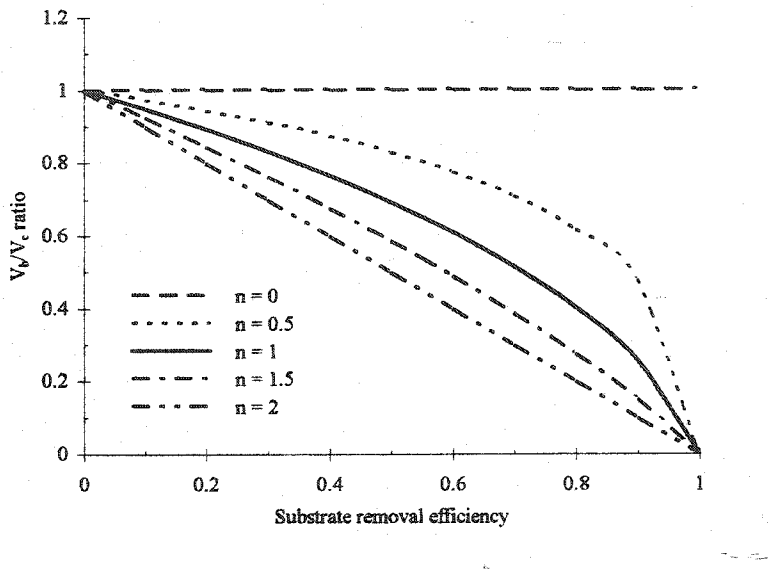


Figure 2-3. Effective volume comparison between BR and CFSTR

The above analysis theoretically verifies the kinetic advantage of a BR. In reality, the operational constraints of an SBR will partly diminish the BR advantage. This will be discussed in detail in Chapter 9 in Part II.

2.3. THE ADVANTAGES OF SBR SYSTEM AND ITS APPLICATION

SBR technology has many theoretical and practical advantages. A number of researchers (Irvine et al., 1977, 1979; Ketchum et al., 1978, 1979; Alleman and Irvine, 1980a, 1980b;

Silverstein and Schroeder, 1983; Palis and Irvine, 1985; Arora et al., 1985; Manning and Irvine, 1985; Chiesa and Irvine, 1985; Mandt, 1985; Abufayed and Schroeder, 1986) have concluded that an SBR system possesses many advantages as discussed below:

1. Theoretically reaction in an SBR has plug flow (PF) kinetics for substrate degradation, which results in a larger driving force for mass transfer and other substrate transformation reactions than a CFSTR and other non-PF reactors because of greater concentration gradients in a PF flow pattern. The flow regime, of course, does not dictate the metabolic regime (first-order, second-order, etc.) but directly influences the overall treatment efficiency in terms of unit substrate processing rate. The flow regime is not a simple process parameter but a fundamental process embodiment.

2. Because effluent discharge is periodic, influent can be held within a wider range of limits, until it meets a specified requirement: very low chemical oxygen demand (COD) or biological oxygen demand (BOD), nitrification, denitrification, and phosphorus removal. Flexible operation modes can be selected for different requirements.

3. Aeration for the activated sludge and sedimentation occur in the same basin. During the latter period, sludge settles under nearly ideal quiescent conditions and no short-circuiting or other disturbances, such as channeling and bypassing, occur providing highly clarified effluent. Solids separation is more challenging in the secondary sedimentation basin of a CFS. Besides deteriorating effluent quality, loss of solids in the clarified effluent results in uncontrolled loss of biomass.

4. Sludge bulking caused by filamentous growth can be controlled to some extent by

varying the operating mode (in particular oxygen supply) during the fill period of the operating cycle. The PF or batch regime that naturally occurs in an SBR tank is known to promote the growth of the zoogloeal microorganisms that settle quickly and compact to a high degree.

5. It can tolerate shock loading including very high feed concentration and peak flow because of higher concentrated sludge held in the reactor which results in lower ratio of food to microorganisms (F/M ratio).

6. No sludge recycle pumping is needed which leads to cost saving in both capital and operation.

The above advantages have re-established SBR as a viable technology for wastewater treatment. Irvine and Busch (1979) reported applications of a full-scale single tank SBR system to treat meat-packing waste in Ada, OK, and a two-tank system to treat dairy waste. Bloemer et al. (1980) and Bloemer and Irvine (1982) introduced a three-tank SBR system at Eaton Corporate Manufacturing services Center in Willoughby Hills, OH, to deal with municipal wastewater flowing at 9.46 m^3/d which was only 25% of the original design flow rate but had no adverse effect on performance. Later Irvine et al. (1983 and 1985) reported on full-scale operation of a SBR system in the town of Culver, IN, which was shifted from a conventional continuous flow activated sludge treatment plant with a capacity of 1400 m^3/d. Other researchers also reported on applications of SBR technology (Barth, 1983; Wilderer, 1984; and Sudo and Okado, 1984).

However, no comparative experiments have been made between SBR and CFSTR systems

to systematically verify the above advantages. It is usually assumed that the same values of the kinetic coefficients apply to a batch, PFR, or CFSTR system. But the situation is quite different among the three. A CFSTR reactor provides relatively uniform conditions at all times compared to the continuously changing environment (at least with respect to substrate) in a PFR or batch reactor that is in a quasi-steady state condition. There are other differences between a batch and a CFSTR or continuous flow PFR. The major one being that the concentration of sludge is very high at the beginning of the fill (inflow) period of a batch cycle and it decreases, as the batch reactor is filled, to concentration levels that exist with minor variation throughout a PFR and the constant concentration that exists in a CFSTR reactor at steady state.

2.4. MODELS FOR A SBR SYSTEM

Irvine and Ritcher (1978), Orhon et al. (1986) and Droste (1990) presented mathematical models to predict SBR process performance. However, these models still have some basic deficiencies for describing SBR system performance because their basis is the Lawrence and McCarty model (1970) which is the most commonly used model in wastewater treatment. A set of the model parameters tends to only depict the activated sludge process in a narrow range (Droste, 1990). Newer more sophisticated models have been proposed for the activated sludge process but there are few studies where these models have been applied. In particular, their application to an SBR system has not been attempted until 1991 (Nakazawa and Tanaka, 1991).

2.4.1. Lawrence & McCarty Model

Lawrence and McCarty (1970) proposed a unified basic model for biological treatment design and operation based on a mass balance for a continuous flow system. Considering substrate removal, the mass balance of the system can be expressed as follows:

Inflow – Outflow + Net removal = Accumulation

$$QS_0 - QS - \frac{kXS}{K_S + S}V = \frac{dS}{dt}V$$

where

S_0 = substrate concentration of influent (mg/L);

S = substrate concentration in the reactor at any time (mg/L);

Q = flow rate of the influent (L/d);

V = volume of reactor (L);

X = concentration of biomass in the reactor (mg/L);

k = specific substrate removal rate (d^{-1});

K_S = half velocity constant (mg/L);

t = time (d).

At steady state around the system dS/dt = 0, and the resulting equation is:

$$S_0 - S = \frac{kXS}{K_S + S}t_d$$

where $t_d = V/Q$.

The Lawrence and McCarty model has clear mechanistic meanings for each term. Unfortunately, there is a large deviation when applying it to an SBR system which will be discussed later in this chapter.

2.4.2. Irvine and Ritcher' s Model

Irvine and Ritcher (1976, 1978) proposed a model based on a first-order reaction for substrate removal:

$$\frac{d(VS)}{dt} = QS_0 + Vr_s \text{ and}$$

$$\frac{d(VX)}{dt} = QX_0 + Vr_x$$

where r_S and r_X are rate expressions for the substrate degradation and sludge decay.

$r_s = k_1SX$ when $S < S''$;

$r_s = k_1S''X$, when $S \geq S''$;

$r_x = Yk_1SX - k_eX$ when $S < S''$,

$r_x = Yk_1S''X - k_eX$ when $S \geq S''$;

S'' = constant, limiting waste concentration (mg/L);

S = substrate concentration (mg/L);

S_0 = substrate concentration of influent (mg/L);

V = liquid volume at any time (L);

Q = influent flow rate (L/d);

X_0 = the concentration of volatile suspended solids (VSS) in the influent, which generally equals zero (mg/L);

X = the concentration of VSS (mg/L);

k_1 = substrate removal rate constant (d^{-1});

k_e = endogenous decay rate (d^{-1});

Y = yield coefficient;

t = time (d).

The boundary conditions for these equations are: At t = 0, $V(0) = V_i$, $S(0) = S_e$ (from the last cycle) and S_0 are known; after the fill time t_f, $dV/dt = Q = 0$.

Irvine initiated research on SBR, which had a profound effect for the recovery and re-development of SBR technology. Irvine and Ritcher's model (1976, 1978) is the earliest and simplest model and can only deal with uniform substrate with first-order (if S<S", the concentration of limiting substrate) or zero-order (if S>S") reactions, the two extremes of Monod kinetics. It cannot describe the process behavior between the two ends. Therefore, its deficiencies are evident.

2.4.3. Orhon's Model

Orhon et al. (1986) used a model based on Monod kinetics and fashioned after the

Lawrence and McCarty model (1970):

$$\frac{dS}{dt} = \frac{Q(S_0 - S)}{V_0 + Qt} - \frac{\mu_m SX}{Y(K_s + S)}$$

$$\frac{dX}{dt} = -\frac{QX}{V_0 + Qt} + \frac{\mu_m SX}{K_s + S} - k_e X$$

where

μ_m = maximum specific growth rate (d^{-1});

K_S = half velocity constant (mg/L);

V_0 = initial volume in an SBR tank (L).

Other definitions are the same as in Irvine's model.

Although Orhon's model uses the Monod rate expression, using a uniform substrate does not allow more accurate prediction for the entire process.

2.4.4. Droste's Model

Droste (1990) made an extensive theoretical analysis of the influence of SBR system parameters on the extent of substrate removal using the Monod and first-order models for substrate removal kinetics. Also the influence of physical operating conditions between SBR and CFSTR systems was analyzed. Droste's model is derived from an expression based on a mass balance:

$$\frac{dS}{dt} = \frac{Q}{V}(S_0 - S) + r_s$$

where

$r_s = kXS/(K_S + S)$ in the Monod expression or

$r_s = k' XS$ in a first-order form, and

$dV/dt = Q$.

The dimensionless expression of the model for Monod kinetics is:

$$\frac{d\xi}{d\tau} + \frac{\xi}{\tau} + \Phi\left(\frac{\xi}{1+\lambda\varepsilon}\right) - \frac{1}{\tau} = 0$$

where

$\xi = S/S_0$, dimensionless substrate concentration;

$\tau = t/t_{dc}$, dimensionless time;

$t_{dc} = V_c/Q$ = detention time in CFSTR;

$$\Phi = \frac{\phi}{\alpha}\left[\frac{\tau_f - \tau + (\tau - \tau_0)}{\tau_f - \tau_0}\right]$$

is variable kinetic parameter and subscripts f and 0 refer to fill and initial conditions;

$\phi = kXt_{dc}/K$ for Monod kinetics or $\phi = k' Xt_{dc}$ for a first-order reaction;

$\alpha = V_i/V_b$ = ratio of initial reactor volume to total available reactor volume

$\lambda = S_0/K_S$, dimensionless saturation constant.

The other definitions are the same as for the above two models.

Droste made the proposed model dimensionless to identify important parameter groups but the basic model still had no substantial difference from Irvine and Ritcher's and Orhon's models. But his extensive theoretical analysis about the characteristics of SBR and the comparison between SBR and CFSTR made progress in the development of SBR technology which will be discussed in Chapter 8.

2.4.5. Silverstein and Schroeder's Model

Silverstein and Schroeder (1983) proposed a kinetic model to predict organic removal during the aerated fill period based on the mass balance of substrate, filtered total organic carbon (FTOC) and sludge mass. For substrate:

$$\frac{d(VC)}{dt} + QC_0 = Vr_c$$

where

C = reactor concentration of FTOC (g/m^3);

C_0 = influent concentration of FTOC (g/m^3);

$r_c = k\,\overline{X}$, the rate of substrate removal (g FTOC/m^3 min.);

$\overline{X}$ = average activated sludge concentration (g/m^3)

Other definitions are the same as above.

For the activated sludge mass:

$$\frac{d(VX)}{dt} = V\mu$$

where

X = suspended solid concentration (g/m^3);

μ = rate of increase of solids ($g/m^3/min$).

It was assumed by the authors that μ accounted for an eligible fraction of the solids mass during filling, which was supported by the MLSS data. Therefore, the mass balance on suspended solids becomes:

$$\frac{d(VX)}{dt} = 0$$

The paper did not provide kinetic predictions for the periods after fill.

Application of Silverstein and Schroeder's model is very limited since physical and biological considerations are limited to FTOC and the model only applies to the fill period with first-order kinetics.

2.4.6. Nakazawa and Tanaka's Model

Nakazawa and Tanaka (1991) developed a mathematical model to deal with the behaviors of biomass and substrate containing colloidal and solid forms within one cycle. Their model is based on the dynamic model for the CFSTR activated sludge process under cyclic loading conditions developed by Ekama and Marais (1979) and on the study of actual municipal wastewater treatment by an SBR activated sludge process.

For soluble and particulate BOD_L in the fill period, the mass balance equations are:

$$\frac{d(VS_s)}{dt} = QS_{si} + Vr_{ss}$$

$$\frac{d(VS_p)}{dt} = QS_{pi} + Vr_{sp}$$

where

S_s = soluble substrate (mg BOD_L/L);

S_p = particulate substrate (mg BOD_L/L);

and subscript "i" indicates influent.

$$r_{ss} = \frac{k_{ms} S_s X_a}{K_{ss} + S_s}$$

and

$$r_{sp} = -K_a S_p X_a \left(f_{ma} - \frac{X_s}{X_a}\right) + p(1-\kappa) k_d X_a$$

where

k_{ms} = maximum specific substrate utilization rate constant for soluble substrate;

K_{ss} = half-saturation coefficient for heterotrophic cell synthesis for soluble substrate;

X_a = active biomass concentration;

K_a = particulate substrate adsorption rate constant;

X_s = stored BOD_L concentration;

p = BOD/VSS ratio;

κ = aerobically nonbiodegradable fraction of organic primary solids;

k_d = rate constant for degradation of degradable biomass;

f_{ma} = the authors define this coefficient as a "parameter related to adsorption and storage" with the units of mg VSS/mg VSS.

After fill, Q in the above two equations is equal to zero. Mass balances of stored BOD_L, X_s, active mass, X_a, and oxygen, O_r, are expressed by the following equations:

$$\frac{d(VX_s)}{dt} = Vr_{xs}$$

$$\frac{d(VX_a)}{dt} = Vr_{xa}$$

$$\frac{d(VO_r)}{dt} = -Vr_{oc} + VR_a$$

where

$$r_{xs} = \frac{K_a S_p X_a (f_{ma} - \frac{X_s}{X_a})}{p} - \frac{k_{mp} X_s p}{K_{sp} + X_s p} X_a$$

is the overall rate of change of stored BOD_L ;

$$r_{xa} = Y \frac{k_{ms} S_s}{K_{ss} + S_s} + \frac{k_{mp} X_s p}{K_{sp} + X_s p} X_a - k_d X_a$$

the overall rate of change of active mass;

$$r_{oc} = (1 - pY)\left(\frac{k_{ms}S_s}{K_{ss} + S_s} + \frac{k_{mp}X_s p}{K_{sp} + X_s p}\right)X_a$$

the overall carbonaceous oxygen consumption rate;

K_{sp} = half-saturation coefficient for heterotrophic cell synthesis for stored substrate;

Y = organism yield coefficient in term of BOD_L.

The authors did not define R_a. Other terms are the same as above. The biokinetic base of Nikazawa and Tanaka's model is that of Ekama and Marais (1979). This model categorizes influent substrate into soluble and insoluble forms and employs two equations, one for each type of substrate, to predict substrate removal but it is different from Ekama and Marais's approach to sub-categorize the soluble organics into biodegradable and non-biodegradable fractions. From the model expressions it can be seen that during fill, since no rate term describes stored BOD_L degradation, the model does not consider this or assumes no accumulation of stored BOD_L in this period although no such assumption was indicated in the paper. And also during fill, there is no influence by dilution of biomass on substrate removal since there is no mass balance equation for the active biomass for the entire cycle but only for the periods after fill. The paper did not give a systematic procedure to estimate the model parameters.

These factors suggest that work needs to be done for dynamic modelling of an SBR system. Further criticism of the biokinetic base of Nakazawa and Tanaka's model will be presented in the next section.

2.4.7. Summary of Analysis of Earlier SBR Models

From above, it can be seen that there is no substantial difference among the first four models. To calibrate the earlier SBR models, a wide range of values of parameters for each model were carefully selected by trial and error. Then each model was run with a computer program, which was developed by the thesis author especially for simulation of SBR system, until reaching a steady state around the system. Finally, the data from the model simulation were compared with preliminary experimental results.

Comparison of the earlier SBR models and the experimental results reveals that these models are unable to predict the entire SBR operation cycle. The model simulation can either fit the fill stage but fail at the beginning and the period after the fill stage or fit the beginning and the period after the fill stage but fail in the fill period. The former prediction occurs with a normal range of rate constant values and the latter with very low values. Figure 2-4 shows the former case where the substrate concentration quickly drops close to zero after fill is stopped. Preliminary experimental results revealed that the COD remaining after the fill period was quite high due to the presence of refractory organic substances produced from sludge digestion and from raw influent and intermediate products of metabolism. The results of the simulation are readily understood from the batch kinetics derived earlier. If no feed is provided after the fill stage, the remaining substrate in the reactor, according to the earlier SBR model reaction rate expressions with either a first-order or Monod formulation, will be completely consumed as long as enough time is provided for the react period.

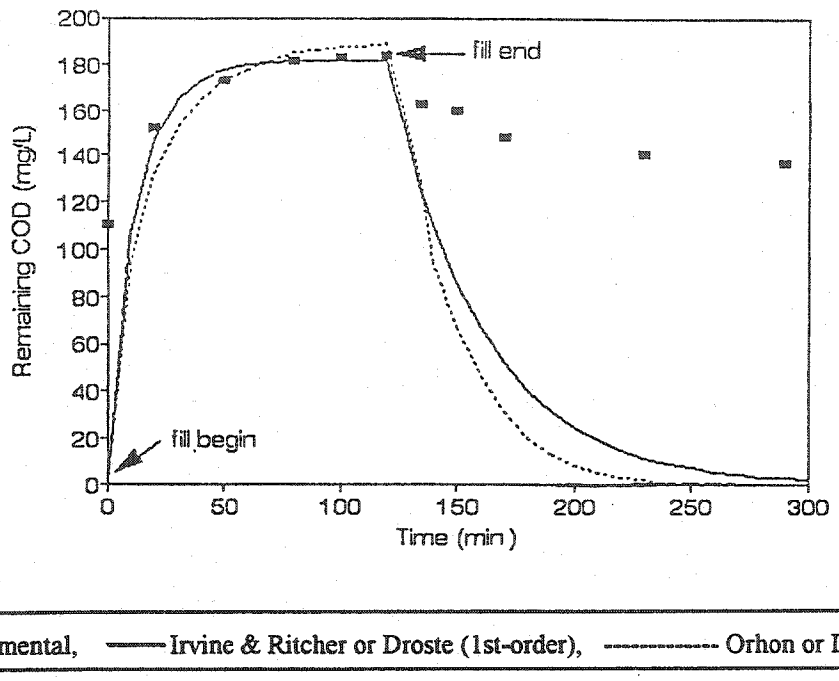


Figure 2-4. Comparison of earlier SBR models with experimental result

The theoretical results from the models in Irvine and Ritcher (1976, 1978) and Orhon et al. (1986) papers are the same, i.e., the predicted substrate concentration curve falls to zero after fill. There are two reasons for the models' failure to describe substrate removal for the entire cycle. One is, as indicated above, that these models ignore the refractory organic materials in the influent and the byproducts of substrate metabolism and sludge decay during the SBR cycle. Also inert organic matter is not incorporated into these models. These kinds of organic materials directly influence effluent quality. The other is that these models did not classify soluble substrate, treating substrate as uniformly degradable. Similar problems arise when these models are applied to continuous flow PFR or CFSTR systems although they may not be as serious as in an SBR system.

It should be noted that the deficiencies of the above models come from the Lawrence and McCarty model (1970). Lawrence and McCarty were among the first to present a unified model of the activated sludge process. This model remains the most widely used model to date but it has some obvious deficiencies. The model deals with a uniform substrate and ignores the production of substances from metabolism which are largely slow or difficult to degrade, and similarly byproducts from sludge decay are difficult-to-degrade. In any activated sludge process, sludge decay is always significant due to the necessity of operating any system at starved conditions which promotes the highest degree of treatment (i.e., there is excess sludge in the system). Ignoring this phenomenon with respect to production of difficult-to-degrade soluble organics clouds the comparison of different systems because the effluent COD largely consists of these byproducts; the readily biodegradable substrate present in the influent has been removed. Furthermore, systems must be operated at comparatively high sludge ages (high biomass concentrations) to maintain sludge settleability. Therefore, effluent quality is similar among all systems but the safety factor for removal of readily degradable substrate is unable to be appraised.

2.5. SOME IMPORTANT MODELS FOR ACTIVATED SLUDGE PROCESS

2.5.1. IAWPRC Model No. 1

Leaders in the field of biological wastewater treatment through the International Association on Water Pollution Research and Control (IAWPRC) formed a task group and proposed an activated sludge model called IAWPRC Model No. 1 (Grady et al., 1986;

Henze et al., 1986, 1987; Bidstrup and Grady, 1988) that had foundations in the work of Ekama and Marais (1979), Dold et al. (1980), Cech et al. (1985) and Ekama et al. (1986) for single-sludge wastewater treatment systems carrying out carbon oxidation, nitrification and denitrification. This model (Henze et al., 1986) is expressed by a matrix system comprising 13 components, 8 process rates and 20 parameters. Because of space limitations, details on the model should be obtained from the original publication. Recently, Sollfrank and Gujer (1991) developed a procedure to characterize organic materials in domestic wastewater in view of the model and Griffiths (1994) modified the model with addition of an approach to phosphorus removal.

There are some important developments in the model:

In contrast to the single (uniform) substrate classification in the earlier models, substrate in this model is classified into readily (soluble), slowly (insoluble) biodegradable and biologically inert (soluble and insoluble) materials which makes it possible to separately depict the degradation processes of substrate with different rates of biodegradation.

Oxygen is considered as negative COD. With this transfer, oxygen uptake rate (OUR) is employed to continuously depict the biodegradation process instead of COD with which only interval tests can be done for the process description.

The model divides biomass into two categories: heterotrophic and autotrophic. Heterotrophic bacteria grow in both aerobic and anoxic environments by utilizing readily biodegradable substrate for carbon and energy while autotrophics grow only in an anoxic condition by using nitrate nitrogen. This classification allows more detailed prediction of

nitrification and denitrification.

The introduction of the death-regeneration concept differs from traditional concepts of endogenous respiration. In the new approach, sludge is degraded into slowly biodegradable materials and dead solids without COD change. The former will hydrolyze into readily biodegradable substrate adding to the soluble COD and the latter is still incorporated into the sludge. In the traditional endogenous respiration approach, the sludge degrades directly into CO_2 and H_2O and no products contribute to soluble or insoluble COD.

On the other hand, the IAWPRC Model No. 1 has at least three major weaknesses.

First, there is no efficient method to measure many of the kinetic parameters and stoichiometric coefficients because of its complicated structure. Generally, model parameters are estimated by experimental measurement or by regression approaches.

Next, the estimation of some model parameters is done by measuring OUR as the response instead of directly measuring oxygen demand, COD or BOD. However, no report proves the sensitivity of the OUR test to parameter variance, which may result in very large errors in the model parameter estimation. For the OUR test itself, Sollfrank and Gujer (1991) reported that in their research OUR measurement was calibrated under steady state conditions by COD continuity and was found to be subject to an error of less than 5% of the true value. The standard COD method has about 5% error (APHA-AWWA-WPCF, 1989), which means that OUR measurement could double the error of the COD method.

Lastly, the approach to treat slowly biodegradable substrate as insoluble has very limited meaning and could result in a large error as well for model prediction of a real process because there are many organic substances that are very slowly biodegradable but they are soluble. Polyvinyl alcohol (PVA), for example, that is found in printing and dyeing wastewater is very slowly biodegradable but completely water soluble. Its presence even with smaller fragments in the effluent will significantly affect the soluble COD level. Furthermore, colloidal materials ranging in size from 10^{-5} to 10^{-3} μm, are not separable by common filtering or other physical processes (except by membrane separation). Therefore, they are considered as water soluble and will contribute to soluble COD of an effluent. Unfortunately, in the IAWPRC Model No. 1, this type of slowly biodegradable substrate is artificially considered as a particulate form that leaves the reactor with discharged sludge instead of with effluent and does not affect the soluble COD of the effluent except for the portion hydrolyzed through sludge decay into a readily biodegradable form. This approach is obviously unreasonable when describing degradation of a slowly biodegradable but water soluble material. Grady (1989), one of the researchers in the Task Group, indicated that the hydrolysis expression was one of the weakest links in the modelling of activated sludge dynamics and is badly in need of further experimental research.

The above analysis shows that there is still much room to modify or simplify the most complicated model to date for more efficient and convenient use.

2.5.2. Application of IAWPRC Model No. 1 to SBR System

Oles and Wilderer (1991) developed a modified version of the IAWPRC model to describe the performance of laboratory and pilot scale SBR systems. Changes of ammonia and NO_X during the SBR process cycle could be reliably predicted after the model parameters were adapted to SBR conditions. The version also gives an approach for SBR plant design with some restrictive rules. However, Oles and Wilderer's work showed no COD degradation data at all and no nitrogen changes in the cycles with various operational conditions. For model parameter estimation, only the maximum specific growth rate of heterotrophic organisms, μ_{max}, and its decay rate, b_H, were experimentally measured and all other model parameters were suggested by the IAWPRC Task Group (Henze et al., 1986, 1987).

2.5.3. Models Concerned with Soluble Microbial Products (SMP)

Many researchers (Chudoba, 1967; Chudoba et al., 1968a, 1968b; Grady et al., 1972; Grady and Williams, 1975; Daigger and Grady, 1977a, 1977b; Baskir and Hansford, 1980; Siber and Eckenfelder, 1980; Saunders and Dick, 1981) revealed that most effluent soluble COD from a biological wastewater treatment process is not from original influent but from microbial metabolism. Numerous studies (Strange et al., 1963; Demain et al., 1965; Mateles and Chian, 1969; McGregor and Finn, 1969; Thomas and Batt, 1969; Hunter, 1971; Pavoni et al., 1972; DeWalle and Chian, 1980; Chudoba et al., 1980; Gaudy and Gaudy, 1980; Parkin and McCarty, 1981; Saunders and Dick, 1981; Grady et al., 1984; Chudoba, 1985; Namkung and Rittmann, 1986; Amy et al., 1987; Rittmann et al., 1987;

and Boero et al., 1991) also found that soluble COD in biological wastewater treatment effluent is composed of a wide variety of high and low molecular compounds although some of the research cases solely use simple compounds in the feed. This fact indicates that the effluent quality consists largely of soluble microbial products (SMP). Some earlier literature (Luedeking and Piret, 1959; Pirt, 1975) categorized SMP formation into two types: growth-associated and non-growth-associated. Growth-associated SMP formation was related to the substrate utilization rate and non-growth-associated SMP formation was proportional to the biomass concentration. Rittmann (1987) and Rittmann et al. (1987) and Furumai and Rittmann (1992) more recently named the two products utilization-associated products (UAP) and biomass-associated products (BAP).

Luedeking and Piret (1959) proposed a simple model of SMP formation in fermentation processes. Baskir and Hansford (1980) incorporated Luedeking and Piret's model into the existing activated sludge theory to predict the effluent soluble COD in the activated sludge system and obtained reasonable results.

Furumai and Rittmann (1992) proposed a model that considered the formation and exchange of SMP. This new model has three equations for biomass and seven equations for substrate and SMP degradation and exchange with a total of 26 parameters. The most important development of the model is the concept of SMP formulated by the following equations:

$$V\frac{dP}{dt} = -QP_0 + \Sigma(R_{1j} + R_{2j})X_j V - R_3 X_h V$$

$$V\frac{dP_0}{dt} = -QP_0 + \Sigma(R_{1j} + R_{2j})X_jV$$

where

P = soluble microbial products (SMP);

P_0 = the total of originally formed SMP;

R_1 = specific UAP formation rate = k_1M and M is specific substrate consumption rate;

R_2 = specific BAP formation rate = k_2;

R_3 = specific SMP consumption rate = $k_3m(P/P_0)$;

k_1 = UAP formation coefficient;

k_2 = BAP formation coefficient;

k_3m = SMP degradation coefficient.

Although they developed the model incorporating formation of SMP from both heterotrophs and nitrifiers, Furumai and Rittmann did not conduct any experiments to verify the proposed model. Another weakness of the modelling work is that all model parameter values are assumed or taken from the literature. These two major weaknesses affect the model's application and reliability.

The above discussions on related activated sludge process models, especially when applied to an SBR system further prove that there is a need and scope to develop a new mathematical model for the SBR activated sludge system.

CHAPTER 3 EXPERIMENTAL APPROACH

3.1. EXPERIMENTAL APPARATUS AND GENERAL CONDITIONS

The experimental approach for this project is based mainly on three considerations. The first is that the experimental results can verify the simulation of the SBR performance by the new SBR model over a wide range of operational conditions. The second is that the model can provide systematic comparison between SBR and CFSTR systems under the same or equivalent operational conditions. The third is that specific methods for the experimental measurement of most parameters of the new SBR model must be developed for the application of the new model.

Irvine (1978) and Norcross (1990) reported that most SBR systems were designed with only 2 or 3 reactors. According to the above considerations and earlier researchers' work, two different systems, SBR and CFSTR, were to be run in parallel for modelling the SBR system and also for a systematic comparison between the two systems. The standard approach to biological treatment kinetic studies commonly evaluates system performance at three sludge ages and three detention times. Therefore, three reactors are set in each system, respectively, under the same equivalent detention time defined by Eq. (8-3) and the same feed concentration. In a system, each reactor is operated at a different sludge age to provide three sludge ages. Figure 3-1 is the schematic outline of the two sets of experimental devices.

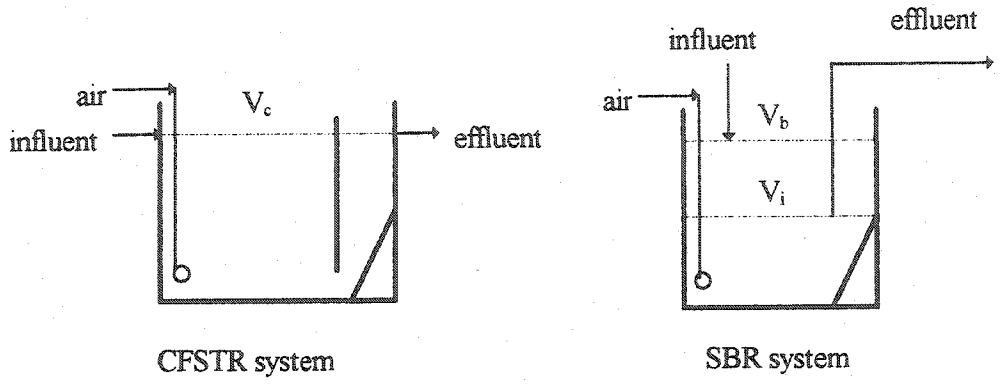


Figure 3-1. Schematic outline of the two experiment devices of SBR and CFSTR systems

The maximum volume of each SBR reactor was V_b = 8 L while the volume of each CFSTR reactor is 10 L with a 2 L sedimentation volume. Aeration was supplied to agitate the mixed liquid and to provide bacteria with suitable DO at 2 to 4 mg/L during fill and react phases and > 0.5 mg/L at the end of settling phase. Feed solution pH was adjusted to 7 to 9 and in the mixed liquor pH was controlled at 6 to 7. The experiment was conducted under room temperature range of 22 to 24°C to render its influence on the rate constants negligible.

3.2. OPERATIONAL PARAMETERS

High substrate removal rate, capability of withstanding high loading shock and low operation cost are the features required for any biological wastewater treatment process. There are several parameters relating to the above factors in an SBR system:

(1) The initial volume V_i or the ratio of V_i /V_b.

At the beginning of each cycle, the volume (mass) of concentrated settled sludge is

included in the volume V_i and it is impossible to exceed V_i because of the volume withdrawn in each cycle. When V_i decreases, the ultimate microorganism concentration (VSS) in the reactor during the react period will also decrease. Consequently, the organic loading rate will increase. If V_i, however, becomes larger, the V_i/V_b ratio increases. The volume capacity of the reactor, therefore, will decrease and the effective reaction time will also decrease. On the other hand, V_i is also limited by sludge volume index (SVI) of the solids and the required X_i.

(2) Fill time, t_f and the ratio of t_f/t_T

In one cycle, increasing t_f will cause decreasing t_T. For a highly concentrated influent, prolongation of t_f is beneficial to avoid a loading shock. But, there is a limit to the length of t_f, i.e., $t_f = (V_b - V_i)/Q$. On the other hand, long t_f causes a higher operation cost if it is not necessary for a weak influent. Therefore different t_f/t_T ratios should be applied to the different situations.

(3) The number of reactors n

A system with more reactors requires lower investment in reactor volume, but higher operation cost because more frequently alternate operations will occur among these reactors. Thus, the number of SBRs should be considered in the experiment.

The experimental plan was designed on practical considerations in accord with the objectives of the study. Comparatively higher substrate concentrations will result in higher concentrations of all substances and minimize experimental error. Furthermore the systems will be more highly stressed. Experience with SBR systems has shown that

sludge does not regularly compact to a volume of 25% of the total reactor volume. Hence, the V_i/V_b ratios were chosen to be 1/3 and 1/2.

Generally the cycle time should integrally divide into 24 h per day for easy operation, therefore, t_c times of 3 and 6 h were selected. Based on experience, the settle and draw times, t_s and t_w, were set at a total time, t_{sw}, of 1 h with which the two options of the sum of fill and react times are determined for each cycle time: $t_f + t_r$ = 1 + 1 h and 1.5 + 0.5 h for t_c = 3 h, and $t_f + t_r$ = 2 + 3 and 3 + 2 h for t_c = 6 h.

The 2 and 3 tank systems were chosen for the comparison of different multi-tank systems. Because each tank works individually, the entire system performance can be determined from results for one tank.

From above considerations, all factors considered in the experiment are summarized in Table 3-1 for convenience.

Table 3-1. Summary of factors in the experiments

The number of reactors n	2		3
The initial volume ratio $\alpha = V_i/V_b$	1/3		1/2
The cycle time t_c; $(t_f + t_r)$ (h)	3; (1+1 and 1.5+0.5)		6; (2+3 and 3+2)
Substrate concentration S_0 (mg/L)	250		500
Observed sludge age θ_{xob} (d)	5	10	15

Table 3-2 lists all experimental runs based on the parameters in Table 3-1 where t_{ed} is an HRT equivalent to the one in a CFSTR system based on the same total system volume and Q is fill flow rate during the fill phase of an operational cycle, and calculated from the

definitions developed in Section 8.3.

Table 3-2. Operational mode design and related parameter values of SBR experiments

Set	S_0	t_{ed}	Reactor No.	V_b	V_i	α	t_c	t_f	t_r	t_{sw}	Q
#	mg/L	h	_	L	L	_	h	h	h	h	L/h
1-250	250	3.5	2	8	2.67	1/3	3	1.5	0.5	1	3.56
1-500	500	3.5	2	8	2.67	1/3	3	1.5	0.5	1	3.56
2-250	250	3.5	3	8	2.67	1/3	3	1	1	1	5.33
2-500	500	3.5	3	8	2.67	1/3	3	1	1	1	5.33
3-250	250	8	2	8	2.67	1/3	6	3	2	1	1.78
3-500	500	8	2	8	2.67	1/3	6	3	2	1	1.78
4-250	250	8	3	8	2.67	1/3	6	2	3	1	2.67
4-500	500	8	3	8	2.67	1/3	6	2	3	1	2.67
5-250	250	5	2	8	4	1/2	3	1.5	0.5	1	2.67
5-500	500	5	2	8	4	1/2	3	1.5	0.5	1	2.67
6-250	250	5	3	8	4	1/2	3	1	1	1	4.00
6-500	500	5	3	8	4	1/2	3	1	1	1	4.00
7-250	250	11	2	8	4	1/2	6	3	2	1	1.33
7-500	500	11	2	8	4		6	3	2	1	1.33
8-250	250	11	3	8	4	1/2	6	2	3	1	2.00
8-500	500	11	3	8	4	1/2	6	2	3	1	2.00

The number of runs for the SBR system listed in Table 3-2 are 16 and multiplying by 3

sludge ages, the total runs were 48. For the SBR system, volumetric loading is not available here until new definitions for it are developed in Section 8.3.

Correspondingly, the experimental design for the CFSTR system is listed in Table 3-3. There were 8 runs per set. Each set contains three sludge ages. Thus the total runs for the CFSTR system was 24.

Table 3-3. Operational mode design and related parameter values of CFSTR experiments

No	t_d	V_e	V_s	t_r	t_s	L_v
	h	L	L	h	h	g COD/L/d
1-250	3.5	10	2	3.5	0.7	2667
1-500	3.5	10	2	3.5	0.7	5333
2-250	5	10	2	5	1	1846
2-500	5	10	2	5	1	3692
3-250	8	10	2	8	1.6	1000
3-500	8	10	2	8	1.6	2000
4-250	11	10	2	11	2.2	667
4-500	11	10	2	11	2.2	1333

The parameters that are compared between the two systems are COD removal efficiency, η, volumetric loading rate, L_v, specific substrate removal rate, R, reactor volume utilization rate, β, biomass decay coefficient, k_e, yield factor, Y, sludge concentration, X_v, and SVI.

3.3. FEED SELECTION

Most of the researchers use mono-, di-saccharides and fatty acids as carbon sources for

bacteria and to perform biokinetics tests to obtain the kinetic rate constants. There is a remarkable weak point associated with using these substrates to simulate real wastewater processes. Since these chemicals are easily consumed by bacteria, a very high concentration has to be employed in the test to avoid too quick degradation to obtain the necessary data for the kinetic parameters. Unfortunately, very high concentrations of limited kinds of substrates will differ by far from real situations and the obtained kinetic mechanisms, therefore, cannot explain the processes properly. Hence, a vegetable protein (commercial product) was selected as feed because it is a multiple component substrate and gives a proper degradation rate in the batch test at a moderate initial concentration.

Table 3-4 lists the components of the protein product provided by the manufacturer. The COD/protein (w/w) ratio was about 1.3. The COD concentration of the vegetable protein feed drops at a moderate rate over 3 to 5 h at an initial concentration of 500 mg/L in a batch test. In contrast, in a batch test of feed mainly containing sugar and beer syrup with yeast, COD decreased so quickly that an initial concentration of 1000 mg/L could drop to near zero in less than ten minutes. This could give a large error in the test to estimate kinetic parameters.

Proteins are poly-molecular substances and not that easily biodegraded. When making feed, a basic hydrolysis method was used in which base was added while heating the protein solution to the boiling point for about half an hour. This procedure can hydrolyze some proteins into amino acids and even smaller molecular substances that could be kinds of easily biodegradable substrate.

Table 3-4 The Components* of the Vegetable Protein
(Product of WEIDER HEALTH PRODUCTS)

Total	**20 g**
Protein	18 g
Glutamic acid	3405 mg
Aspartic acid	2059 mg
Leucine	1470 mg
Arginine	1347 mg
Lysine	1128 mg
Serine	932 mg
Phenylalanine	929 mg
Proline	919 mg
Valine	901 mg
Isoleucine	878 mg
Alanine	768 mg
Glycine	745 mg
Tyrosine	683 mg
Threonine	682 mg
Histidine	465 mg
Methionine	239 mg
Cystine	233 mg
Tryptophan	233 mg
Fat	0.2 g
Carbohydrate	0 g

* as given on the package label

The bacteria can use protein as its carbon source although the protein contains much organic nitrogen. This feed also offers enough phosphorus for bacteria growth. The experimental results have proved that the feed benefited the test procedure and the modelling.

Because of time and other condition limits, the project only concentrated on the modelling of carbonaceous substrate removal in an SBR activated sludge system.

3.4. Batch Test for the Estimation of Stoichiometric and Kinetic Coefficients

The approaches for measuring the stoichiometry and kinetics coefficients will be presented with the SBR model description in Chapter 5.

3.5. Analysis methods

The analytical methods include the methods for COD, total amino acid, carbohydrates, pH, DO, TSS, VSS, sludge settled volume and SVI. All these methods are described in Appendix A or in related references.

PART I DYNAMIC MODELLING OF AN SBR SYSTEM

CHAPTER 4 A NEW MODEL FOR SEQUENCING BATCH REACTOR SYSTEM

4.1. SUBSTRATE CLASSIFICATIONS IN THE NEW MODEL

The analysis of earlier SBR models shows that a unified substrate cannot describe the carbonaceous energy dynamics properly. Conversely, the very detailed classification of substrate in the IAWPRC model results in such a complicated model that it is very difficult to estimate the important parameters. If there is a middle point to classify the substrate in basic categories that can explain the carbonaceous energy removal process properly but the parameters of the model can be easily determined, this is an alternative for the modelling of activated sludge process and especially important for the SBR system.

In the case of carbonaceous substrate removal, treating biomass with particulate volatile organic matter originating from the influent as one phase, i.e., VSS, can simplify the modelling without loss of accuracy for model simulation.

Substrate classification in the new model is based on the following definitions. The organic matter that contributes to COD in a wastewater can be divided into soluble and insoluble or particulate fractions:

$$S_T = S_s + S_p \qquad (4\text{-}1)$$

where

S_T = total COD (mg/L);

S_s = soluble COD (mg/L);

S_p = particulate COD (mg/L).

All the organic materials including molecular and colloidal organic substances that can be separated from particulate by physical separation processes (for example filtration and high G centrifugation) are thought of as soluble organics and those that are rejected by the processes are insoluble or particulate organics. This principle is reasonable considering the real situation of wastewater treatment since particulate organic materials can be removed by sludge entrapment and settling in secondary clarifier but the soluble portion can only be removed by biological oxidation and other types of physical-chemical processes.

The soluble portion is subdivided again into three categories based on biodegradability as shown below:

$$S_S = S_1 + S_2 + S_3 \qquad (4\text{-}2)$$

where

S_1 = soluble easy-to-biodegrade substrate (EBS) (mg COD/L);

S_2 = soluble difficult-to-biodegrade substrate (DBS) (mg COD /L);

S_3 = soluble inert organic materials (IOM) (mg COD /L).

Particulate COD in the influent, S_p, is assumed to be removed instantaneously by sludge entrapment and become part of VSS. The pathway of its degradation is parallel with sludge decay. As in sludge aerobic digestion, some particulate COD is decomposed to

CO_2 and H_2O providing energy to bacteria, and some degrades and serves for cell synthesis, while the remainder, mainly biologically inert components, is discharged with excess sludge. Probably the true rate of degradation of this substrate is different from that of biomass decay. However, it is only a small part of total VSS and when measuring decay rate, k_e, and yield, Y, the VSS contains these particulate materials. The VSS change during a test period is an overall mass change including the particulate decomposition. Thus, the decay rate constant k_e includes the contribution from this amount of particulate materials. By employing such an approach, the model can be simplified without loss of accuracy.

EBS COD is equivalent to readily biodegradable substrate in the IAWPRC Model No. 1 and can directly be used by biomass for synthesis. On the other hand, the new SBR model rejects the IAWPRC Model No. 1 approach that the slowly degradable COD is insoluble and adsorbed instantaneously as soon as it contacts the sludge and is then hydrolyzed into readily biodegradable material. Instead, the new model considers its real characteristic as soluble, but degraded at a lower rate than EBS COD. In the IAWPRC Model No. 1, colloidal organic materials are thought of as particulate and adsorbed to the cell particle surface. Then they are hydrolyzed to readily biodegradable COD and released to the bulk liquid by the action of extracellular enzymes secreted by the biomass. There are some questions about this approach. First, the adsorption rates for particulates and colloids should not be the same or necessarily close. Particulates and colloids with positive charges are very easily adsorbed by activated sludge that has negative charges on its particle surface (Metcalf and Eddy, 1991). Thus, these two can be thought of as adsorbed

instantaneously as they contact with sludge. Colloids with neutral and negative charges are not easily adsorbed; therefore, the approach of the IAWPRC Model No. 1 will cause large errors by employing one equation to describe the hydrolysis of particulate COD including true particulates that can be separated by physical processes and colloids that can only be separated by physical-chemical or chemical processes (Weber, 1972). Second, it is not clear that the portion of hydrolyzed COD released to the bulk liquid is readily biodegradable substrate. The hypothesis that all the particulate COD can finally add to readily biodegradable substrate (Henze et al., 1986) lacks experimental validation. The new SBR model considers DBS COD as soluble and removed at a lower rate, which can avoid the weakness of the approach in the IAWPRC Model No. 1.

Following the above subdivision rule, the effluent soluble COD can also be divided into the three portions below:

$$S_e = S_{1e} + S_{2e} + S_{3e} \qquad (4\text{-}3)$$

S_{1e} in the effluent should approximately equal zero in a well operated activated sludge process.

This model adopts the death-regeneration concept of the Task Group Model No. 1. When activated sludge degrades aerobically, the products can be classified as follows:

Decomposition of X_v = Soluble portion S_s + Non-volatile particulate portion P_{nv}

But the soluble part is the only consideration in this transformation because it affects the soluble COD. Generally, the released soluble S_s consists of three components as those in

the influent although the percentage of each component could be different. The released non-volatile particulate matter is still incorporated into the sludge and discharged by wasting sludge, which is also a difference from the IAWPRC Model No. 1. The classification of substrate and the new model mechanisms are summarized and illustrated by Fig. 4-1.

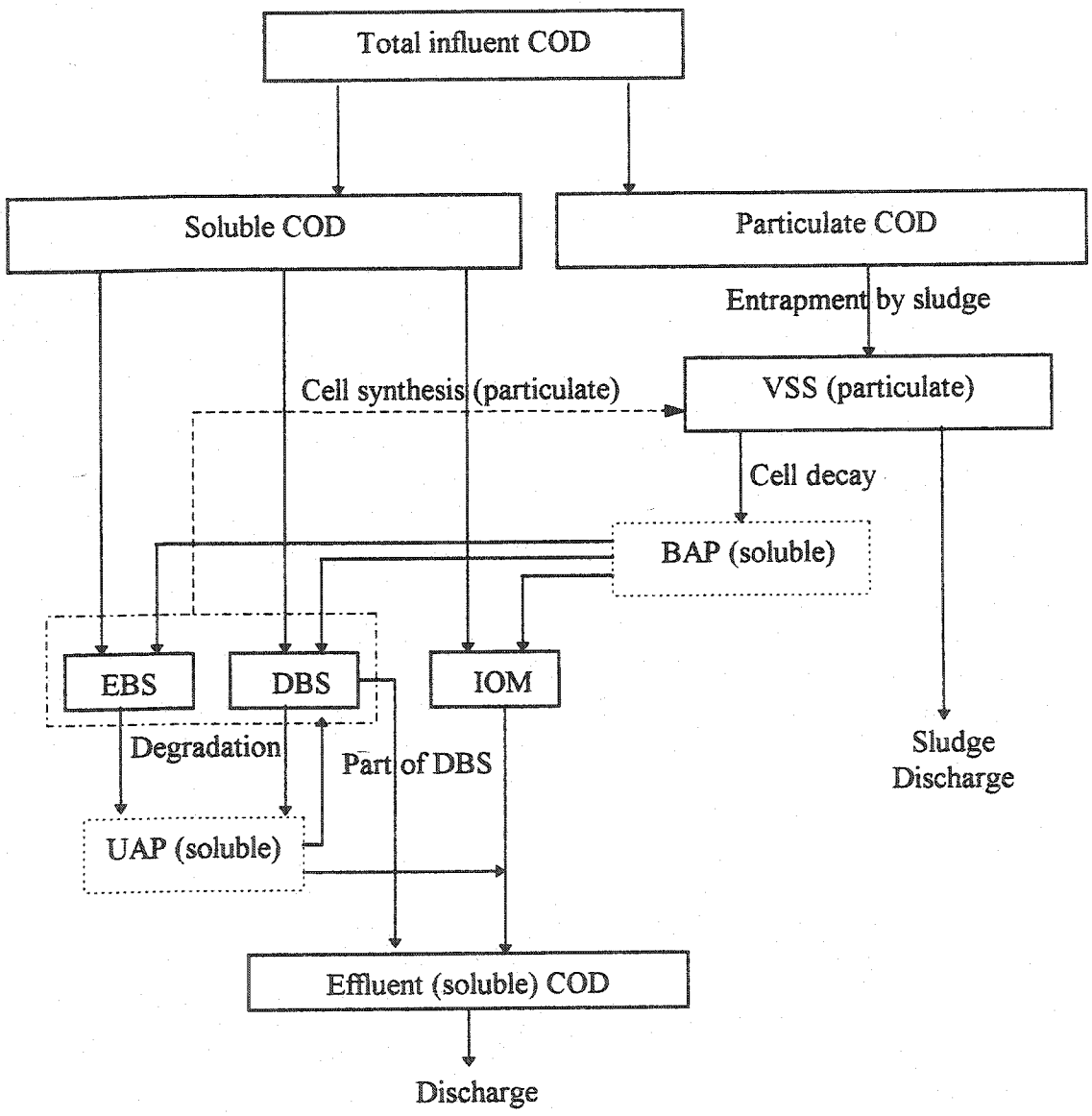


Figure 4-1. Substrate classification and the new SBR model mechanisms

4.2. THE DEVELOPMENT OF THE NEW DYNAMIC MODEL FOR SBR SYSTEM

4.2.1. Assumptions for the New Model

Before the development of the new dynamic model for SBR system, some assumptions must be made.

1. Each SBR reactor is CM in the fill and reaction periods and the substrate and biomass are evenly distributed throughout the reactor during these two stages.
2. The activity of microorganisms only occurs during aeration periods, i.e., in the fill and react stages. Their activity stops when aeration is terminated. No activity occurs during settle and withdraw periods. This assumption will be discussed in more detail in Section 5.4.6.
3. Sequencing degradation of different substrates is valid and depends on their biodegradability, i.e., the most easily biodegradable substrate will be degraded first by bacteria.
4. The particulate substrate will be entrapped by activated sludge and removed at once as it contacts with activated sludge to become part of VSS.
5. The temperature effect on the kinetic process can be neglected over the relatively constant room temperature range.

4.2.2. The Development of the New SBR Model

In the new SBR model, three differential equations are used to describe the degradation or change of the three categories of substrate, and one differential equation is used to describe the change of biomass in the system. The widely accepted Monod expression for substrate removal rate is adopted here.

The rate for EBS is

$$r_{s_1} = -\frac{k_1 S_1 X_v}{K_{S_1} + S_1} \qquad (4\text{-}4)$$

where

k_1 = specific removal rate for EBS (d^{-1});

S_1 = EBS concentration (mg COD/L);

X_v = VSS concentration (mg/L);

K_{S_1} = half-velocity constant for EBS degradation (mg/L).

The rate for DBS is

$$r_{s_2} = -\frac{k_2 S_2 X_v}{K_{S_2} + S_2} \qquad (4\text{-}5)$$

where

k_2 = specific removal rate for DBS (d^{-1});

S_2 = DBS concentration (mg COD/L);

K_{S_2} = half-velocity constant for DBS degradation (mg/L).

The biomass growth rate is

$$r_{X_v} = Y\left(\frac{k_1 S_1 X_v}{K_{S_1} + S_1} + \frac{k_2 S_2 X_v}{K_{S_2} + S_2}\right) \quad (4\text{-}6)$$

where Y = biomass yield factor (mg/mg).

The first-order reaction will be applied to biomass aerobic decay, i.e.

$$r_{X_{vd}} = -k_e X_v \quad (4\text{-}7)$$

where k_e = biomass decay rate constant (d^{-1}).

As discussed in the Section 2.5.3 that the majority of the effluent soluble COD from a biological process is not from influent but from microbial metabolism and from bacteria decomposition. Based on this, the new SBR model contains expressions for SMP that come from two sources: substrate utilization and biomass decay. These are defined as UAP and BAP, respectively by Namkung and Rittmann (1986). The two researchers also found that the rate of UAP formation was proportional to the substrate removal rate and the formation rate of BAP was proportional to the concentration of biomass. The new SBR model adopts these expressions to describe these two portions of COD. The advancement here is that SMP also consists of EBS, DBS and IOM. Their formation rates are:

$$r_{XS_1} = f_{X_1} \gamma_X k_e X_v \quad (4\text{-}8)$$

for EBS formation of BAP;

$$r_{XS_2} = f_{X_2} \gamma_X k_e X_v \quad (4\text{-}9)$$

for DBS formation of BAP;

$$r_{XS_3} = f_{X_3}\gamma_X k_e X_V \qquad (4\text{-}10)$$

for IOM formation of BAP;

$$r_{UAP} = \gamma_S[(-r_{S_1})+(-r_{S_2})] = \gamma_S\left(\frac{k_1 S_1 X_V}{K_{S_1}+S_1}+\frac{k_2 S_2 X_V}{K_{S_2}+S_2}\right) \qquad (4\text{-}11)$$

for the IOM portion of UAP; where

γ_s = the coefficient for the formation of IOM portion of UAP (dimensionless), also a function of sludge age, i.e., $\gamma_s = f(\theta_X)$;

γ_x = the conversion coefficient of decayed VSS to soluble COD (dimensionless), also a function of sludge age, i.e., $\gamma_x = g(\theta_X)$;

f_{X_1}, f_{X_2} and f_{X_3} = fractions of EBS, DBS and IOM of BAP (%), respectively.

There is no specific rate expression for the formation of EBS and DBS portions of UAP because these rates are involved in and slow the degradation rates of EBS and DBS.

From entire mass balances within a SBR system, a group of differential equations for change of EBS, DBS, IOM and VSS, or, X_v will be derived.

During fill with a constant flow rate Q:

(1) For EBS or S_1

$$QS_0 f_1 + r_{S_1} V + r_{XS_1} V = \frac{d(VS_1)}{dt}, \text{ then}$$

$$\frac{d(VS_1)}{dt} = S_1\frac{dV}{dt} + V\frac{dS_1}{dt} = QS_1 + V\frac{dS_1}{dt}$$

where $V = V_i + Qt$ during fill and $V = V_b$, constant after fill; and $dV/dt = Q$. S_0 is the total soluble COD concentration of the influent and f_1 the fraction of EBS in the influent.

Rearranging this equation yields:

$$\frac{dS_1}{dt} = \frac{Q}{V}(S_0 f_1 - S_1) + r_{s_1} + r_{xs_1}$$

Substituting rate expressions Eqs. (4-4) and (4-8) in the above leads to:

$$\frac{dS_1}{dt} = \frac{Q}{V}(S_0 f_1 - S_1) - \frac{k_1 X_v S_1}{K_{S_1} + S_1} + f_{x_1}\gamma_x k_e X_v \qquad (4\text{-}12)$$

(2) For DBS or S_2:

$$QS_0 f_2 + r_{s_2} V\left(\frac{K_0}{K_0 + S_1}\right) + r_{xs_2} V = \frac{d(VS_2)}{dt}$$

where f_2 is the fraction of DBS in the influent; $K_0/(K_0+S_1)$ is a switching function because DBS degradation depends on the concentration of EBS. K_0 is a constant which, after careful selection, makes the switching function close to unity when S_1 is very low and near zero when S_1 is high. Microorganisms will attack the most readily degradable substrate first as observed by Monod (1949). Gaudy (1963) indicated that DBS will not be degraded when EBS exists. The "switch" function incorporates this phenomenon into the model by reducing the DBS degradation rate to insignificant values when the EBS concentration is high.

Rearranging the above equation results in:

$$\frac{dS_2}{dt} = \frac{Q}{V}(S_0 f_2 - S_2) + r_{s_2}\left(\frac{K_0}{K_0 + S_1}\right) + r_{xs_2}$$

Using Eqs. (4-5) and (4-9) to replace the rate expressions yields:

$$\frac{dS_2}{dt} = \frac{Q}{V}(S_0 f_2 - S_2) - \left(\frac{k_2 X_v S_2}{K_{S_2} + S_2}\right)\left(\frac{K_0}{K_0 + S_1}\right) + f_{x_2}\gamma_x k_e X_v \qquad (4\text{-}13)$$

(3) For IOM or S_3

$$QS_0 f_3 + r_{s_3} V + r_{xs_3} V = \frac{d(VS_3)}{dt}$$

Rearranging this equation yields:

$$\frac{dS_3}{dt} = \frac{Q}{V}(S_0 f_3 - S_3) + r_{s_3} + r_{xs_3}$$

Replacing rate expressions in the equation with Eqs. (4-10) and (4-11) results in:

$$\frac{dS_3}{dt} = \frac{Q}{V}(S_0 f_3 - S_3) + \gamma_s\left(\frac{k_1 X_v S_1}{K_{s_1} + S_1} + \frac{k_2 X_v S_2}{K_{S_2} + S_2}\frac{K_0}{K_0 + S_1}\right) + f_{x_3}\,\gamma_x k_e X_v$$

where f_3 is the fraction of IOM in the influent. After computer simulation, the switch function was removed from the above equation because it had an insignificant effect on the final model results. Therefore, the above equation becomes:

$$\frac{dS_3}{dt} = \frac{Q}{V}(S_0 f_3 - S_3) + \gamma_s\left(\frac{k_1 X_v S_1}{K_{s_1} + S_1} + \frac{k_2 X_v S_2}{K_{S_2} + S_2}\right) + f_{x_3}\gamma_x k_e X_v \qquad (4\text{-}14)$$

(4) For VSS, X_v:

$$QX_{v0} + r_{X_v} V + r_{X_{vd}} V = \frac{d(VX_v)}{dt}$$

After rearrangingthe equation, it becomes:

$$\frac{dX_v}{dt} = \frac{Q}{V}\left(X_{v0} - X_v\right) + r_{X_v} + r_{X_{vd}}$$

Substituting Eqs. (4-6) and (4-7) into it yields:

$$\frac{dX_v}{dt} = \frac{Q}{V}\left(X_{v0} - X_v\right) + Y\left(\frac{k_1 X_v S_1}{K_{S_1} + S_1} + \frac{k_2 X_v S_2}{K_{S_2} + S_2}\frac{K_0}{K_0 + S_1}\right) - k_e X_v \qquad (4\text{-}15)$$

(5) For effluent S_e, Eq. (4-3) is the correct expression

$$S_e = S_{1e} + S_{2e} + S_{3e}$$

where S_{1e}, S_{2e} and S_{3e} are the effluent concentrations of S_1, S_2 and S_3, respectively. In the normal operation, $S_{1e} \approx 0$. Other definitions in the new model are the same as those in the earlier models.

After the fill period, Q = 0, then the first term in each equation equals zero. The equations become the expressions for batch reactor kinetics.

4.2.3. The Boundary Conditions of the New SBR Model

By assuming an overall steady state around the system and drawing excess activated sludge at the end of each cycle based on the designed sludge age, i.e., both the total VSS mass and the effluent quality in the system approach constant levels. The boundary conditions for these equations are:

when t = 0, after settle, $t = t_f + t_r + t_s$ and after draw, $t = t_f + t_r + t_s + t_w$,

$V(0) = V_i$;

$S_1(0) = S_1(t_f + t_r + t_s) = S_1(t_f + t_r + t_s + t_w) = S_{1e} \approx 0$;

$S_2(0) = S_2(t_f + t_r + t_s) = S_2(t_f + t_r + t_s + t_w) = S_{2e}$;

$S_3(0) = S_3(t_f + t_r + t_s) = S_3(t_f + t_r + t_s + t_w) = S_{3e}$;

$X(0) = X(t_f + t_r + t_s) = X_v/\alpha$;

where $\alpha = V_i/V_b$.

When $t = t_f$,

$V(t_f) = V_b$;

$X(t_f) = X_v$.

4.3. A NEW MODEL FOR CFSTR ACTIVATED SLUDGE SYSTEM

Based on a mass balance, a new steady state model for a CFSTR system can also be derived by using the same definitions as in the SBR system:

(1) For EBS or S_1:

$$QS_0f_1 - QS_1 - \frac{k_1X_vS_1}{K_s + S_1}V + f_{x_1}\gamma_x k_e X_v V = \frac{d(VS_1)}{dt} = 0 \qquad (4\text{-}16)$$

(2) For DBS or S_2:

$$QS_0f_2 - QS_2 - V\left(\frac{k_2X_vS_2}{K_{S_2}+S_2}\right)\left(\frac{K_0}{K_0+S_1}\right)+f_{x_2}\gamma_x k_e X_v V = \frac{d(VS_2)}{dt} = 0 \qquad (4\text{-}17)$$

(3) For IOM or S_3

$$QS_0f_3 - QS_3 + \gamma_{s_3}\left(\frac{k_1X_vS_1}{K_{S_1}+S_1}+\frac{k_2X_vS_2}{K_{S_2}+S_2}\right)V + f_{x_3}\gamma_x k_e X_v V = \frac{d(VS_3)}{dt} = 0 \qquad (4\text{-}18)$$

(4) For VSS or X_V:

$$QX_{v0} - QX_v + Y\left(\frac{k_1X_vS_1}{K_{S_1}+S_1}+\frac{k_2X_vS_2}{K_{S_2}+S_2}\frac{K_0}{K_0+S_1}\right)V - k_eX_vV = \frac{d(VX_v)}{dt} = 0 \qquad (4\text{-}19)$$

These two models can be used to predict the operations of SBR and CFSTR and to compare the two systems under equivalent operational conditions.

CHAPTER 5 ESTIMATION OF PARAMETERS IN THE NEW SBR MODEL

Many researchers have used batch biological reactors for multiple purposes. Moser (1977) reported that in a BR or in the forward zone of a PFR, the readily biodegradable compounds will be eliminated first after a short reaction time, while poorly degradable compounds will be eliminated last, i.e., towards the end of the reaction time in a BR or in the end zone of a PFR. This suggested that it is possible to differentiate EBS and DBS by a batch test. Another advantage of a biological BR test is that it can be used to determine biokinetic parameters and is easy to operate, saving time and expense compared to other methods. Braha and Hafner (1987) used lab scale BRs to model biokinetics of a CFS activated sludge process although they found biomass needs to quickly adapt in the batch test. If the biomass is previously acclimated in a BR, then moved to the testing reactor, it is already adapted.

Based on the above information, a set of batch biological reactor testing techniques were developed to differentiate the various types of COD produced and transformed during the treatment cycle.

5.1 PRINCIPLE, ASSUMPTIONS AND PROCEDURE OF BATCH REACTOR TEST

5.1.1. Principle

There are two basic relationships in a biological batch test. One is substrate COD degradation vs time and the other is substrate COD degradation rates vs corresponding COD concentrations, S, i.e., $dS/dt = f(S)$.

From $dS/dt = f(S)$, the different COD categories can be defined due to their different dS/dt rates at different S concentrations. EBS degradation will have the highest rate. The rate for DBS will be lower than that of EBS while IOM degrades with a rate near zero.

At any moment after starting a BR test, soluble COD comes from two sources: (a) feed and (b) decomposed VSS or BAP. Decomposed VSS is transformed into smaller molecular organic substances first, then further degrades to inorganic materials or is utilized by other portion of biomass for cell synthesis. The part of decomposed VSS that disappears within the reaction period is degradable BAP (BAP_d) which also includes EBS and DBS. Some BAP compounds cannot be degraded further and stays in the clarified effluent leaving the reactor. These are non-degradable BAP (BAP_{nd}) and belong to IOM. These relationships can be described by three basic equations:

$$S_t = S_s + BAP_t = S_1 + S_2 + S_3 + BAP_T \quad (5\text{-}1)$$

$$BAP_T = BAP_d + BAP_{nd}; \quad (5\text{-}2)$$

$$\Delta COD_p = \Delta BAP_T = \Delta BAP_d + \Delta BAP_{nd} \quad (5\text{-}3)$$

where

S_t = total soluble COD;

BAP_t = total BAP;

ΔCOD_p = decomposed VSS (particulate) COD.

In a fed reactor, degradation rate of substrate COD should include rates for both feed and BAP_d. However, generated BAP is mixed with fed COD. Degradation of BAP_d takes place concurrently with fed substrate and is "hidden" in the measured soluble ΔCOD. Thus, direct measurement of BAP_d degradation is not possible. This problem can be solved by employing a parallel blank BR in which the same amount of washed sludge as in a fed reactor is held. BAP in the blank is negligible at the beginning of the test. Total COD (COD_T) change through an entire test cycle in a blank BR, which mainly includes COD_p, can be used to calculate the generation of BAP. Degradation of COD_T in the blank BR indicates the degradation of BAP_d because released BAP_{nd} with remaining COD_p is still included in the measured COD_T. Therefore, it is reasonable to assume that the soluble COD accumulated is BAP_{nd}. BAP_{nd} can be obtained by measuring the soluble COD change in the blank BR.

The following is a procedure to estimate the true biodegradable amount of COD during a test cycle based on the above basic equations:

At t = 0 in the fed reactor, measured soluble COD = S_0. At the same time in the blank reactor, $BAP_{d,0} = 0$, $BAP_{nd,0} \approx 0$ also and total COD = $COD_{T,0}$. At any moment t in the fed reactor, measured soluble COD is S_t. At the same time in the blank reactor, $BAP_{nd,t}$

and $COD_{T,t}$ can be measured. Thus, BAP_d in the blank at any time t can be obtained by the following equations:

$$BAP_{d,t} = COD_{T,0} - COD_{T,t}$$

and

$$BAP_{T,t} = BAP_{d,t} + BAP_{nd,t} = COD_{T,0} - COD_{T,t} + BAP_{nd,t} \quad (5\text{-}4)$$

Considering BAP_d, actual soluble COD concentration, S' for the calculation of fed COD degradation rate at this moment should be

$$S' = S_t - BAP_{d,t} = S_t - (COD_{T,0} - COD_{T,t}) \quad (5\text{-}5)$$

S_t is directly measured from fed reactors while $COD_{T,0} - COD_{T,t}$ is measured from a blank reactor initially containing the same amount of washed sludge as that of a fed reactor. Now the corrected rate, dS'/dt, may be used to describe degradation rate in the fed reactor. The points on the dS'/dt curves are determined by the following calculation:

$$\frac{dS'}{dt} \approx \frac{\Delta S'}{\Delta t} = \frac{S'_{t+1} - S'_t}{\Delta t} \quad (5\text{-}6)$$

where S'_t and S'_{t+1} are the corrected COD concentrations at times t and t + 1, respectively, and calculated according to Eq. (5-5).

The corresponding S value is the average of measured COD from time t to t + 1

$$\bar{S} = \frac{S_{t+1} + S_t}{2} \quad (5\text{-}7)$$

Both fed COD and BAP degrade at the measured COD concentration and their related

rate constants estimation should be made at these corresponding COD values.

Based on the $\frac{dS'}{dt} = f(S)$ curve, the reaction types throughout the entire degradation process can be judged and defined. With proper procedures, the rate constants can also be measured and calculated.

The values of f_{x1}, f_{x2} and f_{x3} may also be estimated from the above data. To do this, BAP_d and BAP_T at any time period of t to t + 1, defined as $BAP_{d,\ t/t+1}$ and $BAP_{T,\ t/t+1}$, are calculated first:

$$BAP_{T,\ t/t+1} = COD_{T,\ t} - COD_{T,\ t+1} \qquad (5\text{-}8)$$

$$BAP_{d,\ t/t+1} = (COD_{T,\ t} - COD_{T,\ t+1}) - (COD_{s,\ t+1} - COD_{s,\ t}) \qquad (5\text{-}9)$$

Then the ratios of $BAP_{d,\ t/t+1}$ /$BAP_{T,\ t/t+1}$ for any period of t to t+1 can be obtained. The estimations of f_{x1}, f_{x2} and f_{x3} will be introduced in Section 5.2.2.

5.1.2. Test Conditions

To simplify analysis, the sludge produced during a test cycle is ignored (it is very small) compared to the original bulk quantity and the total amount of activated sludge in the reactor is treated as a constant. This assumption can be realized by using the average activated sludge concentration throughout the testing period.

Primary conditions

The activated sludge used in the BR test should have a sludge age of at least 10 d which has more stable composition than younger sludge. The sludge should also be taken from

an activated sludge reactor that has been operating for at least two sludge ages (Henze et al., 1986). The F/M ratio should be 0.3 to 0.6 mg COD/mg VSS, which is a common range in activated sludge processes for the measurement.

Apparatus

For the measurement of biological kinetic and stoichiometric parameters, a set of batch tests was conducted with four 2L beakers with an aeration stone in each beaker.

Evaporation losses due to aeration were restored before sampling for analyses. The volume reduction to be restored was measured by aerating the same initial volume of distilled water in the beaker for 24 h.

Test procedure

Step 1: Settle the total 6000 mL volume of mixed liquor taken from aeration tank of an SBR or a CFSTR and decant the supernatant. Wash the settled sludge with distilled water to remove soluble COD. Repeat the washing step at least 3 times. Then divide the washed sludge into four equal portions, and dilute each one to 1500 mL with distilled water. Finally put them into four 2000 mL beakers, respectively.

Step 2: Add three different quantities of concentrated feed to three of the four washed sludge samples. Ensure that the added feed volume is negligible compared to the 1500 mL of the mixed sludge. The beaker without feed addition is the blank sample.

Step 3: Aerate the samples and test the soluble COD of clarified water at time intervals of 0, 0.05, 0.1, 0.2, 0.3, 0.5, 1, 2, 3.5, 5, 7, 12 and 24 h for the three fed samples and at time

intervals of 0, 3.5, 7, 12 and 24 h for the blank sample to obtain S-time curves.

Step 4: Measure COD_T of the blank at time intervals of 0, 3.5, 7, 12 and 24 h and draw the COD_T-time and $dCOD_T/dt$ curves to determine the reaction type of biomass degradation and the released BAP_{nd} and BAP_d.

Step 5: Subtract BAP_d from the three S-time curves for fed samples to correct them for COD released from sludge decay to obtain the adjusted COD degradation, S′, values.

Step 6: Plot three dS′/dt-S curves from the three sets of adjusted S′ values to determine the ranges for different COD categories and the type of their degradation.

Step 7: The rate constant, k_1, and half-velocity constant, K_{S_1}, for EBS degradation were estimated with the Lineweaver-Burke method applied to the initial COD change in each of the three samples that were fed a different amount of COD. At the beginning bacteria always utilize EBS and there is a large amount at this time (Grau et al., 1975; Moser, 1977; Ekama et al., 1986).

Figure 5-1 provides a flow chart as a summary of procedures for the new SBR model parameter estimation with batch test techniques.

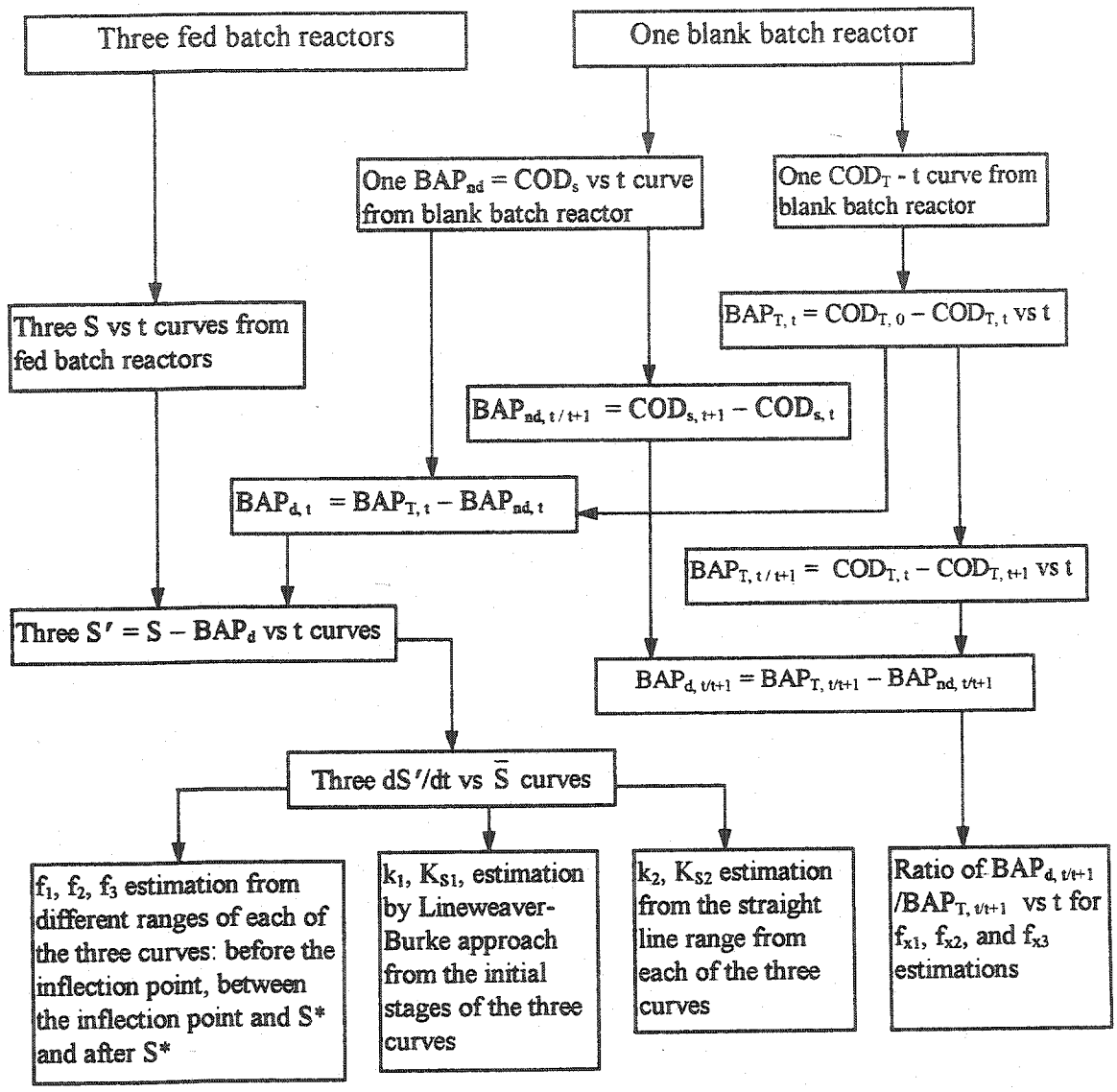


Figure 5-1. A flow chart for experimental estimations of the new SBR model parameters

5.2 QUANTITATIVE TEST OF INFLUENT COD FRACTIONS

5.2.1. Measurement of f_1, f_2 and f_3

Typical remaining soluble COD vs time curves with three different initial soluble COD concentrations are shown in Figure 5-2a (and 5-2b which shows the same figure with a y-

axis range of 0-100 mg/L and provides a detailed look at the ascending trend of the curves after 5 h areation).

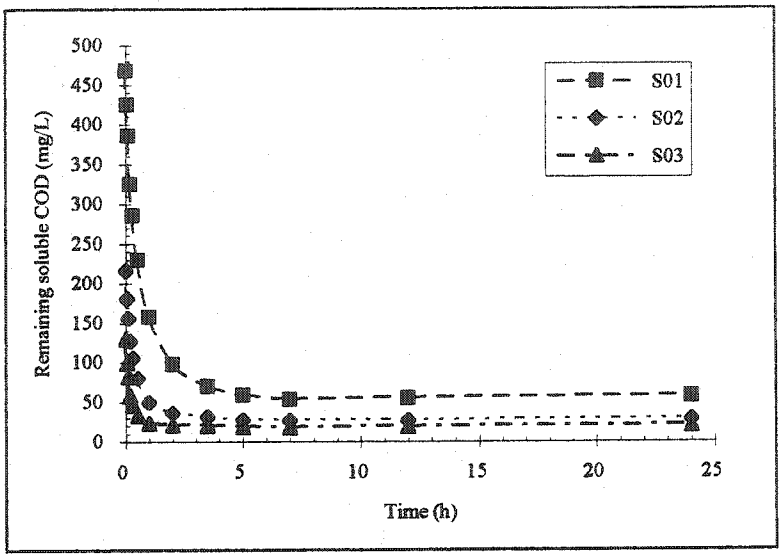


Figure 5-2a. Soluble COD degradation curves from a batch test with three different initial concentrations (sludge from run No. 8-500 for an SBR system and θ_{xob} = 15 d).

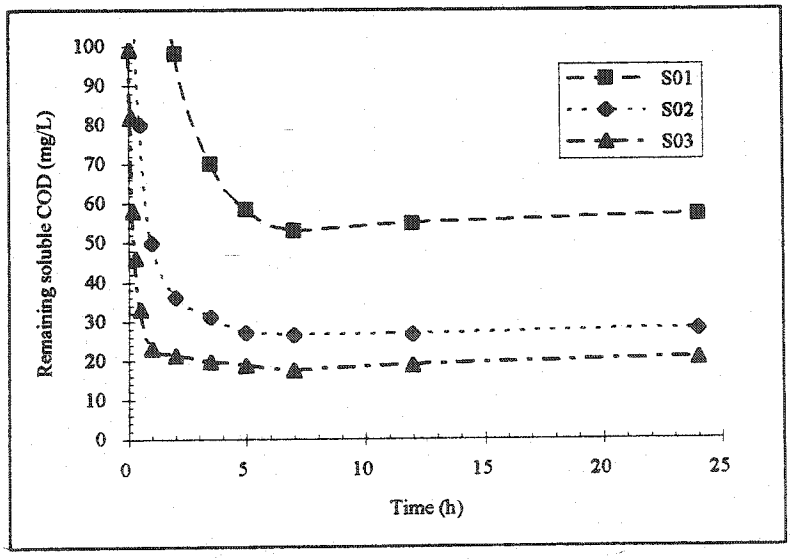


Figure 5-2b. Soluble COD degradation curves from a batch test with three different initial concentrations (the same Fig. as 5-2a with a y-axis range of 0 - 100 mg/L).

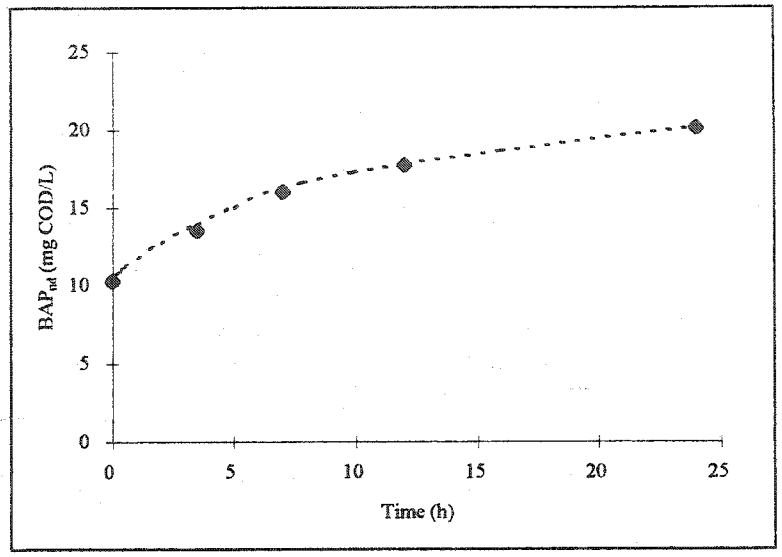


Figure 5-3. BAP$_{nd}$ - time curve from the blank BR test

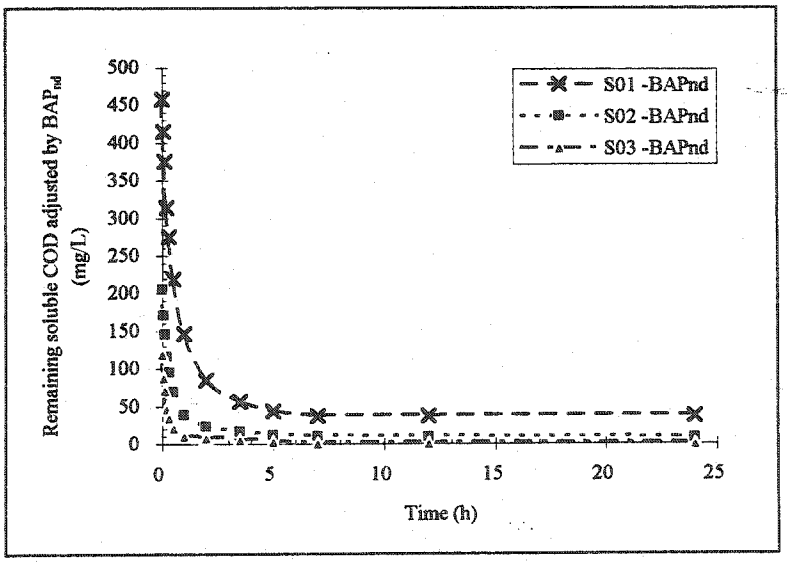


Figure 5-4. Remaining soluble COD- time curves adjusted by BAP$_{nd}$

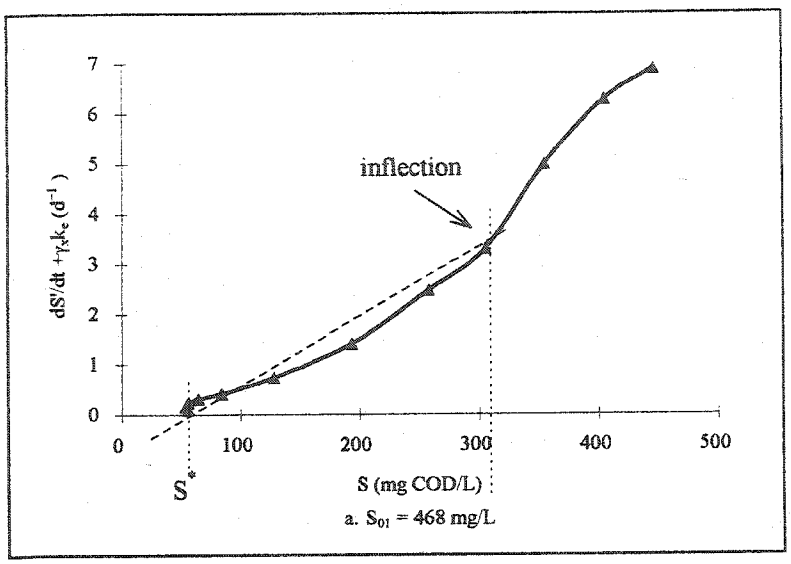


Figure 5-5a. dS′/dt-S curve from a batch test with S_{01} = 468 mg/L

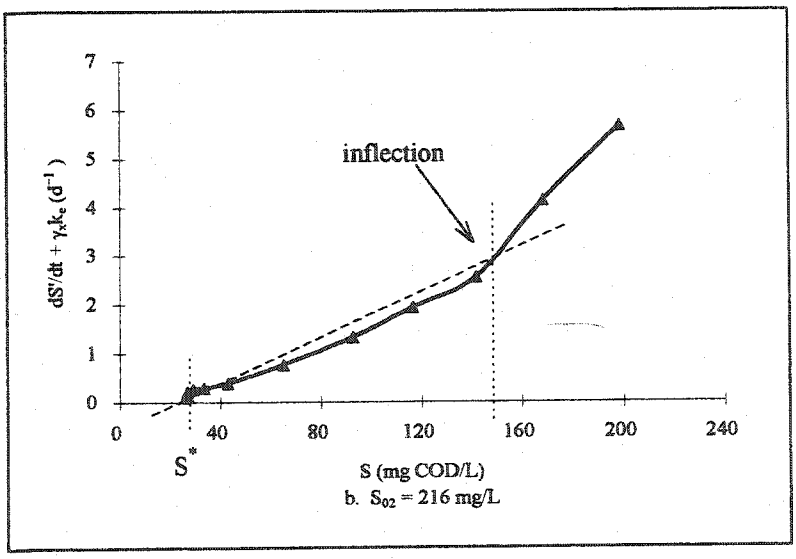


Figure 5-5b. dS′/dt-S curve from a batch test with S_{02} = 216 mg/L

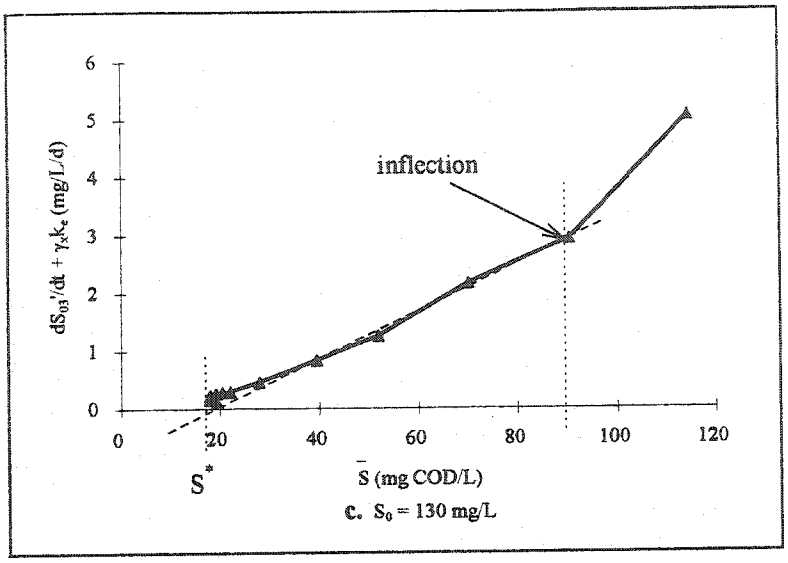


Figure 5-5c. dS′/dt-S curve from a BR test with S_{03} = 130 mg/L

Figure 5-3 is the BAP_{nd}-time curve. Fig. 5-4 is the S-time curves adjusted by subtracting BAP_{nd}, which shows that the measured COD degradation curves are affected by BAP_{nd}. The latter added to the former made them higher than their "true" values. This phenomenon becomes obvious when the remaining COD is lower. The BAP_{nd} can cause COD curves to ascend after 5 h reaction (Fig. 5-2b).

Figures 5-5a, 5-5b and 5-5c are dS′/dt-S curves with different initial COD concentrations. An adjustment for the COD concentration, S, has been made by subtracting BAP_d to obtain true substrate removal rate which includes fed COD removal and decomposed VSS degradation. The other sets of curves are in Appendix B.

From the dS′/dt-S curves in Figs. 5-5a to 5-5c, it can be seen that the substrate removal rate dS′/dt has a quick drop (dS′/dt curve has a larger slope) at the beginning that lasted only a few minutes for lower initial substrate concentration or about ten min for the higher

initial concentrations. The rapid drop of COD concentration is EBS metabolism. In the IAWPRC Model No. 1, researchers (Ekama et al., 1986) have proven that there is a sharp drop in OUR after feeding is terminated when testing readily biodegradable substrate with a daily cyclic square wave feeding pattern.

After the quick drop of dS'/dt, a linear trend of the dS'/dt curve occurs with a smaller slope that shows a slower degradation of substrate at this stage with a constant rate change or a first-order style reaction. This group of substrates is much different from EBS, comprising a mixture of colloidal and soluble organic materials of complex organic structure, and degrades at a slower rate than EBS. Many researchers (Lawrence and McCarty, 1970; Dold et al., 1980; Dold and Marais, 1986; and Henze et al., 1986) found that a first-order reaction can properly describe the degradation of DBS.

Ekama and Marais (1979) treated DBS of domestic waste as particulate COD and proposed a first-order reaction to describe the COD utilization based on the work of Morris and Stumm (1960), Ford and Eckenfelder (1967) and Wilson and Marais (1976) who found that 60 to 70% of the COD in domestic wastewater is in a fine particulate form. Dold et al. (1980) adopted the approach to develop a general model for the activated sludge process. In their model, they hypothesized that DBS is adsorbed by activated sludge and then hydrolyzed into readily biodegradable substrate. The limiting rate is determined by the rate of the hydrolysis. They further hypothesized that there is no energy consumed and no COD degradation during hydrolysis and employed a modified adsorption mechanism (a first-order reaction) of particulate COD in domestic wastewater proposed by Blackwell (1971) to formulate the rate limiting process. This approach was

finally adopted into the IAWPRC Model No. 1 (Henze et al., 1986).

Approaching the end of the batch test, the S-time curves became horizontal and the dS′/dt curve is close to zero, which demonstrates that the leftover COD is biologically inert. There are three sources of this inert COD: influent, non-biodegradable UAP (UAP_{nd}) and BAP_{nd}. Grady and Lim (1980) stressed the importance of correcting the specific rate of substrate removal by subtracting this portion from the initial COD concentration, S_0 and from the effluent COD, S_e. However, they did not suggest correcting this by tracking and deducting the nondegradable BAP in the blank batch test from the entire dS′/dt-S curve.

After defining each range of the dS′/dt-S curve, the fractions of different types of substrates can be calculated. From the beginning to the point where the dS′/dt curve changes to a "straight" line, the COD change can be considered as EBS removal. Its percentage, f_1, is calculated by the corresponding COD change to the inflection point divided by the total added soluble COD, COD_s, that is:

$$f_1 = [(COD_{s,\,t=0} - BAP_{nd,\,0}) - (COD_{s,\,\text{at inflection}} - BAP_{nd\ \text{at corresponding}\ t})]/$$
$$(COD_{s,\,t=0} - BAP_{nd,\,0}) \qquad (5\text{-}10)$$

The straight line portion indicates the degradation of DBS COD and its portion, f_2, is computed by the corresponding COD drop divided by total soluble COD added:

$$f_2 = [(COD_{s,\,\text{at inflection}} - BAP_{nd,\,\text{at corresponding}\ t}) - (S^* - BAP_{nd,\,\text{at corresponding}\ t})]/$$
$$(COD_{s,\,t=0} - BAP_{nd,\,0}) \qquad (5\text{-}11)$$

The dS'/dt curve terminated at S^*, which indicates that DBS in solution at this moment is almost consumed and the remaining COD is IOM. Originally, the COD at the S* point contains three parts. The first is the inert soluble COD from feed, the second UAP_{nd} from the metabolism of both EBS and DBS and the third is BAP_{nd} from biomass decay. Because the curve has been corrected by deducting the BAP_{nd} accumulation curve, the S^* now contains only inert organic material from the influent and UAP_{nd}. But UAP_{nd} is proportional to the amount of degraded substrate which is proportional to the influent concentration, S_0, and therefore, UAP_{nd} is proportional to S_0 as well as to the fraction of IOM in the influent. At present, there is no simple technique to distinguish between IOM and UAP_{nd} in effluent from a biological wastewater treatment system accepting multi-substrate feed. For convenience and simplification of the estimation of the model parameters, one coefficient, f_3, is employed to describe this term.

f_3, the sum of inert fraction of the feed and UAP_{nd} is calculated by the following equation:

$$f_3 = (S^* - BAP_{nd,\ \text{at corresponding } t})/(COD_{s,\ t=0} - BAP_{nd,\ 0}) \qquad (5\text{-}12)$$

or simply by the equation:

$$f_3 = 1 - f_1 - f_2 \qquad (5\text{-}13)$$

Table 5-1 lists the results of the three different categories of COD in the feed and in the released COD from sludge decomposition from 13 sets of BR tests. The values of $f_{x1} + f_{x2}$ listed in the last column are discussed in the next section. (The series numbers, x - xxx - xx, in the second column: experiment set - S_0 - θ_{xob}).

Table 5 -1 The measured f_1, f_2 and f_3 values from thirteen sets of BR tests

Test No.	Sludge from	$\bar{X}_V$ mg/L	θ_{xob} d	S_0 mg/L	f_1 -	f_2 -	f_3 -	$f_{x1} + f_{x2}$ -
#1	8-500-5	1650	5	144	0.32	0.65	0.03	0.91
				110	0.35	0.6	0.05	
				65	0.35	0.65	0.01	
#2	8-500-15	3150	15	468	0.28	0.64	0.08	0.98
				216	0.31	0.69	0.04	
				130	0.24	0.74	0.02	
#3	7-500-15	2176	15	465	0.29	0.65	0.06	0.91
				220	0.33	0.65	0.03	
				115	0.36	0.63	0.02	
#4	3-500-10	2250	10	367	0.30	0.67	0.03	0.90
				184	0.35	0.61	0.04	
				93	0.37	0.6	0.03	
#5	6-250-15	3960	15	367	0.30	0.69	0.01	0.91
				184	0.33	0.63	0.03	
				93	0.34	0.64	0.02	
#6	2-250-10	1900	10	889	0.24	0.72	0.04	0.91
				445	0.29	0.68	0.03	
				221	0.32	0.68	0	
#7	2-250-15	3487	15	888	0.29	0.68	0.03	0.95
				443	0.32	0.32	0.04	
				220	0.32	0.68	0	
#8	5-500-10	3418	10	886	0.33	0.66	0.01	0.96
				665	0.30	0.69	0.01	
				443	0.32	0.67	0.01	
#9	5-500-15	4195	15	884	0.32	0.67	0.01	0.97
				663	0.34	0.66	0	
				442	0.34	0.65	0.01	
#10	5-500-10	4340	10	936	0.30	0.66	0.04	0.96
				702	0.29	0.68	0.03	
				468	0.30	0.68	0.01	

Table 5-1 (cont'd)

Test No.	Sludge from	$\overline{X}_V$ mg/L	θ_{xob} d	S_0 mg/L	f_1 -	f_2 -	f_3 -	$f_{x1} + f_{x2}$ -
#11	5-500-15	5513	15	936	0.29	0.68	0.03	0.97
				702	0.28	0.7	0.02	
				468	0.36	0.61	0.03	
#12	5-250-10	1518	10	583	0.29	0.68	0.03	0.97
				350	0.29	0.7	0.01	
				117	0.35	0.65	0	
#13	5-250-15	2680	15	583	0.31	0.67	0.02	0.98
				350	0.31	0.68	0.01	
				117	0.42	0.57	0.01	
Average					**0.316**	**0.653**	**0.024**	**0.945**

Table 5-2 presents the results of the statistical estimation of f_1, f_2, f_3 and $(f_{x1} + f_{x2})$.

Table 5 -2 Statistics of measured f_1, f_2 , f_3 and $(f_{x1} + f_{x2})$ values from BR tests

Statistical Data	f_1	f_2	f_3	$f_{x1} + f_{x2}$
Mean	**0.316**	**0.653**	**0.024**	**0.945**
Standard Error	0.006	0.010	0.003	0.0082
Standard Deviation	0.034	0.064	0.017	0.030
Sample Variance	0.0012	0.0041	0.0003	0.0009
Minimum	0.24	0.32	0	0.90
Maximum	0.42	0.74	0.08	0.98
Count	39	39	39	13
Confidence Level (95.0%)	± 0.011	± 0.021	± 0.006	± 0.018

The results shows that $f_1 = 0.316 \pm 0.011$, $f_2 = 0.653 \pm 0.021$ and $f_3 = 0.024 \pm 0.006$, all at 95% confidence levels.

5.2.2. Measurement of f_{X_1}, f_{X_2} and f_{X_3}

Using a similar method the soluble COD fractions released from sludge digestion can be calculated.

First, COD_T of the blank sample is measured. This is the total COD including VSS and BAP_{nd}. At the beginning of the test, the sample only contains COD of VSS since soluble COD has been removed by washing the sludge. Then, the sample is continuously aerated for 24 h. Soluble COD (BAP_{nd}) and COD_T are measured at time intervals of 3.5, 7, 12 and 24 h. The COD changes for BAP_{nd} and COD_T vs time curves are plotted and also the curves of their change rates, $dBAP_{nd}/dt$ and $dCOD_T/dt$ vs COD_T concentration. By using Eq. (5-4), BAP_T can be calculated. Figure 5-6 is a typical plot of BAP_{nd} and BAP_T changes for a blank reactor with a washed sludge.

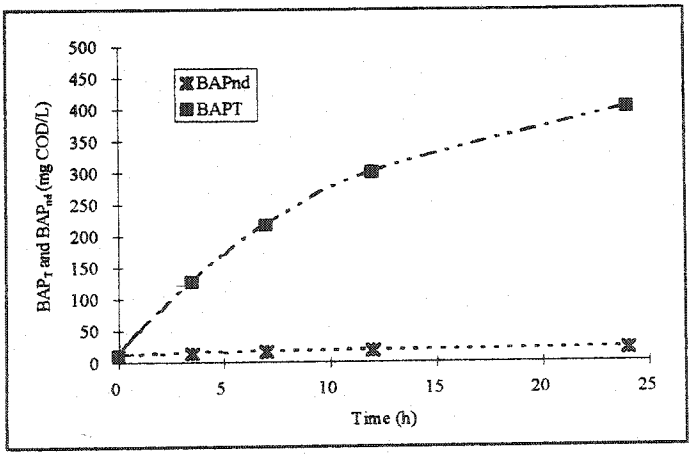


Figure 5-6. BAP_T and BAP_{nd} vs time curves from a blank BR test; sludge from No. 8-500 SBR reactor and θ_{xob} = 15 d.

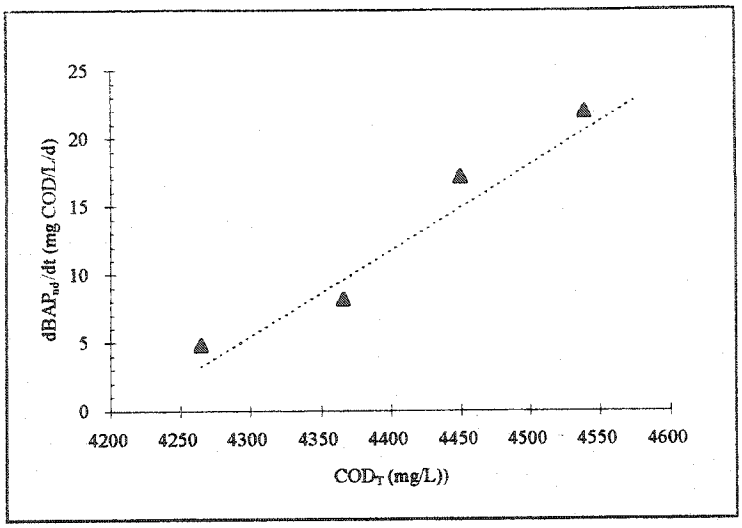


Figure 5-7. The linear relationship of BAP_{nd} accumulation rate to COD_T from a blank BR test; sludge from No. 8-500 SBR reactor and θ_{xob} = 15 d.

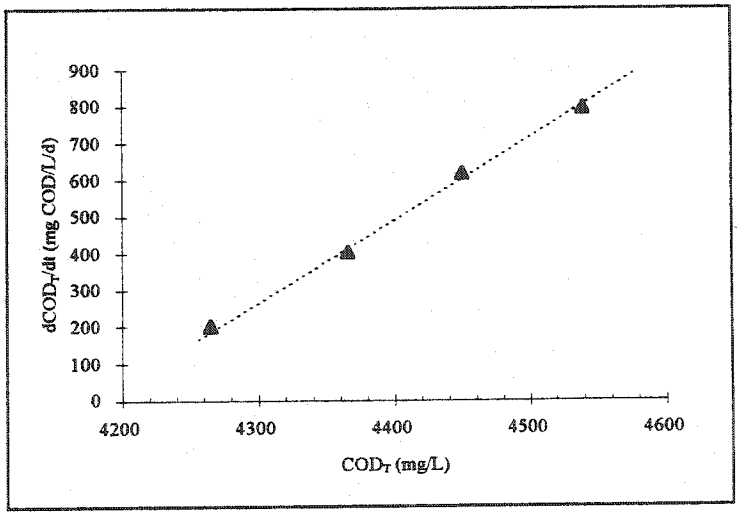


Figure 5-8. The linear relationship of BAP_T degradation rate to COD_T from a blank BR test; sludge from No. 8-500 SBR reactor and θ_{xob} = 15 d.

Figure 5-7 demonstrates that BAP_{nd} accumulation rate is linearly proportional to the COD_T concentration. Figure 5-8 shows that the COD_T degradation rate is also

proportional to COD_T as well. This suggests that the BAP_{nd} production rate can be expressed by a proportionality relation with the concentration of VSS, $dS_3/dt \propto COD_T$, then, $dS_3/dt \propto k_e X_v$, because all the soluble COD in the blank system comes from decomposition of VSS. Therefore, considering that the rate of release of soluble COD is controlled by sludge decay rate and using the conversion coefficient $\gamma_X \approx 1.42$ mg COD/ mg VSS (Hoover and Porges, 1952; Grady and Lim, 1980) to calculate the soluble COD converted from decomposed VSS, the BAP_{nd} rate expression can be written as

$$r_{xs_1} = f_{x_1} \gamma_x k_e X_v$$

where f_{x_3} is the percentage of BAP_{nd} in the released soluble COD.

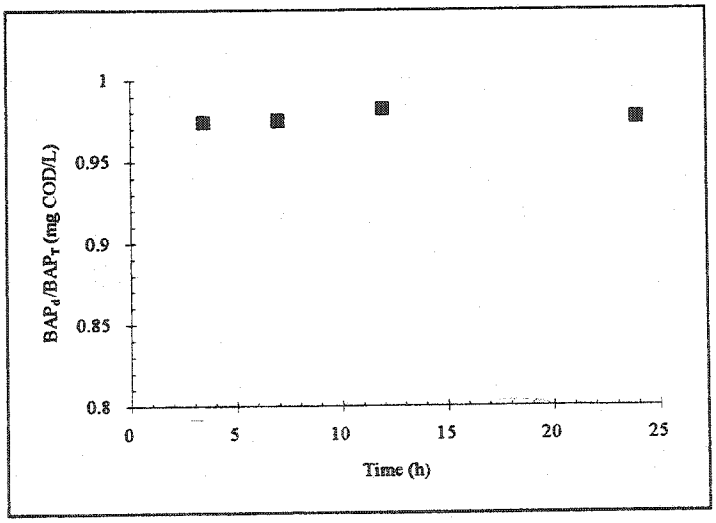


Figure 5-9. The ratio of BAP_d/BAP_T showing most of BAP degradable.

On the other hand, comparison of the BAP_T change curve and the BAP_{nd} change curve in Fig. 5-6 reveals that the COD_T change was primarily due to degraded BAP at all time intervals and very little of it contributed to BAP_{nd}. From the 13 sets of BR tests, the ratio

of BAP_d/BAP_T ($f_{x1} + f_{x2}$) varied from 90 to 98% (refer to the last column in Table 5-1) and the average degradable BAP_T was about 94.5% which provides a basis for the estimation of f_{X3}.

The degraded COD_T should be classified as the sum of easily and slowly biodegradable substrates. Both of their release rates are the same and determined by biomass decay rate, k_e, which is first-order with respect to COD_T or to total VSS concentration, X_v, as stated above but zero-order with respect to EBS, S_1, and DBS, S_2. Logically, these two rates are not related to the concentrations of EBS and DBS in the bulk mixed liquid but they are controlled by k_e.

Treating all BAP_d as EBS is reasonable because there was no accumulation of it during any time interval. This is equivalent to assuming $f_{x_2} = 0$. These results are different from the approach of the IAWPRC Model No. 1, in which the decomposed VSS is treated as slowly degradable substrate, then converted into readily degradable substrate.

Finally summarizing the BAP_d and BAP_{nd} rate equations:

$$r_{xs_1} = f_{x_1}\gamma_x k_e X_v \tag{5-13}$$

$$r_{xs_2} = f_{x_2}\gamma_x k_e X_v = 0 \tag{5-14}$$

$$r_{xs_3} = f_{x_3}\gamma_x k_e X_v \tag{5-15}$$

where $f_{x_1} \approx 0.95$, $f_{x_2} = 0$, $f_{x_3} = 0.05$ and $\gamma_x \leq 1.42 = f(\theta_x)$.

5.2.3. Determination of γ_x and γ_s

The first experimental results showed that both γ_x and γ_s were affected by sludge age. The younger sludge produced more BAP and UAP per unit biomass. Considering this fact, the new model introduces sludge age θ_x into the two conversion coefficients. The expressions are

$$\gamma_x = \frac{A_x}{C_x + \theta_x} \tag{5-16}$$

$$\gamma_s = \frac{A_s}{C_s + \theta_x} \tag{5-17}$$

A_x, A_s, C_x and C_s are constants and will be determined by selection of proper values to make the new model fit the experimental results. C_x and C_s have only methamatical meanings and keep the expressions within the reasonable ranges to meet the practical situation when sludge ages approach very small values, for exsample, $\theta_x < 0.1$ d.

5.3. THE EXPERIMENTAL VALIDATION OF UAP AND BAP EXPRESSIONS IN THE NEW SBR MODEL

As mentioned before, many researchers have shown the existence of UAP and BAP in a biological process. They are different from their counterparts in the influent. Previous research has also demonstrated that the effluents from biological processes mainly contain complex molecular substances. Grady et al. (1972) concluded from their study that metabolic products, another term for UAP and BAP, constituted an average of 85% of the

effluent COD in single-substrate systems and nearly 100% in a multi-component system. Later, Grady and Blachly (1985) used bench-scale reactors to study the molecular weight distributions in activated sludge effluents. They found that the largest amount of material was in the <1,000 and > 100,000 molecular weight ranges. Painter (1973) found 60% of the organic carbon in a secondary effluent to have a molecular weight greater than 10,000, consisting partially of proteins and polysaccharides. Manka and Rebhun (1982) found that most of the soluble organic compounds in the secondary effluents from oxidation ponds had molecular weights greater than 20,000 and humic acids and proteins were the two major groups. Amy et al. (1987) reported that the two major components of secondary effluent COD were fulvic acids and proteins. Anionic detergents were the third highest component for activated sludge and trickling filter systems.

On the other hand, Chudoba (1985) reported that COD compounds in an effluent from a biological process always corresponded to the feed composition. Concentrations in the effluent were proportional to their concentrations in the feed and almost always were 1 to 3.5% of their original concentration, even if the compounds in the feed were easy-to-biodegrade, such as glucose, sucrose, acetic acid or alamine.

To confirm the existence of UAP and BAP which have been expressed in the new SBR model and to compare them with original COD components fed to the systems, two sets of experiments in two systems, respectively, were carried out. One was a protein feed system and the other used sucrose as a sole carbon source.

5.3.1. Analysis Result of Remaining Amino Acids

A set of analyses was conducted to determine amino acids in the effluent from a batch reactor test at time intervals of 0, 3.5, 7, 12 and 24 h. The acclimated sludge was from No. 5-500-10 SBR. Table 5-3 shows the results of the analyses.

In the table, the second column is the estimated concentrations of various amino acids, fat and carbohydrates based on the information (Table 3-4) provided by the vegetable protein manufacturer. The COD for this feed is about 500 mg/L when 80 g of vegetable protein is dissolved 200 L of water. The third column is the concentrations of the feed ingredients at t = 0 in the batch test. The fourth to tenth columns list the concentrations of amino acids, carbohydrates and COD at the corresponding time intervals. The remainder of the columns are the results for sludge from an SBR with observed sludge age of 10 d and from CFSTR1, CFSTR2 and CFSTR3 with sludge ages of 5, 10 and 15 d, respectively. Total amino acid is the sum of individual amino acids in the same column while total carbohydrate and COD are the direct test results.

Comparison of the second and third columns reveals that measured amino acid concentrations corresponded well to the estimations. With reaction time, most of the amino acids from the feed were transformed or degraded. The total number of typical amino acids decreased from 17 to 4 (except tyrosine which was used as a calculation reference or standard and tryptophan which was not found at the beginning and was missing in the later periods) and the corresponding concentrations of the individual amino acids decreased to about 1 mg/L. The total amino acid concentration decreased from 393.2 mg/L initially to 4.6 mg/L after only 7 h reaction time as shown in the fifth column

Table 5-3 Measured amino acids, carbohydrates and COD for the batch reactor and other systems with the vegetable protein as feed

	Estim. feed conc. mg/L	Tested feed conc. mg/L	Fed batch 3.5 h mg/L	Fed batch 7 h mg/L	Fed batch 12 h mg/L	Fed batch 24 h mg/L	Blank batch 0 h mg/L	Blank batch 7 h mg/L	Blank batch 24 h mg/L	SBR2 eff. mg/L	CFSTR 1 eff. mg/L	CFSTR 2 eff. mg/L	CFSTR 3 eff. mg/L
Total amino acid	**360.3**	**393**	**54**	**4.6**	**4.5**	**3.9**	**2.4**	**2.1**	**3.1**	**1.8**	**4.4**	**5.7**	**3.0**
Glutamic acid	68.1	80.4	3.2	<d.l.	<d.l.	<d.l.	<d.l.	<d.l.	<d.l.	<d.l.	<d.l.	<d.l.	<d.l.
Aspartic acid	41.2	47.9	<d.l.	0.5	0.5	0.9	0.3	0.3	0.7	0.4	1.0	1.1	0.8
Leucine	29.4	35.0	4.4	<d.l.	<d.l.	<d.l.	<d.l.	<d.l.	<d.l.	<d.l.	<d.l.	<d.l.	<d.l.
Arginie	26.9	30.5	<d.l.	<d.l.	<d.l.	<d.l.	<d.l.	<d.l.	<d.l.	<d.l.	<d.l.	<d.l.	<d.l.
Lysine	22.6	26.7	2.9	<d.l.	<d.l.	<d.l.	<d.l.	<d.l.	<d.l.	<d.l.	<d.l.	<d.l.	<d.l.
Serine	18.6	21.1	14.6	1.3	1.2	0.9	1.0	0.4	1.3	0.5	1.3	1.4	1.1
Phenylalanine	18.6	21.9	<d.l.	<d.l.	<d.l.	<d.l.	<d.l.	<d.l.	<d.l.	<d.l.	<d.l.	<d.l.	<d.l.
Proline	18.4	21.6	<d.l.	<d.l.	<d.l.	<d.l.	<d.l.	<d.l.	<d.l.	<d.l.	<d.l.	<d.l.	<d.l.
Valine	18.0	20.9	2.7	<d.l.	<d.l.	<d.l.	<d.l.	1.0	0.1	<d.l.	<d.l.	<d.l.	<d.l.
Isoleucine	17.6	20.9	2.9	<d.l.	<d.l.	<d.l.	<d.l.	<d.l.	<d.l.	<d.l.	<d.l.	<d.l.	<d.l.
Alanine	15.4	18.4	5.5	0.6	<d.l.	<d.l.	<d.l.	<d.l.	<d.l.	<d.l.	<d.l.	<d.l.	<d.l.
Tyrosine (*Noleucine Std*)	13.7	*Std.*	*Std.*	*Std.*	*Std.*	*Std.*	*Std.*	*Std.*	*Std.*	*Std.*	*Std.*	*Std.*	*Std.*
Threonine	13.6	17.3	5.1	<d.l.	0.9	<d.l.	<d.l.	<d.l.	<d.l.	<d.l.	<d.l.	0.8	<d.l.
Glycine	14.9	17.7	8.0	1.7	1.0	1.1	0.6	<d.l.	0.5	0.6	1.2	1.5	0.2
Histidine	9.3	10.5	4.8	<d.l.	<d.l.	<d.l.	<d.l.	<d.l.	<d.l.	<d.l.	<d.l.	<d.l.	<d.l.
Methionine	4.8	1.9	<d.l.	<d.l.	<d.l.	<d.l.	<d.l.	<d.l.	<d.l.	<d.l.	<d.l.	<d.l.	<d.l.
Cysteine	4.7	0.5	<d.l.	0.5	0.9	1.0	0.5	0.4	0.5	0.3	0.9	0.9	0.9
Tryptophan	4.7	<d.l.	<d.l.	<d.l.	<d.l.	<d.l.	<d.l.	<d.l.	<d.l.	<d.l.	<d.l.	<d.l.	<d.l.
Total Carbohydrate	**0**	**9.4**	**5.2**	**4.0**	**4.2**	**6.6**	**0.4**	**3.7**	**5.1**	**4.2**	**4.4**	**7.7**	**6.2**
Sucrose	0	<d.l.	<d.l.	<d.l.	<d.l.	<d.l.	<d.l.	<d.l.	<d.l.	<d.l.	<d.l.	<d.l.	<d.l.
Glucose	0	<d.l.	<d.l.	<d.l.	<d.l.	<d.l.	<d.l.	<d.l.	<d.l.	<d.l.	<d.l.	<d.l.	<d.l.
Fructose	0	<d.l.	<d.l.	<d.l.	<d.l.	<d.l.	<d.l.	<d.l.	<d.l.	<d.l.	<d.l.	<d.l.	<d.l.
Fat	**4**	n/a	n/a	n/a	n/a	n/a	n/a	n/a	n/a	n/a	n/a	n/a	n/a
Acetate	n/a	<d.l.	<d.l.	<d.l.	<d.l.	<d.l.	<d.l.	<d.l.	<d.l.	<d.l.	<d.l.	<d.l.	<d.l.
Propionate	n/a	<d.l.	<d.l.	<d.l.	<d.l.	<d.l.	<d.l.	<d.l.	<d.l.	<d.l.	<d.l.	<d.l.	<d.l.
Butyrate	n/a	<d.l.	<d.l.	<d.l.	<d.l.	<d.l.	<d.l.	<d.l.	<d.l.	<d.l.	<d.l.	<d.l.	<d.l.
COD	**≈ 500**	**519**	**77**	**13**	**14**	**20**	**4.2**	**11**	**18**	**19**	**55**	**35**	**34**

* <d.l. = below detection limit, ** n/a = not analyzed, *** Std = Standard.

in Table 5-3, which is about 1% of total amino acids in the feed. This level remained until

24 h, the end of the test.

The test results of carbohydrates also showed that each effluent sample contained no sucrose, glucose, fructose, acetate, propanate or butyrate, i.e., no simple carbohydrates. But total carbohydrate results demonstrate that it degraded from 9.2 mg/L initially to 4.0 mg/L at 7 h, then increased to 4.2 mg/L at 12 h and to 6.6 mg/L at 24 h, which can only be carbohydrates other than simple molecular carbohydrates. They have more complex molecular structure and larger molecular weight. COD, initially at 519 mg/L, steadily decreased to 13 mg/L at 7 h and increased to 20 mg/L at the end of the test cycle.

From the preliminary experiment on the feed selection, the measured ratio of COD:amino acids was about 1.3 mg/mg and the measured ratio for COD:carbohydrate was about 1.0 mg/mg. The following equation involving the two ratio values is employed to estimate the unknown organic materials other than the typical amino acids and carbohydrates:

$$\text{Unknown Organics} \approx \text{COD} - (\text{Total Amino Acid} \times 1.3 + \text{Total Carbohydrate} \times 1.0)$$

The fourth row in Table 5-4 lists the calculation results, which show a trend of increasing portion of unknown organic materials in both the fed reactor and the blank reactor with increasing reaction time. Also, unknown organic materials with total carbohydrates, the portion of complex molecular substances, steadily increased with reaction time.

The last row shows that the ratio of the complex molecular organics to COD increased from 2% at the beginning of the batch test to 75% at the end for the fed system and from 26 to 78% for the blank test. From the last row, it can also be seen that the complex molecular: COD ratio is higher for the effluents from SBR and CFSTR processes than for

Table 5-4 Approximate estimation of the organic materials other than typical amino acids and carbohydrates for the various protein systems

	Estim. feed conc. mg/L	Tested feed conc. mg/L	Fed batch 3.5 h mg/L	Fed batch 7 h mg/L	Fed batch 12 h mg/L	Fed batch 24 h mg/L	Blank batch 0 h mg/L	Blank batch 7 h mg/L	Blank batch 24 h mg/L	SBR 2 eff. mg/L	CFSTR 1 eff. mg/L	CFSTR 2 eff. mg/L	CFSTR 3 eff. mg/L
Total Amino acid	360.3	393.2	54.1	4.6	4.5	3.9	2.4	2.1	3.1	1.8	4.4	5.7	3.0
Total Carbohydrate	4	9.4	5.2	4.0	4.2	6.6	0.4	3.7	5.1	4.2	4.4	7.7	6.2
Unknown Organics	≈ 0	≈ 0	1.5	3	3.5	8.3	0.7	4.6	8.9	12.5	46.2	19.9	23.9
COD	≈ 500	519	77	13	14	20	4.2	11	18	19	55	35	34
Complex Molecular/ COD	< 0.01	0.02	0.09	0.54	0.55	0.75	0.26	0.75	0.78	0.88	0.90	0.79	0.89

the batch test. This is because SBR and CFSTR processes had reached steady state and there were accumulations of the complex molecular materials in their supernatants. But in the BR, the sludge was washed before returning it to the reactors; most of the accumulated soluble organics were removed by washing. Washing the sludge resulted in a lower concentration of soluble complex molecular substances at the end of the test cycle.

All the above results prove that the original substrates that contributed to the feed COD no longer existed in the remaining soluble COD, instead, COD from UAP and BAP became the main components.

5.3.2. Sucrose as a Sole Carbon Source for an SBR Run

An SBR system with sucrose, one type of EBS COD, as its sole carbon source was run until steady state around the system was reached. Then following the same procedure for the BR test described in Section 5.1, a set of samples from the system was analyzed.

Table 5-5 demonstrates that the results of the amino acids and carbohydrates analyses for

this system were similar to those from the protein system. The sucrose degraded quickly and completely disappeared after 2 h reaction despite its very high initial concentration (S_0 = 2000 mg COD/L), from 2.2 to 8 times that (250 to 900 mg COD/L) for the system with the vegetable protein as feed. During the testing cycle, acetic acid, a simple intermediate product, exists at 24 to 128 mg/L before 3.5 h of reaction time, and so does propionate but only at concentrations less than 6 mg/L. After sucrose concentration decreased to less than 60 mg/L, the intermediate organic acids degraded and disappeared quickly and there was neither simple molecular carbohydrate nor common amino acids found in the supernatant although its COD was still high (around 463 mg/L) and total carbohydrate was 165 mg/L at a reaction time of 2 h.

One different result of this system from that of the protein system was that there was no simple molecular carbohydrate left in the supernatant after 3.5 h reaction or in the effluent, compared to total amino acids at about 1% of the feed concentration which always remained in the effluent from the protein system. Although sucrose was the sole carbon source and no amino acids were added, more amino acids were generated with extended reaction time in the fed reactor compared to the protein fed reactor. This phenomenon could result from reaction equilibrium because of low amino acid concentration in the sucrose system, which induced more lysis of protein in the bacterial cells. These generated amino acids, therefore, belong to BAP. Also the blank from the sucrose fed sludge generated more amino acids than the blank from the protein fed sludge.

The last two rows in Table 5-5 present the measurement and calculation results of the

Table 5-5 Measured amino acids, carbohydrates and COD for the batch test with sucrose as sole carbon source

	Fed 0 h mg/L	Fed 0.5 h mg/L	Fed 1 h mg/L	Fed 2 h mg/L	Fed 3.5 h mg/L	Fed 8 h mg/L	Fed 24 h mg/L	Blank 0 h mg/L	Blank 3.5 h mg/L	Blank 8 h mg/L	Blank 24 h mg/L
Total amino acid	<d.l.	n/a	n/a	n/a	**3.3**	**7.2**	**12**	**0.0**	**3.3**	**13**	**22**
Glutamic acid	<d.l.	n/a	n/a	n/a	<d.l.	<d.l.	<d.l.	<d.l.	<d.l.	<d.l.	<d.l.
Aspartic acid	<d.l.	n/a	n/a	n/a	1.0	<d.l.	1.0	<d.l.	<d.l.	1.2	1.0
Leucine	<d.l.	n/a	n/a	n/a	<d.l.	<d.l.	1.6	<d.l.	<d.l.	0.3	5.2
Arginie	<d.l.	n/a	n/a	n/a	<d.l.	<d.l.	<d.l.	<d.l.	<d.l.	<d.l.	<d.l.
Lysine	<d.l.	n/a	n/a	n/a	<d.l.	<d.l.	<d.l.	<d.l.	<d.l.	<d.l.	<d.l.
Serine	<d.l.	n/a	n/a	n/a	1.2	1.5	1.3	<d.l.	1.3	2.2	1.1
Phenylalanine	<d.l.	n/a	n/a	n/a	<d.l.	<d.l.	<d.l.	<d.l.	<d.l.	<d.l.	<d.l.
Proline	<d.l.	n/a	n/a	n/a	<d.l.	<d.l.	<d.l.	<d.l.	<d.l.	<d.l.	<d.l.
Valine	<d.l.	n/a	n/a	n/a	<d.l.	1.6	3.6	<d.l.	<d.l.	2.2	6.4
Isoleucine	<d.l.	n/a	n/a	n/a	<d.l.	1.4	2.9	<d.l.	<d.l.	1.9	5.9
Alanine	<d.l.	n/a	n/a	n/a	<d.l.	<d.l.	<d.l.	<d.l.	<d.l.	1.9	<d.l.
Tyrosine	*Std.*	n/a	n/a	n/a	*Std.*	*Std.*	*Std.*	*Std.*	*Std.*	*Std.*	*Std.*
Threonine	<d.l.	n/a	n/a	n/a	<d.l.	0.8	1.0	<d.l.	<d.l.	1.0	1.4
Glycine	<d.l.	n/a	n/a	n/a	0.2	1.0	<d.l.	<d.l.	1.0	1.2	<d.l.
Histidine	<d.l.	n/a	n/a	n/a	<d.l.	<d.l.	<d.l.	<d.l.	<d.l.	<d.l.	<d.l.
Methionine	<d.l.	n/a	n/a	n/a	<d.l.	<d.l.	<d.l.	<d.l.	<d.l.	<d.l.	<d.l.
Cysteine	<d.l.	n/a	n/a	n/a	0.9	0.9	0.9	<d.l.	1.0	0.9	1.0
Tryptophan	<d.l.	n/a	n/a	n/a	<d.l.	<d.l.	<d.l.	<d.l.	<d.l.	<d.l.	<d.l.
Total Carbohydrates	**2060**	**748**	**361**	**165**	**21**	**28**	**46**	**3.1**	**15**	**24**	**45**
Sucrose	1990	755	356	57	<d.l.	<d.l.	<d.l.	<d.l.	<d.l.	<d.l.	<d.l.
Glucose	39	<d.l.	<d.l.	<d.l.	<d.l.	<d.l.	<d.l.	<d.l.	<d.l.	<d.l.	<d.l.
Fructose	38	<d.l.	<d.l.	<d.l.	<d.l.	<d.l.	<d.l.	<d.l.	<d.l.	<d.l.	<d.l.
Acetate	22	112	128	24	<d.l.	<d.l.	<d.l.	<d.l.	<d.l.	<d.l.	<d.l.
Propionate	33	3	6	1	<d.l.	<d.l.	<d.l.	<d.l.	<d.l.	<d.l.	<d.l.
Butyrate	41	<d.l.	<d.l.	<d.l.	<d.l.	<d.l.	<d.l.	<d.l.	<d.l.	<d.l.	<d.l.
COD	**2200**	**1808**	**1324**	**463**	**53**	**62**	**92**	**11**	**29**	**54**	**98**
Unknown Organics	**140**	**938**	**834**	**381**	**28**	**25**	**30**	**7.9**	**9.7**	**2.4**	**24**
Complex Molecular / COD Ratio	**0.06**	**0.52**	**0.63**	**0.82**	**0.92**	**0.85**	**0.83**	**0.72**	**0.85**	**0.69**	**0.71**

complex molecular : COD ratio in the effluents from the sucrose BR system. One difference for the calculation from the previous one in Section 5.3.1 is that between reaction time 0 and 3.5 h, total carbohydrates include sucrose, glucose and fructose which are simple molecular organics and should be deducted from the total carbohydrates for the calculation of the complex molecular fraction. Another difference that should be indicated is that the level of amino acids between reaction time 0 and 3.5 h could be neglected because this level is below the detection limit at the beginning and only 3.3 mg/L at 3.5 h.

Analysis of Table 5-5 reveals that there is a similar trend of increasing ratio of complex molecular COD to total COD with reaction time for either the fed reactor or the blank reactor. For the fed reactor, the ratio rose from 6% initially to 83% at the test end. Meanwhile for the blank, this ratio was consistently higher around 70% except for one measurement, 85%, at 3.5 h which could be caused by random errors. On average, the fed reactor contained a higher complex molecular : COD ratio than the blank although the quantities of sludge for both were the same. The difference must result from the feed which is the only difference between the two, therefore, the difference must be due to UAP.

Referring to Table 5-4, the ratios of complex compounds to COD in the protein system are close between the fed reactor and the blank reactor, which is different from the sucrose system. It is likely that a biological process with protein as feed would generate less UAP than the system with sucrose as the sole carbon source.

From the above analysis, it can be concluded that the unknown effluent organic materials

and total carbohydrates are different from the feed components and come from UAP and BAP. This matches other results noted at the beginning of Section 5.3. This confirms that kinetic terms for UAP and BAP in the new SBR model are necessary.

The residual COD from the protein system always contained about 1% of its original feed content which is similar to Chudoba's results (1985). But the residual COD from the sucrose system contained no original feed ingredient, which is different from Chudoba's results.

5.4. EXPERIMENTAL DETERMINATION OF KINETIC CONSTANTS

5.4.1. Evaluation of k_1 and K_{S_1}

The remaining kinetic constants of the new model can be determined via the method of initial rates by differential analysis (Levenspiel, 1972; Roberts, 1977 and Speitel and DiGiano, 1988). The batch test for determining the COD fractions is also used for determination of the rate constant k_1, half-velocity constant K_{S_1} for EBS and rate constant k_2 for DBS which will be discussed in the next paragraph. Recalling the work of Moser (1977) at the beginning of Section 5.1 and the test results presented in Section 5.1.3, it can be concluded that the kinetic coefficients of EBS removal, k_1 and K_{S_1}, can be measured by testing the initial degradation rate in the BR. Figure 5-10 illustrates the data for three initial substrate concentrations from the BR test.

As described in Section 4.1.1, EBS in multiple substrates will be utilized by bacteria first. Grau et al. (1975) expected that for a multi-component substrate, if the measurements are

carried out over a short time at the beginning of a batch test when single substrates are present in the mixture, the substrate removal kinetics can be described by Monod kinetics. Using at least three different initial COD concentrations in batch tests and measuring their initial degradation rates is necessary to determine kinetic parameters of k_1 and K_{s_1} in the Monod expression.

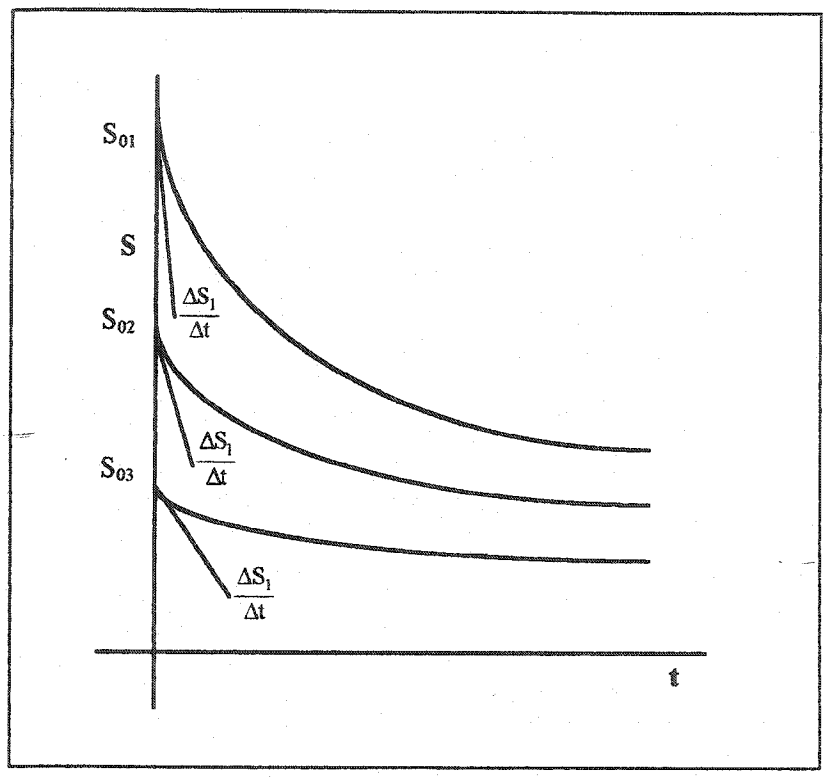


Figure 5-10. Plot for the differential method

From Eq. 4-7 with Q = 0 and $r_{s_1} = \Delta S_1/\Delta t$ for a time interval Δt from t to t + 1,

$$r_{s_1} = \frac{(S_1)_{t+1} - (S_1)_t}{\Delta t} = -\frac{k_1 \overline{X}_v S_1}{K_{S_1} + S_1} + f_{x_1} \gamma_x k_e \overline{X}_v$$

where $\overline{X}_v$ is the average sludge concentration through the batch test. Moving the term of

released COD from sludge decay to the left side, exchanging the positions of two S_1 values at t + 1 and t, changing the signs before every term and dividing both sides by $\overline{X}_v$ results in

$$\frac{(S_1)_t - (S_1)_{t+1}}{(\Delta t)\overline{X}_v} + f_{x_1}\gamma_x k_e = -\frac{r_{s_1}}{\overline{X}_v} + f_{x_1}\gamma_x k_e = \frac{k_1 S_1}{K_{S_1} + S_1}$$

Its reciprocal expression is

$$\frac{1}{-\frac{r_{s_1}}{\overline{X}_v} + f_{x_1}\gamma_x k_e} = \frac{K_{S_1} + S_1}{k_1 S_1} = \frac{K_{S_1}}{k_1}\frac{1}{S_1} + \frac{1}{k_1}$$

A straight line is plotted with a slope of K_{S_1}/k_1 and an ordinate intercept of $1/k_1$ as shown in Fig. 5-11. The value of f_{x_1} is known from the test methods given in Section 5.2.2 and the slope and the intercept can be found from the plot. k_1 and K_{S_1} can now be calculated.

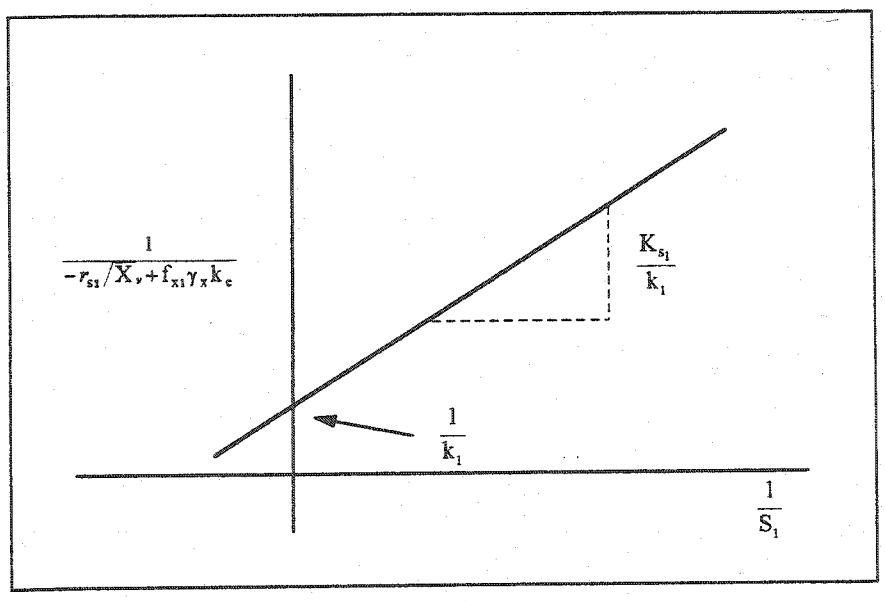


Figure 5-11. A plot to determine k_1 and K_{S1}

5.4.2. The Results of Experimental Testing k_1 and K_{S_1}

The sixth and seventh columns in Table 5-6 are results for k_1 and K_{S_1}. The correlation R values (the eighth column in Table 5-6) for the 13 tests are quite high, ranging from 0.956 to 1.00 which indicates the high reliability of the experimental estimation.

Table 5-6 Kinetic rate constants determined from the BR tests

Test No.	Sludge from	$\overline{X}_v$ mg/L	θ_{xob} d	S_0 mg/L	k_1 d^{-1}	K_{S1} mg/L	Corr. R	$k_2'_{test}$ L/mg-d	Corr. R	ρ	$k_2'_{adj}$ L/mg-d
#1	8-500-5	1650	5	144	11.9	80.9	0.974	0.04	0.995	0.007	0.092
				110				0.053	0.995	0.005	0.105
				65				0.066	0.998	0.003	0.105
#2	8-500-15	3150	15	468	7.3	55.9	0.958	0.012	0.974	0.012	0.063
				216				0.019	0.984	0.015	0.056
				130				0.038	0.990	0.009	0.082
#3	7-250-15	2176	15	465	9.9	96.3	1.00	0.011	0.969	0.013	0.057
				220				0.023	0.983	0.011	0.069
				115				0.041	0.984	0.008	0.083
#4	3-500-10	2250	10	367	11.9	86.2	0.988	0.022	0.981	0.007	0.095
				184				0.047	0.995	0.004	0.125
				93				0.066	0.992	0.002	0.121
#5	6-500-15	3960	15	367	8.1	67.0	0.977	0.018	0.979	0.009	0.079
				184				0.025	0.982	0.012	0.066
				93				0.047	0.973	0.008	0.086
#6	2-250-10	1900	10	889	9.5	77.0	0.993	0.004	0.979	0.021	0.036
				445				0.012	0.988	0.013	0.060
				221				0.024	0.995	0.011	0.072
#7	2-250-15	3487	15	888	7.3	54.6	1.00	0.006	0.958	0.014	0.054
				443				0.011	0.986	0.014	0.055
				220				0.024	0.987	0.011	0.072
#8	5-500-10	3418	10	884	14.7	110	0.970	0.006	0.985	0.013	0.056
				663				0.01	0.990	0.011	0.070
				442				0.014	0.984	0.011	0.070

Table 5-6 (Cont'd)

Test No.	Sludge from	[mg/L	θ_{xob} d	S_0 mg/L	k_1 d^{-1}	K_{S1} mg/L	Corr. R	k_2' test L/mg-d	Corr. R	ρ	k_2' adj L/mg-d
#9	5-500-15	4195	15	884	16.9	91.9	1.00	0.009	0.976	0.009	0.083
				663				0.013	0.980	0.008	0.091
				442				0.023	0.985	0.006	0.114
#10	5-500-10	4340	10	936	14.7	110	0.956	0.008	0.993	0.009	0.077
				702				0.011	0.992	0.009	0.080
				468				0.023	0.985	0.005	0.120
#11	5-500-15	5513	15	936	14.7	112	0.970	0.008	0.960	0.010	0.074
				702				0.01	0.975	0.010	0.073
				468				0.017	0.978	0.008	0.089
#12	5-250-10	1518	10	583	13.6	97.5	0.997	0.012	0.978	0.010	0.075
				350				0.022	0.997	0.008	0.091
				117				0.043	0.983	0.007	0.088
#13	5-250-15	2680	15	583	16.2	135	0.980	0.013	0.959	0.009	0.084
				350				0.027	0.993	0.006	0.112
				117				0.063	0.997	0.002	0.129
Avg					**12.1**	**93.7**				**0.009**	**0.082**

5.4.3. Estimation of k_2 and K_{S2}

From Figs. 5-5a to 5-5c, it can be seen that there is a linear relation between specific substrate utilization rate, r_s, and substrate concentration, S, after a quick drop of r_s at the beginning of the test. Degradation of DBS occurs after EBS is almost consumed by bacteria (Section 5.2.2.). The slope of the linear range of the curves can be calculated as k_2', the kinetic coefficient of a first-order reaction, with regression while treating $K_{S2} >> S_2$ in the Monod equation and $k_2' = k_2/K_{S2}$.

The ninth column in Table 5-6 presents measured k_2' results, $k_2'_{test}$. It is interesting to note that there is a decreasing trend of $k_2'_{test}$ values as the initial substrate concentration increases. This is one type of feedback inhibition that can yield a so called "fine control" over the degradation (reaction) sequence (Lehninger, 1975; Grady and Lim, 1980). The fine control effect is especially conspicuous for bacteria because of their basic need to conserve nitrogen sources. This type of inhibition typically exists in a bacterial system using proteins or amino acids as a feed. In such a system, one type of amino acid reacts with an enzyme and, after a reaction sequence, produces an "end product" that is still an amino acid but with lower molecular weight and is ready to be decomposed further into simpler and lower grade non-amino acid molecules. The end product is a specific inhibitor of an enzyme at or near the beginning of the reaction sequence to prevent enzymes from wasting energy, nitrogen and carbon. Added amino acids containing the "inhibitor" will form or aggravate the fine control inhibition. It is capable of second-by-second adjustment of the reaction rate to the steady state level of the end product concentration. As a result, the rate of the entire sequence of reaction is determined by the steady-state concentration of the end product. From the test results in Table 5-6, it is known that this type of inhibition does not affect EBS degradation but it does affect DBS degradation. Therefore an adjustment needs to be applied to the estimation of DBS degradation rate constant, k_2'.

5.4.4. The Correction of Feedback Inhibition on k_2

For the correction of k_2, illustrating the relation of slope of dS'/dt curve and initial

concentration S_0 results in a linear line on semi-log graph paper as shown in Fig. 5-12 from which the true k_2' value can be read at different S_0 concentrations.

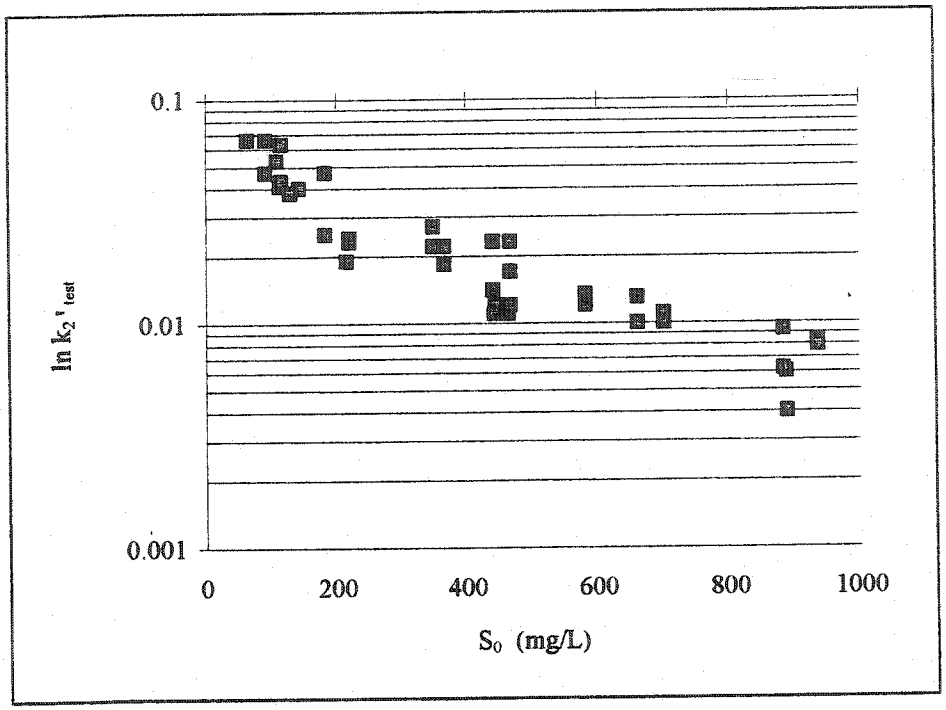


Figure 5-12. The linear relation between S_0 and ln $k_2'_{test}$

Applying the Lineweaver-Burk approach (Metcalf and Eddy, Inc., 1991), which has been extensively used in the literature, to Eq. (4-8) and putting the switch function aside because it is only active when EBS exists,

$$\frac{dS_2}{dt} = r_{s_2} = -\frac{k_2 X_v S_2}{K_{S_2} + S_2}$$

leads to

$$\frac{1}{-r_{s_2}/X_v} = \frac{K_{S_2}}{k_2}\frac{1}{S_2} + \frac{1}{k_2} \qquad (5\text{-}18)$$

According to the inhibition theory of enzymatic kinetics (Lehninger, 1975), the above equation becomes:

$$\frac{1}{-r_{s_2}/X_v} = \frac{K_{S_2}}{k_2}\left(1+\frac{[I]}{K_I}\right)\frac{1}{S_2}+\frac{1}{k_2}\left(1+\frac{[I]}{K_I}\right)$$

where the first term refers to the slope of the Lineweaver-Burk plot curve and second term to its intercept. [I] is the inhibitor concentration and K_I the inhibition constant. As the experimental results showed that DBS degradation followed a first-order reaction which means $K_{S_2} >> S_2$, the second term can be neglected. Hence,

$$\frac{1}{-r_{s_2}/X_v} \approx \frac{K_{S_2}}{k_2}\left(1+\frac{[I]}{K_I}\right)\frac{1}{S_2} = \frac{1}{k_2'}\left(1+\frac{[I]}{K_I}\right)\frac{1}{S_2} \qquad (5\text{-}19)$$

The inhibitor comes from the feed and should be proportional to the influent COD concentration. Then, using P_I as the percentage of inhibitor in the feed and letting $[I] = P_I S_0$ results in

$$\frac{1}{-r_{s_2}/X_v} = \frac{1}{k_2'}\left(1+\frac{P_I S_0}{K_I}\right)\frac{1}{S_2} = \left(\frac{1+\rho S_0}{k_2'}\right)\frac{1}{S_2} \text{ or}$$

$$k_2' = -\frac{r_{s_2}}{X_v}\left(\frac{1+\rho S_0}{S_2}\right) \qquad (5\text{-}20)$$

where $\rho = P_I/K_I$.

By using Eq. (5-18) to express the inhibited system without the correction term of $(1+[I]/K_I)$ and considering $K_{S_2} >> S_2$, Eq. (5-18) becomes

$$\frac{1}{-r_{si}/X_v} = \left(\frac{1}{k_2'_{test}}\right)\frac{1}{S_2} \qquad (5\text{-}21)$$

where $k_2'_{test}$ is the measured value of k_2' directly from the slopes of dS'/dt-S curves under various initial concentrations of S_0.

Comparing Eq. (5-20) with Eq. (5-21), there should be a relationship of

$$\frac{1}{k_2'_{test}} = \frac{(1+\rho S_0)}{k_2'}$$

$$\rho = \left(\frac{k_2'}{k_2'_{test}} - 1\right)/S_0 \qquad (5\text{-}22)$$

To obtain ρ, k_2' can be first assumed as the intercept of the $k_2'_{test}$ - S_0 curve extended to the Y axis where $S_0 = 0$. After ρ is obtained from Eq. (5-22), the true k_2' can be adjusted by either Eq. (5-20) or Eq. (5-22). ρ values for each test are given in Table 5-6.

Table 5-7 Statistic results of the adjusted $k_2'_{test}$ values

Corrected k_2	
Mean	0.0823
Standard Error	0.0035
Standard Deviation	0.0219
Sample Variance	0.0005
Range	0.0933
Count	39
Confidence Level (95.0%)	± 0.0071

The last column in Table 5-6 lists the corrected $k_2'_{adj}$ values. The mean of the corrected $k_2'_{adj}$ is 0.0823. Table 5-7 is the statistical description of the estimation which suggests that $k_2'_{adj} = 0.0823 \pm 0.0071$ at a 95% confidence level.

5.4.5. Determination of k_e and Y Coefficients

As stated in the section of model development (Section 4.1), the new model deals with carbonaceous COD metabolism and treats the activated sludge as uniform biomass. Therefore, a single set of yield factor, Y, and endogenous decay rate constant, k_e was applied to the model. The Lineweaver-Burke plot (Metcalf and Eddy, Inc., 1991) is adopted here to calculate k_e and Y in a CFSTR system.

Before applying this approach to the CFSTR system, the Lawrence and McCarty model in Section 2.4.1 must be reviewed. For a CFSTR system with a settling tank, two assumptions must be made in the development of the kinetic model:

1. Substrate degradation by microorganisms occurs only in the reactor unit.
2. The volume used in calculating the mean cell residence time, or sludge age, for the system includes only the reactor volume.

These two assumptions are reasonable for most activated sludge systems with settling tanks because substrate metabolism by microorganisms in the clarifier is negligible due to the quick separation of sludge and wastewater and to the lack of oxygen in the sludge layer. The following equation is the mass balance of activated sludge in a CFSTR system:

$$\frac{dX}{dt}V = QX_0 - [Q_wX + (Q - Q_w)X_e] + \left(Y\frac{kXS}{K_s + S} - k_eX\right)V$$

Assuming that steady-state conditions prevail (dX/dt = 0) and the microorganism concentration in the influent is zero, yields

$$\frac{1}{\theta_x} = Y\frac{Q(S_0 - S)}{VX} - k_e \qquad (5\text{-}23)$$

This is a linear equation. By fitting a straight line, Y and k_e can be obtained from its slope and intercept, respectively.

For a SBR system, reaction and clarification occur in the same vessel. The space-time characteristics of the batch system are different from those of a CFSTR system. During fill and react in an operation cycle, the volume of an SBR reactor acts as a reactor for degradation of substrate by microorganisms. Afterwards during settle and draw periods in an SBR system, similar to the situation in a clarifier of a CFSTR system, microorganism activities decline significantly such that they should not be considered in the estimation of kinetic parameters, and Y and k_e must be calculated in an approach equivalent to the CFSTR system. Therefore, two similar assumptions are applied to an SBR system:

1. Substrate degradation by microorganisms occurs only in the periods of fill and react, and the metabolism of microorganism during settle and draw periods is negligible because the biomass is separated from the liquid and aeration is absent in the latter two phases.

2. The total biomass, $M_x = VX_v$, used in calculating the mean cell residence time or

sludge age for the system only includes the biomass under reactive conditions, i.e., in the fill and react stages.

Assuming the time fraction of reactive conditions for a 24 hour period in the operation of an SBR reactor is φ, from a mass balance, the equation of biomass change in the system by definition is:

Total biomass accumulation within the system each day	=	Biomass in influent into the system per day	−	Biomass discharged from the system per day	−	Biomass washed with effluent from the system per day	+
		+ Biomass growth in the system per day	−	Biomass decayed in the system under reactive conditions per day			

or in mathematical form:

$$\frac{d\overline{M}_X}{dt} = Q_d X_0 - Q_{wd} X_w - (Q_d - Q_{wd}) X_e + Y Q_d (S_0 - S_e) - k_e \overline{M}_X \varphi \qquad (5\text{-}24)$$

where

$\overline{M}_X$ = the total biomass in the reactor;

$\overline{M}_X \varphi$ = the total effective biomass adjusted by the reactive time portion of a cycle;

$Q_d = Qt_f N_c$, the flow rate per day;

$$\varphi = \frac{(t_f + t_r)N_c}{t_c N_c} = \frac{t_f + t_r}{t_c};$$

N_c = the number of operation cycle per day;

t_f = fill period duration in one operational cycle;

t_r = react period duration in one operational cycle;

t_c = a cycle time;

$Q_{wd} = Q_w t_w N_c$, the sludge volume wasted per day;

X_0, X_w and X_e = biomass concentrations in the influent, wasted sludge stream and effluent, respectively.

$\overline{M}_X$ is the average of total biomass during an operational cycle, which is the approach adopted by Lawrence and McCarty (1970) to handle the variable biomass concentration in modelling a PFR system.

The reactive time fraction, φ, applies to $\overline{M}_X$ but not to the term of biomass yield because substrate degradation is controlled by the effective biomass which includes the reactive time fraction. The term of biomass yield is only a stoichiometric parameter.

Assuming the total mass change in the system is negligible after a quasi-steady state is reached around the entire system ($d\overline{M}_X/dt = 0$) and biomass in the influent equals zero, Eq. (5-24) becomes:

$$\frac{1}{\theta_{xob}\,\varphi} = Y\frac{Q_d(S_0 - S_e)}{\overline{M}_X\,\varphi} - k_e \qquad (5\text{-}25)$$

where θ_{xob} is observed sludge age and calculated by

$$\theta_{xob} = \frac{\overline{M}_x}{Q_{wd}X_w + (Q_d - Q_{wd})X_e} \tag{5-26}$$

The term of $\theta_{xob}\,\varphi$ is a true sludge age or true mean cell residence time of an SBR system. Substituting $Q_d = Q_f\, t_f\, N_c$, $Q_f = (V_b - V_i)/t_f$ and $\overline{M}_x = V_b\overline{X}_v$ into the above equation yields:

$$\frac{1}{\theta_{xob}\,\varphi} = Y\frac{N_c(V_b - V_i)(S_0 - S_e)}{V_b\overline{X}_v\,\varphi} - k_e = Y\frac{N_c(1 - V_i/V_b)(S_0 - S_e)}{\overline{X}_v\,\varphi} - k_e \tag{5-27}$$

where $\overline{X}_v$ is average biomass concentration through the react period when the reactive liquid volume reaches its maximum at V_b.

Now Y and k_e can be calculated by Eq. (5-27) after influent concentration, treatment efficiency, observed sludge age and operational mode are determined. The slope of the line from the equation is Y and the absolute value of the intercept is k_e.

5.4.6. The Results of Experimental Testing k_e and Y

Table 5-8 lists the measurement results of k_e and Y based on 14 sets of tests. The average correlation coefficient was R = 0.966 which means the tested values of Y and k_e are highly reliable. If the aeration fraction φ is not included in the calculation, the Y value will not change but k_e will be φ times larger than its true value since $\varphi < 1$.

Table 5-8 The results of Y and k_e adjusted with φ in the SBR system

No.	t_{ed}	R_{tr} (g COD/g VSS day)			k_e	Y	Corr. R
-	(h)	SBR 1 ($\theta_{xob}\varphi$ = 3.3 - 4.2 d)	SBR 2 ($\theta_{xob}\varphi$ = 6.7 - 8.3 d)	SBR 3 ($\theta_{xob}\varphi$ = 10 - 12.5 d)	(d^{-1})	(gVSS/ gCOD)	-
2-25	3.5	1.099	0.536	0.465	0.0244	0.297	0.980
5-25	5	1.209	0.639	0.476	0.0261	0.270	0.999
	5	0.938	0.546	0.472	0.0864	0.414	0.991
5-50	5	1.029	0.639	0.449	0.0642	0.351	0.993
	5	1.141	0.659	0.474	0.0457	0.302	0.999
6-25	5	1.052	0.671	0.492	0.0846	0.363	0.994
6-50	5	1.298	0.797	0.502	0.0386	0.256	0.982
7-25	11	0.785	0.468	0.351	0.0516	0.371	0.999
	11	0.740	0.489	0.316	0.0514	0.385	0.939
7-50	11	0.855	0.526	0.362	0.0452	0.330	0.90
	11	0.871	0.528	0.393	0.0558	0.338	0.851
8-25	11	0.768	0.516	0.331	0.0539	0.373	0.924
8-50	11	0.874	0.471	0.379	0.0347	0.316	0.996
	11	0.828	0.482	0.386	0.0557	0.358	0.981
Average					0.0512	0.337	0.966

Table 5-9 provides the statistical information for the experimental estimation of the two parameters, which suggests that k_e equals 0.0512 ± 0.0106 d^{-1} and Y will be 0.337 ± 0.0259 g VSS/g COD at a 95% confidence level.

Table 5-9 Statistics for the measurement of Y and k_e in the SBR system

	k_e (d^{-1})	Y
Mean	**0.0512**	**0.337**
Standard Error	0.0049	0.012
Standard Deviation	0.0184	0.045
Sample Variance	0.0003	0.002
Range	0.0621	0.157
Minimum	0.0864	0.256
Maximum	0.0244	0.414
Count	14	14
Confidence Level (95.0%)	± 0.0106	± 0.0259

5.4.7. Determination of Switch Function Constant K_0

The switch function constant in Eq. (4-8) allows the degradation of DBS when EBS concentration is very low or stops the degradation of DBS if the EBS concentration is high. The value of K_0 is determined by trial and error. The computer program developed to simulate an SBR process can also be used to predict results from a BR test by setting influent flow rate to zero. Several K_0 values were carefully selected for the batch test simulation and one or two values were chosen that made the dS'/dt curve smooth at the inflection from dS_1/dt to dS_2/dt range. This K_0 value was put into the SBR model for computer simulation. If the operational results were not predicted with this K_0 value, it was adjusted slightly until good simulations were obtained. It was found that K_0 ranged between 20 to 40 and 30 was around the best value. Therefore, $K_0 = 30$ was used in all simulations.

CHAPTER 6 DYNAMIC MODELING OF SBR WITH MEASURED KINETIC AND STOICHIOMETRIC PARAMETERS

6.1. NEW MODEL SIMULATION OF SBR PROCESS

The new SBR model is solved by a computer program which is able to simulate the acclimatization of the system until it reaches steady state when any change of kinetic coefficients or initial conditions is given. Then the final simulation results of an SBR operational cycle are output. If the initial or intermediate value of a parameter exceeds the model's boundary, the program will indicate a failure of simulation and terminate. This function is especially important for maintaining a proper sludge concentration at the beginning of a cycle. Otherwise, the simulation would produce an unreasonable result.

To verify the new SBR model, the 48 SBR experimental runs (refer to Table 3-2 for details on the runs) were to be simulated with the model.

Table 6-1 lists the ranges of the kinetic and stoichiometric parameter values for the SBR system with the vegetable protein as feed. Except for the value of K_0 and conversion coefficients for UAP and BAP, γ_{s_3} and γ_X, all other parameter values were experimentally measured according to the approaches developed in the previous sections. One set of parameter values that were the middle values of the data listed in Table 6-1, was selected for the computer simulation of the 48 SBR experimental runs with the new model.

Table 6-1. The typical range of kinetic and stoichiometric parameters of the new SBR model

Parameters	Values	Units
k_1	11 to 13	d^{-1}
K_{s_1}	87 to 100	mg/L
k_2	0.07 to 0.09	$(mg/L\text{-}d)^{-1}$
K_0	20 to 40	mg/L
k_e	0.050 to 0.052	d^{-1}
Y	0.30 to 0.35	mg/mg
f_1	0.31 to 0.33	–
f_2	0.63 to 0.67	–
f_3	0.02 to 0.03	–
f_{x_1}	0.93 to 0.96	–
f_{x_2}	0	–
f_{x_3}	0.04 to 0.07	–
$\gamma_s = A_s/(C_s + \theta_x)$	0.3 to 1.8	–
$\gamma_x = A_x/(C_x + \theta_x)$	0.01 to 0.05	–

Of the 48 experimental runs, 13 failed because the initial reactor volume, V_i, was unable to maintain the amount of sludge required for the designed sludge ages. These failures were three runs of set No. 2-500, three runs of set No. 3-250, one run of set No. 3-500 and six runs of the No. 4 series. All the runs that failed occurred with V_i = 1/3 V_b, (the lower V_i of the two experimental design values), and higher L_{vtr}. Logically, all six runs of set No. 1 did not operate because they had the highest L_{vtr} and lower V_i. Although the volumetric loadings for three runs of set No. 3-250 and six runs of No. 4 series were not high, their failure was caused by fixing V_i = 1/3 V_b at the beginning of acclimation and poor sludge settling and compacting qualities caused the sludge to be washed out during

each operational cycle. The proper procedure should be to reduce V_i gradually until reaching the designed value during acclimation, since sludge settling and compacting qualities could be improved as acclimation occurs. However, the sludge SVI, the key parameter describing sludge settling and compacting qualities, can never be recovered if the sludge concentration is far below the value required for the volumetric loading rate.

An SBR system is prose to this situation if V_i is low. The amount of sludge above V_i is removed each cycle and the remaining amount of sludge is unable to meet the designed L_{vtr}. The above analysis also suggests that V_i is the most restrictive operational parameter for the SBR system. Section 9.5 will discuss the operational constraints of an SBR in detail.

Figures 6-1 to 6-10 are the results of the new model predictions for the experimental runs of the SBR system. The left side of each figure is the soluble COD remaining vs time during an operational cycle and the right side is the VSS vs cycle time. The designed operational mode or the Set No. of the run is at the top of each curve. The last number of the Set No. is the observed sludge age (defined in Section 5.4.5).

General observation of these figures reveals that the model successfully simulates the actual performances although the cycle modes vary from t_f/t_r =1.5/0.5 to 2.0/3.0, with a wide range of L_{vtr} from 545 to 3429 mg COD/L d and t_{ed} (see Chapter 8) from 3.5 to 11 h. The model also depicted well the operations with different true sludge ages ranging from 3.33 to 10 d (observed sludge age from 5 to 15 d).

All the soluble COD curves quickly ascend at the beginning of the fill stage. This is

because the rate of substrate degradation is less than the feed addition rate. Acclimation of microorganisms to the substrate could be a factor and also there is less liquid volume to dilute the feed. The driving force of substrate concentration in reaction expressions is still low which also predicts a lower reaction rate. After this period, substrate degradation is accelerated in accord with a higher substrate concentration driving force in the reaction rate expression, which reduced the accumulation of feed, then reached an equilibrium with feed rate. The curves become flat at this moment. This trend persisted until fill ended. Some curves have a slight downward trend at the later fill stage, such as runs No. 3-500-5, No. 3-500-10, No. 5-250-10, No. 5-500-10, No. 5-500-15, No. 6-500-15, No. 7-500-5, No. 7-500-10, No. 7-500-15. In these runs, sludge concentrations were higher, corresponding sludge ages were longer, and there was more degradation of substrate. These reactors have the capacity to accept more substrate than provided.

At the point of feed termination, the curves turned down sharply. The equilibrium of degradation and feed addition was broken by feed termination and by consumption of the remaining substrate in the solution. The downward trend of the curves became more gentle and later flat, with the complete consumption of fed substrate and the production of UAP and BAP.

Finally some curves, such as those for runs No. 2-250-15, No. 3-500-15, No. 6-500-10, No. 6-500-15, No. 7-500-10, No. 7-500-15, and nearly all No. 8 runs rose slightly because of large accumulation of BAP at higher sludge concentrations which lowered the sludge loading and caused more sludge decomposition. Careful observation of the curves reveals that the final rise of the curve occurred only in the longer react modes: t_r = 60 min

for series No. 2 and No. 6, and t_r = 120 min for series No. 3 and No. 7 and t_r = 180 min for series No. 8. Comparing runs No. 5 with No. 6 and No. 7 with No. 8, on the other hand, shows that shorter fill time did not affect the effluent quality. Furthermore, those runs that had a slightly downward trend in the COD curve at the higher flat range can treat more substrate during the fill phase and have potential to shorten their t_f. The above two analyses suggest that cycle time could be shortened by shortening both t_f and t_r in order to ensure better effluent quality by control of sludge decomposition from over reaction or aeration after feed termination. Shortening t_f and t_r is equivalent to shortening t_{ed} which means more efficient HRT because of its PF type kinetics, especially for influent containing mainly EBS.

In each set of runs, the COD curve rose higher for the lower sludge age reactor and descended for the longer sludge age reactor. The reason is that the longer sludge age reactor contained a higher sludge concentration which could degrade more substrate within the same period.

Also among each set of runs, the reactor with the longer sludge age produced better effluent quality. In set No. 5-250 in Fig. 6-3, for example, SBR3 had a 15 d sludge age with VSS of 6000 mg/L at the beginning of the cycle and VSS at about 3000 mg/L at the end of the reaction phase producing an effluent with around 20 mg/L soluble COD, whereas SBR1 with a 5 d sludge age and about 2400 mg/L VSS at the beginning of the cycle decreasing to 1200 mg/L at the end of the cycle generated an effluent of about 30 mg/L COD. SBR2 had an effluent COD closer to that of SBR3 with a 10 d sludge age. The situation for the No. 5-500 series is very similar. The model predictions clearly show

this difference among the three runs. From the end of the solid line, it can be found that the predicted COD is 15 mg/L for SBR3 effluent, 17 mg/L for SBR2 and about 22 mg/L for SBR1.

One more phenomenon can be observed from these figures. The run with higher S_0 produced higher S_e. In the No. 5 series, for example, the three runs with S_0 = 250 mg/L and three sludge ages generated effluents with COD concentrations at approximately 16, 18 and 22 mg/L respectively, while the three runs with S_0 = 500 mg/L and same three sludge ages produced effluents with COD concentrations at approximately 28, 31 and 40 mg/L, respectively. These results demonstrate that the effluent concentration would rise but not be doubled when doubling the influent concentration and it supports the conclusion in Section 5.3. The main explanation for this is that the released BAP and UAP could be degraded to a greater extent under longer reaction time or HRT (Grady and Blachly 1985).

The new SBR model prediction of VSS concentration changes within the operational cycle were very close to the experimental data.

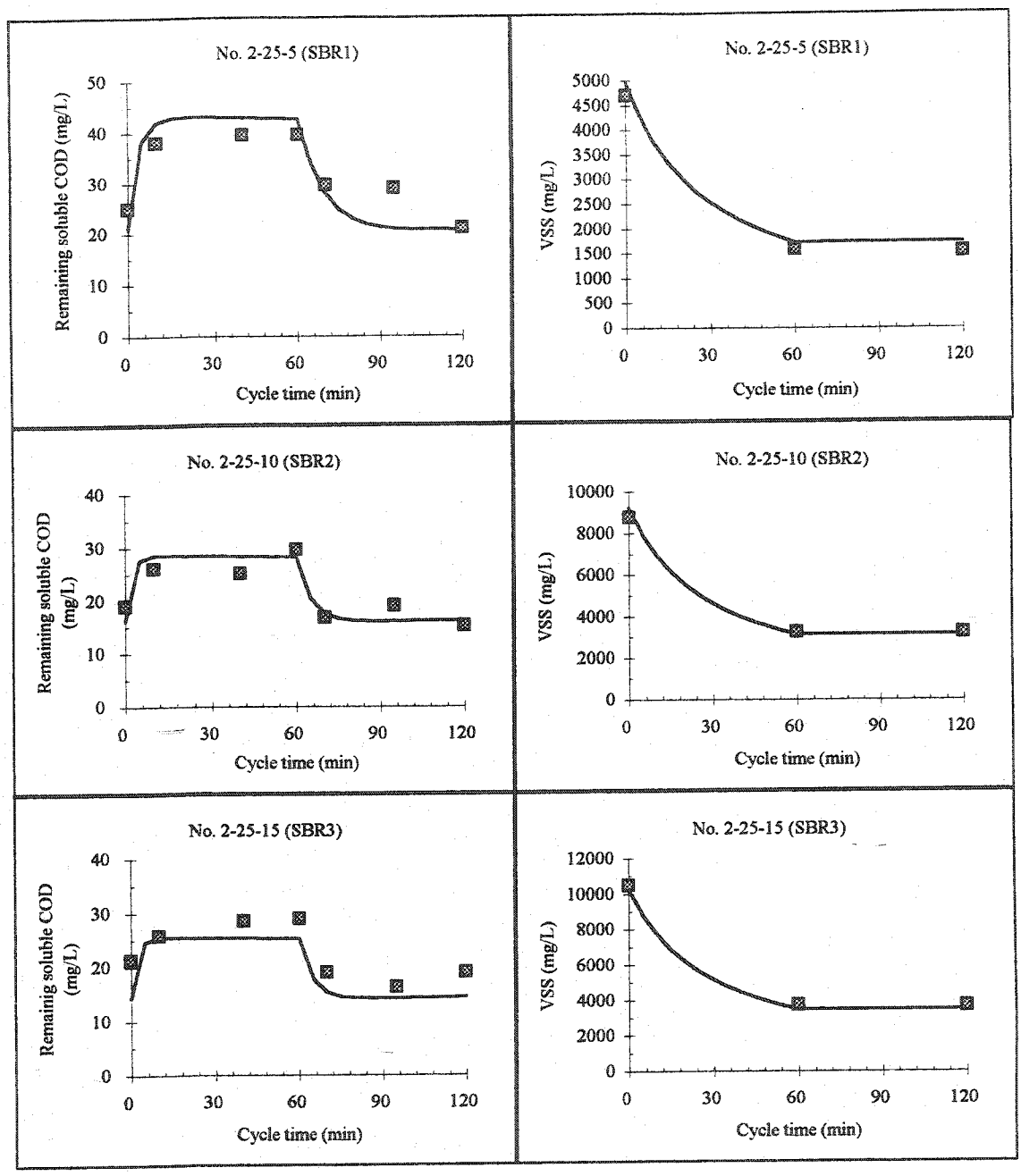


Figure 6-1 New model prediction of SBR performance: Experimental series No. 2-250, the left side showing remaining soluble COD and right side VSS changes within one operational cycle. (Line: model prediction; Marker: experimental verification)

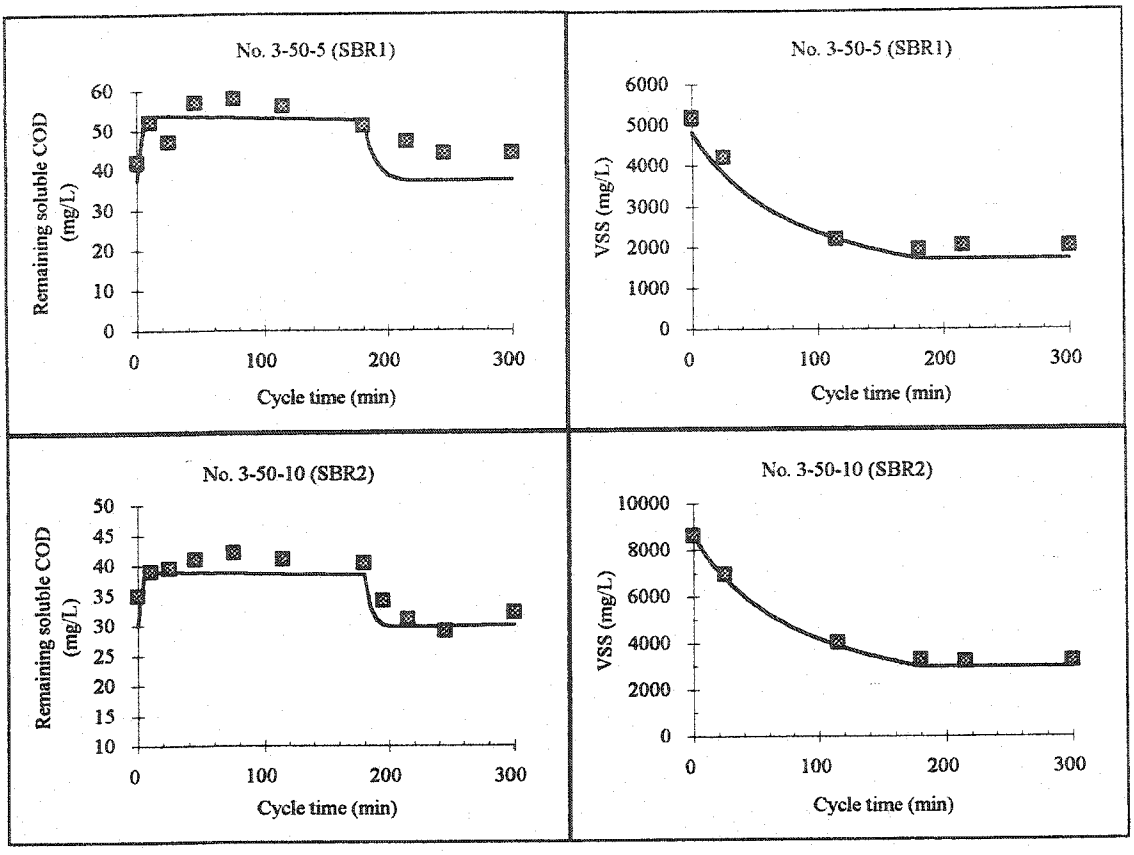


Figure 6-2 New model prediction of an SBR performance: Experimental set No. 3-500 series, the left side showing remaining soluble COD and right side VSS changes within one operational cycle. (Line: model prediction; Marker: experimental verification)

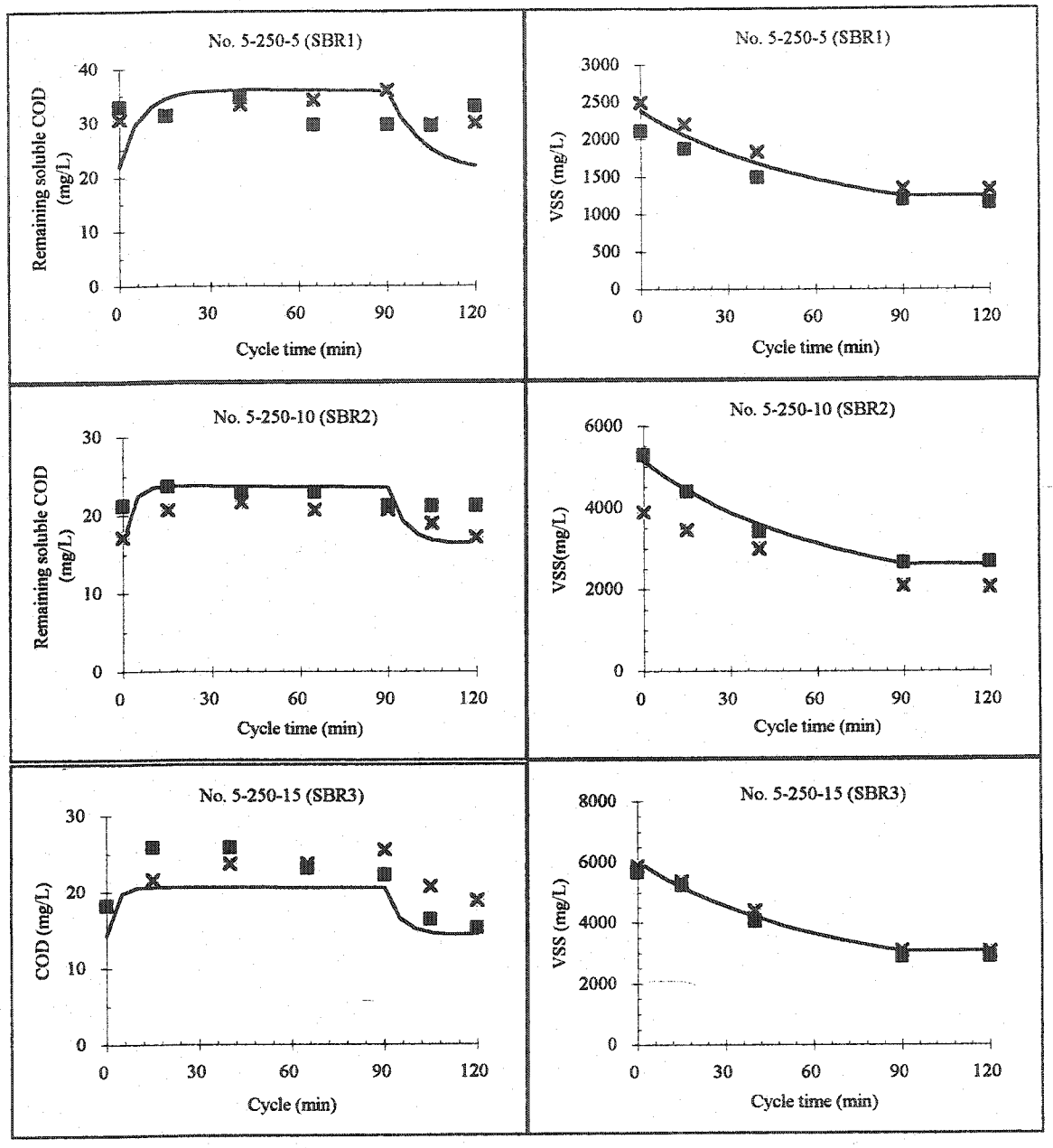


Figure 6-3 New model prediction of SBR performance: Experimental series No. 5-250, the left side showing remaining soluble COD and right side VSS changes within one operational cycle. (Line: model prediction; Marker: experimental verification)

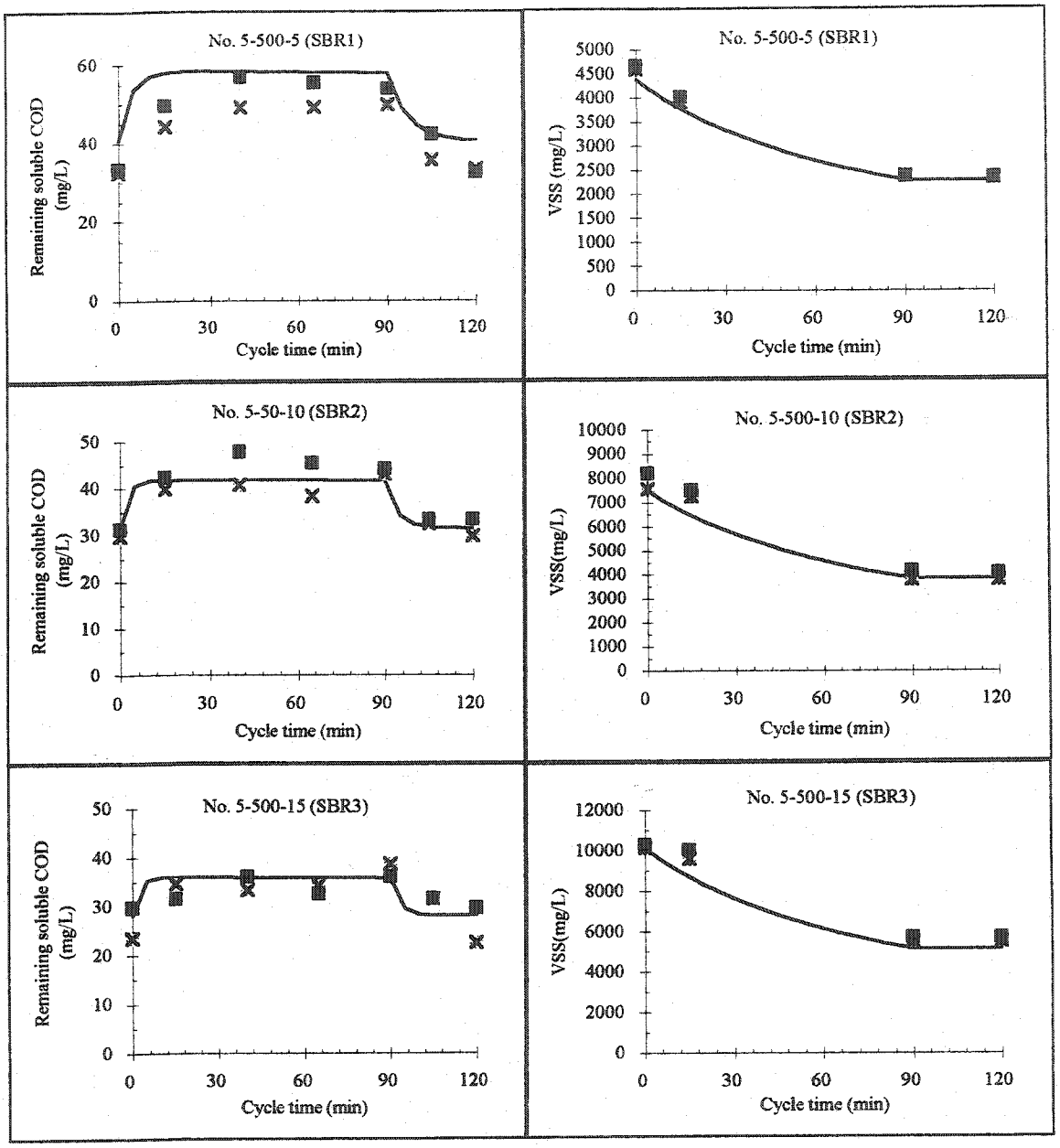


Figure 6-4 New model prediction of SBR performance: Experimental series No. 5-500, the left side showing remaining soluble COD and right side VSS changes within one operational cycle. (Line: model prediction; Marker: experimental verification)

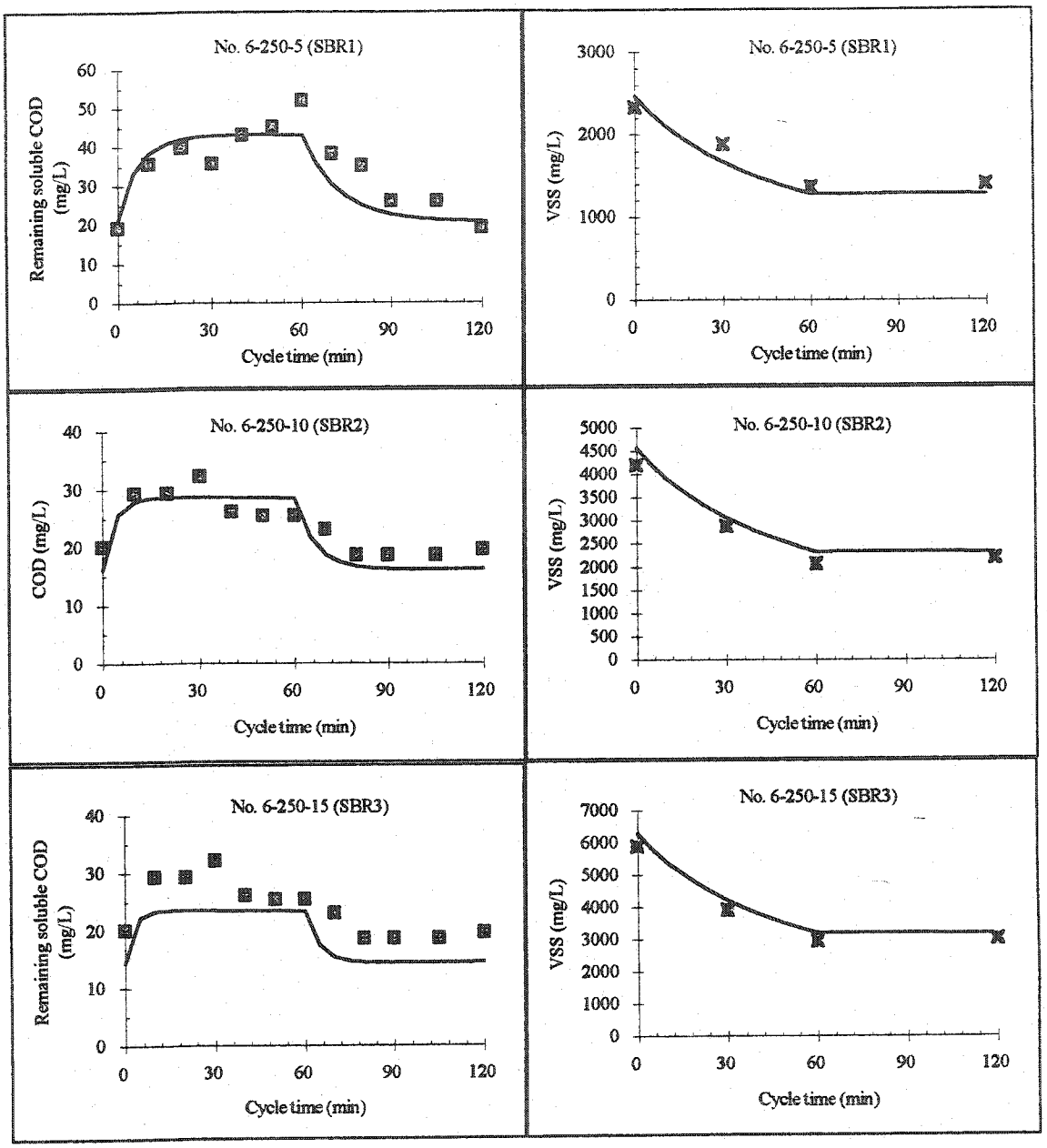


Figure 6-5 New model prediction of SBR performance: Experimental series No. 6-250, the left side showing remaining soluble COD and right side VSS changes within one operational cycle. (Line: model prediction; Marker: experimental verification)

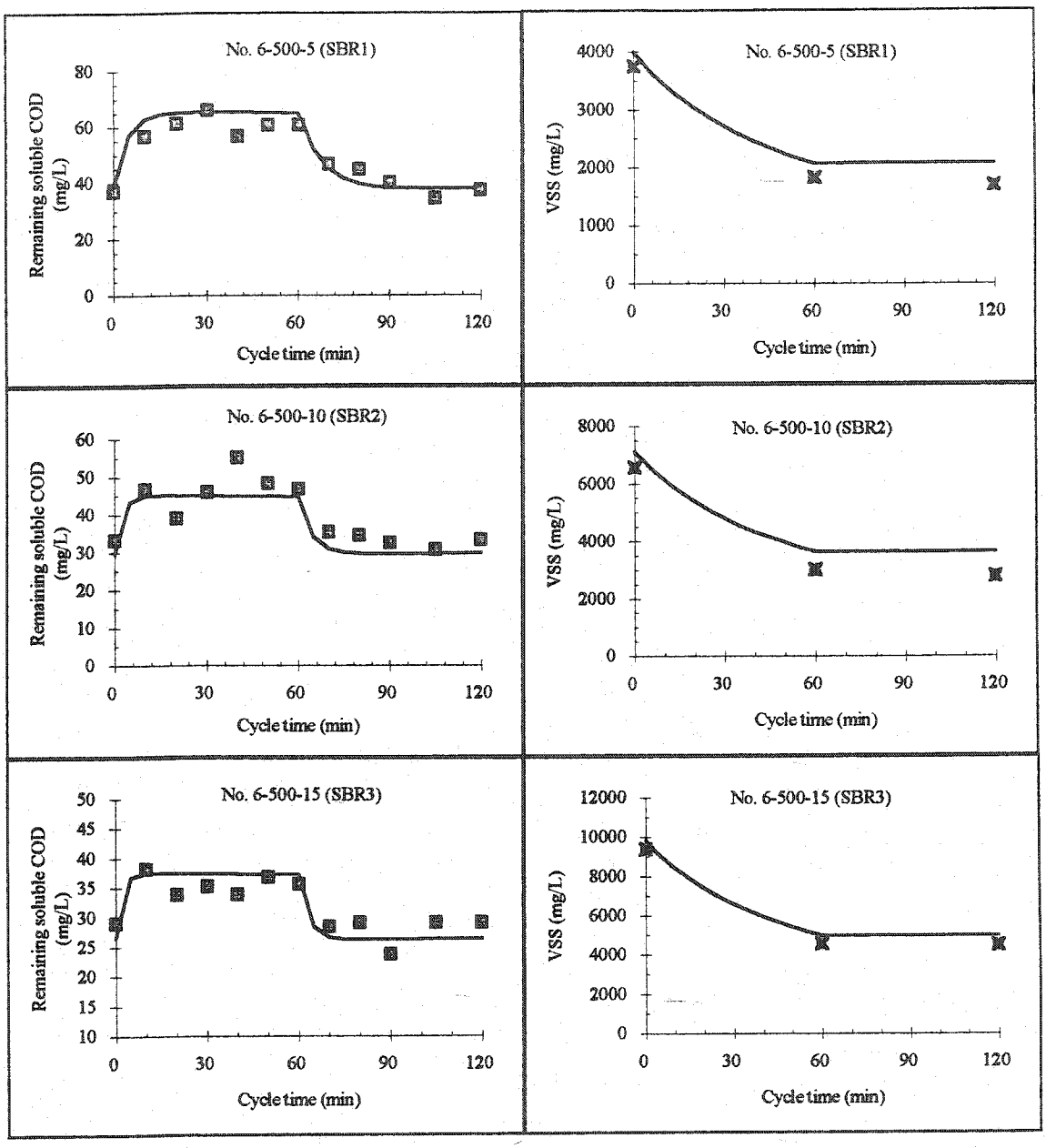


Figure 6-6 New model prediction of SBR performance: Experimental series No. 6-500, the left side showing remaining soluble COD and right side VSS changes within one operational cycle. (Line: model prediction; Marker: experimental verification)

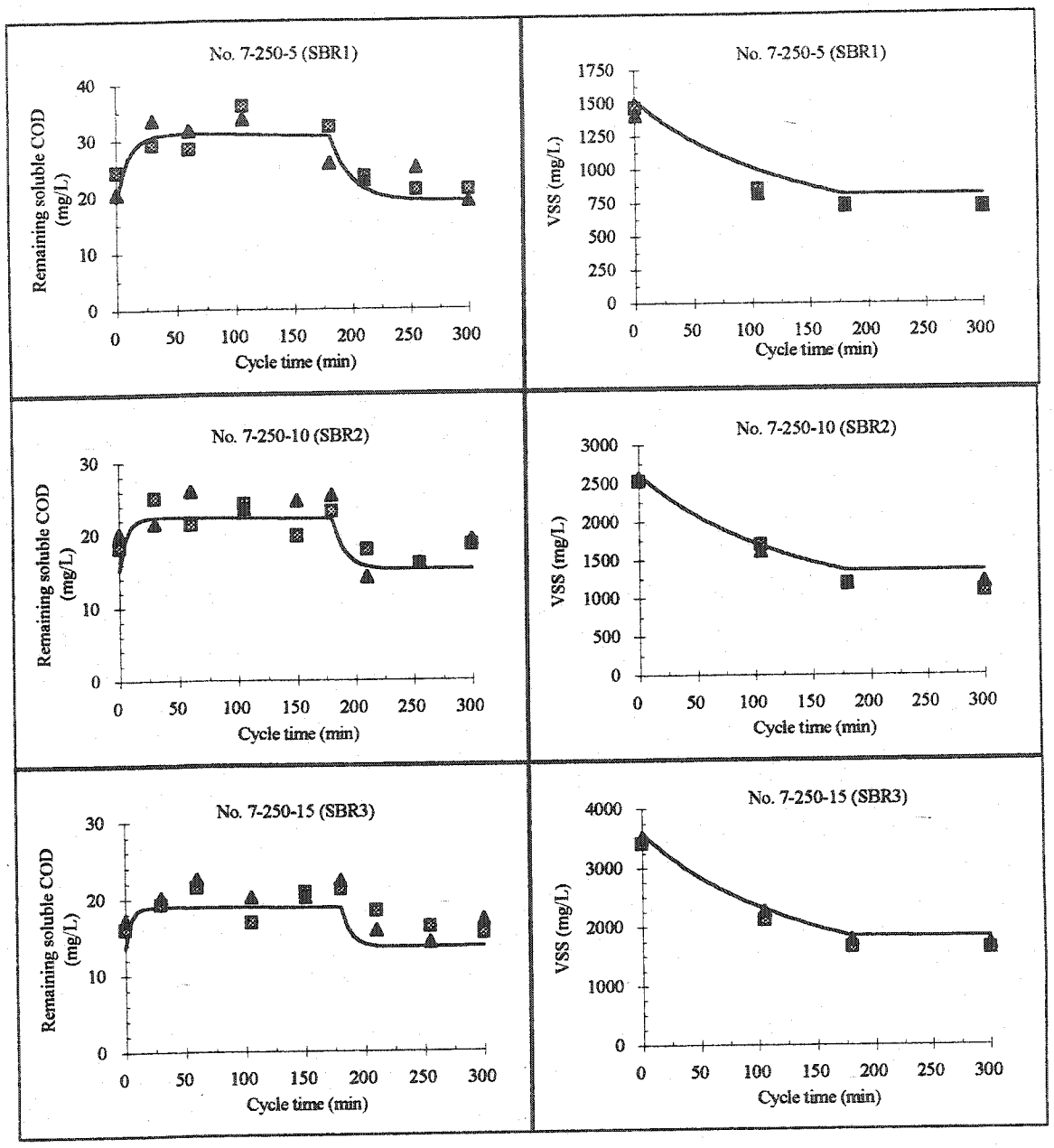


Figure 6-7 New model prediction of SBR performance: Experimental series No. 7-250, the left side showing remaining soluble COD and right side VSS changes within one operational cycle. (Line: model prediction; Marker: experimental verification)

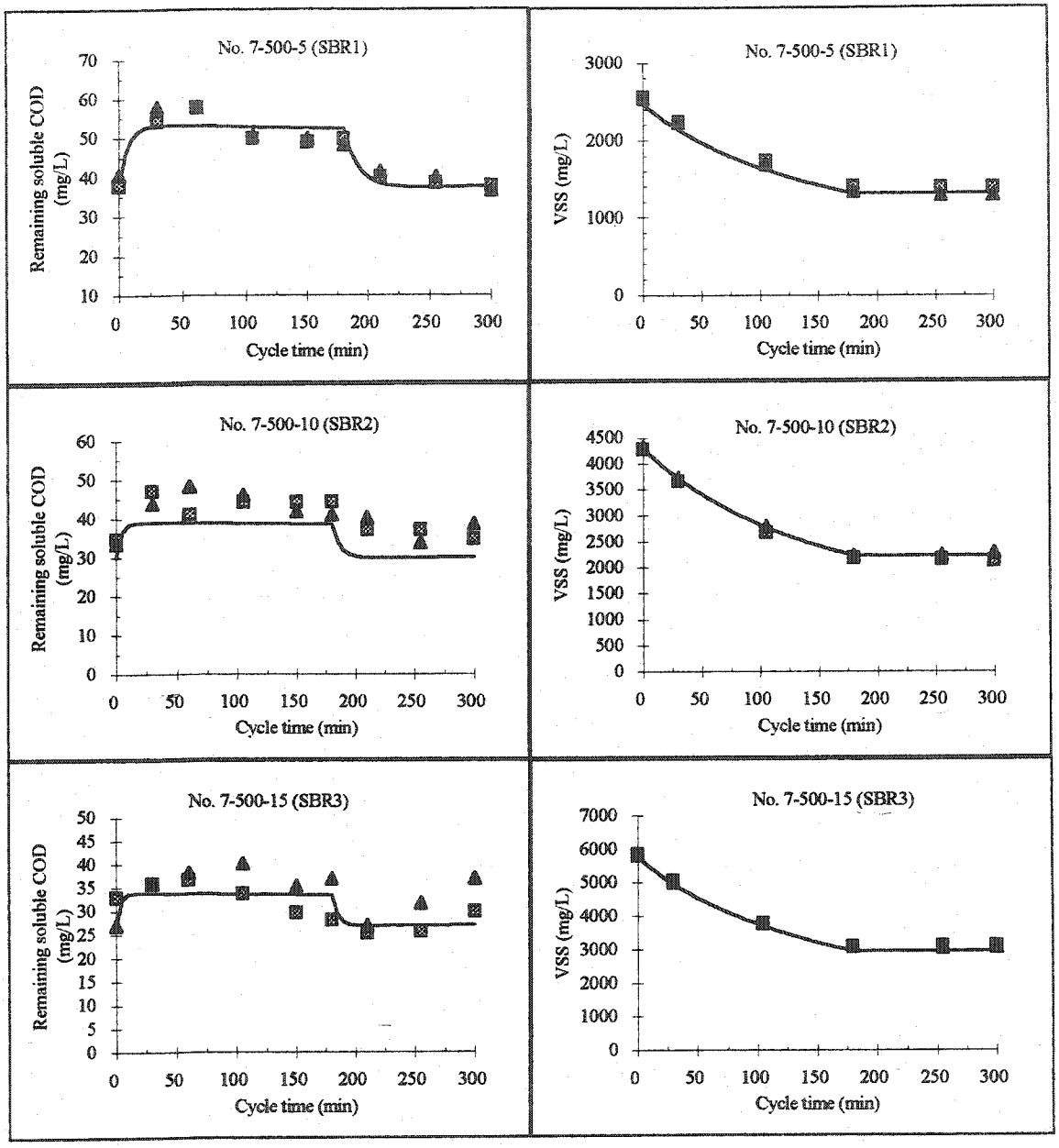


Figure 6-8 New model prediction of SBR performance: Experimental series No. 7-500, the left side showing remaining soluble COD and right side VSS changes within one operational cycle. (Line: model prediction; Marker: experimental verification)

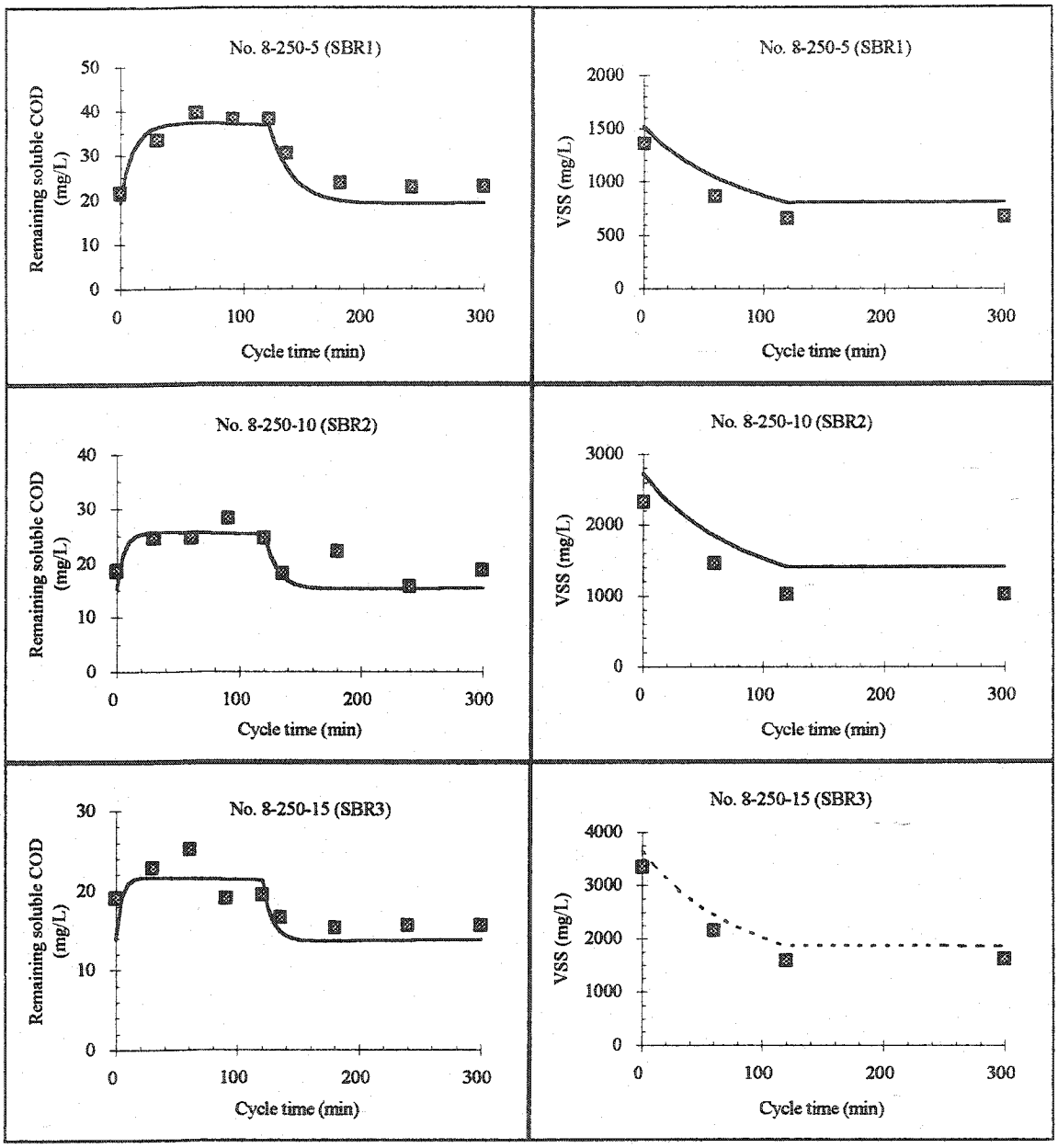


Figure 6-9 New model prediction of SBR performance: Experimental series No. 8-250, the left side showing remaining soluble COD and right side VSS changes within one operational cycle. (Line: model prediction; Marker: experimental verification)

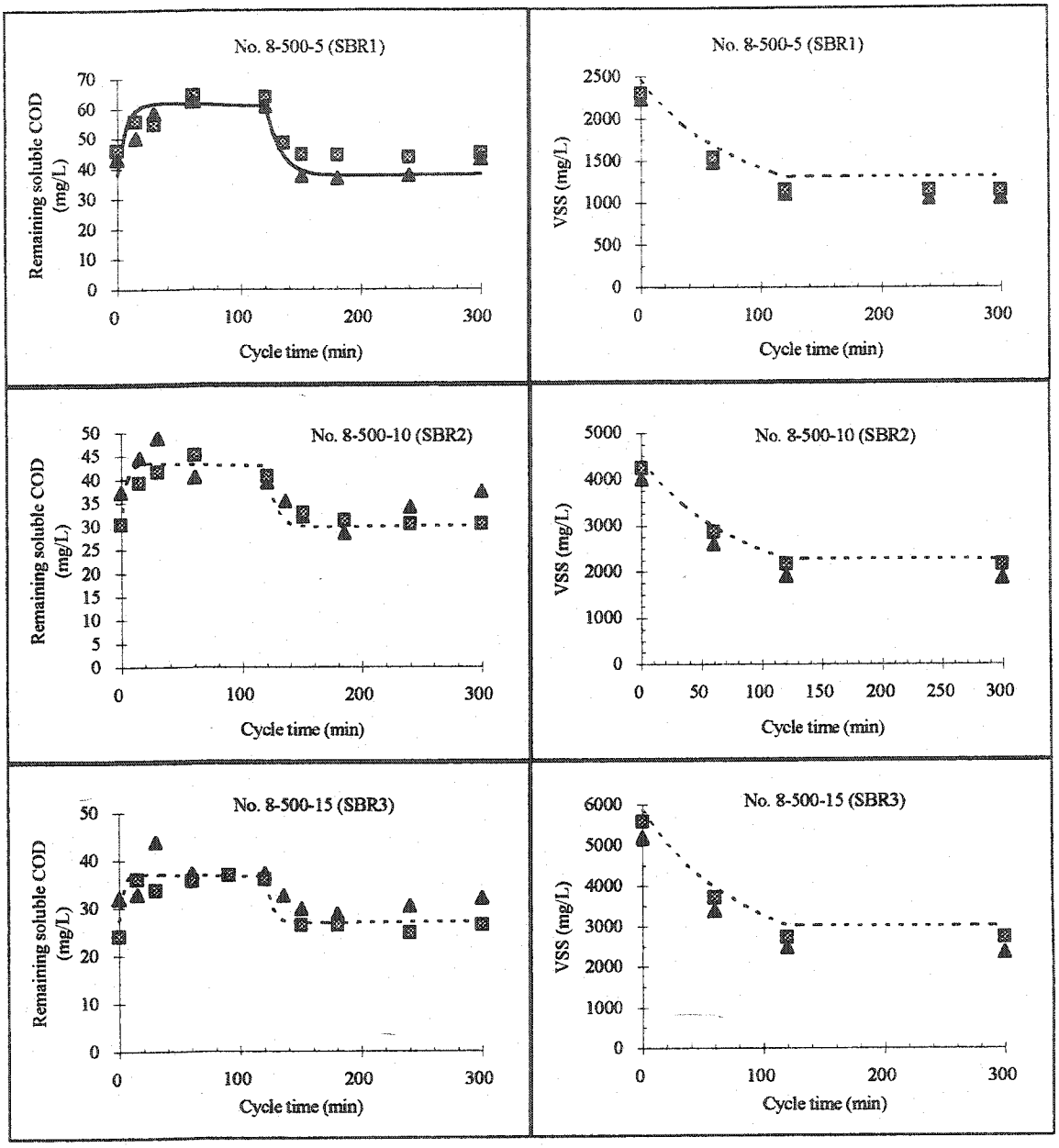


Figure 6-10 New model prediction of SBR performance: Experimental series No. 8-500, the left side showing remaining soluble COD and right side VSS changes within one operational cycle.

(Line: model prediction; Marker: experimental verification)

6.2. PRELIMINARY STATISTICAL ANALYSIS FOR THE FIT OF THE NEW SBR MODEL

From Section 6.1, it can be seen that the new model with one set of measured parameters depicted SBR performance well over a wide range of operational modes. In this section, analysis of variance (ANOVA) is employed to evaluate the success of the new model.

Assume y_u is a vector of the u'th experimental measurement at each time interval during an SBR operational cycle, η_u is a vector of the new model's predicted results for the u'th reading and ε_u a vector of random errors for the u'th set of tests. The relation of the three vectors can be expressed by the following equation:

$$y_u = \eta_u + \varepsilon_u \qquad (u = 1, 2, \ldots\ldots, n \text{ test}) \tag{6-1}$$

All the measured soluble COD results from the SBR cycle tests are taken as the observed data set, y_u, with random errors, ε_u, and the model simulation readings at the corresponding time (to the experimental measurement) intervals as the predicted data set, η_u. Each data set is in a column and each time interval is a row. There is a pair of data (the u'th set), predicted and observed, in each row. Total pairs of the data are n = 389. Any pair of data is independent from any other because there is no relation between any two measurements at different time intervals. The relation of the two data sets or columns is to be determined.

Equation (6-1) is equivalent to a linear regression equation

$y_a = b_0 + bx_a + \varepsilon_a$

where, a = 1, 2, ..., n, is n times of tests, or measurements with $b_0 = 0$ (the line passes through the origin) and b = 1 (the slop of the regression equation is 45°). Therefore, the following method is used as a preliminary statistical analysis for the fit of the new SBR model.

H_0: b = 0, is hypothesized to check the linear relation of Eq. 6-1. It can be proved that, the sum of regression variance squares with degrees of freedom ($df_R = 1$), $S_R / \sigma^2 \sim \chi^2$ (1), the sum of error variance squares with degrees of freedom ($df_{err} = n - 1$), $S_{err} / \sigma^2 \sim \chi^2$ (n – 1), and the two are independent each other, and sum of total variance squares, $S_T = S_R + S_{err}$, with degrees of freedom ($df_T = n$).

Then, it is quite common to use $F < F_\alpha$ (1, n – 1) relation to confirm the above hypothesis, where, $F = (S_R/df_R)/(S_{err}/df_{err})$. If $F > F_\alpha$ (1, n – 1), which means $b \neq 0$ and a linear relation between y and x is significant.

The following statistical parameters can be determined from the data in Appendix I. Preliminary values are listed in Table 6-2. Table 6-3 is the ANOVA results.

From Table 6-3, it can be seen that the F value of S_R, 3867.2, is much larger than $F_{\alpha = 0.001}$ (388, 1) = 1.37 at $\alpha = 0.001$ or a 99.9% confidence level. This indicates that the linear relation between y and η is significant. Thus, the model's predicted results are significant for the experimental measurements and the model is satisfied.

Table 6-2 Preliminary values of ANOVA calculation

$\bar{y} = 32.61$	$\bar{\eta} = 31.40$	
$\Sigma y = 12685$	$\Sigma \eta = 12214$	
$\Sigma y^2 = 464138.6$	$\Sigma \eta^2 = 442235.8$	$\Sigma y\eta = 450089.6$
$(\Sigma y)^2 = 1.61E+08$	$(\Sigma \eta)^2 = 1.49E+08$	
$(\Sigma y)^2/n = 413616.4$	$(\Sigma \eta)^2/n = 383495.7$	$(\Sigma y \Sigma \eta)/n = 398271.4$
$l_{yy} = \Sigma y^2 - (\Sigma y)^2/n$ $= 50522.2$	$l_{\eta\eta} = \Sigma y^2 - (\Sigma y)^2/n$ $= 58740.1$	$l_{y\eta} = \Sigma y\eta - (\Sigma y \Sigma \eta)/n$ $= 51818.2$

Table 6-3 The final results of ANOVA for the new SBR model fit

Source of variance	S	df	MS	F	$F_{\alpha=.001}$ (388,1)
Regression	$(l_{y\eta})(l_{y\eta}/l_{\eta\eta}) =$ 45711.9	1	45711.9	3867.2	1.37
Error	$(l_{yy}) - (l_{y\eta})(l_{y\eta}/l_{\eta\eta}) =$ 4810.3	388	12.40		
Total	$l_{yy} =$ 50522.2	389			

Figure 6-11 is a plot of the predicted results against the observed results. From the plot, the linear relationship between the two data sets is remarkable with R = 0.94 or $R^2 = 0.88$ (Table 6-4).

Table 6-4 Regression results between the model predictions and the experimental measurements

Multiple R	0.938156
R^2	0.880137
Standard Error	3.950645
Observations	389

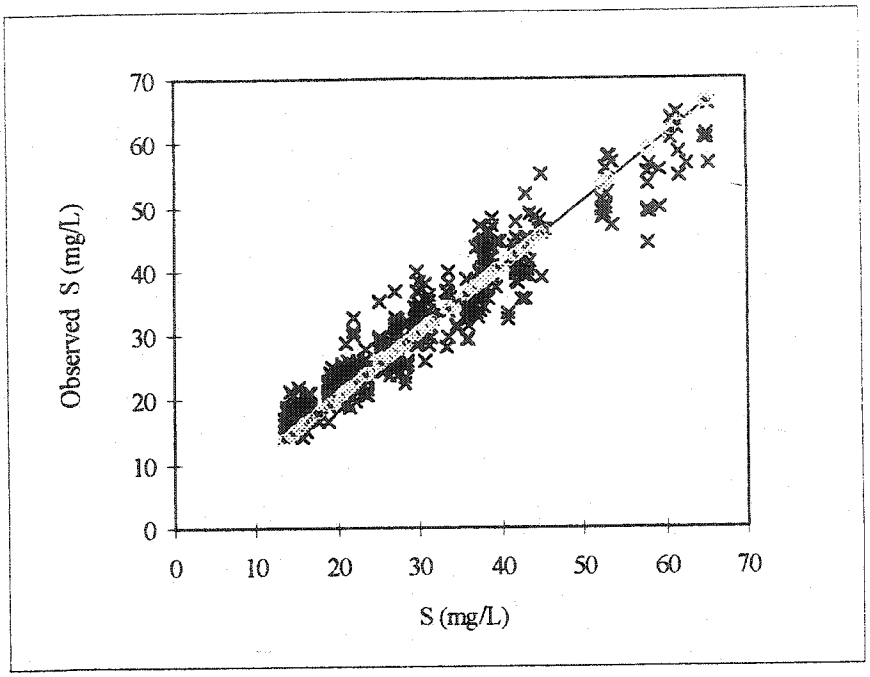


Figure 6-11 The fit of the model predicted results

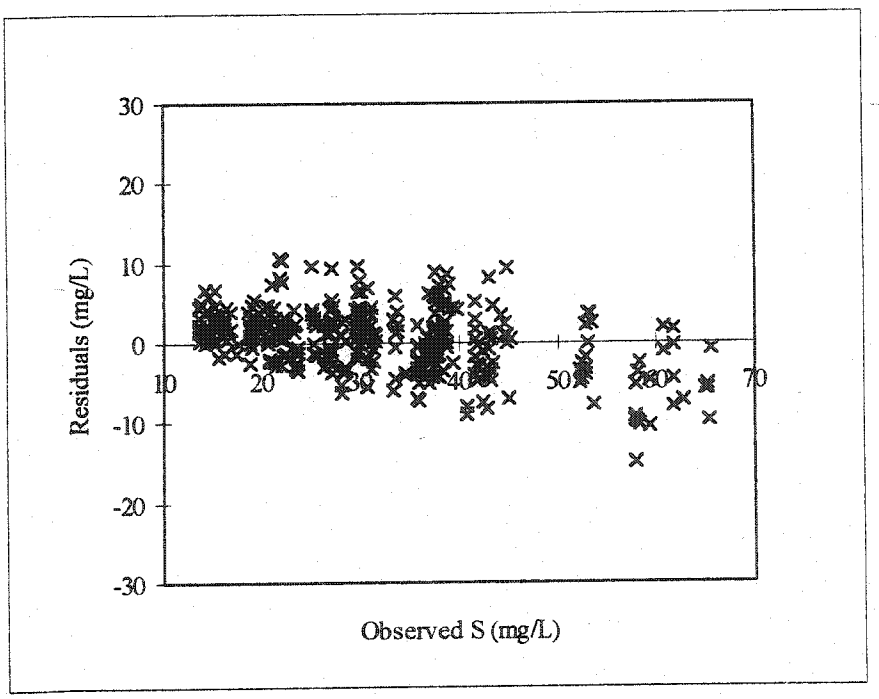


Figure 6-12 The residuals of the observed results

Figure 6-12 presents a plot of the residuals of the observed results. The residual distribution is basically even, although a slightly downward trend exists.

Both Figs. 6-11 and 6-12 confirm that the model successfully predicted the SBR performance over a wide range of operational modes.

Another statistical method to determine the relationship of the two data sets is correlation, ρ, which is used to measure the closeness level of the two data sets moving together if they are linearly related. The correlation is calculated by dividing the covariance of the two data sets by the product of their standard deviations, i.e.,

$$\rho_{x,y} = \frac{\text{Cov}(X,Y)}{\sigma_x \sigma_y} \qquad (-1 \le r \le 1) \qquad (6\text{-}2)$$

where $\rho_{x,y}$ = the correlation of the two data sets;

Cov (X, Y) = covariance of the two data sets;

σ_x and σ_y = the standard deviations of the two data sets.

From the total 389 pairs of data, it was found that $\rho = 0.951$ (Table 6-5) which shows that the predicted S has a strong relation to the observed S.

Table 6-5 The results of the correlation of the two data sets

	Predicted S	*Observed S*
Predicted S	1	
Observed S	0.951	1

CHAPTER 7 CONCLUSION OF PART I: DYNAMIC MODELLING SBR SYSTEM

SBR technology has been an innovation in the past two decades and has been increasingly used in wastewater treatment due to its kinetic and operational advantages. Previous SBR models predicted SBR behaviors to a certain extent but have obvious deficiencies. One of them is that the models were unable to properly depict the performance after the fill period. The major reason is that the models do not address soluble COD formation from both substrate degradation and sludge decay.

A new mathematical model has been developed for the SBR activated sludge system. It is based on the standard Lawrence and McCarty model and IAWPRC model No. 1 and contains four differential equations and one algebraic equation and twelve parameters.

In contrast with previous models, the most important developments of the new model are the consideration of different degradabilities of major classes of substrate and inclusion of the organic materials formed from substrate metabolism and released from activated sludge decay. In the new model total COD is divided into two parts: soluble and insoluble. The soluble part is further subdivided into EBS, DBS and biologically IOM. The classification of the substrate makes it possible to describe the degradation process of organic substance more precisely.

Addition of the expressions for soluble refractory COD formation from metabolism or from activated sludge decay, that contribute to the soluble COD in the clarified water and

significantly affect effluent quality, greatly improve the new model's accuracy and applicability.

It was found that the soluble COD from substrate metabolism is closely related to the type of substrate degraded while the soluble COD released from activated sludge decay is not. Experiments also revealed that the major portion of soluble COD from sludge decay (BAP) is easily biodegradable which is different from expectations.

Considering the major weaknesses of the IWAPRC model No. 1 and the applicability of the new SBR model, necessary simplifying work was done when adopting some features of the IWAPRC model and other related models, that leads to experimental measurement of most model parameters.

Quantitative test methods for the classification of the substrate have been devised to aid in characterizing and developing the coefficient values of the new SBR model. Batch test techniques were employed for measuring three different soluble COD categories, EBS, DBS and IOM, while considering the three portions formed or released from metabolism and sludge decay. The kinetic constants of the new model can also be estimated by the techniques. It was found that EBS degradation followed Monod kinetics and DBS followed a first-order reaction.

With the set of experimental testing methods, the measured kinetic constants and other coefficients, and supported by a computer program, the model successfully predicted SBR performance over a wide range.

PART II AN OVERALL COMPARISON OF SBR AND CFSTR SYSTEMS

CHAPTER 8 THEORETICAL COMPARISON OF SBR AND CFSTR SYSTEMS

SBR and CFSTR systems should be compared under equivalent conditions. The basic terms that can be used to compare the two systems are effective reactor volume which is truly "effective" in practice or under certain physical constraints of the operation, true HRT, volumetric loading rate and specific substrate loading rate (or sludge loading rate). For a CFSTR, these terms are easily expressed mathematically because of its "constant" hydraulic and kinetic conditions. However, there is no standard mathematical expression for any of these terms for an SBR reactor since it is running under an open and unsteady system during fill. The reactor volume (reaction liquid volume) varies (increases) greatly and the concentrations of both biomass and substrate are changing. Under a closed system during the react stage, substrate and biomass continue to change. Few researchers have examined the issue. Based on their long term work, Irvine and Ketchum (1989) reported that the above parameters are convenient for use in both design and operation calculations but not available due to the dramatic impact of aeration and mixing strategies on overall performance of an SBR system.

For an SBR system, there is no evaluation in the literature of true sludge age, effective reactor volume, true HRT, true sludge loading rate and true volumetric loading rate to date. The following sections develop these concepts as they pertain to SBR systems and compare them with those of a CFSTR.

8.1. THEORETICAL BASIS

The effective reactor volume is the space in which the reactive media, normally wastewater and biomass solids in a wastewater treatment process, can be held and reacted until a desired effluent quality is reached. For an SBR, the space depends on the reactive media or mixed liquor volume in the reactor. The time which accounts for the reactive media staying in the reactor is HRT or theoretical average liquid age.

In a CFS, there are two typical types of reactors: CFSTR and PFR. The flow pattern is CM in the former and PF in the later. Any other type of CFS reactor has a flow regime between these two extremes. The effective volume of any CFS reactor is its reactor volume (assuming no dead zone), V_c, which can hold the reactive media or liquid. It is fixed and constituent. The HRT, t_{dc}, is also determined and constant as long as a steady flow Q is delivered. For a given quantity of reactive media or wastewater with the flow rate Q, it needs time, t_{dc}, to complete reaction with biomass to reach a designed effluent quality. At least Qt_{dc} reactor volume is needed for the treatment. This amount of wastewater stays in the reactor for average time t_{dc} or the average liquid age equals t_{dc} although portions of the wastewater stay in the reactor shorter than t_{dc} and others longer than t_{dc} due to mixing, short-circuiting and dead zone in the reactor. But the average HRT in the reactor is still t_{dc} regardless of non-ideal flow patterns in the reactor.

In an SBR reactor, the hydraulic condition is CM while the kinetics are PF. At any reaction time and any position in the vessel, the situation is identical to that of a cross-section in an ideal PFR. Compared to a CFS, an important difference of an SBR is that

the volume of the reactive media is changing (increasing) during the fill period while that in a CFS is constant. This difference must result in a variable effective reactor volume for an SBR reactor. Another difference is that the operational phases of fill, react, settle, draw and idle take place in the SBR vessel, which leads to a significant reduction of effective reactor volume according to the preset operational mode. One more difference between an SBR and a CFS is that the biomass concentration in SBR is very high at the beginning of the fill period of a batch cycle and it decreases, as the reactor is filled, to concentration levels that exist with minor variation throughout a PFR and the constant concentration that exists in a CFSTR reactor at steady state. Because these hydraulic and kinetic conditions in an SBR system are different from those in CFSs, the approaches applied for the latter are no longer fully valid. Some new concepts and definitions are therefore needed for the former.

8.2. DROSTE'S APPROACH FOR THE RELATIONSHIP OF SBR AND CFSTR SYSTEMS AND FIRST ANALYSIS OF PHYSICAL CONSTRAINTS OF SBR OPERATION

Droste (1990) analyzed some operational constraints diminishing the above advantages of SBR. He concluded that the system model should incorporate these constraints.

It is well known that, in the batch system, reactor volume must be increased relative to a PFR reactor because of the additional time required to fill, draw and settle a BR. There are physical relationships between the two systems (Droste, 1990). For a given detention time, t_{dc}, in a CFSTR reactor, there is an equivalent detention time, t_{ed}, in an SBR reactor

based on an equal total volume in each system. The total volume in a CFSTR system consists of the reactor and the sedimentation basin. The SBR system is comprised of the number of tanks in the system. The following is Droste's derivation.

$$t_{dc} = \frac{V_c}{Q} = t_{ed} \tag{8-1}$$

where V_c is reactor volume of CFSTR system and Q is flow rate. But, for an n-tank SBR system,

$$nV_b = V_c + V_{sc}$$

where

$V_{sc} = Qt_{sc}$;

V_{sc} is the volume of the sedimentation basin in the CFSTR system;

t_{sc} = detention time of sedimentation in a CFSTR system;

V_b = volume of an SBR reactor.

$$V_c = nV_b - V_{sc} = nV_b - Qt_{sc} \tag{8-2}$$

From Eqs. (8-1) and (8-2)

$$t_{dc} = t_{ed} = \frac{nV_b - Qt_{sc}}{Q} \tag{8-3}$$

In an SBR system, the cycling time t_c is the sum of fill time, t_f, reaction time, t_r, settling time, t_s and draw time, t_w (idle time is neglected here), i.e.,

$$t_c = t_f + t_r + t_s + t_w = t_f + t_r + t_{sw} \tag{8-4}$$

where $t_{sw} = t_s + t_w$ is the non-aeration period.

If there are n reactors (n > 1) in the SBR system, no equalization basin for the system and a continuous flow is treated,

$$t_f = \frac{t_c}{n} \tag{8-5}$$

Eqs . (8-4) and (8-5) yield

$$t_r = (n-1)t_f - t_{sw} \tag{8-6}$$

The same flow rate Q as in the CFSTR system will apply to the SBR system and the initial volume in one SBR is V_i, therefore

$$Q = \frac{V_b - V_i}{t_f} \tag{8-7}$$

The two systems are related by the above equations. Under an equivalent condition, the total volume of an SBR system, compared to that of a CFSTR, should equal $V_c + V_{sc}$, the total volume of a CFSTR system. Systematic comparison between the two systems will be made in Chapter 9 under the above equivalent conditions.

8.3. THE EFFECTIVE VOLUME V_{ef} AND TRUE HYDRAULIC RETENTION TIME, t_{tr}, IN THE SBR SYSTEM

In an SBR system, as mentioned above, the reactor volume is partially used during the fill period, fully used in the stage of reaction, and completely idle as a sedimentation basin of a CFS during the settle and draw period, t_{sw}. The effective volume , V_{ef}, and the true HRT, t_{tr}, of an SBR reactor are different from those of a CFS reactor. Proper definitions of

these parameters is important for standardizing the design of SBRs.

8.3.1. Defining the Effective Volume, V_{ef}, and True HRT, t_{tr}, in an SBR System

For the estimation of effective volume and average age of reactive liquid or true HRT in an SBR, the operational characteristics must be considered and some assumptions must be made.

An operational cycle starts from fill. That is, at $t = t_0$,

$$V = V_i$$

After Δt at $t_0 + \Delta t$, the total liquid volume becomes

$$V_i + \Delta V = V_i + Q\Delta t$$

When $t = t_f$, the total liquid volume reach its maximum V_b.

$$V_b = V_i + Qt_f, \text{ or}$$

$$V_b - V_i = Qt_f$$

After t_f, the reactor enters react stage during which the volume as a reactor equals V_b and remains constant until the react period finishes. After the react period, the volume as a reactor equals zero,

$$V_b = 0$$

because the vessel is used as a sedimentation tank for the separation of liquid and solids and for decanting clarified water until the next cycle begins.

To develop the related mathematical expressions, consider the two extreme situations in

the effective periods. First, set fill at an infinitesimal t_f and large Q such that fill finishes instantly with a total fill volume of Qt_f. In this situation, the vessel acts as an ideal BR with a total volume of V_b throughout the entire react period. The effective volume (V_{ef}) of the reactor is given by

$$V_{ef} = V_b$$

For the whole cycle, the space-time under non-react periods must be deducted. V_b should be reduced by the reactive ratio of $(t_f + t_r)/t_c$, where t_r is the reaction time, and $t_f = 0$, therefore

$$V_{ef} = V_b \frac{t_r}{t_c}$$

In one cycle, the total amount of treated liquid is Qt_f. Averaging this volume throughout an entire cycle provides an equivalent flow rate, Qt_f/t_c, to that of a CFS. The true HRT of the reactive liquid in an SBR is now

$$t_{tr} = \frac{V_{ef}}{Q\frac{t_f}{t_c}} = V_b \frac{t_r}{t_c} \Big/ Q\frac{t_f}{t_c}$$

$$t_{tr} = t_r \frac{V_b}{V_b - V_i} \qquad (8\text{-}8)$$

The right side can be physically interpreted as the true HRT equaling react time, t_r, multiplied by the liquid dilution time of $V_b/(V_b - V_i)$.

The another extreme of operation is that fill period is carried out for the entire react period and $t_r = 0$. In this situation, the effective reactor volume is

$$V_{ef} = \frac{1}{2}(V_b - V_i) + V_i = \frac{1}{2}(V_b + V_i)$$

Consider this as the deduction of non-react time by multiplying the effective reactor volume by the aeration time ratio, $(t_f + t_r)/t_c$, and $t_r = 0$ in this case.

$$V_{ef} = \frac{1}{2}(V_b + V_i)\frac{t_f}{t_c}$$

and the true HRT is

$$t_{tr} = V_{ef} \Big/ Q\frac{t_f}{t_c}$$

$$= \frac{(V_b + V_i)t_f/t_c}{2Qt_f/t_c}$$

$$= \frac{(V_b + V_i)}{2Q}$$

But $Q = (V_b - V_i)/t_f$

therefore

$$t_{tr} = \frac{(V_b + V_i)}{2Q} = \frac{t_f(V_b + V_i)}{2(V_b - V_i)} = \frac{V_b}{V_b - V_i}t_f - \frac{1}{2}t_f \qquad (8\text{-}9)$$

The physical meaning of the left side is that true HRT equals fill time multiplied by the liquid dilution ratio minus half of the fill time because of the half utilization of the volume $(V_b - V_i)$ throughout the fill period.

From the above analysis of effective volumes and true HRT at the two extreme

operational conditions, the two parameters are variables and their values will be between the two end conditions. The procedure to derive general expressions for of V_{ef} and t_{tr} follows.

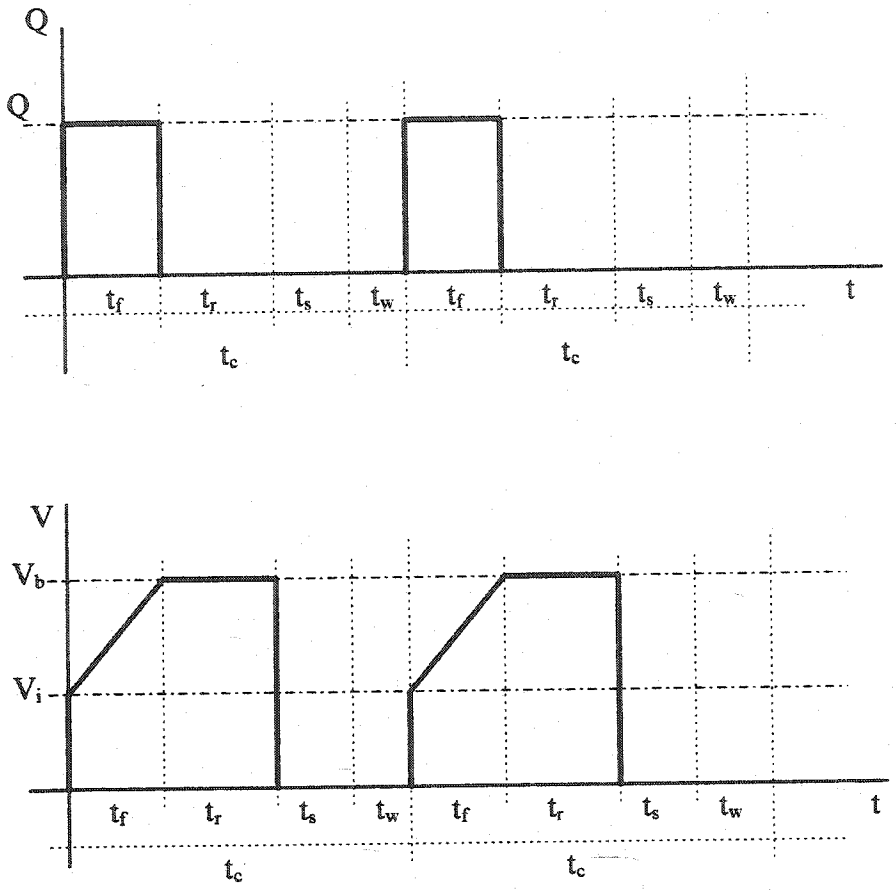


Figure 8-1 The effective reactor volume change in an SBR operational cycle

Figure 8-1 illustrates the relationship of flow rate Q, fill time t_f, and the liquid volume or effective volume change with time in an SBR operational cycle.

With start of fill, for a constant Q, liquid volume increases form its initial V_i at the rate of Qt. When fill ends and react starts, Q = 0 and the reactor volume reaches its maximum

that is maintained until react finishes. After react, the reactor transits to a settling tank and effective reaction volume equals zero until the beginning of the next cycle.

Based on the above description, the effective volume, or, the average liquid volume occupying the reactor over one operation cycle is:

$$V_{ef} = \frac{1}{t_c}\left(\int_{t_0}^{t_1} v\,dt + \int_{t_1}^{t_2} v\,dt \right)$$

where $(t_1 - t_0) = t_f$ and $v = V_i + Qt$ in the fill stage and $(t_2 - t_1) = t_r$ and $v = V_b$ in the react stage. To consider the reactor volume used as a "reactor" under aeration time within a cycle, the integration expression is divided by t_c. Substituting for v

$$V_{ef} = \frac{1}{t_c}\left(\int_{t_0}^{t_1} (V_i + Qt)dt + \int_{t_1}^{t_2} V_b dt \right) = \frac{1}{t_c}\left[V_i(t_1 - t_0) + \frac{1}{2}Q(t_1 - t_0)^2 + V_b(t_2 - t_1) \right]$$

$$= \frac{1}{t_c}\left(V_i t_f + \frac{1}{2}Qt_f^2 + V_b t_r \right)$$

But $Qt_f = (V_b - V_i)$, therefore,

$$V_{ef} = \frac{1}{t_c}\left[V_i t_f + \frac{1}{2}(V_b - V_i)t_f + V_b t_r \right]$$

$$= \frac{1}{t_c}\left(V_i t_f + \frac{1}{2}V_b t_f - \frac{1}{2}V_i t_f + V_b t_r \right)$$

$$= V_b \frac{t_f + t_r}{t_c} - \frac{1}{2}(V_b - V_i)\frac{t_f}{t_c}$$

$$V_{ef} = V_b\varphi - \frac{1}{2}(V_b - V_i)\frac{t_f}{t_c} \quad (8\text{-}10)$$

where

$$\varphi = \frac{(t_f + t_r)N_c}{t_c N_c} = \frac{t_f + t_r}{t_c} \quad (8\text{-}11)$$

is the reactive ratio for each day or each cycle. Or,

$$V_{ef} = V_b\frac{t_c - t_{sw}}{t_c} - \frac{1}{2}(V_b - V_i)\frac{t_f}{t_c} \quad (8\text{-}12)$$

This formula has clear mechanistic meaning. The first right-hand side term refers to the total reactor volume under the reactive period which includes the fill stage and the second to the unused portion of the reactor volume during fill in one cycle or on a daily basis.

Shortening the fill time and increasing react time can provide more effective reactor volume. A higher difference of $(V_b - V_i)$ results in a lower effective volume V_{ef}. This is understandable because a greater value of $(V_b - V_i)$ means more empty reactor volume in operation which reduces the effective volume. However, a lower difference of $(V_b - V_i)$ results in smaller flow rate Q or volume treated in one cycle which will increase operation costs.

The volume utilization coefficient, β, can be calculated by dividing V_{ef} by V_b, that is,

$$\beta = \frac{V_{ef}}{V_b} = \varphi - \frac{1}{2}\left(1 - \frac{V_i}{V_b}\right)\frac{t_f}{t_c} = \varphi - \frac{1}{2}(1 - \alpha)\frac{t_f}{t_c} \quad (8\text{-}13)$$

or

$$\beta = \frac{V_{ef}}{V_b} = \frac{1}{2}(1+\alpha)\frac{t_f}{t_c} + \frac{t_r}{t_c} \qquad (8\text{-}14)$$

where $\alpha = V_i/V_b$ is the ratio of initial rector volume to the maximum reactor volume. It is useful to define HRT in an SBR based on the concept of average liquid age in a vessel because of its time orientation, multi-phase operation and unsteady state nature.

The true HRT, t_{tr}, can be computed based on V_{ef} and total amount of influent treated during a cycle. The periods of settle, draw and idle if it is needed, should not be included in the calculation. Thus

$$t_{tr} = \frac{V_{ef}}{\frac{1}{t_c}\int_{t_0}^{t_f} Q dt} = \frac{V_{ef}}{Qt_f/t_c}$$

Substituting the expression for Q and V_{ef} into above equation results in

$$t_{tr} = \frac{1}{Qt_f/t_c}\left[V_b\frac{t_f+t_r}{t_c} - \frac{1}{2}(V_b - V_i)\frac{t_f}{t_c}\right] = \frac{t_c}{V_b - V_i}\left[V_b\frac{t_f+t_r}{t_c} - \frac{1}{2}(V_b - V_i)\frac{t_f}{t_c}\right]$$

Rearranging the equation yields:

$$t_{tr} = \frac{1}{1-V_b/V_i}(t_f+t_r) - \frac{1}{2}t_f = \frac{1}{1-\alpha}(t_f+t_r) - \frac{1}{2}t_f \qquad (8\text{-}15)$$

or

$$t_{tr} = \frac{1}{1-\alpha}(t_c - t_{sw}) - \frac{1}{2}t_f \qquad (8\text{-}16)$$

This is the mathematical expression of true HRT in an SBR which shows that t_{tr} is a

function of dilution rate, $V_b/(V_b - V_i) = 1/(1 - \alpha)$, fill time, t_f, and react time, t_r. After V_b, V_i, t_{sw} and t_c are set, the true HRT, t_{tr}, will only be determined by t_f, since t_r is determined by t_c, t_f and t_{sw}.

By using Eqs. (8-10) and (8-15), V_{ef} and t_{tr} can be verified at the two extreme operational conditions described earlier in this section. For one extreme end condition in which the volume of $(V_b - V_i)$ is filled instantly with $t_f = 0$ and t_r dominates the effective space-time, the above two equations become:

$$V_{ef} = V_b \frac{t_f}{t_c}$$

and

$$t_{tr} = \frac{V_b}{V_b - V_i} t_r = \frac{1}{1-\alpha} t_r$$

When the operational condition goes to the other extreme in which $t_r = 0$ and t_f dominates the entire effective process, the two equations change to

$$V_{ef} = V_b \frac{t_f}{t_c} - \frac{1}{2}(V_b - V_i)\frac{t_f}{t_c} = \frac{t_f}{2t_c}(V_b + V_i) \text{ and}$$

$$t_{tr} = \frac{V_b}{V_b - V_i} t_f - \frac{1}{2} t_f = \frac{t_f}{2}\left(\frac{V_b + V_i}{V_b - V_i}\right) \text{ or}$$

$$t_{tr} = \frac{t_f}{2}\left(\frac{1 + V_i/V_b}{1 - V_i/V_b}\right) = \frac{t_f}{2}\left(\frac{1+\alpha}{1-\alpha}\right)$$

These two expressions for the two extremes are exactly the same as Eqs. (8-8) and (8-9).

8.3.2. Defining Volumetric Loading Rate of an SBR System

The volumetric loading rate of a CFS reactor, L_v, is

$$L_v = \frac{(24\ h/day)QS_0}{V} = \frac{S_0}{t_D}$$

where

V = effective volume of the reactor.

t_D = 24 V/Q is the HRT based on a daily flow rate. Similar to a CFS, the volumetric loading rate for an SBR system, L_{vtr}, can be based on a daily flow rate Q_d:

$$L_{vtr} = \frac{Q_d S_0}{V_{ef}} = \frac{Q_f t_f N_c S_0}{V_b\left[\varphi - \frac{1}{2}(1-\alpha)\frac{t_f}{t_c}\right]} = \frac{N_c(V_b - V_i)S_0}{V_b\left[\varphi - \frac{1}{2}(1-\alpha)\frac{t_f}{t_c}\right]} \qquad (8\text{-}17)$$

Rearranging Eq. (8-17) yields

$$L_{vtr} = \frac{N_c(1-\alpha)S_0}{\varphi - \frac{1}{2}(1-\alpha)\frac{t_f}{t_c}} \qquad (8\text{-}18)$$

Compared to the parameters of a CFS reactor, effective reactor volume, true HRT and volumetric loading rate of an SBR system are variables affected by the operational mode. Table 8-1 lists differences between the two systems.

Table 8-1 Hydraulic characteristics comparison of the two systems

	Effective volume	True HRT	Effective volume ratio in the system	Volumetric loading rate
CFS	V_c constant	V_c/Q constant	$V_c/(V_c + V_s)$ constant	S_0/t_D constant
SBR	$V_b\ \varphi - 1/2(V_b - V_i)t_f/t_c$ variable	$t_f/(1-\alpha) - 1/2t_f$ variable	$\varphi - 1/2(1-\alpha)t_f/t_c$ variable	$N_c(1-\alpha)S_0/[\varphi - 1/2(1-\alpha)t_f/t_c]$ variable

8.3.3. Sample Calculation of V_{ef}, t_{tr} and L_{vtr}

A set of sample calculation results for V_{ef}, t_{tr} and L_{vtr} is given in Fig. 8-2 for a general examination of the relationships among these parameters. The values of basic parameters are: V_b = 8 L for all calculations; φ = 2/3, 3/4 and 5/6 while t_c = 3, 4, 6 h from graphs A1 to A3, respectively. In each graph, the solid line represents the results of V_i = 2 L or α = 0.25, dashed line of V_i = 4 L or α = 0.5 and dotted line of V_i = 6 L or α = 0.75.

The Graph A series shows how fill time affects effective reactor volume. V_{ef} increases linearly when t_f is decreased and reaches its maximum value at t_f = 0 as indicated in the derivation. Decreasing V_i (from dotted line to solid line) will decrease V_{ef} as well even if t_f is unchanged, because less V_i results in more available volume ($V_b - V_i$). This effect diminishes as t_f is shortened until there is no effect at $t_f \approx 0$. From Graphs A1 to A3 it can be seen that longer cycle time, t_c, which leads to larger reactive time ratio will increase V_{ef} under the same t_f because the fraction of t_c for the settle and draw phases is reduced.

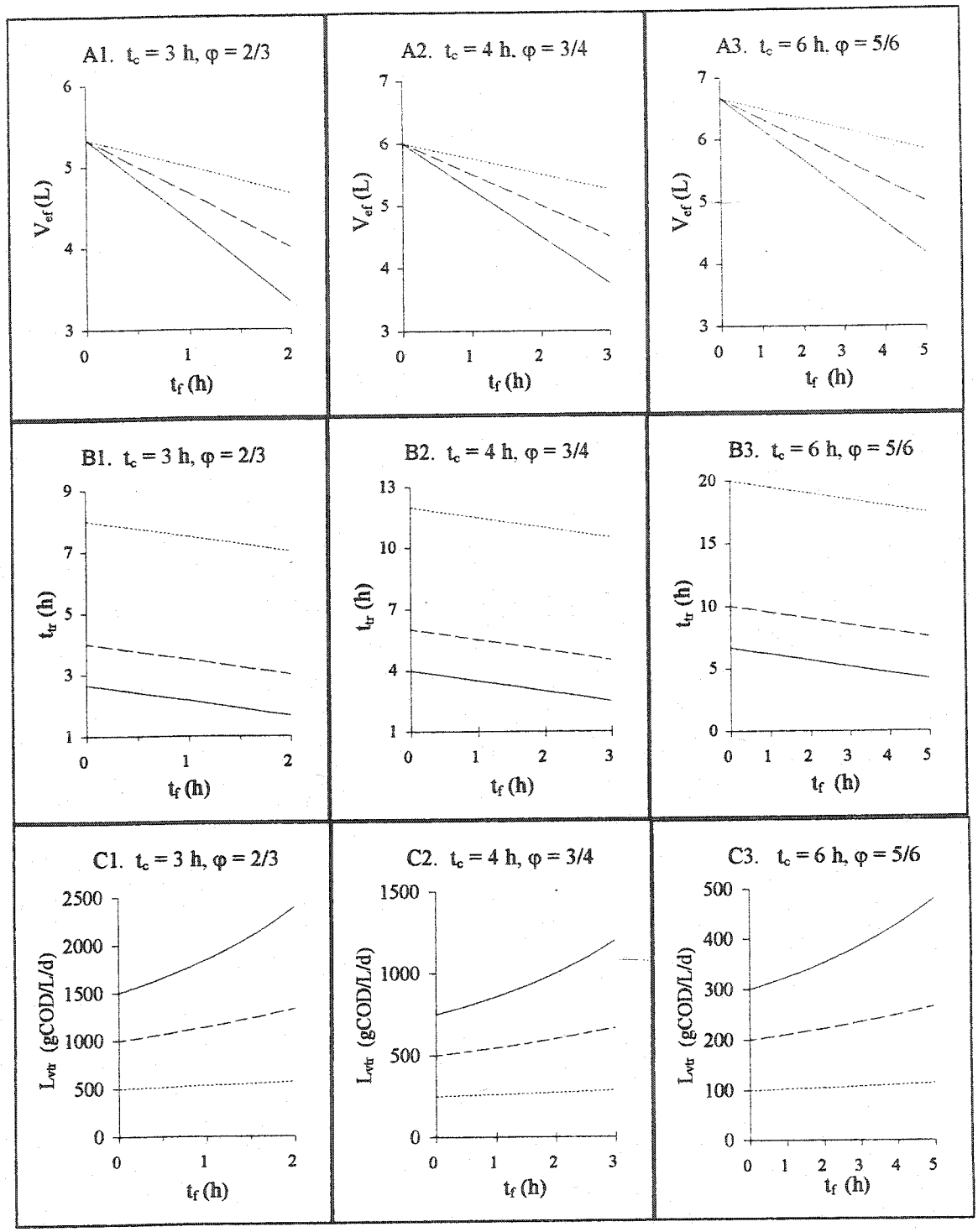


Figure 8-2. The relationships of fill time to effective reactor volume, V_{ef}, true HRT, t_{tr} and volumetric loading rate, L_{vtr}. The solid line represents V_i = 2 L or α = 0.25, dashed line V_i = 4 L or α = 0.5 and dotted line V_i = 6 L or α = 0.75.

The Graph B series reveals a linear relationship of true HRT, t_{tr}, and t_f. Similar to the Graph A series, t_{tr} increases as t_f decreases, reaching its maximum at $t_f \approx 0$. At the same t_f, changing V_i or α has a significant effect on t_{tr}. Increasing α from 0.25 to 0.5 yields about a 50% increase in t_{tr} and doubles t_{tr} as α is increased from 0.5 to 0.75. Increasing α increases V_i, which results in less available reactor volume and a lower Q to fill it. With unchanged t_f and a lower Q, a smaller total volume of reactive liquid resides in the reactor and causes longer t_{tr}. Longer cycle time always benefits t_{tr} as shown from Graphs B1 to B3. For example, t_{tr} is more than doubled when t_c increases from 3 to 6 h while φ increases from 2/3 to 5/6.

The nonlinear relationship between volumetric loading rate, L_{vtr}, and t_f in the graph C series clearly illustrates an increasing trend of L_{vtr} with lengthening t_f but with reducing V_i or α. As stated in the above two paragraphs, longer t_f leads to smaller V_{ef} and shorter t_{tr} all of which contribute to a higher loading rate. However, lengthening cycle time t_c can dramatically reduce the loading which can be seen from graphs C1 to C3. A reduction of L_{vtr} by more than 50% can be obtained with t_c of 4 h instead of 3 h and about four-fifths reduction with 6 h t_c instead of 3 h. Unfortunately with this reduction capacity for treating reactive media is lost as t_c increases from 3 to 4 h, for example, and the number of cycles n is reduced from 8 to 6 per day. Under the condition of no change in V_i and t_f, this reduction results in a 25% loss in reactor capacity. Therefore, all of these parameters should be very carefully considered and weighted in a design of an SBR system.

8.3.4. Definition of Basic Biokinetic Parameters for an SBR System

Biomass decay rate k_e and yield factor Y in an SBR In Section 5.4.1, the definitions of these two parameters have been made. Eq. (5-27) has been derived to estimate the values of the two parameters with the adjustment by φ.

Specific substrate removal rate R_{tr} If Eq. (5-27) is changed to a form similar to that of a CSTR,

$$\frac{1}{\theta_{xob}\varphi} = YR_{tr} - k_e \tag{8-19}$$

where

$$R_{tr} = \frac{N_c(V_b - V_i)(S_0 - S_e)}{V_b \bar{X}_V \varphi}$$

and then

$$R_{tr} = \frac{N_c(1 - V_i/V_b)(S_0 - S_e)}{\bar{X}_V \varphi} = \frac{N_c(1-\alpha)(S_0 - S_e)}{\bar{X}_V \varphi} \tag{8-20}$$

can be defined as true specific substrate removal rate of an SBR system. The linear relation of the inverse of true sludge age and the specific substrate removal rate in an SBR reactor can be expressed by a straight line.

In Eq. (8-20), $\alpha = V_i/V_b$ is a very important parameter because it affects both t_{tr} and R_{tr}.

8.3.5. Another Derivation of True Specific Substrate Removal Rate R_{tr} in an SBR

For the computation of true specific substrate removal rate, R_{tr}, it can be proved that the

results are the same either by using basic definitions or by using the true HRT. The following is the verification.

From the definitions in Section 5.4.1 and considering a quasi-steady state condition around a reactor over a cycle, i.e., applying $d\overline{M}_x/dt = 0$ to Eq. (5-17), the expression of the specific substrate removal rate is

$$R_{tr} = \frac{N_c(V_b - V_i)(S_0 - S_e)}{V_b \overline{X}_v \varphi} = \frac{N_c(1-\alpha)(S_0 - S_e)}{\overline{X}_v \varphi}$$

Because $N_c = 24\ h/t_c$ and $\varphi = (t_f + t_r)/t_c$, thus

$$R_{tr} = \frac{24(1-\alpha)(S_0 - S_e)}{\overline{X}_v (t_f + t_r)} \qquad (8\text{-}21)$$

R_{tr} is adjusted to a daily basis in a manner similar to a CSTR based on the true HRT, t_{tr}, and effective activated sludge concentration, X_{ef}, which is calculated from total effective biomass, $V_b \overline{X}_v \varphi$, divided by effective reactor volume, V_{ef}.

$$R_{tr} = \frac{(S_0 - S_e)}{X_{ef}\ t_{tr}\ (day/24\ h)} \qquad (8\text{-}22)$$

But $24\ h/day = N_c\ t_c$, therefore,

$$R_{tr} = \frac{N_c t_c (S_0 - S_e)}{X_{ef}\ t_{tr}} = \frac{N_c t_c (S_0 - S_e)}{\left(\frac{V_b \overline{X}_v \varphi}{V_{ef}}\right)\left(\frac{V_{ef}}{Q_f \frac{t_f}{t_c}}\right)} = \frac{N_c Q_f t_f (S_0 - S_e)}{V_b \overline{X}_v \varphi}$$

Rearranging the equation yields

$$R_{tr} = \frac{N_c(V_b - V_i)(S_0 - S_e)}{V_b \bar{X}_v \varphi} = \frac{N_c(1-\alpha)(S_0 - S_e)}{\bar{X}_v \varphi} \quad (8\text{-}23)$$

or

$$R_{tr} = \frac{24(1-\alpha)(S_0 - S_e)}{\bar{X}_v(t_f + t_r)} \quad (8\text{-}24)$$

This is the exact expression derived from the definition.

8.3.6. Sludge Loading Rate, L_{xtr} of an SBR System

From the specific removal rate expression, another parameter, sludge loading rate, L_x, can be derived. For a CFS

$$L_x = \frac{(24\ h/day)QS_0}{VX_v} = \frac{S_0}{X_v t_D} \quad (8\text{-}25)$$

For an SBR system

$$L_{xtr} = \frac{Q_d S_0}{V_b \bar{X}_v \varphi} = \frac{N_c Q_f t_f S_0}{V_b \bar{X}_v \varphi}$$

$$L_{xtr} = \frac{N_c(V_b - V_i)S_0}{V_b \bar{X}_v \varphi} = \frac{N_c(1 - V_i/V_b)S_0}{\bar{X}_v \varphi} = \frac{N_c(1-\alpha)S_0}{\bar{X}_v \varphi} \quad (8\text{-}26)$$

Both specific substrate removal rate, R_{tr}, and sludge loading rate, L_{xtr}, in an SBR system are a function of initial reactor volume, V_i, while a CSTR system has no such terms.

All the defined parameters can be used either in design of an SBR system or in the comparison of different operational modes of the system. In design, the expressions of V_{ef}, t_{tr} with L_{xtr} and L_{vtr} determine the reactor dimensions.

In design of operational mode, t_f should be as short as possible to increase V_{ef} and t_{tr} However, the pump capacity and shock loading should also be carefully considered to find the optimum operational mode. The R_{tr} expression will be useful to determine the Y and k_e values that are compatible with the design. Design of an SBR system will be discussed in detail in Chapter 10.

The new defined parameters can also apply to an anaerobic SBR (ASBR) system. In this application, the assumption of no reaction in the settle and draw periods is still applied and reactive time ratio refers to the fill and react stages when influent is mixed completely with anaerobic activated sludge in the reactor.

CHAPTER 9 EXPERIMENTAL COMPARISON OF SBR AND CFSTR SYSTEMS

References from the 1960s to date show no systematic experimental comparison of SBR and CFSTR under equivalent operational conditions. Such a comparison is important to practically verify the reported advantages of the SBR system over the CFSTR system.

9.1. COMPARISON OF SUBSTRATE REMOVAL EFFICIENCY

Droste (1990) suggested that higher substrate removal efficiency based on equivalent operational conditions can prove the advantages of an SBR system over a CFSTR system. The efficiencies from the two systems can be compared based on either the equivalent HRT or the volumetric loading.

9.1.1. Comparison of COD Removal Efficiency based on the Equivalent HRT

An SBR has PF kinetics for substrate degradation. Recalling its definition in Section 8.2, the equivalent HRT of an SBR, t_{ed}, is the same as the value of HRT, t_{dc}, of a CFSTR. It is calculated by Eq. (8-3):

$$t_{ed} = \frac{nV_b - Qt_{sc}}{Q} = t_{dc} = \frac{V_c}{Q} \qquad (8\text{-}3)$$

Based on the equivalent HRT, t_{ed}, an SBR system should have an advantage of higher

substrate removal efficiency. It is the most important practical advantage that should be verified. Figures 9-1 and 9-2 are the average values of soluble COD removal efficiencies vs t_{dc} (CFSTR) or t_{ed} and t_{tr} (SBR) in the two systems.

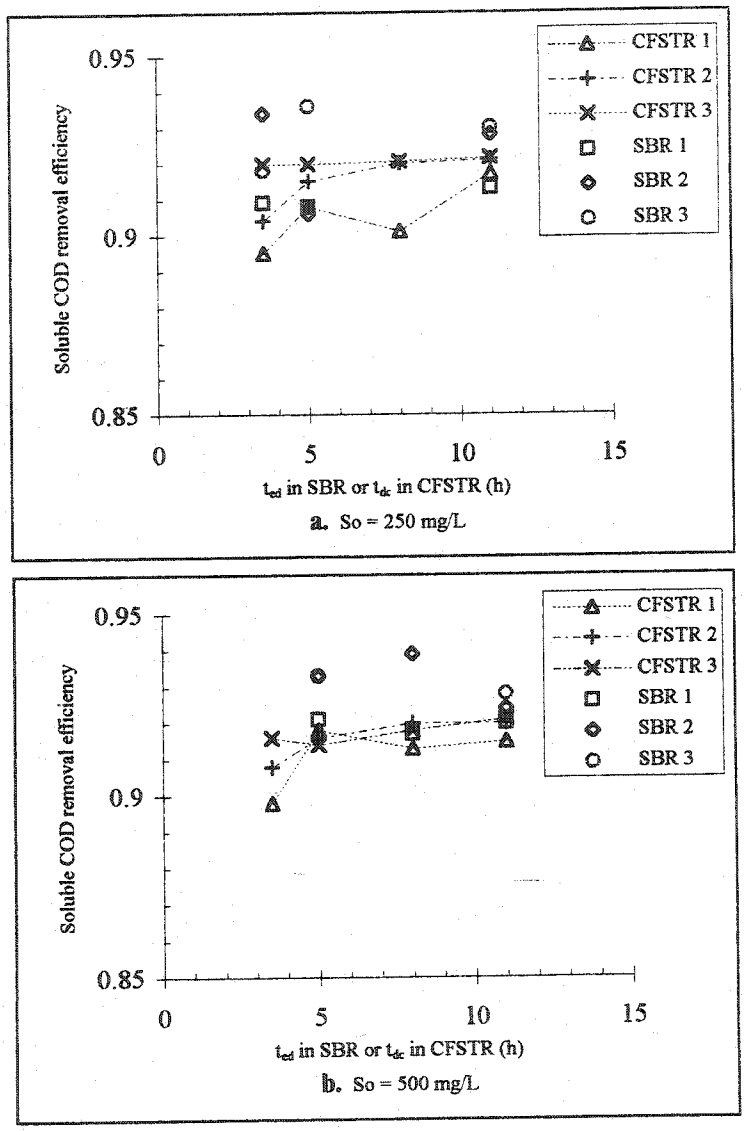


Figure 9-1 Comparison of soluble COD removal efficiency η vs HRT in the two systems (a. S_0 = 250 and b. S_0 = 500 mg/L)

Figure 9-1 shows that under equivalent HRTs from 3.5 to 11 h, the SBR system has a

slightly higher soluble COD removal efficiency than the CFSTR system at either S_0 = 250 mg/L or S_0 = 500 mg/L. The overall average soluble COD removal efficiency in the SBR system was 0.923 based on 44 runs while this efficiency was 0.913 in the CFSTR system based on 16 runs, about one percent higher in the former system.

Table 9-1 is the analysis of variances (ANOVA) for the two systems based on the averages of soluble COD removal efficiencies corresponding to different equivalent HRTs. The F value, 2.77, is higher than F_α = 2.048 at α = 0.05 level but lower than F_α = 2.785 at α = 0.01 level.

Table 9-1 ANOVA results of soluble COD removal comparison between the two systems

Groups	Count	Sum	Average	Variance
SBR system	17	15.7	0.923	10^{-4}
CFSTR system	21	19.23	0.913	6×10^{-5}

Source of Variation	SS	*df*	MS	F	$P_{\text{-value}}$	$F_{\alpha = 0.05}$	$F_{\alpha = 0.01}$
Between two systems	3.905	22	0.177	**2.770**	0.01	**2.048**	**2.785**
Within each system	0.271	1	0.271	4.225	0.052	4.301	7.945
Error	1.410	22	0.064				
Total	5.585	45					

This comparison shows a slight kinetic advantage of the SBR system although it is diminished by shorter true HRTs in the SBR system, which were 1/3 to 1/6 shorter than those in the CFSTR.

Both Figs. 9-1 and 9-2 also reveal that HRT does not affect the COD removal efficiency in

the SBR system under the designed experimental conditions, even under the lowest t_{tr} of 2.55 h. Completion of most substrate degradation within the shortest designed HRT is the main reason. From the experimental results of batch tests in Section 5.2.3, it is known that almost all original substrates were degraded during the first 3 to 4 h. But COD does not drop further because of IOM from influent, SAP from substrate degradation and BAP from biomass decay. All these organic compounds are biologically inert or refractory which cause total COD in the system to remain at a certain level, regardless of the length of the HRT when the time is above the minimum HRT required.

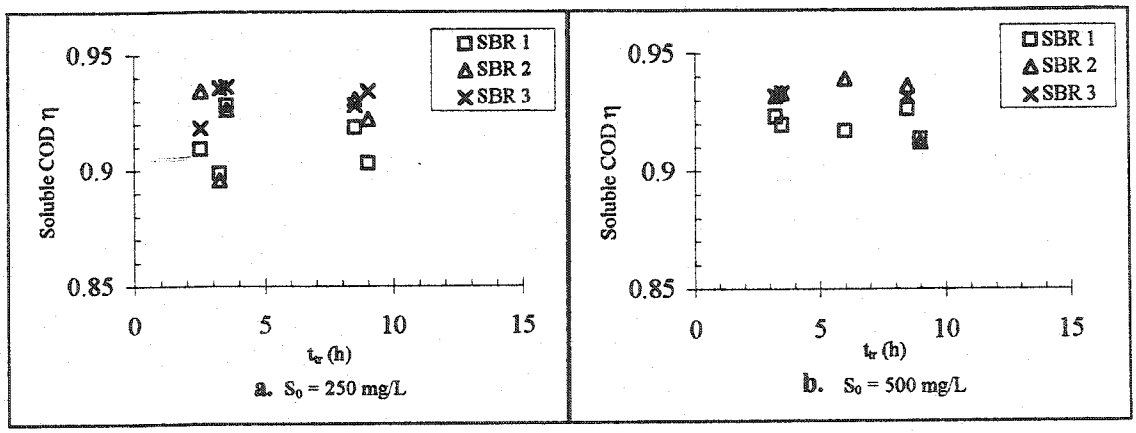


Figure 9-2 COD removal efficiency η vs t_{tr} of the SBR system (a. S_0 = 250 and b. S_0 = 500 mg/L)

In the CFSTR system, this trend was only shown in the runs with HRT from 5 to 11 h. Lower COD removal efficiencies were observed in the runs at the shortest HRT of 3.5 h and shorter sludge ages of 5 and 10 d. The CFSTR reactors with shorter sludge ages contained lower sludge concentrations. When they dealt with substrate at a short HRT, DBS could exit by the CM flow pattern, which could deteriorate effluent quality. By

extending sludge age and HRT, DBS could be degraded more completely and effluent quality, therefore, can be improved significantly as shown in the figures at HRT longer than 5 h for the CFSTR system.

9.1.2 Comparison of COD Removal Efficiency based on the Volumetric Loading

Another important comparison of substrate removal efficiency between the two systems was based on the volumetric loading. Figures 9-3a and 9-3b show that volumetric loading did not affect the COD removal efficiencies in both SBR and CFSTR systems. The reason is the same as stated above for HRT because, after the reactor volume is chosen, there are two ways to change volumetric loading: one is to change HRT and the other is to change influent concentration. Changing volumetric loading is equivalent to changing HRT with no change in influent concentration.

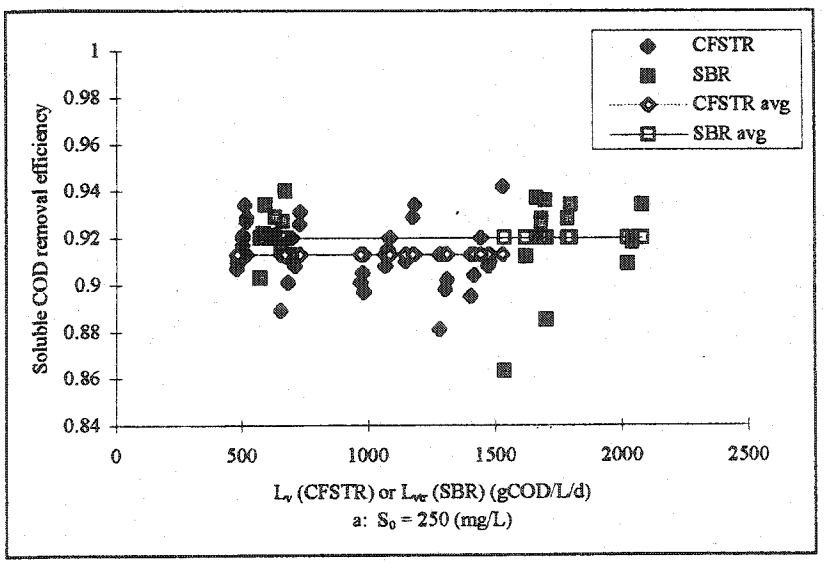


Figure 9-3a Comparison of soluble COD removal efficiency vs volumetric loading in the two systems ($S_0 = 250$ mg/L).

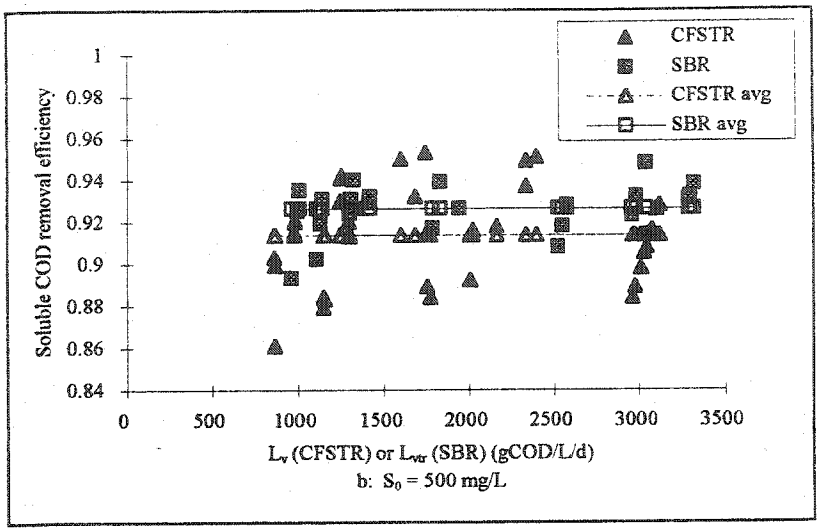


Figure 9-3b Comparison of soluble COD removal efficiency vs volumetric loading in the two systems (S_0 = 500 mg/L).

Figures 9-3a and 9-3b also show that the SBR system provides a slightly higher COD removal efficiency than the CFSTR.

ANOVA results in Tables 9-2a and 9-2b reveal that this difference is not significant with F = 2.678 against $F_{\alpha=0.05}$ = 4.016 for the runs of S_0 = 250 mg/L and significant with F = 6.253 against $F_{\alpha=0.05}$ = 4.007 for the runs of S_0 = 500 mg/L. This suggests that the SBR system does not overwelm the CFSTR system. Therefore, other considerations are necessary to select an SBR system for a wastewater treatment process.

Table 9-2a ANOVA results of soluble COD removal efficiencies vs volumetric loadings between the two systems (S_0 = 250 mg/L)

Groups	Count	Sum	Average	Variance
CFSTR system	36	32.875	0.9132	0.000182
SBR system	21	19.323	0.9201	0.000340

Table 9-2a (cont'd)

Source of Variation	SS	df	MS	F	P_{-value}	$F_{\alpha=0.05}$
Between two systems	0.00064	1	0.00064	**2.678**	0.107	**4.016**
Within each system	0.01315	55	0.00024			
Total	0.01379	56				

Table 9-2b ANOVA results of soluble COD removal efficiencies vs volumetric loadings between the two systems (S_0 = 500 mg/L)

Groups	Count	Sum	Average	Variance
CFSTR system	36	32.886	0.9135	0.0005
SBR system	24	22.233	0.9264	0.0002

Source of Variation	SS	df	MS	F	P_{-value}	$F_{\alpha=0.05}$
Between two systems	0.002	1	0.0024	**6.253**	0.0152	**4.007**
Within each system	0.022	58	0.0004			
Total	0.025	59				

9.2. COMPARISON OF KINETIC COEFFICIENTS

The comparison in this section includes specific substrate removal rates, yield factors and biomass decay rates.

9.2.1. Comparison of Overall Specific Substrate Removal Rates

For an SBR system, the specific substrate removal rate, R_{tr}, has been defined in Section 8.3.6:

$$R_{tr} = \frac{N_c(1 - V_i/V_b)(S_0 - S_e)}{\overline{X}_v \varphi} = \frac{N_c(1-\alpha)(S_0 - S_e)}{\overline{X}_v \varphi}$$

while for a CFSTR system it is

$$R = \frac{(S_0 - S_e)}{\overline{X}_v t_{dc}}$$

The following figures give experimental results from CFSTR and SBR systems under equivalent operational conditions. Figures 9-4 a, b and c are results from the reactors with sludge age or observed sludge age of approximately 5, 10 and 15 d, respectively, and S_0 = 250 mg/L. Figures 9-5 a, b and c are for the same sludge ages as Figs. 9-4 a, b and c, and S_0 = 500 mg/L. The R and R_{tr} values from all runs in both systems are arithmetically averaged based on the different t_{dc} of CFSTR or t_{ed} of SBR.

It is interesting to note that, when S_0 = 250 mg/L, the trend of R_{tr} values in the SBR system was from high values at shorter t_{ed} to lower values at longer t_{ed} while the R values in the CFSTR were flat over the experimental t_{dc} range.

Comparison of the two systems reveals that the R_{tr} values of the SBR were higher than those of the CFSTR at the shorter t_{ed} or t_{dc} but became close at the longest t_{ed} or t_{dc}. There are several factors that contribute to the specific substrate removal rate: COD concentrations of influent and effluent, HRT and biomass concentration in the reactor. Higher R_{tr} could be caused by less biomass with higher SVI at shorter HRT in the SBR system. Recalling Fig. 9-1 at the shortest HRT, the SBR showed higher COD removal efficiency than the CFSTR when S_0 = 250 mg/L, which means that, at shorter HRT but

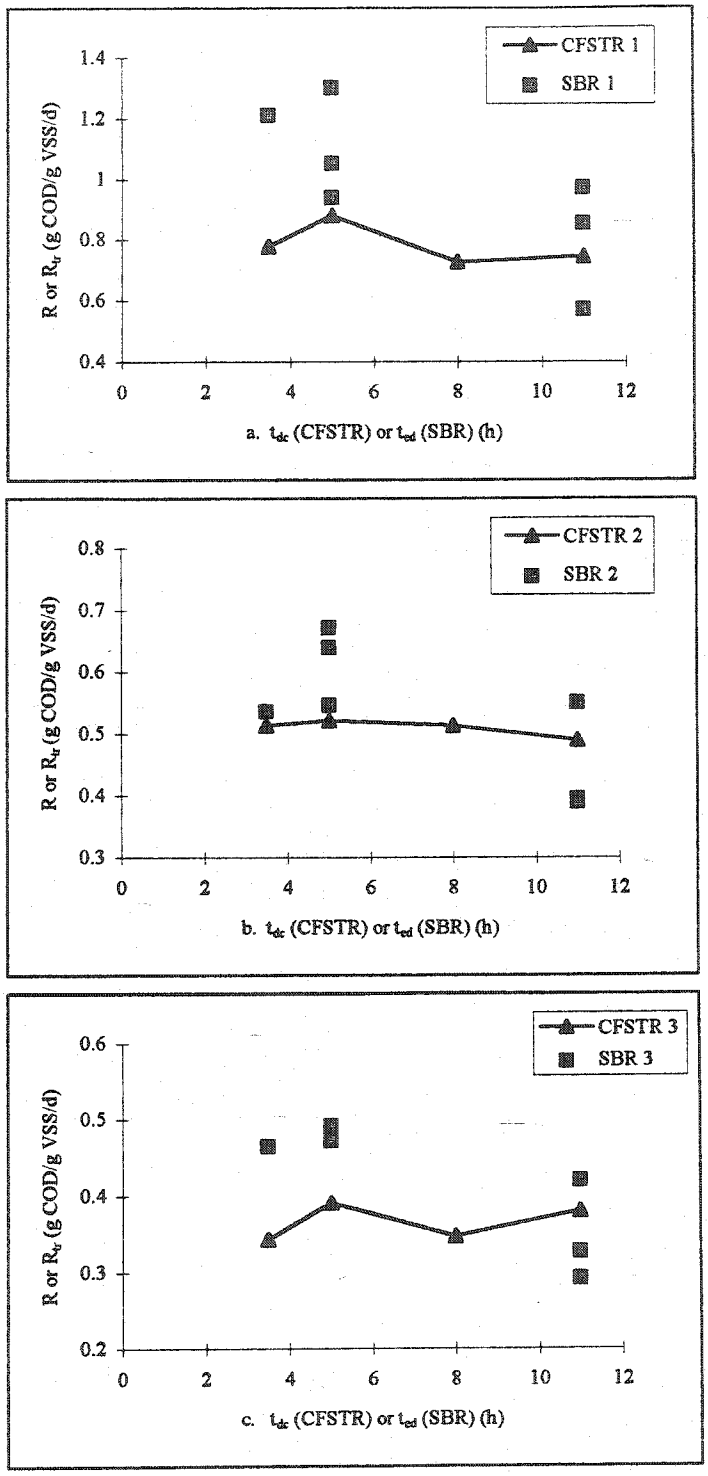


Figure 9-4 Specific substrate removal rate vs t_{dc} or t_{ed} in the two systems (S_0 = 250 mg/L, a: $\theta_x = \theta_{xob}$ = 5 d; b: $\theta_x = \theta_{xob}$ = 10 d; c: $\theta_x = \theta_{xob}$ = 15 d)

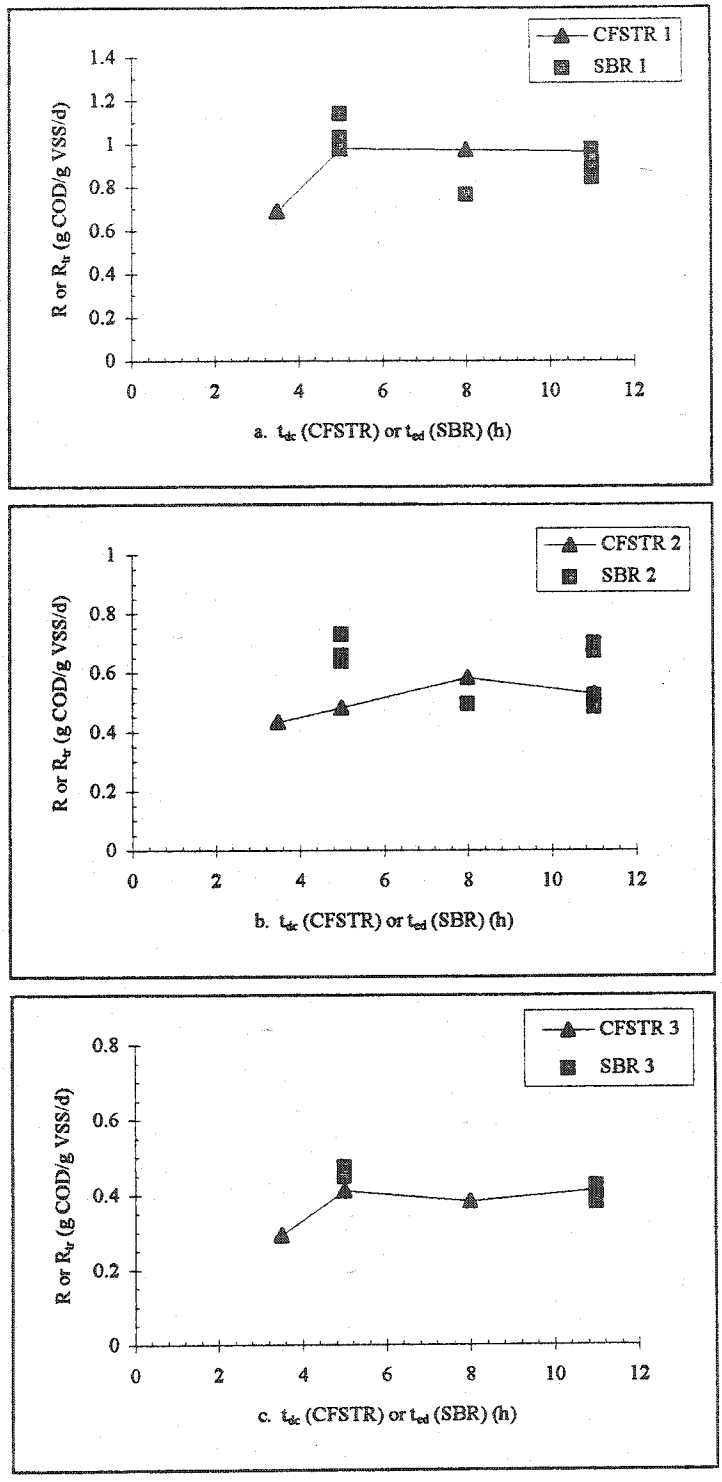


Figure 9-5 Specific substrate removal rate vs t_{dc} or t_{ed} in the two systems (S_0 = 500 mg/L, a: $\theta_x = \theta_{xob}$ = 5 d; b: $\theta_x = \theta_{xob}$ = 10 d; c: $\theta_x = \theta_{xob}$ = 15 d)

PF kinetics, SBR with less biomass is able to deal with more substrate fed and degrades it more fully than a CFSTR under the same condition.

It is also interesting that lower R values in the CFSTR system were observed at the shortest HRT runs when S_0 = 500 mg/L; no such trend was observed in the SBR system. Comparatively, the CFSTR system held higher sludge concentrations at shorter HRT than the SBR system possibly because the higher but constant loading rate generated lower SVI and better settling sludge in the former system. However, lower R values at the shortest t_{dc} did not lead to higher COD removal efficiency in the CFSTR system (refer to Fig. 9-1b). On the contrary, the CFSTR had a lower removal efficiency than the SBR system.

The overall average R_{tr} in SBR system is 0.649 g COD/g VSS/d based on 44 runs, 0.094 g COD/g VSS/d higher than CFSTR which had an average of 0.555 (g COD/g VSS/d) from 16 runs. ANOVA results in Table 9-3 for R and R_{tr} comparison in the two systems show that the difference of the two values is significant at $\alpha = 0.05$ but is not significant at $\alpha = 0.01$, which suggests a biological kinetic advantage of SBR but no overwhelming evidence for it.

Table 9-3 ANOVA results of specific substrate removal rates, R and R_{tr}, in the two systems

Source of Variation	SS	df	MS	F	$P_{\text{-value}}$	$F_{\alpha = 0.05}$	$F_{\alpha = 0.01}$
Between two systems	0.222	1	0.222	**4.187**	0.0431	**3.926**	**6.867**
Within each system	5.926	112	0.0529				
Total	6.148	113					

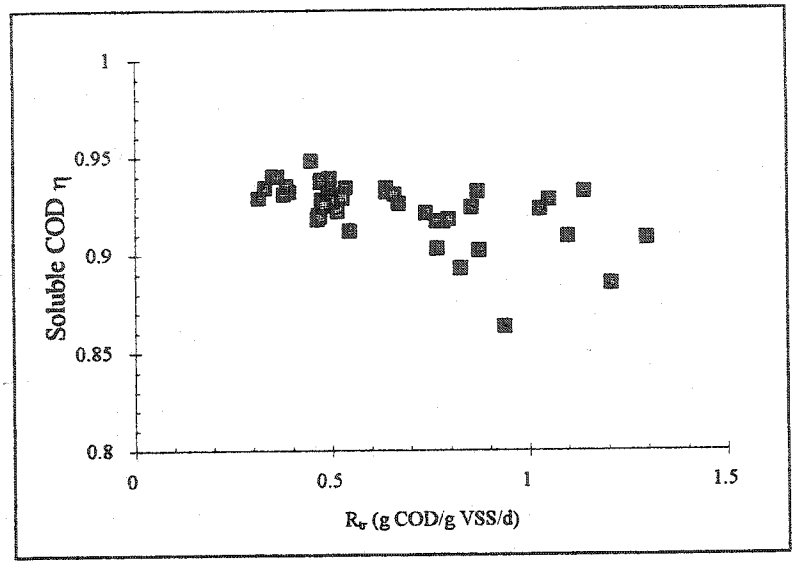


Figure 9-6 The relationship of soluble COD removal efficiency, η, vs true specific substrate removal rate R_{tr} in the SBR.

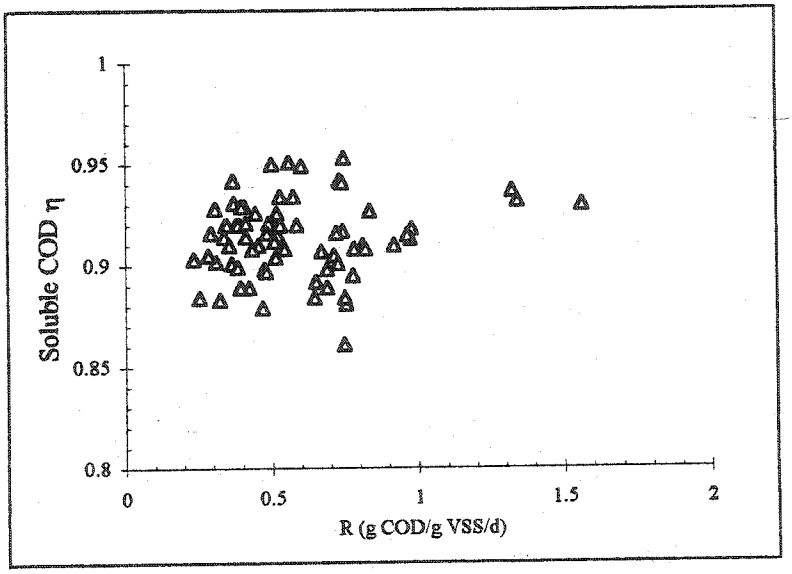


Figure 9-7 The relationship of soluble COD removal efficiency, η, vs specific substrate removal rate R in the CFSTR system.

Figures 9-6 and 9-7 provide another comparison, COD removal efficiency vs specific

substrate removal rate, between the two systems. The two figures demonstrate, similar to the situation in the comparison of volumetric loading vs HRT, that COD removal efficiency η varied in a more narrow range for the SBR compared to the CFSTR.

ANOVA results in Table 9-4 proved that the variance of soluble COD removal efficiency of the SBR is 2.49×10^{-4}, less than 3.53×10^{-4} for the CFSTR system.

Table 9-4 ANOVA of soluble COD removal efficiencies vs specific substrate removal rates in the two systems

Groups	Count	Sum	Average	Variance
CFSTR system	72	65.761	0.913347	0.000353
SBR system	44	40.63	0.923409	0.000249

Source of Variation	SS	df	MS	F	P_{-value}	$F_{\alpha = 0.01}$
Between two systems	0.00277	1	0.00277	**8.809**	0.00365	**6.863**
Within each system	0.0358	114	0.000314			
Total	0.038546	115				

Also in this table, F value for COD removal comparison is 8.809, greater than $F_{\alpha = 0.01}$ = 6.863, which indicates the SBR possess better substrate removal kinetics.

9.2.2. Comparison of Y and k_e

The yield factor Y and biomass decay rate k_e of SBR reactors have been calculated based on the definitions developed in Section 5.4.7. Table 5-8 in that section lists the results.

The k_e and Y values of the CFSTR system running under the equivalent operational

conditions were also measured according to the traditional method (Metcalf & Eddy, Inc., 1979; 1991). Table 9-5 gives the measured values of k_e and Y.

Table 9-5 Measured Y and k_e of the CFSTR system

t_d (h)	Sludge Loading Rate (kg COD/kg VSS day)			k_e (d^{-1})	Y (g VSS/ g COD)
	CFSTR 1 (θ_x = 5 d)	CFSTR 2 (θ_x = 10 d)	CFSTR 3 (θ_x = 15 d)		
	S_0 = 250 mg/L				
3.5	0.78	0.513	0.34	0.048	0.31
5	0.88	0.52	0.39	0.048	0.29
8	0.81	0.51	0.35	0.041	0.29
11	0.78	0.56	0.38	0.071	0.34
	S_0 = 500 mg/L				
3.5	0.69	0.43	0.29	0.038	0.34
5	0.73	0.43	0.35	0.049	0.34
8	0.88	0.56	0.38	0.042	0.27
11	0.82	0.53	0.41	0.071	0.33
Average				0.0511	0.314

From the results shown in Table 5-8 and Table 9-5, it can be seen that average values of Y and k_e in the SBR are close to those in the CFSTR system, k_e = 0.0512 d^{-1} and Y = 0.337 in the former against 0.0511 d^{-1} and 0.314, respectively in the latter. From Eq. (5-20) for the calculation of k_e and Y, mathematically, Y as a slope, should have no change when reactive time ratio factor φ applies to the equation. Failure to adjust the equation by φ will cause a large error in the estimation of k_e and possibly make Y meaningless because

the intercept, $-k_e$, may be positive without the correction.

Using k_c and Y values of a CFSTR system as a substitution for those of an SBR system provides an accurate estimation for model simulation of the latter. After accounting for the hydraulic difference between the two system, their biological characteristics should be similar when their operations are under equivalent conditions.

9.3. COMPARISON OF SLUDGE COMPACTIBILITY AND THE EFFECT OF V_i ON THE PERFORMANCE OF SBR

Sludge loading rate significantly affects sludge compactibility. It is the key parameter for successful operation of an SBR because supernatant must be withdrawn until the designed V_i remains to provide sufficient available volume for influent for the next cycle. Also a sufficient quantity of sludge must settle and compact within V_i. Many researchers reported that SVI varies with sludge loading change. Sludge loading should be examined before comparing sludge compactibilities in the two systems. In some sludge loading ranges, SVI increases with a loading increase but in some ranges the trend of SVI change is opposite. Also differences of SVI in the two systems could exist even under equivalent operational conditions.

9.3.1. Comparison of Sludge Loading Rate

The expression of sludge loading rate, L_X, is very similar to the specific substrate removal rate. For a CFSTR system

$$L_x = \frac{S_0}{\overline{X}_v t_d}$$

and for an SBR system:

$$L_{xtr} = \frac{N_c(1 - V_i/V_b)S_0}{\overline{X}_v \varphi} = \frac{N_c(1-\alpha)S_0}{\overline{X}_v \varphi}$$

Comparing these with the expressions of R and R_{tr} in Section 8.2.3, it can be seen that the difference between sludge loading and specific substrate removal rates is the absence of an effluent COD concentration term in the equation for sludge loading L_x. In other words, L_x or L_{xtr} is $(1 - \eta)$ times greater than R or R_{tr}. Therefore, the relationship of sludge loading to other parameters is nearly the same as that of specific substrate removal rate and the information from R or R_{tr} can be used for analysis of L_x or L_{xtr}.

Equation (8-29) shows that sludge loading rate changes are directly proportional to the influent concentration and inversely proportional to the HRT and biomass concentration. Figures 9-8 and 9-9 present the R_{tr} and R distributions under various t_{tr} in SBR and t_{dc} in CFSTR, respectively. The R_{tr} distribution in SBR shows an interesting trend which declines with longer t_{tr} while R in CFSTR does not. This phenomenon, as discussed in Section 9.2.1, may be caused by better settling and compactable sludge developed under longer HRT in the SBR system, which allows more sludge to be held in the reactor and lowers the sludge loading. Further analysis of SVI, will give more support to this point.

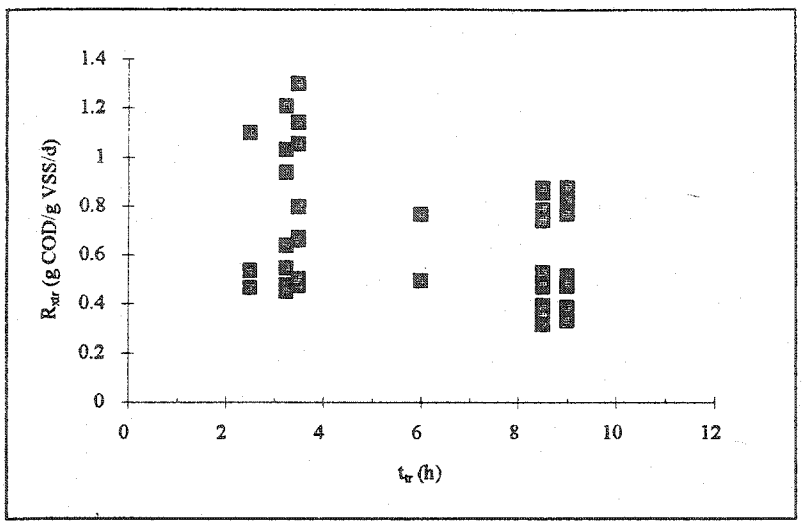


Figure 9-8. Relationship of true sludge loading R_{tr} vs t_{tr} in the SBR system

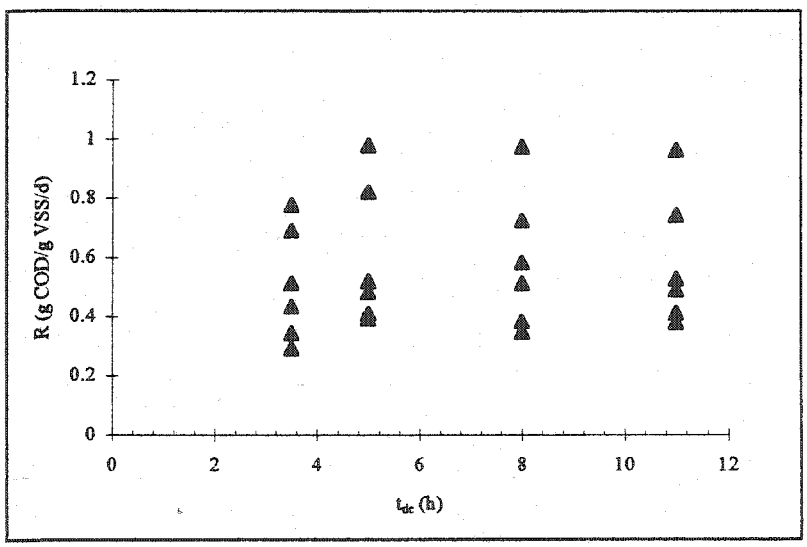


Figure 9-9. Relationship of sludge loading R vs t_{dc} in the CFSTR system

9.3.2. Comparison of SVI in the Two Systems

SVI is used for the evaluation of activated sludge compactibility. There are two sets of data illustrated in Figs. 9-10 and 9-11 to show the relationships of SVI vs true sludge

loading and vs true sludge age in the SBR system and two sets in Figs. 9-12 and 9-13 for the CFSTR system.

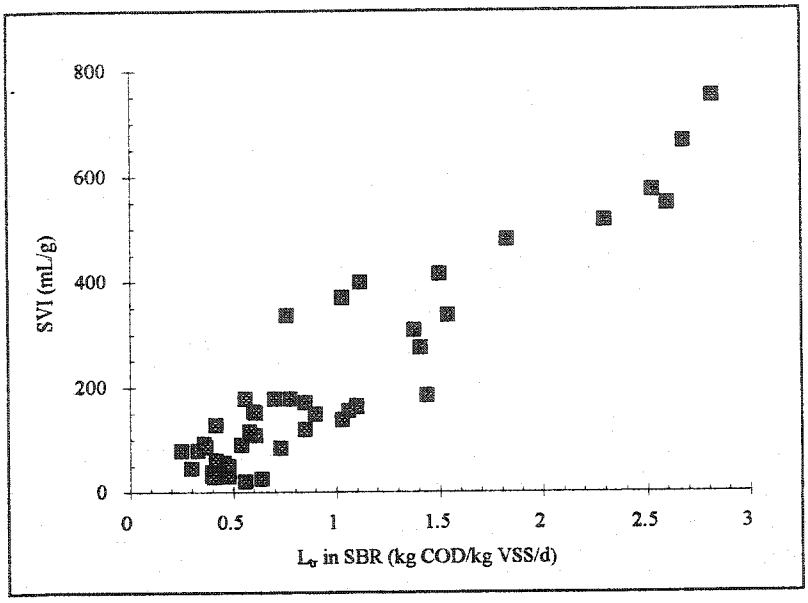


Figure 9-10. Relationship of true sludge loading and SVI in the SBR system

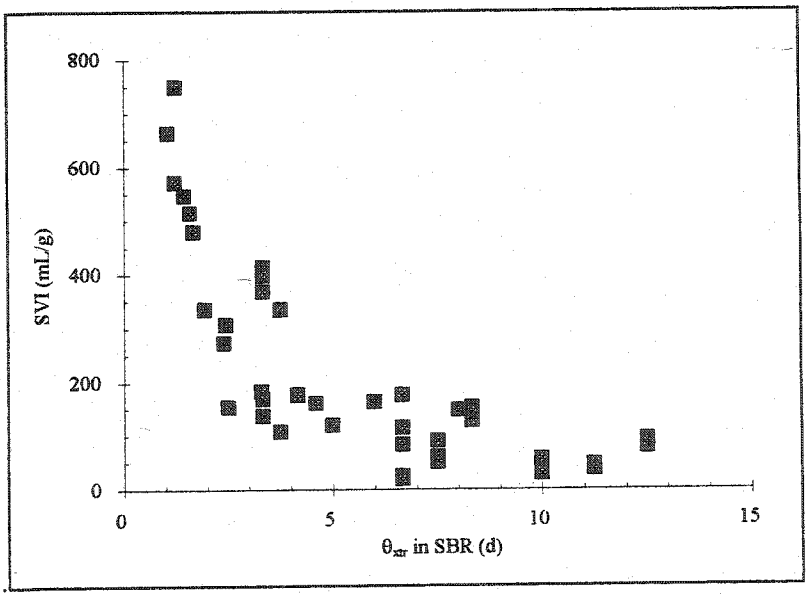


Figure 9-11. Relationship of true sludge age and SVI in the SBR system

From Fig. 9-10, it can be seen that in the SBR system, SVI increase is linear with increasing sludge loading. Within the common sludge loading range 0.3 to 0.6 g COD/g VSS/d, this value is under 200 mL/g.

Figure 9-11 demonstrates that SVI decreases in an exponential manner with increasing true sludge age. Its values are below 200 mL/g when true sludge age reaches 4 d or longer, which suggests that the steady operation of the SBR system with the feed used in this study requires a sludge age longer than 4 d.

On the other hand, Fig. 9-12 for the CFSTR system shows a trend of higher SVI than the SBR when sludge loading increases. By comparing the two systems within the same sludge loading range from 0 to 1 g COD/g VSS/d (referring to Fig. 9-14 for the SBR system), CFSTR still shows a positive trend of higher SVI than SBR. This difference suggests that much higher SVI or poorer settling sludge under higher sludge loading could

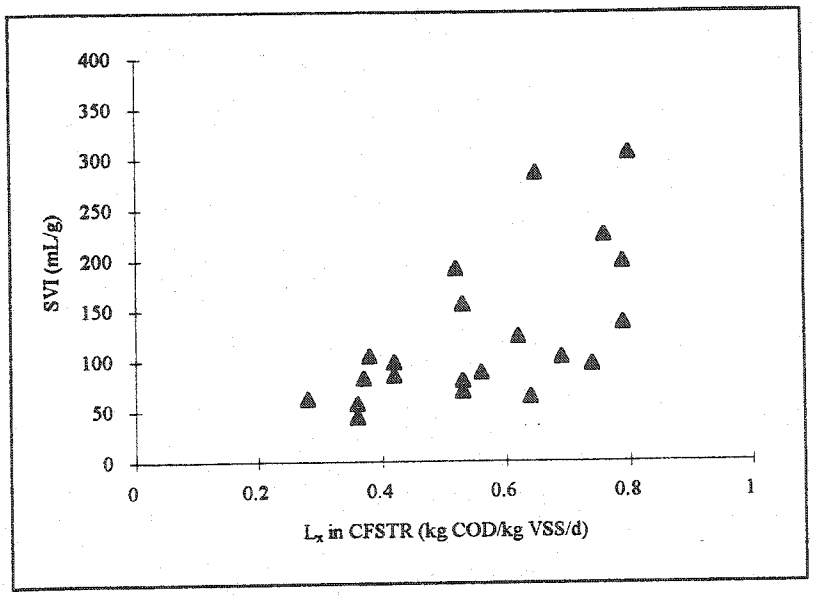


Figure 9-12. Relationship of sludge loading and SVI in the CFSTR system

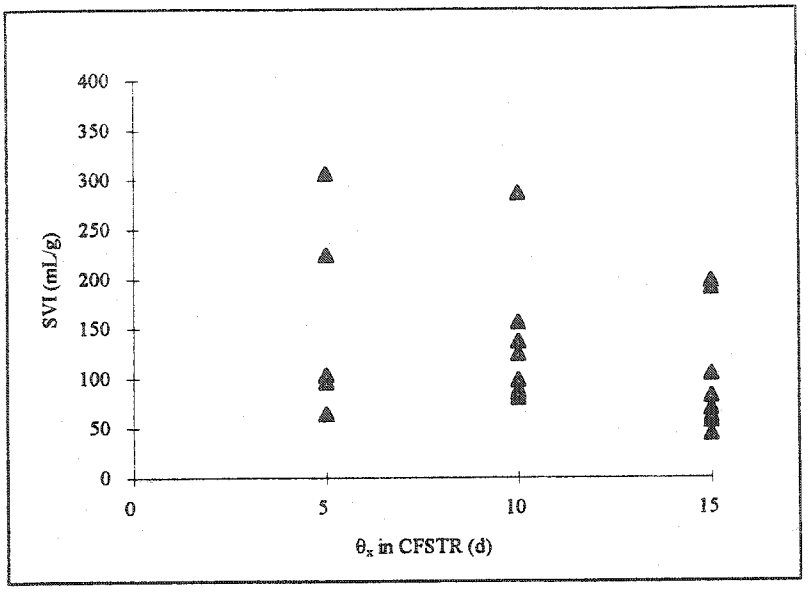


Figure 9-13. Relationship of sludge ages and SVI in the CFSTR system

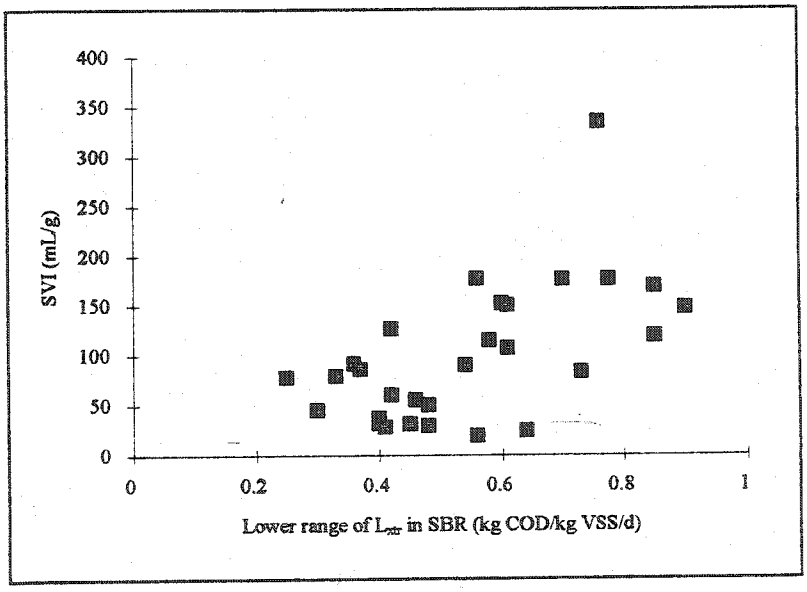


Figure 9-14. Relationship of true sludge loading and SVI in the SBR system (L_{xtr} = 0 - 1 g COD/g VSS/d range)

appear in a CFSTR compared to an SBR.

Meanwhile, the comparison of SVI vs sludge age between the two systems demonstrates

that a CFSTR has higher SVI sludge than the SBR under the same sludge age range. Careful observation of Figs. 9-11 and 9-13 reveals that for a CFSTR operating between sludge ages of 5 to 15 d, SVI values range from 50 to 300 mL/g, higher than those, 30 to 200 mL/g, in the SBR over the same range of sludge age.

Table 9-6 gives ANOVA results for the SVI comparison of the two systems. From the table, F = 3.092 larger than $F_{\alpha = 0.01} = 2.604$ indicates that the difference of SVI in the two is significant. The lower average of SVI, 93.6 mL/g in the SBR than 126.4 mL/g in the CFSTR suggests that the SBR system generates better settling and compactable sludge than the latter. Also from the table, the lower variance of SVI, 4979, in the SBR than 5529, in the CFSTR suggests that settlibility and compactibility of the sludge in the SBR system is more stable than sludge in the CFSTR system.

Table 9-6 ANOVA of SVI in the two systems within specific substrate removal rate range of 0 to 0.8 g COD/g VSS/d

Groups	Count	Sum	Average	Variance
SBR system	26	2433	93.6	4979
CFSTR system	21	2654	126.4	5529

Source of Variation	SS	*df*	MS	F	$P_{\text{-value}}$	$F_{\alpha = 0.01}$
Between two systems	226356	25	9054	3.092	0.003	2.604
Within each system	939	1	939	0.321	0.576	7.770
Error	73210	25	2928			
Total	300505	51				

Thus, it can be concluded that, under equivalent operational conditions within the experimental parameter range, the SBR system generates better settling and more

compactable sludge than the CFSTR system, which allows an SBR system to run at comparatively lower sludge loading and provide higher capacity for shock loading.

9.4. COMPARISON OF REACTOR VOLUME UTILIZATION EFFICIENCY

Whether a reactor volume is used efficiently or not is important to evaluate the kinetics and the economy of the reactor. Volumetric loading rate and the physical volume utilization ratio describe the reactor volume utilization efficiency. Volumetric loading rate is specific substrate input rate based on unit effective reactor volume while physical reactor volume utilization ratio is a ratio of effective reactor volume to total system volume. Effective reactor volume has been defined in Section 8.2.6.

9.4.1. Comparison of Volumetric Loading

The volumetric loading rate for a CFSTR is

$$L_v = \frac{QS_0}{V} = \frac{S_0}{t_d}$$

According to Eq. (8-18), the volumetric loading rate for the SBR system is

$$L_{vtr} = \frac{Q_d S_0}{V_{ef}} = \frac{N_c(1-\alpha)S_0}{\varphi - \frac{1}{2}(1-\alpha)\frac{t_f}{t_c}}$$

Figure 9-15 provides a comparison of volumetric loading of the two systems based on t_{ed}. Although the SBR system has higher volumetric loading than the CFSTR, it does not

suggest that the former can treat more substrate than the latter as explained in the next paragraph. With t_{ed} extending to longer than 10 h, the loading rates in the two systems

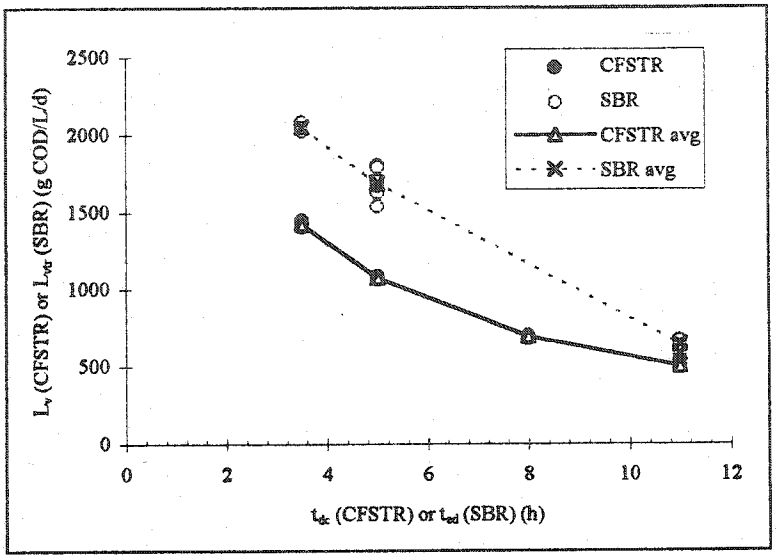


Figure 9-15. Comparison of volumetric loading, L_v or L_{vtr} vs HRT, t_{dc} or t_{ed} between CFSTR and SBR systems, respectively. (Average data from S_0 = 250 mg/L runs)

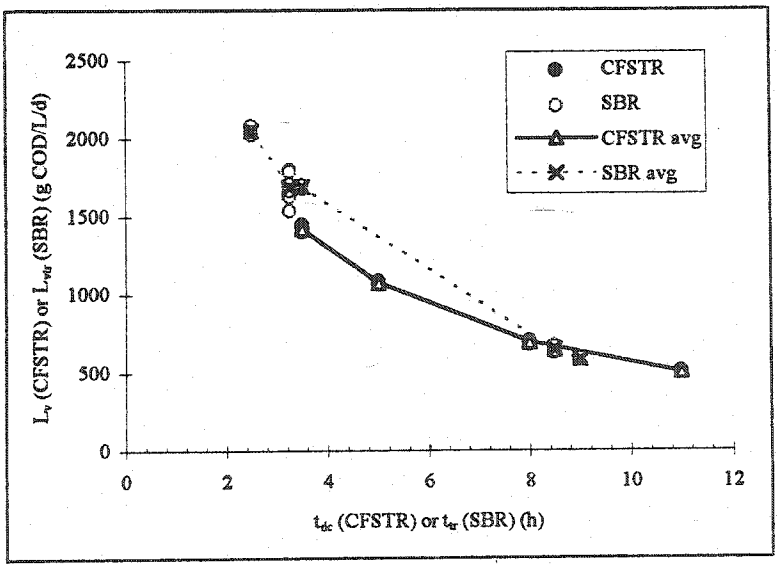


Figure 9-16. Comparison of volumetric loading, L_v or L_{vtr} vs t_{dc} or t_{tr}, between CFSTR and SBR systems, respectively. (Average data from S_0 = 250 mg/L runs)

become close. This trend reveals that under longer HRT, SBR becomes similar to an extended aeration process, losing its kinetic advantage.

An important finding is shown in Fig 9-16. If the comparison of volumetric loading between the two systems is made based on t_{tr} instead of t_{ed} (defined in Section 8.3.1) for the SBR, the relationship of volumetric loading and HRT of the two systems is almost the same. Under the same HRT (t_{ed} for the SBR system), higher L_{vtr} in the SBR system reveals its kinetic priority over the CFSTR system. However, t_{tr} in the SBR, from which the corresponding L_{vtr} is obtained, is always shorter than t_{ed} due to the aeration (or reaction) time ratio φ <1. Shorter t_{tr} corresponds to higher volumetric loading rate or the benefit of SBR kinetic advantage. From Fig. 9-17 and when considering true reaction time, t_{tr} for SBR and t_{dc} for CFSTR, it can be seen that there is no obvious improvement of volumetric utilization efficiency for the SBR system.

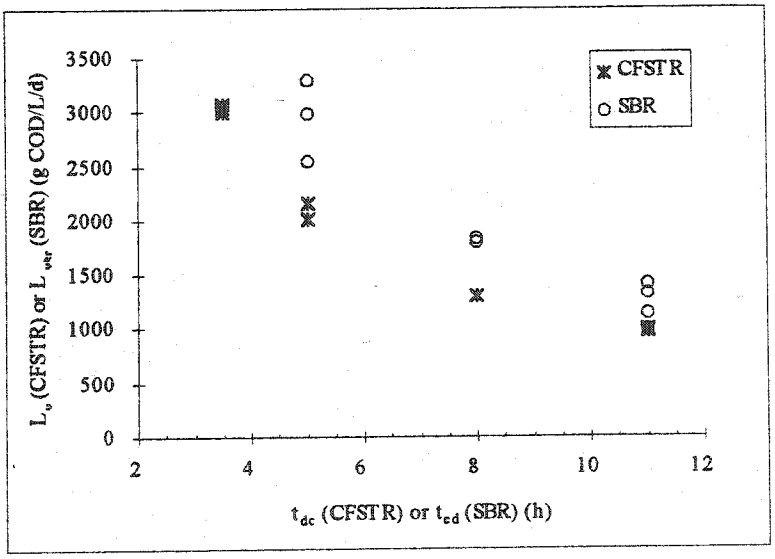


Figure 9-17. Comparison of volumetric loading L_v or L_{vtr}, vs t_{dc} or t_{ed} between the two systems (Average data from S_0 = 500 mg/L runs)

The comparison from Figs. 9-17 and 9-18 (S_0 = 500 mg/L) is very similar to that from Figs. 9-15 and 9-16. The only difference is L_v or L_{vtr} values in the figures are almost double those in Figs. 9-15 and 9-16 due to doubled influent concentration.

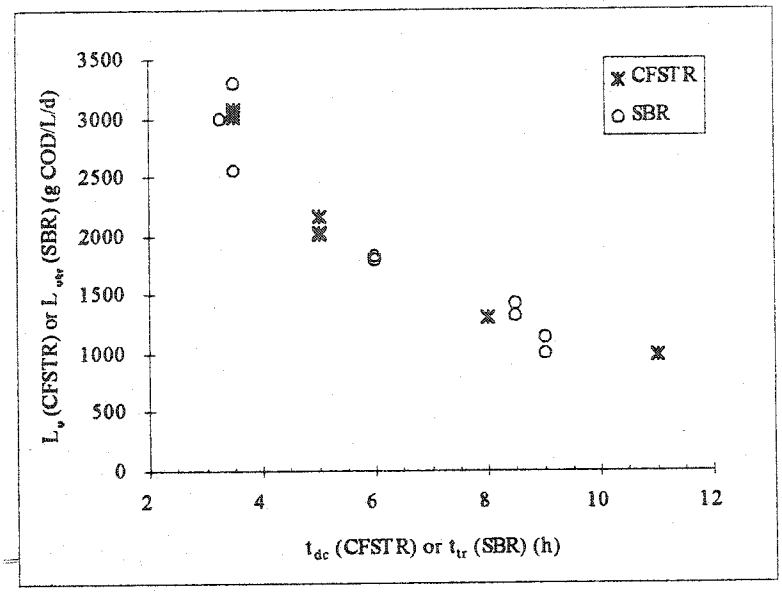


Figure 9-18. Comparison of volumetric loading L_v or L_{vtr}, vs t_{dc} or t_{tr} between the two systems (Average data from S_0 = 500 mg/L runs)

9.4.2. Comparison of Physical Volume Utilization Ratios of SBR and CFSTR

Physical volume utilization ratio, β, is the ratio of effective reactor volume to total system volume. For an SBR system this ratio has been defined in Section 8.2.3 and calculated by Eqs. (8-13) or (8-14). For the CFSTR system β is calculated by:

$$\beta = V_c / (V_c + V_{sc})$$

Table 8-1 lists the β related parameters and their values for the experimental sets. Due to a batch operational mode in the SBR system, β is a variable while it is a constant in a CFSTR system as shown in Table 9-7.

Table 9-7 Operational mode design and related parameter values of CFSTR experiments

No	t_d (h)	V_e (L)	V_s (L)	t_T (h)	t_s (h)	V_{ef} (L)	L_v (g COD/L/d)	β
1-250	3.5	10	2	3.5	0.7	10	2667	0.83
1-500	3.5	10	2	3.5	0.7	10	5333	0.83
2-250	5	10	2	5	1	10	1846	0.83
2-500	5	10	2	5	1	10	3692	0.83
3-250	8	10	2	8	1.6	10	1000	0.83
3-500	8	10	2	8	1.6	10	2000	0.83
4-250	11	10	2	11	2.2	10	667	0.83
4-500	11	10	2	11	2.2	10	1333	0.83

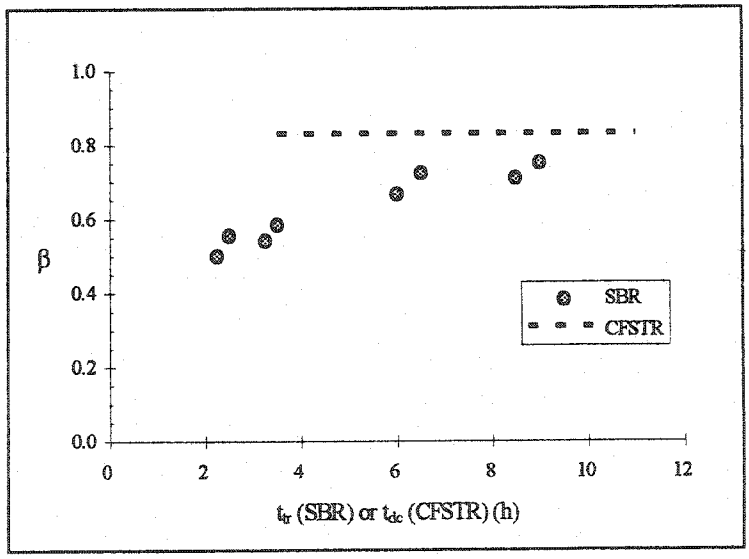


Figure 9-19. The relationship of β (V_{ef}/V_b) and t_{tr} in the SBR system, dotted-line is β value of the CFSTR system

Comparison of Tables 8-1 and 9-7 shows that the CFSTR system always has a higher physical volume utilization rate than the SBR. This difference is especially larger in the shorter HRT range, illustrated in Fig. 9-19.

9.5. COMPARISON OF OPERATIONAL CONSTRAINTS OF THE TWO SYSTEMS

Operational constraints of a biological wastewater treatment process are the limits beyond which the system can fail. These constraints could be physical, biological or a combination of the two.

For a CFSTR system, a high flow rate can disturb the laminar flow pattern in the secondary clarifier and then wash out a significant amount of the sludge, which causes return sludge of lower concentration to the aeration basin. Finally, lack of enough sludge in the aeration basin results in system failure. This situation is a physical constraint for a CFSTR system. Another example is that too high influent substrate concentration could produce activated sludge with a high SVI that is difficult to settle in the secondary clarifier and quite easily washed out due to continuous flow mode of the system, causing failure in the system. Also too low sludge age applied to the system can result in very poor settling sludge that can lead to system failure. The latter two examples are biological or physical-biological constraints for the CFSTR system. There could be other kinds of biological factors such as toxic chemicals that may cause system failure. These kinds of constraints were not considered in this research.

Actually, an SBR system has some operational constraints that are more strict than a CFSTR but some are less strict based on the large quantity of experimental data gathered in this study over a wide operational range. The strictest constraint for a SBR system is its initial volume, V_i, to accept feed.

In each SBR reactor, the effective volume will be limited by the length of the fill period and by the settling velocity and the compatibility of activated sludge. During the entire fill period, on average only half of the volume ($V_b - V_i$) can be used as react space. As t_f increases and consumes a larger portion of the total cycle time, the reactor volume utilization over the entire cycle decreases because the reactor is not full for a longer period of time. If the total volume, nV_b, is not changed, decreasing the number of reactors, n, will lengthen the fill period, t_f, and shorten the react period, t_r, and therefore, decrease the treatment efficiency.

Sludge that settles slowly or does not compact well will also decrease the reaction time. Slowly settling sludge increases the time required for the settling period at the expense of reaction time. Sludge that does not settle to a high degree of compaction decreases the available volume in a reactor. The latter two factors are dependent on the characteristics of the activated sludge that are largely dependent on the influent quality and the treatment provided. A high strength influent will tend to cause sludge bulking or produce a sludge with poor settleability and compatibility (Norcross, 1990).

If the above factors cause poor settling and less compactable sludge, there will not be enough sludge left in V_i after withdrawal at the end of a cycle. For the next cycle the sludge will be under a higher F/M ratio and could result in even poorer settling and less compactable sludge than that from the last cycle. This situation will continue if there is no increase in V_i to retain more sludge. Finally system failure will occur. Under these circumstances, more reactor volume has to be provided to hold enough sludge to maintain

treatment, thus, the effective volume for react will be remarkably decreased. These constraints diminish the advantages of an SBR.

Tables 9-8 and 9-9 provide a comparison of successive situations in the two systems. In Table 9-8, wk/fl (work/fail) indicates that part of an operation worked and part failed. For each set of V_i and t_{ed}, there are two operational modes: a shorter and a longer t_f, respectively, where one failed and the other did not. Referring to Table 3-2, Set No. 1 series failed in which t_f was longer and No. 2 series worked because t_f was shorter.

In the experiment, Set No. 1 with t_{ed} = 3.5 h, S_0 = 250 or 500 mg/L, all three designed sludge ages failed because high substrate loading at sludge age of 5 d or longer generated too much sludge with a compacted volume that was much larger than V_i. For each cycle more sludge was removed than produced. The sludge age decreased with each withdrawal. SVI rose to 1000 mL/g which resulted in system failure. Similar situations were observed in Set 2 with S_0 = 500 mg/L at all three sludge ages, and in Set 3 with S_0 = 500 mg/L and sludge age of 15 d.

In contrast, no such failure occurred in the CFSTR system under the equivalent experimental conditions. From these results, an SBR system has a more strict physical constraint, V_i, than a CFSTR.

The mechanisms of failure or resistance to substrate shock loading in the two systems are different. In a CFSTR system, microorganism species are acclimated at constant conditions: stable concentration of substrate, DO and other physical, chemical and biological conditions. A shock loading applied to microorganisms may change their bio-

Table 9-8 Comparison of successive operations in the two systems (S_0 = 250 mg/L)

t_{ed} h	SBR V_i = 1/3 V_b			SBR V_i = 1/2 V_b			CFSTR		
	θ_{xoh} 5 d	θ_{xoh} 10 d	θ_{xoh} 15 d	θ_{xoh} 5 d	θ_{xoh} 10 d	θ_{xoh} 15 d	θ_x 5 d	θ_x 10 d	θ_x 15 d
3.5	wk/fl*	wk/fl	wk/fl	-	-	-	work	work	work
5	-	-	-	work	work	work	work	work	work
8	work	work	work	-	-	-	work	work	work
11	-	-	-	work	work	work	work	work	work

* wk/fl (work/fail); one condition worked and one condition failed

Table 9-9 The succeed comparison of the two systems (S_0 = 500 mg/L)

t_{ed} h	SBR V_i = 1/3 V_b			SBR V_i = 1/2 V_b			CFSTR		
	θ_{xoh} 5 d	θ_{xoh} 10 d	θ_{xoh} 15 d	θ_{xoh} 5 d	θ_{xoh} 10 d	θ_{xoh} 15 d	θ_x 5 d	θ_x 10 d	θ_x 15 d
3.5	fail	fail	fail	-	-	-	work	work	work
5	-	-	-	work	work	work	work	work	work
8	work	work	fail	-	-	-	work	work	work
11	-	-	-	work	work	work	work	work	work

flocculating and settling abilities, sludge becomes bulked, then easily washed out of the reactor. In an SBR system, shock loading can cause sludge bulking temporarily but sludge can recover due to the presence of more species that are used to the changing environment within an operational cycle. Also the batch mode is beneficial to hold sludge in the reactor. These conditions may buffer an SBR system against failure.

Experimental results shown in Table 9-9 reveal that under the equivalent HRT and low SBR initial volume (V_i = 1/3 V_b), an SBR shows a narrower operational range than a

CFSTR. But an SBR has flexibility to change operational mode by increasing V_i to 1/2 V_b and shortening the feed time, t_f, to reach the same equivalent HRT. The system worked properly.

Another difference between the two systems is hydraulic shock loading. For an SBR system, feed flow rate variation has a minimal effect. It can accept a certain amount of feed within a very short period to obtain the highest kinetic rate as a true BR. But a CFSTR can only accept a flow rate from which there is no danger to wash out a significant amount of sludge.

9.6. CHARACTERIZATIONS AND CONCLUSION OF THE SBR SYSTEM

Under the equivalent conditions, i.e., under the same

$$t_{dc} = t_{ed} = \frac{nV_b - Qt_{sc}}{Q}$$

the SBR system exhibited a little higher substrate removal efficiency than the CFSTR by about one percent, although the former has much lower reactor volume utilization rate than the latter, 0.5 to 0.75 against 0.83. The lower physical volume utilization rate did not completely eliminate the kinetic advantage of the SBR.

Under the equivalent HRT, t_{ed}, the SBR also possesses slightly higher volumetric loading than the CFSTR, which reveals a higher substrate removal rate per unit reactor volume for the SBR system from an engineering point of view, although there is no such an advantage for the SBR based upon true HRT, t_{tr}. From statistical analysis under t_{ed}, the SBR system

has, on average, a slightly higher specific substrate removal rate than the CFSTR system as shown in Table 9-1. Obviously, these advantages of an SBR over a CFSTR are seriously diminished under some circumstances because an SBR must pay the cost for ideal PF type kinetics by lower physical volumetric utilization ratio, which finally deteriorates most of the kinetic advantage.

Under the circumstances of low and comparatively stable feed concentration, easy-to-biodegrade organic components and stable influent flow rate, an SBR will not have a high kinetic advantage. Only under the circumstances of the strengthening and refractory organic components in or unstable flow rate and concentration of the influent, will an SBR be expected to perform better than a CFSTR. These situations require a treatment system that can provide low F/M ratio, flexible HRT and sludge age to deal with various organic components.

The weakest constraint of an SBR system is its initial reactor volume, V_i. To overcome it, a design engineer could select higher V_i with short t_c and t_f to balance low volume utilization rate. On the other hand, large V_i will reduce the available reactor volume to accept feed. Proper selection of V_i is one of the key considerations for designing a SBR system.

CHAPTER 10 DESIGN PROCEDURES OF SBR SYSTEMS

This chapter provides a set of procedures to design an SBR system. Some parameters must be known before design calculations. These parameters are wastewater flow rate Q, influent COD or BOD concentration, effluent requirement or removal efficiency η, and the coefficients, Y, k_e and SVI. Other kinetic parameters, k_1, K_S, k_2, γ_s, γ_x, f_1, f_2, f_3, f_{x1}, f_{x2} and f_{x3}, will also be necessary if model simulation needs to be conducted.

10.1. TEST OF KINETIC RATE CONSTANTS

Most kinetic constants can be tested by the methods described in Chapter 5. Those which are not experimentally available can be assumed initially and then adjusted by the new SBR model.

10.2. THE NUMBER OF REACTORS IN THE SYSTEM, n, THE CYCLE TIME t_c, THE NUMBER OF CYCLES EACH DAY, N_c

The number of reactors in an SBR system and the total volume of the system are two important parameters that are directly related to the capital costs. Generally more reactors can provide a higher reactor volume utilization rate but will lead to higher capital cost and increase of shift frequency between the reactors. Commonly the number of reactors is two or three. An SBR system with more than four reactors is not normally recommended.

The number of cycles each day, N_c, or the length of a cycle, t_c, is another parameter that is decided based on experience. For operational convenience, t_c should be integrally divided by 24 h, with which an operator easily knows what the operational stage is at any time of a day. Therefore, t_c = 24, 12, 8, 6, 4, 3 and 2 h are recommended and, correspondingly, $N_c = 24/t_c$ = 1, 2, 3, 4, 6, 8 and 12. In some cases, t_c could be longer than 24 h. Following the same principle, t_c = 36, 48, 60, 72 h .... are convenient for operation.

10.3. DETERMINATION OF INITIAL REACTOR VOLUME RATIO, FILL TIME, REACT TIME, SETTLE TIME, DRAW TIME AND REACTIVE TIME RATIO

The initial reactor volume ratio $\alpha = V_i/V_b$ is a key parameter that influences reactor volume utilization rate and success of operation. Its value, theoretically, can be chosen from very low, for example, 5%, to very high 95%. But a low V_i could easily cause failure of operation and a value too high is meaningless because there is not enough volume to accept the feed. Common values for α could be 25 to 75% depending on sludge settling and compacting qualities and on the feed concentration. If the sludge has a low SVI, a low value can be chosen. If feed concentration is high, the value could be up to 75% for better dilution and for lower risk of shock loading. When there are no data, α = 50% is recommended and later it can be adjusted in practice if it is not suitable.

For designing t_f, there are two options. One is to calculate it directly by Eq. (8-5):

$$t_f = \frac{t_c}{n}$$

as long as t_c and t_r are set. A long t_f, when the number of reactors is only two or even one, will largely reduce SBR reactor utilization rate and diminish its rate of treatment.

Fill time should be as short as possible to obtain a "pure" batch mode which is ideal PF kinetics. For this option, an equalization basin will be required to hold the incoming wastewater because required flow rate is much higher than the normal wastewater flow rate. This will allow one to shorten t_f and to reach the same fill volume ($V_b - V_i$) during fill. But this approach will add another vessel. Duration of t_f will depend on the fill pump capacity. A balance of capital for the pump facilities, cost of operation of the pump and the benefit of PF kinetics must be carefully considered. t_f could be selected for 0.5 or 1 h, thereafter, $t_r = t_c - t_f$.

Determination of settle time requires a settling test and SVI data. Compared to about 2 h settling time in a secondary clarifier in a CFS, t_s = 1 h or less for an SBR is reasonable. Draw time, t_w, depends on the capacity of the withdrawal apparatus. Draw can be completed by a gravity type decanter or a decanter with a pumping system. The former needs a large diameter pipe system because of the low hydraulic head. The latter needs more power to run the pump. Whatever method is chosen, the level of the decanter should be adjustable to meet different V_i requirements later on and the draw flow rate should minimally disturb the quiescent liquid. Generally t_w can be about 0.5 h or less. Thus total time for settle and draw should not be longer than 1.5 h.

Now reaction or aeration time ratio, φ, another key parameter of SBR, can be calculated by Eqs. (8-4) and (8-11), $t_r = t_c - t_f - t_s - t_{sw}$, and $\varphi = (t_f + t_r)/t_c$.

10.4. REACTOR VOLUME, TOTAL SYSTEM VOLUME AND TRUE HYDRAULIC RETENTION TIME

From known Q, α and time periods of an operational cycle, a single SBR reactor volume, V_b, can be calculated. Since

$V_b - V_i = Qt_f$ or

$V_b = Qt_f + V_i$, but

$V_i = V_b\alpha$

Substituting the V_i expression into the above equation and rearranging it results in

$$V_b = \frac{Qt_f}{1-\alpha}$$

Thus the total system volume will be nV_b. The true HRT for each reactor can be calculated by Eq. (8-15):

$$t_{tr} = \frac{1}{1-\alpha}(t_f + t_r) - \frac{1}{2}t_f$$

and the effective reactor volume for each reactor, calculated by Eq. (8-10), is

$$V_{ef} = V_b\varphi - \frac{1}{2}(V_b - V_i)\frac{t_f}{t_c}$$

10.5. THE VERIFICATION OF SPECIFIC SUBSTRATE REMOVAL RATE R_{sr} AND THE MODIFICATION OF nV_b

With Eq. (8-23)

$$\frac{1}{\theta_{xob}\varphi} = Y\frac{N_c(V_b - V_i)(S_0 - S_e)}{V_b\overline{X}_v\varphi} - k_e$$

The above parameters, especially V_b and V_i, can be checked and modified if necessary. Putting all necessary given parameters and V_b, V_i, φ and N_c, into the equations and assuming an observed sludge age θ_{xob}, calculate the average VSS concentration, $\overline{X}_v$, then calculate the settled VSS volume with α and SVI.

If $\overline{X}_v/\alpha < 10^6/SVI$, the assumed θ_{xob} is theoretically obtainable but it may not the best value. The best θ_{xob} value should be greater than double the minimum sludge age and make $\overline{X}_v/\alpha \approx 10^6/SVI$.

If settled VSS volume is larger than V_i, there are two options. First, re-select sludge age and repeat the above calculation procedure until the VSS volume meets V_i. Second, change V_i and α, and recalculate them until desired θ_{xob} is reached.

CHAPTER 11 CONCLUSION OF PART II: AN OVERALL COMPARISON OF SBR AND CFSTR SYSTEMS

The second important contribution of this thesis is systematic development of design definitions and engineering parameters. An SBR system is not as popular as a continuous flow system for many reasons. One of the reasons is lack of widely accepted design standards. Design standards should be made based on both theoretical and practical work. To date, environmental engineers and researchers directly employed approaches that are widely used for CFS to design SBR systems. Unfortunately, these approaches lead to errors when applied to the design of SBR, or to the description of the performance of SBR process which can result in incorrectly sizing an SBR reactor or wrongly setting operational strategies. The causes of the above situations come from the multiple operational phases based on the pre-designed time sequences and the biokinetically unsteady state in the SBR process which are completely different from conditions in a steady state CFS.

The major parameters of the SBR that are different from those in steady state CFS are effective reactor volume, true HRT, true mean cell retention time or sludge age, total effective biomass; yield factor; sludge decay rate constant; true specific substrate removal rate, true sludge loading rate and volumetric loading rate. These parameters have been redefined and the relationships among them have been derived.

In the SBR system, the effective reactor volume is variable and depends on both the aeration time and fill time length in an operational cycle. The true HRT is also variable and a function mainly of the fill duration when total and initial reactor volumes and cycle length have been decided. The total effective biomass in an SBR reactor is significantly affected by the operational mode and consequently the biokinetic parameters. The true mean cell retention time or sludge age is also affected by the operational mode. The true sludge loading rate is calculated based on the total effective biomass and the true volumetric loading rate based on the effective reactor volume. The new definitions are also supported by the extensive experimental and related SBR model building work.

The third important development of the project is the completion of an overall experimental comparison between SBR and CFSTR systems. Systematic comparison of three SBR and three CFSTR reactors was conducted under equivalent operational conditions. The SBR system showed slightly improved kinetics over the CFSTR, while having more strict physical constraints than the latter. The major physical constraint is initial reactor volume V_i which reduced reactor volume utilization rate and limited the quantity of sludge held in the reactor. As a result of the constraints, the advantages of the SBR system compared to the CFSTR system are seriously diminished. Based on equivalent operational condition, the overall average COD removal efficiency by the SBR system was about one percent higher than the CFSTR system. Also based on the equivalent condition, the SBR system possessed slightly higher volumetric loading and slightly higher specific substrate removal rates. The SBR showed more stable operation than the CFSTR with slightly more narrow variations of COD removal efficiency and of

specific removal rate as well. The analysis of variance (ANOVA) results reveal that these SBR advantages are significant at $\alpha = 0.05$ level but not significant at $\alpha = 0.01$. From the comprehensive comparison of the systems, it can be concluded that under the circumstances of low and comparatively stable feed concentration, easy-to-biodegrade organic components and stable influent flow rate, the SBR system will show minimal advantage over a CFSTR system. Only under the circumstances of high strength or refractory organic components or unstable flow rate or unstable concentration, will an SBR system be expected to perform better treatment than CFSTR because these situations require a treatment system that can provide low F/M ratio, flexible HRT and sludge age to deal with various organic components and hydraulic or organic shock.

REFERENCES

Abufayed, A.A. and Schroeder, E.D. (1986). Kinetics and stoichiometry of SBR/denitrification with a primary sludge carbon source. **J. WPCF**, 58, 5, 398-405.

Alleman, J.E. and Irvine, R.L. (1980). Storage induced denitrification using sequencing batch reactor operation. **Wat. Res.**, 14, 1483-1488.

Alleman, J.E. and Irvine, R.L. (1980). Nitrification in the sequencing batch reactor. **J. WPCF**, 52, 11, 2747-2754.

Amy, G.L., Bryant, C.W., Jr, and Belyani, M. (1987). Molecular weight distributions of soluble organic matter in various secondary and tertiary effluents. **Wat. Sci. Tech.**, 19, 529 - 538.

Arden, E. and Lockett, W.T. (1914a). Experiments on the oxidation of sewage without the aid of filters. **J. Soc. of Chem. Industries.**, 33, 523-539.

Arden, E., and Lockett, W.T. (1914b). Experiments on the oxidation of sewage without the aid of filters II. **J. Soc. of Chem. Industries.**, 33, 1122-1124.

Arden, E. and Lockett, W.T. (1915). Experiments on the oxidation of sewage without the aid of filters III. **J. Soc. of Chem. Industries.**, 34, 937-943.

Arora, M.L. Barth, E.F. and Umphres, M.B. (1985). Technology evaluation of sequencing batch reactors. **J. WPCF**, 57, 8, 867-875.

Artan, N. and Orhon, D. (1989). The effect of reactor hydraulics on the performance of activated sludge systems -II. the formation of microbial products. **Wat. Res.**, 23, 12, 1519-1525.

APHA-AWWA-WPCF. (1989). Standard methods for the examination of water and wastewater. 17th Edition. Publisher: American Public Health Association. Washington, DC.

Barth, E.F. (1983). Implementation of sequencing batch reactor for municipal treatment. **6th Symposium on Wastewater Treatment**, sponsored by Environment Canada, Ottawa.

Baskir, C. I. And Hansford, G.S (1980). Product formation in the continuous culture of

microbial populations grown on carbohydrates. **Biotechnol. Bioengr.**, 22, 1857-1875.

Bidstrup, S.M. and Grady, C.P.L., Jr. (1988). SSSP-Simulation of single-sludge process. PART 1, **J. WPCF**, 351-361.

Blackwell, L.G. (1971). A theoretical and experimental evaluation of the transient response of the activated sludge process. **Ph.D. thesis, Clemson Univ.**, Clemson, SC.

Bloemer, J.W.; Farrell, R. P. and Kawahata, M. (1980). Sequencing batch reactor (SBR). treatment plant with zero discharge at Eaton Corporation's Willoughby Hills, OH. **Proc. 12th Mid-Atlantic Industrial Waste Conference**, 97-101.

Bloemer, J.W. and Irvine, R.L. (1982). Sequencing batch reactor treatment plant with zero discharge. **PB 82-223256** (U.S. Government Report).

Boero, V. J.; Eckenfelder, W.W., Jr. and Bowers, A.R. (1991). Soluble microbial product formation in biological systems. **Wat. Sci. Tech.**, 23, 1067-1991.

Braha, A. and Hafner, F. (1987). Use of lab batch reactors to model biokinetics. **Wat. Res.**, 21, 1, 73-81.

Cech J.S.; Chudoba, J. and Grau, P. (1985). Determination of kinetics constants of activated sludge microorganisms. **Wat. Sci. Technol.**, 17, 2/3, 259 -272.

Chiesa, S.C. and Irvine, R.L. (1985). Growth and control of filamentous microbes in activated sludge: an integrated hypothesis. **Wat. Res.**, 19, 4, 471-479.

Chudoba, J. (1967). Residual organic matter in activated sludge process effluents. I. Degradation of saccharides, fatty acid and amino acids under batch conditions **Technol. of Water**, 12, 39-75.

Chudoba, J.; Nemec, M. and Nemcova, R. (1968a). Residual organic matter in activated sludge process effluents. II. Degradation of saccharides, fatty acid and amino acids under continuous conditions. **Technol. of Water**, 13, 27-43.

Chudoba, J.; Prasil, M. and Emmerova, H. (1968b). Residual organic matter in activated sludge process effluents. III. Degradation of amino acids and phenols under continuous conditions. **Technol. of Water**, 13, 45-61.

Chudoba, J.; Cervenka, J. and Zima, M. (1969). Residual organic matter in activated sludge process effluents. IV. Treatment of municipal sewage. **Technol. of Water**, 15,

5-21.

Chudoba, J.; Tucek, F.; Lischke, P. and Sames, F. (1980). Residual organic matter in activated sludge process effluents. X. Isolation and identification of a high molecular fraction of polypeptidic character. **Technol. of Water and Environ.**, 23, 79-94.

Chudoba, J. (1985). Quantitative estimation in COD units of refractory organic compounds produced by activated sludge microorganisms. **Wat. Res.**, 19, 1, 37-43.

Daigger, G.T. and Grady, C.P.L., Jr. (1977a). A model for the bio-oxidation process based on product formation concepts. **Wat. Res.**, 11, 1049-1057.

Daigger, G.T. and Grady, C.P.L., Jr. (1977b). Factors affecting effluent quality from fill-and-draw activated sludge reactors. **J. WPCF**, 49, 2390-2396.

Demain, A. L., Burg, R.W., and Hendlin, D., (1965). Excretion and degradation of ribonucleic acid by Bacillus subtilis. **J. Bacterial**, 89, 640-646.

DeWalle, F.B. and Chian, E.S.K. (1980). Kinetics of formation of humic substances in activated sludge systems and their effect on flocculation. **Biotech. and Bioeng.**, 16, 739-755.

Dold, P.L.; Ekama, G.A. and Marais, G.v.R. (1980). A general model for the activated sludge process. **Prog. Wat. Tech.**, 12, 47-77.

Dold, P.L. and Marais, G.v.R. (1986). Evaluation of the general activated sludge model proposed by the IAWPRC task group. **Wat. Res.**, 18, 63-89.

Droste, R.L. (1990). Comparison of continuous flow and sequencing batch reactors for biological wastewater treatment. (for **The Biotech. of Wastewater Management Workshop**, Ottawa).

Dubois, M.; Gilles, K.A.; Hamilton, J.K.; Rebers, P.A. and Smith, F. (1956). Colorimetric method for determination of sugars and related substances. **Analyt. Chem.**, 28, 350-356.

Ekama, G.A. and Marais, G.v.R. (1979). Dynamic behavior of the activated sludge process. **J. WPCF**, 5, 3, 534-556.

Ekama, G.A.; Dold, P.L. and Marais, G.v.R. (1986). Procedure for determining influent COD fraction and the maximum specific growth rate of heterotrophs in activated sludge system. **Wat. Sci. Tech.**, 18, 6, 91-114.

Ford, D.L. and Eckenfelder, W.W., Jr. (1967). The role of enzymes in the contact stabilization process - discussion. Advances in Water Pollution Research, 2. (Article by R.H. Siddinqi, R,S. Engelbrcht and R.E. Speece). **J. WPCF**, 39, 1211-1222.

Furumai, H. and Rittman, B.E. (1992). Advanced modeling of mixed populations of heterotrophs and nitrifiers considering the formation and exchange of soluble microbial products. **Wat. Sci. Tech.**, 26, 3-4, 493-502.

Gaudy, A.F., Jr. (1963). Sequential substrate removal in heterogeneous population. **J. WPCF**, 35, 903-922.

Gaudy, A.F., Jr. and Gaudy, E.T. (1980). Microbiology for environmental scientists and engineers. McGraw-Hill Book Co., New York.

Gaudy, A.F., Jr. and Blachly, T.R. (1985). A study of the biodegradability of "residual COD". **J. WPCF,** 43, 4, 665-676.

Grady, C.P.L., Jr. and Lim, H. C. (1980). Biological Wastewater Treatment, Theory and Applications. Marcel Dekker, New York.

Grady, C.P.L., Jr.; Harlow, L.J. and Reising, R.R. (1972). Effects of growth rate and influent substrate concentration on effluent quality from chemostats containing bacteria in pure and mixed culture. **Biotech. Bioeng.**, 14, 391-410.

Grady, C.P.L., Jr.; Guejer, W.; Henze, M.; Marais, G.v.R. and Matsuo, T. (1986). A model for single sludge wastewater treatment systems. **Wat. Sci. Tech.**, 18, 47-61.

Grady, C.P.L., Jr. (1989). Dynamic modelling and exert system in wastewater engineering. Lewis Publishers Inc., Chelsea, MI.

Grady, C.P.L., Jr. and Williams, D.R. (1975). Effects of influent substrate concentration on the kinetics of natural microbial populations in continuous culture. **Wat. Res.**, 9, 171-180.

Grau, P.; Dohanyos, M. and Chudoba, J. (1975). Kinetics of multicomponent substrate removal by activated sludge. **Wat. Res.**, 9, 637-642.

Griffiths, P. (1994). Modifications to the IAWPRC task group general activated sludge model. **Wat. Res.**, 28,.3, 657-664.

Henze, M.; Grady, C.P.L., Jr.; Gujer, W.; Marais, G.v.R. and Matsuo, T. (1986). Activated sludge model 1. **IAWPRC Scientific and Technical Report 1**.

Henze, M.; Grady, C.P.L., Jr.; Gujer, W.; Marais, G.v.R. and Matsuo, T. (1987). A general model for single sludge wastewater treatment system. **Wat. Res.**, 21, 5, 505-515.

Hoepker, E.C. and Schroeder, E.D. (1979). The effect of loading rate on batch activated sludge effluent quality. **J. WPCF**, 51, 2, 264-272.

Hoover, S.R. and Porges, N. (1952). Assimilation of dairy wastes by activated sludge, II: The equations of synthesis and rate of oxygen utilization, **Sewage Ind. Wastes**, 24, 306-312.

Irvine, R.L. and Avis, W.B. (1971). Use of sequencing batch reactor for wastewater treatment. **Proc. 26th Industrial Waste Conf., Purdue Univ., 1971**. Lafayette, IN.

Irvine, R.L. and Ritcher, R.O. (1976). Computer simulation and design of sequencing batch biological reactors. **Proc. 31st Industrial Waste Conf., Purdue Univ., 1976**.

Irvine, R.L.; Fox, T.P. and Richter, R.O. (1977). Investigation of fill and batch periods of sequencing batch reactors. **Wat. Res.**, 11, 713-717.

Irvine, R.L. and Ritcher, R.O. (1978). Comparative evaluation of sequencing batch reactors. **J. of the Environ. Engr. Division**, June, 503-514.

Irvine, R.L. and Busch, A.W. (1979). Sequencing batch biological reactors ----- an overview. **J. WPCF**, 51, 2, 235-243.

Irvine, R.L.; Ketchum, L.H.; Breyfogle, R. and Barth, E.F. (1983). Municipal application of sequencing batch treatment. **J. WPCF**, 55, 5, 484-488.

Irvine, R.L.; Ketchum, L.H., Jr.; Arora, M.L. and Barth, E.F. (1985). An organic loading study of full-scale sequencing batch reactors. **J. WPCF**, 57, 8, 847-853.

Irvine, R.L. and Ketchum, L.H., Jr. (1989). Sequencing batch reactors for biological wastewater treatment. **CRC Critical Reviews in Environ. Control**., 18, 4, 255-294.

Ketchum, L.H., Jr.; Irvine, R.L. and Dennis, R.W. (1978). Sequencing batch reactors to meet compliance. **AIChE Symposium Series, Water**, 75,190, 186-190.

Ketchum, L. H., Jr. and Liao, P.C. (1979). Tertiary chemical treatment for phosphorus reduction using sequencing batch reactors. **J.WPCF**, 52, 298-304.

Lawrence, A.W. and McCarty, P.L. (1970). Unified basis for biological treatment design

and operation. **J. of the Sanit. Eng. Div., Amer. Soc. of Civil Engineers**, 96, SA3, June, 757-778.

Lessard, P. and Beck, M.B. (1993). Dynamic modelling of the activated sludge process: a case study. **Wat. Res.**, 27, 6, 963-978.

Lehninger, A.L. (1975). Biochemistry. Second Edition. Worth Publishers, Inc. New York, N. Y.

Luedeking, R. and Piret, E.L., (1959). A kinetic study of the lactic acid fermentation batch process at controlled pH. J. **Bioch. Microbial Technol.**, 16, 399 - 403.

Mandt, M.G. (1985). The innovative technology of sequencing batch reactors. **Poll. Eng.**, 17, 7, 26-28.

Manka, J. and Rebhun, M. (1982). Organic groups and molecular weight distribution in tertiary effluents and renovated waters. **Wat. Res.**, 16, 399-403.

Manning, J.F. and Irvine, R.L. (1985). The biological removal of phosphorus in a sequencing batch reactor. **J. WPCF**, 57, 1, 87-94.

McGregor, W.C. and Finn, R.K. (1969). Factors affecting the flocculation of bacteria by chemical additives. **Biotech. Bioeng.**, 11, 127-138.

Metcalf and Eddy, Inc. (1991). Wastewater Engineering-treatment, disposal, and reuse. Third edition. McGraw-Hill Publishing Company, New York.

Monod, J. (1949). The growth of bacterial cultures. **Ann. Rev. Microbial.**, III, 371-392.

Morris, J.C. and Stumm, W. (1960). Colloidal aspects of waste treatment. **Proc. Rudolphs Research Conf.**, Rutgers Univ.

Moser, F. (1977). Ein Rohrreaktor zur Abwasserreinigung. **Verfahrenstechnik**, 11, 670-673.

Nakazawa, H. and Tanaka, K. (1991). Kinetic model of sequencing batch activated sludge process for municipal wastewater treatment. **Wat. Sci. Tech.**, 23, 1097-1106.

Namkung, E. and Rittman, B.E. (1986). Soluble microbial products (SMP). formation kinetics by biofilms. **Wat. Res.**, 20, 795-806.

Norcross, K.L. (1990). Performance and design consideration for SBR treatment of food processing wastewater. **Proc. of 1990 Food Ind. Envir. Conf.**, Nov. 12-14. Atlanta, GA.

Oles, J. and Wilderer, P.A. (1991). Computer aided design of sequencing batch reactors based on the IAWPRC activated sludge model. **Wat. Sci. Tech.**, 23, 1087-1095.

Orhon, D.; Cimsit, Y. and Tunay, O. (1986). Substrate removal mechanism for sequencing batch reactors. **Wat. Sci. Tech.**, 18, 21-33.

Painter, H. (1973). Organic compounds in solution in sewage effluents. **Chemistry and Industry**, 818-822.

Palis, J.C. and Irvine, R.L. (1985). Nitrogen removal in a low-loaded single tank sequencing batch reactor. **J. WPCF**, 57, 1, 82-86.

Parkin, G.F. and McCarthy, P.L. (1981). A comparison of the characteristics of soluble organic nitrogen in untreated and activated sludge treated wastewaters. **Wat. Res.**, 15, 139-149.

Philibrook, D.M. and Grady, C.P.L., Jr. (1985). Evaluation of biodegradation kinetics for priority pollutants. **Proc. 40th Industrial Waste Conf., Purdue Univ., 1985**. J..M. Bell (Ed.). Butterworth Publishers, Stoneham, Mass., 795.

Pirt, S. J. (1975). Principles of microbe and cell cultivation, John Wiley and Sons, Inc., New York.

Rittman, B.E.; Bae, W.; Namkung, E. and Lu, C.J. (1987). A critical evaluation of microbial product formation in biological processes. **Wat. Sci. Tech.**, 19, 517 - 528.

Rittman, B.E. (1987). Aerobic biological treatment. **Environ. Sci. Tech.**, 21, 2, 128-136.

Roberts, D.V. (1977). Enzyme kinetics. Cambridge University Press. Cambridge.

Saunders, F.M. and Dick, R.I. (1981). Effect of mean-cell residence time on organic composition of activated sludge effluents. **J. WPCF**, 53, 201-215.

Siber, S. and Eckenfelder, W.W., Jr. (1980). Effluent quality variation from multi-component substrates in the activated sludge process. **Wat. Res.**, 14, 471-476.

Silverstein, J. and Schroeder, E.D. (1983). Performance of SBR activated sludge processes with nitrification / denitrification. **J. WPCF**, 55, 4, 377-384.

Sollfrank, U. and Gujer, W. (1991). Characterization of domestic wastewater for mathematical modelling of the activated sludge process. **Wat. Sci. Tech.**, 23, 1057-1066.

Speitel, G.E., Jr. and DiGiano, F.A. (1988). Determination of microbial kinetic

coefficients through measurement of initial rates by radiochemical techniques. **Wat. Res.**, 22, 829-835.

Strange, R.E.; Wade, H.E. and Ness, A.G. (1963). The catabolism of proteins and nucleic acids in starved Aerobacter aerogenes. **Biochem. J.**, 86, 197 - 203.

Sudo, R. and Okado, M. (1984). Simultaneous removal of phosphorus and nitrogen by sequencing batch activated sludge process. Presented at the **2nd German-Japanese Workshop on Wastewater and Sludge Treatment**, Karlsruhe, West Germany.

Templeton, L.L. and Grady, C.P.L., Jr. (1988). Effect of culture history on the determination of biodegradation kinetics by batch and fed-batch techniques. **J. WPCF**, 60, 5, 651-658.

Thomas, T.D. and Batt, R. D. (1969). Degradation of cell constituents by starved Streptococcus lactis in relation to survival. **J. Gen. Microb.**, 58, 347 - 362.

Weber, W.J., Jr. (1972). Physicochemical processes for water quality control. John Wiley & Sons, Inc., New York.

Wilderer, P.A. (1984). Application of sequencing batch reactor technology for industrial wastewater treatment. Presented at **The 2nd German-Japanese Workshop on Wastewater and Sludge Treatment**, Karlsruhe, West Germany.

Williamson, K.J. and McCarty, P.L. (1975). Rapid measurement of Monod half-velocity coefficients for bacterial kinetics. **Biotech. Bioeng.**, 17, 915-924.

Wilson, D.E. and Marais, G.v.R. (1976). Adsorption phase in biological denitrification. **Res. Rept.** No. W. 11, Dept. of Civil Eng., Univ. of Cape Town, South Africa.

APPENDIX A

ANALYSIS OF COD

COD analysis follows the method 5023c, Close Flux, in Standard Methods for Water and Wastewater Analysis (APHA,1989).

ANALYSIS OF TOTAL AMINO ACIDS

To verify the effect of SMP on the existing COD in the clarified solution, total amino acids were analyzed to track the feed protein degradation in the biological process.

To analyze total amino acids, mix one volume wastewater sample with one volume of 12 NHCl. The mixture is heated in a sealed tube at 106 C° for 24 h. Dry the digested solution under vacuum at room temperature and the dried sample can be analyzed for total amino acids. All samples were finally analyzed in the laboratory of the Medical School at the University of Ottawa.

ANALYSIS OF SIMPLE MOLECULAR CARBOHYDRATES

In order to compare the difference between the degradations of protein and saccharose for the verification of SMP, one batch test set was conducted with saccharose as the main component in the feed.

The analysis of simple molecular carbohydrates was conducted at the Biotechnology

Research Institute of NRC in Montreal.

Apparatus: The chromatographic system consist of an HPLC pump (Model 590, Millipore, Waters Chromatography Division, USA), a temperature control module (Model TCM, Millipore), a refractive index detector (Model 410, Millipore) and an WISP autoinjector with a variable loop volume (Model 710b, Millipre). The column is an Interaction ION-300 Organic Acid Column (300 mm X 7.8 mm I.D., Interation Chemicals Inc., CA, USA) with a Ion Guard GC-801 guard column (Interation Chemicals Inc.). Data acquisition for two signals and integration is performed on a millennium 2010 chromatographic manager system (Millipore).

Solvent: Sulphuric acid (0.0033N) is prepared form concentrated sulphuric acid (Anachemia Canada Inc.) using a reverse-osmosis treated demineralized water.

Sample preparation: All reference standard solutions are prepared from analytical reagent grade subsistence obtained from different and known companies. All samples are preferably centrifuged for a few min and/or filtered through a 0.2 μm filter (Millex GS, Millipore).

Chromatographic conditions: Most of the time, the flow rate is 0.4 ml per min and should not exceed 0.6 ml per min. The temperature of the column is fixed at 30°C. The column pressure should not exceed 2200 psi. (150 atm). The most frequent column sample volume injected used is 50 μL.

Procedure: The solvent is degassed with helium gas for 5 min before use, and degassed continuously during use. The column is conditioned 30 min before use until a steady and

horizontal baseline is obtained. Inject a known volume in μL from a standard preparation into the chromatography system, record the chromatogram, measure the areas for each peak and identify each of them. Inject the same column in μL of a sample preparation, identify the homology peaks by comparison of the retention times with those from the standard preparation, similarly chromatographed.

Calculation: Calculate the concentration of each component using of a standard curve.

Limit of detection: For the majority of carbohydrates and alcohols, the limit of detection of the refractive index detector is approximately 5-50000 mg/L For the organic acids, the limit of detection is dependent on the wavelength used (on a UV detector) and the structure and chemical composition of the acid analyzed. In most cases, the limit of detection is approximately 1-35000 mg/L by UV and 5-50000 mg/L by RI.

ANALYSIS OF TOTAL CARBOHYDRATES

Total carbohydrates is measured with colorimetric method developed by Dubois et al. (1956), which is simple, sensitive and reproducible.

Apparatus: At least six Pyrex test tubes (18 mm × 150 mm) with a vibrator for vortexing the test tubes are needed. A water bath (30°C) is to stabilize the sample temperature. A spectrophotometer (using 490 nm wavelength) is used for the final measurement.

Solvent: 100 mL 5% phenol solution is made as a color generator. Concentrated analytical grade H_2SO_4 is used to provide a low pH for color generation. D-glucose (BDH Chemicals) solutions at concentrations of 0, 5, 10, 15, 20 and 25 mg/L are prepared

for the calibration curve.

Procedure: 1 mL sample solution and 1 mL 5% phenol solution are added into a test tube. Then, 5 mL concentrated sulfuric acid is added into the tube. Meanwhile, a blank sample is prepared by adding 1 mL distilled water and 1 mL phenol solution into another test tube, and adding 5 mL sulfuric acid into it as well. The tubes are vortexed and cooled for at least 10 min at room temperature. Next, the tubes are put into water bath at 30°C for 10 min to stabilize temperature and the generated yellow color. The absorbances of the solution are then measured with the spectrophotometer at 490 nm against the blank. The absorbance readings can be converted into the concentrations of total carbohydrates by comparison with the calibration curve.

ANALYSIS OF TSS AND VSS

TSS and VSS are analyzed according to methods 2540D and 2540E, respectively, in *Standard Methods for Water and Wastewater Analysis* (APHA,1989).

OTHER ANALYTICAL METHODS

Settled Sludge Volume and SVI is analyzed according to method 2710 in *Standard Methods for Water and Wastewater Analysis* (APHA,1989).

DO is analyzed according to method 4500-OG in *Standard Methods for Water and Wastewater Analysis* (APHA,1989).

APPENDIX B BATCH TEST RESULTS

B-1. Batch Test 1 (S_0 = 144, 110 and 65 mg/L, respectively; acclimated sludge from SBR run No. 8-500 and θ_{xob} = 5 d)

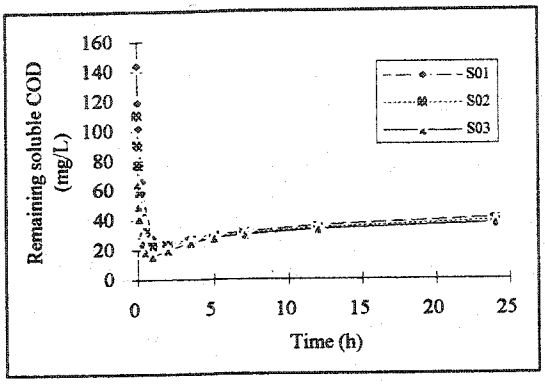


Fig-B-1-1. Soluble COD degradation vs time

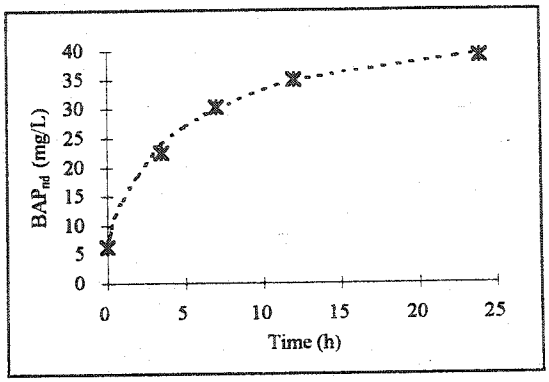


Fig-B-1-2. BAP_{nd} vs time

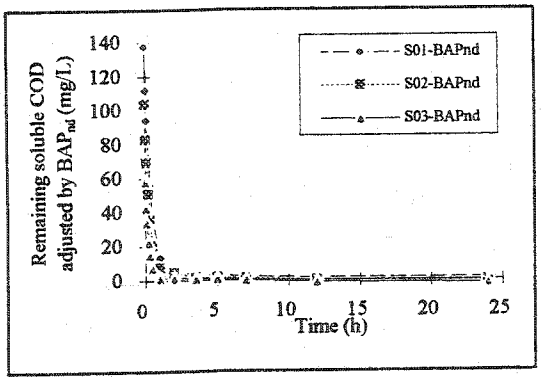


Fig-B-1-3. Soluble COD degradation vs time curves adjusted by BAP_{nd}

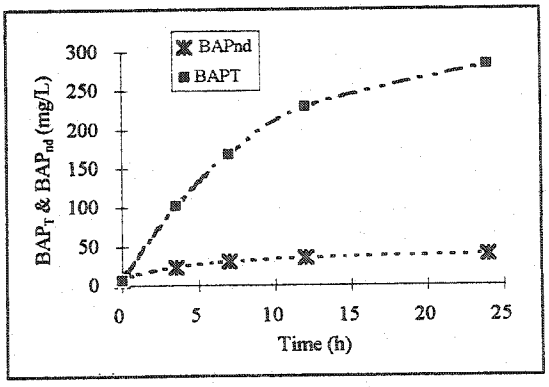


Fig-B-1-4. BAP_T compared to BAP_{nd} vs time

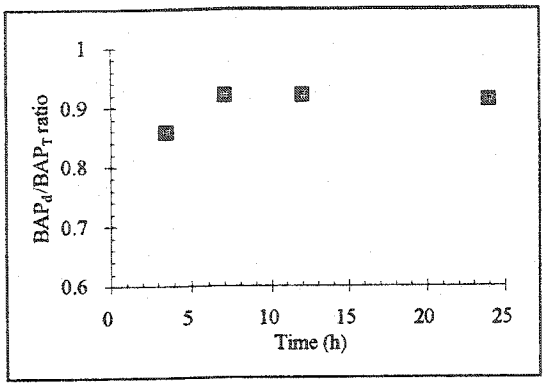


Fig-B-1-5. The ratio of BAP_d to BAP_T

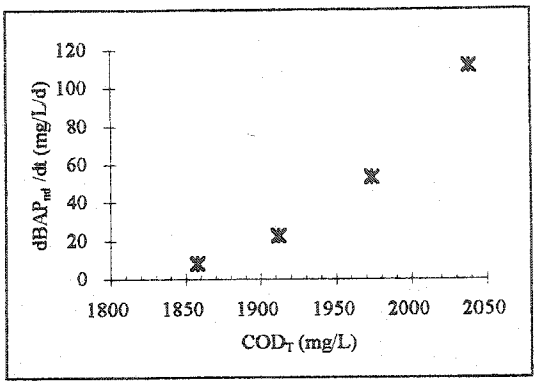


Fig-B-1-6. Linear relation between $dBAP_{nd}$ /dt and COD_T

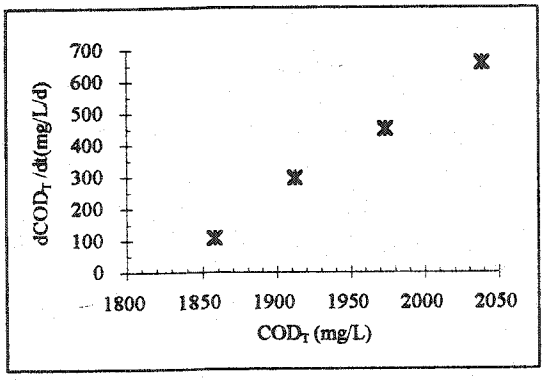


Fig-B-1-7. Linear relation between $dCOD_T/dt$ and COD_T

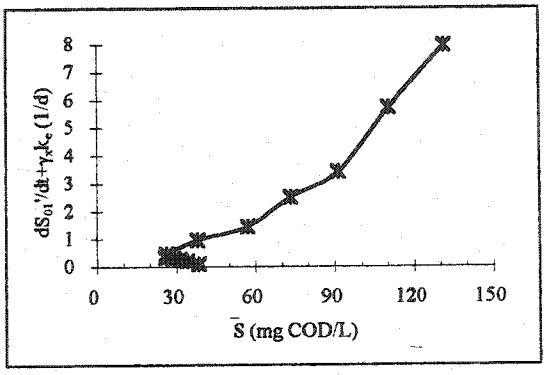


Fig-B-1-8. dS′/dt vs S curve with S_0 = 144 mg/L

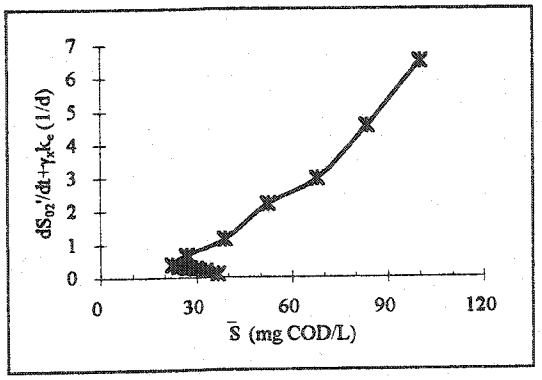


Fig-B-1-9. dS′/dt vs S curve with S_0 = 110 mg/L

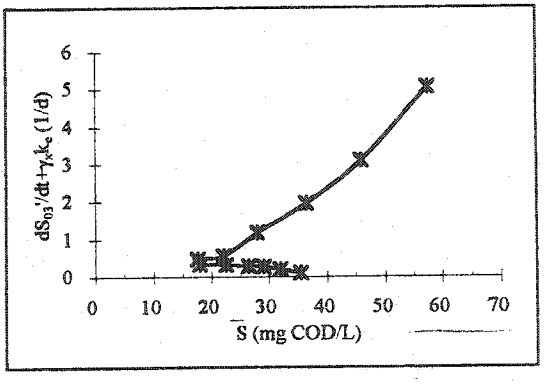


Fig-B-1-10. dS′/dt vs S curve with S_0 = 65 mg/L

APPENDIX B BATCH TEST RESULTS

Batch Test 1. (Sludge from No. 8-500-5)					$\bar{X}_v$ =	1650	mg/L					
Time	S_{01}	S_{02}	S_{03}	$\bar{S}_{01}$	$\bar{S}_{02}$	$\bar{S}_{03}$	$dS_{01}'/dt+\gamma_x k_e$	$dS_{02}'/dt+\gamma_x k_e$	$dS_{03}'/dt+\gamma_x k_e$	BAP_{nd}	$*BAP_{nd}$	$dBAP_{nd}/dt$
h	mg/L	mg/L	mg/L	mg/L	mg/L	mg/L	d^{-1}	d^{-1}	d^{-1}	mg/L	mg/L	mg/L/d
0	144	110	65							6.2	6.2	
0.05	119	90	50	131.5	100	57.5	7.958	6.503	5.049		7	
0.1	102	77	42	110.5	83.5	46	5.718	4.554	3.100		7.5	
0.2	81	59	31	91.5	68	36.5	3.405	2.969	1.950		8.4	
0.3	66	46	25	73.5	52.5	28	2.489	2.198	1.180		9.6	
0.5	48	32	19	57	39	22	1.434	1.143	0.561		11.5	
1	28	22	16	38	27	17.5	0.961	0.670	0.467		14.5	
2	24.1	23	20	26.05	22.5	18	0.457	0.385	0.342		18.6	
3.5	27.6	26	25	25.85	24.5	22.5	0.327	0.332	0.313	22.5	24	164
5	30.2	28.7	28	28.9	27.35	26.5	0.286	0.285	0.283		27	
7	32.1	31.1	30.3	31.15	29.9	29.15	0.265	0.262	0.262	30.3	29.8	53
12	36.1	34.6	33.7	34.1	32.85	32	0.198	0.199	0.200	35	34.7	23
24	40.9	39.2	37.4	38.5	36.9	35.55	0.099	0.099	0.100	39	39.4	8
					$1/\bar{S}$	$1/(dS'/dt+\gamma_x k_e)$		Regression Output for k_1 and K_{S1}:				
f_1	0.324746	0.346821	0.345238		0.008	0.126	k_1	Constant			0.076737	
f_2	0.62119	0.615607	0.603741		0.010	0.154	13	Std Err of Y Est			0.008132	
f_3	0.054064	0.037572	0.05102		0.017	0.198		R Squared			0.975186	
$f_1+f_2+f_3$	1	1	1				K_{S1}	No. of Observations			3	
							92	Degrees of Freedom			1	
								X Coefficient(s)			7.066493	
								Std Err of Coef.			1.127223	
* The data smoothened by the polynomial method (Gerald and Wheatley, 1989)												

APPENDIX B BATCH TEST RESULTS

Bactch Test 1 (Cont.')

S_{01}-BAP_{nd}	S_{02}-BAP_{nd}	S_{03}-BAP_{nd}	COD_T	*COD_T	$dCOD_T/dt$	BAP_T	BAP_T	BAP_T at t	BAP_d/BAP_T	S_{01}'	S_{02}'	S_{03}'
S_{01}-BAP_d	S_{02}-BAP_d	S_{03}-BAP_d										
mg/L	mg/L	mg/L	mg/L	mg/L	mg/L/d	mg/L	mg/L	mg/L	-	mg/L	mg/L	mg/L
137.8	103.8	58.8	2130	2135		6.2	6.2			144	110	65
112	83	43		2132			9.2	3		116.8	87.8	47.8
94.5	69.5	34.5		2129			12.2	3		97.3	72.3	37.3
72.6	50.6	22.6		2126			15.2	3		74.2	52.2	24.2
56.4	36.4	15.4		2123			18.2	3		57.4	37.4	16.4
36.5	20.5	7.5		2120			21.2	3		38.3	22.3	9.3
13.5	7.5	1.5		2105.5			35.7	14.5		6.8	0.8	-5.2
5.5	4.4	1.4		2077			64.2	28.5		-21.5	-22.6	-25.6
3.6	2	1	2050	2039	658	102	102.2	38	0.858	-50.6	-52.2	-53.2
3.2	1.7	1		2008.5			132.7	30.5		-75.5	-77	-77.7
2.3	1.3	0.5	1965	1973.5	449	168	167.7	35	0.920	-105.8	-106.8	-107.6
1.4	-0.1	-1	1930	1912	295	229	229.2	61.5	0.920	-158.4	-159.9	-160.8
1.5	-0.2	-2	1855	1858	108	283	283.2	54	0.913	-202.9	-204.6	-206.4
								Avg.	0.903			

Regression Output for k_2:	S_{01}	S_{02}	S_{03}
Constant	-0.80775	-1.22647	-1.39547
Std Err of Y Est	0.203149	0.240325	0.178167
R Squared	0.978199	0.981677	0.980164
No. of Observations	5	6	5
Degrees of Freedom	3	4	3
X Coefficient(s)	**0.044693**	**0.065909**	**0.0949**
Std Err of Coef.	0.003852	0.004502	0.007794

The figures for Batch Test 2 are in Section 5.2

Batch Test 2. (Sludge from SBR No. 8-500-15)					$\bar{X}_v$=	3150	mg/L					
Time	S_{01}	S_{02}	S_{03}	$\bar{S}_{01}$	$\bar{S}_{02}$	$\bar{S}_{03}$	$dS_{01}'/dt+\gamma_x k_e$	$dS_{02}'/dt+\gamma_x k_e$	$dS_{03}'/dt+\gamma_x k_e$	BAP_{nd}	$*BAP_{nd}$	$dBAP_{nd}/dt$
h	mg/L	mg/L	mg/L	mg/L	mg/L	mg/L	d^{-1}	d^{-1}	d^{-1}	mg/L	mg/L	mg/L/d
0	468	216	130							10.3	10.3	
0.05	425	181	99	446.5	198.5	114.5	6.887	5.668	5.058		10.4	
0.1	386	156	82	405.5	168.5	90.5	6.277	4.144	2.925		10.5	
0.2	325	127	58	355.5	141.5	70	4.982	2.544	2.163		10.7	
0.3	286	106	46	305.5	116.5	52	3.310	1.938	1.253		10.85	
0.5	230	80	33	258	93	39.5	2.474	1.331	0.835		11.1	
1	158	50	23	194	65	28	1.407	0.767	0.463		11.7	
2	98	36	21.2	128	43	22.1	0.738	0.388	0.295		12.7	
3.5	70	31	19.7	84	33.5	20.45	0.415	0.298	0.280	13.5	13.9	24.68571
5	58.5	27.1	18.6	64.25	29.05	19.15	0.311	0.273	0.258		15	
7	53	26.4	17.4	55.75	26.75	18	0.244	0.226	0.228	16	16.2	15.77143
12	54.7	26.6	18.6	53.85	26.5	18	0.168	0.170	0.169	19	17.7	7.2
24	57	27.9	20.4	55.85	27.25	19.5	0.106	0.107	0.106	22	20.1	4.8
								Regression Output for k_1 and K_{S1}:				
									Constant			0.13062
f_1	0.332532	0.312105	0.243943		1/$\bar{S}$	$1/(dS'/dt+\gamma_x k_e)$		k_1	Std Err of Y Est			0.00701
f_2	0.58062	0.635634	0.739348		0.0022	0.145		7.7	R Squared			0.96475
f_3	0.086847	0.052261	0.016708		0.0050	0.176		K_{S1}	No. of Observations			3
$f_1+f_2+f_3$	1	1	1		0.0087	0.198		61	Degrees of Freedom			1
									X Coefficient(s)			7.961481
									Std Err of Coef.			1.521827
* The data smoothened by the polynomial method (Gerald and Wheatley, 1989)												

Batch Test 2 (Cont.')

S_{01} - BAP_{nd}	S_{02} - BAP_{nd}	S_{03}- BAP_{nd}	COD_T	*COD_T	$dCOD_T/dt$	BAP_T	BAP_T	BAP_T at t	BAP_d/BAP_T	S_{01}'	S_{02}'	S_{03}'
S_{01} - BAP_{nd}	S_{02} - BAP_{nd}	S_{03}- BAP_{nd}	COD_T	*COD_T	$dCOD_T/dt$	BAP_T	BAP_T	BAP_T at t	BAP_d/BAP_T	S_{01} -BAP_d	S_{02} -BAP_d	S_{03} -BAP_d
mg/L	mg/L	mg/L	mg/L	mg/L	mg/L/d	mg/L	mg/L	mg/L	-	mg/L	mg/L	mg/L
457.7	205.7	119.7	4655	4656	1/d	10	10.3			468	216	130
414.6	170.6	88.6		4654			12.3			423.1	179.1	97.1
375.5	145.5	71.5		4652			14.3			382.2	152.2	78.2
314.3	116.3	47.3		4648			18.3			317.4	119.4	50.4
275.15	95.15	35.15		4644			22.3			274.6	94.6	34.6
218.9	68.9	21.9		4636			30.3			210.8	60.8	13.8
146.3	38.3	11.3		4618			48.3			121.4	13.4	-13.6
85.3	23.3	8.5		4586			80.3			30.4	-31.6	-46.4
56.1	17.1	5.8	4520	4540	795	126	126.3	46	0.974	-42.4	-81.4	-92.7
43.5	12.1	3.6		4498			168.3			-94.8	-126.2	-134.7
36.8	10.2	1.2	4468	4450	617	216	216.3	48	0.975	-147.1	-173.7	-182.7
37	8.9	0.9	4362	4366	403	300	300.3	84	0.982	-227.9	-256	-264
36.9	7.8	0.3	4283	4265	202	401	401.3	101	0.976	-324.2	-353.3	-360.8
								Avg.	0.977			

Regression Output for k_2:	S_{01}	S_{02}	S_{03}
Constant	-0.58737	-0.36478	-0.55963
Std Err of Y Est	0.224483	0.108031	0.09822
R Squared	0.970748	0.987073	0.991702
No. of Observations	7	8	8
Degrees of Freedom	5	6	6
X Coefficient(s)	0.011942	0.019961	0.037896
Std Err of Coef.	0.000927	0.000933	0.001415

B-3. Batch Test 3 (S_0 = 465, 220 and 115 mg/L, respectively; acclimated sludge from SBR run No. 7-500 and θ_{xob} = 15 d)

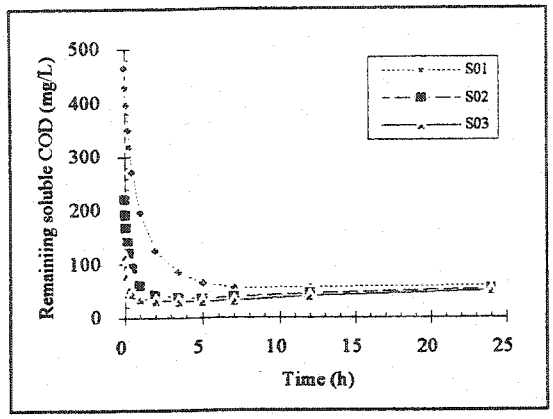


Fig.B-3-1. Soluble COD degradation vs time

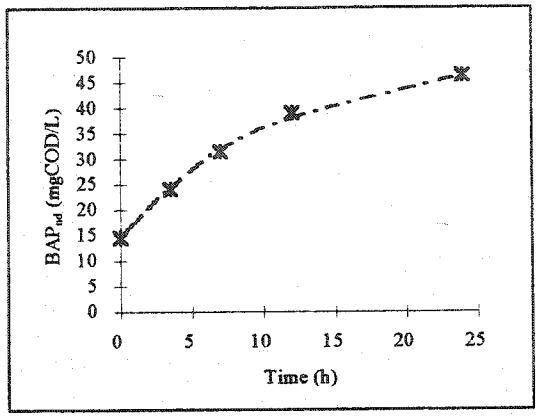


Fig-B-3-2. BAP_{nd} vs time

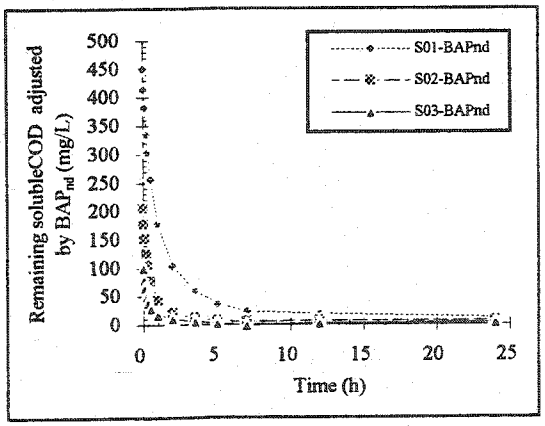


Fig-B-3-3. Soluble COD degradation vs time curves adjusted by BAP_{nd}

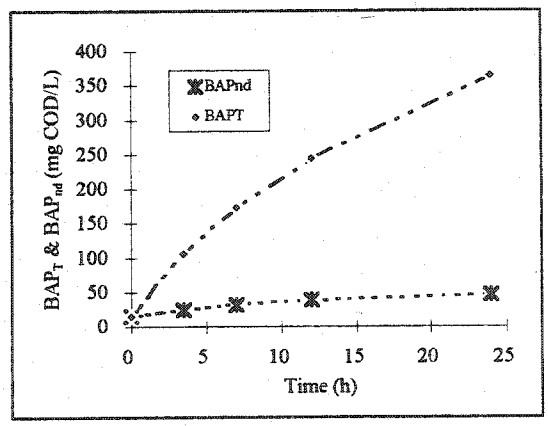


Fig-B-3-4. BAP_T compared to BAP_{nd} vs time

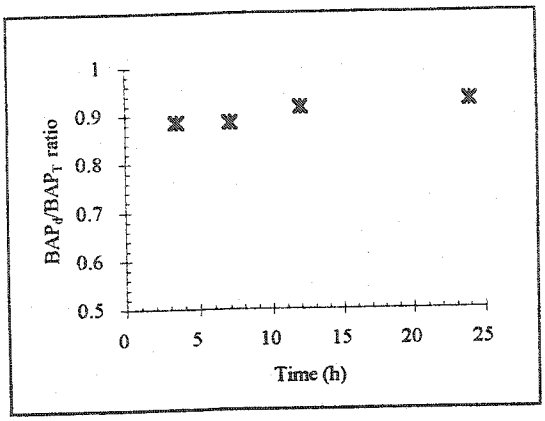


Fig-B-3-5. The ratio of BAP_d to BAP_T

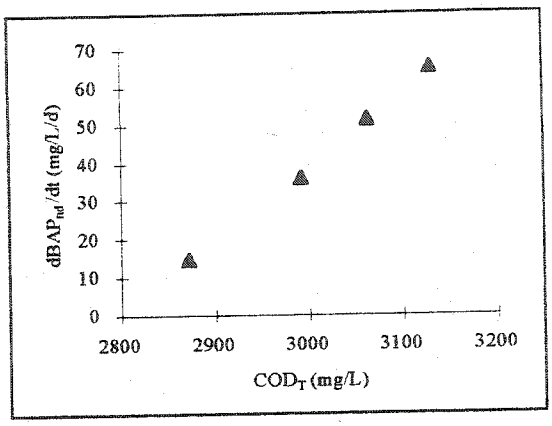


Fig-B-3-6. Linear relation between $dBAP_{nd}$ /dt and COD_T

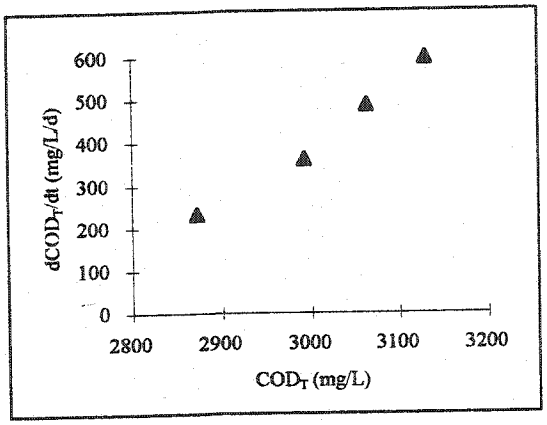


Fig-B-3-7. Linear relation between $dCOD_T/dt$ and COD_T

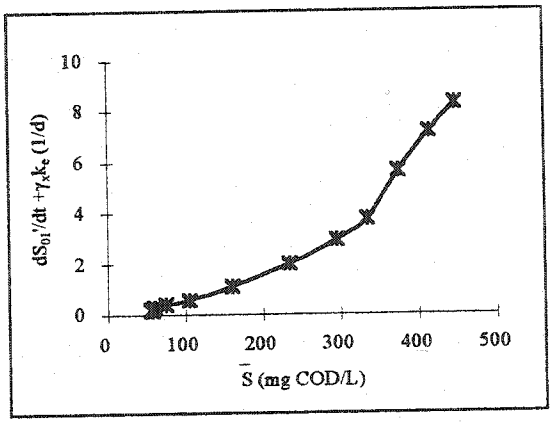


Fig-B-3-8. dS/dt vs S curve with S_0 = 465 mg/L

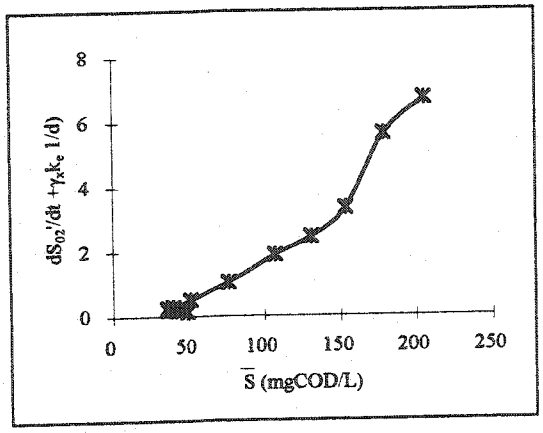


Fig-B-3-9. dS/dt vs S curve with S_0 = 220 mg/L

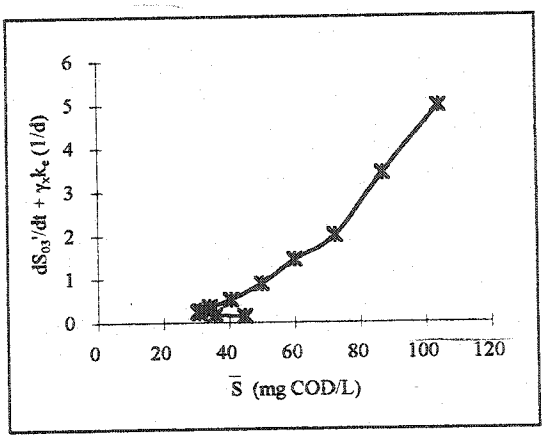


Fig-B-3-10. dS/dt vs S curve with S_0 = 115 mg/L

Batch Test 3. (Sludge from No. 7-500-15)

						$\bar{X}_v$ =	2176	mg/L				
Time	S_{01}	S_{02}	S_{03}	$\bar{S}_{01}$	$\bar{S}_{02}$	$\bar{S}_{03}$	$dS_{01}'/dt+\gamma_x k_e$	$dS_{02}'/dt+\gamma_x k_e$	$dS_{03}'/dt+\gamma_x k_e$	BAP_{nd}	$*BAP_{nd}$	$dBAP_{nd}/dt$
h	mg/L	mg/L	mg/L	mg/L	mg/L	mg/L	d^{-1}	d^{-1}	d^{-1}	mg/L	mg/L	mg/L/d
0	465	220	115							14.5	14.5	
0.05	429	191	94	447	205.5	104.5	8.273	6.729	4.964		14.7	
0.1	398	167	80	413.5	179	87	7.170	5.626	3.420		14.9	
0.2	350	140	65	374	153.5	72.5	5.637	3.321	1.997		15.2	
0.3	319	121	55	334.5	130.5	60	3.762	2.438	1.446		15.5	
0.5	272	93	45	295.5	107	50	2.935	1.887	0.894		16.1	
1	196	60	36	234	76.5	40.5	1.997	1.049	0.519		17.6	
2	125	42	32	160.5	51	34	1.105	0.520	0.366		20.5	
3.5	85	37	30.2	105	39.5	31.1	0.560	0.303	0.280	24	24.4	68
5	65	34.7	30.5	75	35.85	30.35	0.394	0.264	0.245		27.9	
7	55.6	38	31.2	60.3	36.35	30.85	0.273	0.203	0.217	31.5	32	52
12	57	45	40	56.3	41.5	35.6	0.185	0.173	0.169	39	38	29
24	58.7	53.3	49.5	57.85	49.15	44.75	0.147	0.141	0.140	46.3	45	14
					1/$\bar{S}$	$1/(dS'/dt+\gamma_x k_e)$		Regression Output for k_1 and K_{S1}:				
f_1	0.291898	0.327007	0.356219		0.0022	0.1209	k_1	Constant			0.09575	
f_2	0.645283	0.634307	0.619403		0.0049	0.1486	10	Std Err of Y Est			0.000927	
f_3	0.062819	0.038686	0.024378		0.0096	0.2014		R Squared			0.999743	
$f_1+f_2+f_3$	1	1	1				K_{S1}	No. of Observations			3	
							115	Degrees of Freedom			1	
								X Coefficient(s)			11.01723	
								Std Err of Coef.			0.176494	

* The data smoothened by the polynomial method (Gerald and Wheatley, 1989)

Batch Test 3 (Cont.')

S_{01}-BAP_{nd}	S_{02}-BAP_{nd}	S_{03}-BAP_{nd}	COD_T	*COD_T	$dCOD_T/dt$	BAP_T	BAP_T	BAP_T at t	BAP_d/BAP_T	S_{01}'	S_{02}'	S_{03}'
										S_{01}-BAP_d	S_{02}-BAP_d	S_{03}-BAP_d
mg/L	mg/L	mg/L	mg/L	mg/L	mg/L/d	mg/L	mg/L	mg/L	-	mg/L	mg/L	mg/L
450.5	205.5	100.5	3218	3221		15	14.5			465	220	115
414.3	176.3	79.3		3219.5			16	1.5		427.7	189.7	92.7
383.1	152.1	65.1		3218			17.5	1.5		395.4	164.4	77.4
334.8	124.8	49.8		3215			20.5	3		344.7	134.7	59.7
303.5	105.5	39.5		3212			23.5	3		311	113	47
255.9	76.9	28.9		3206			29.5	6		258.6	79.6	31.6
178.4	42.4	18.4		3192			43.5	14		170.1	34.1	10.1
104.5	21.5	11.5		3164			71.5	28		74	-9	-19
60.6	12.6	5.8	3113	3130	624	106	105.5	34	0.885	3.9	-44.1	-50.9
37.1	6.8	2.6		3099			136.5	31		-43.6	-73.9	-78.1
23.6	6	-0.8	3085	3063	459	173	172.5	36	0.886	-84.9	-102.5	-109.3
19	7	2	2980	2992	341	244	243.5	71	0.915	-148.5	-160.5	-165.5
13.7	8.3	4.5	2891	2872	240	364	363.5	120	0.942	-259.8	-265.2	-269
									0.907			

Regression Output for k_2:	S_{01}	S_{02}	S_{03}
Constant	-0.65639	-0.75055	-1.48334
Std Err of Y Est	0.221992	0.131336	0.24977
R Squared	0.977901	0.989727	0.956539
No. of Observations	7	7	8
Degrees of Freedom	5	5	6
X Coefficient(s)	**0.012351**	**0.02532**	**0.051878**
Std Err of Coef.	0.00083	0.001154	0.004514

B-4. Batch Test 4 (S_0 = 367, 184 and 93 mg/L, respectively; acclimated sludge from SBR run No. 3-500 and θ_{xob} = 10 d)

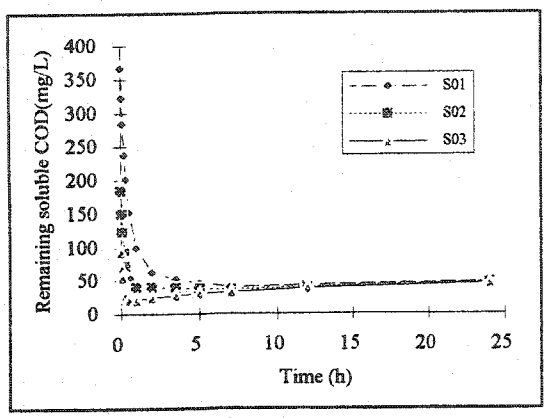


Fig.B-4-1. Soluble COD degradation vs time

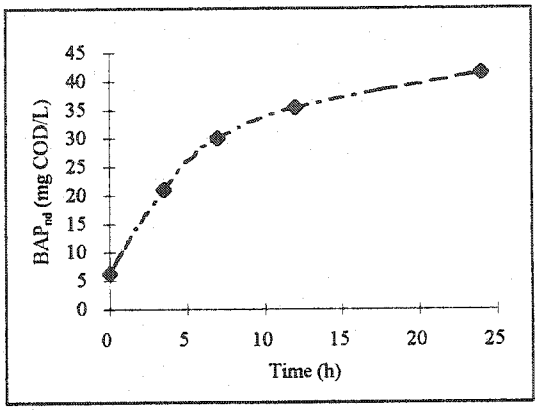


Fig-B-4-2. BAP_{nd} vs time

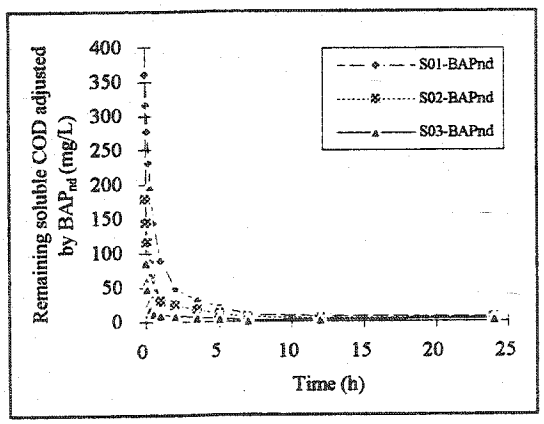


Fig-B-4-3. Soluble COD degradation vs time curves adjusted by BAP_{nd}

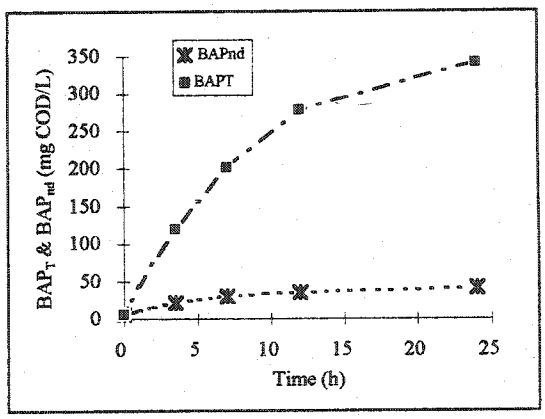


Fig-B-4-4. BAP_T compared to BAP_{nd} vs time

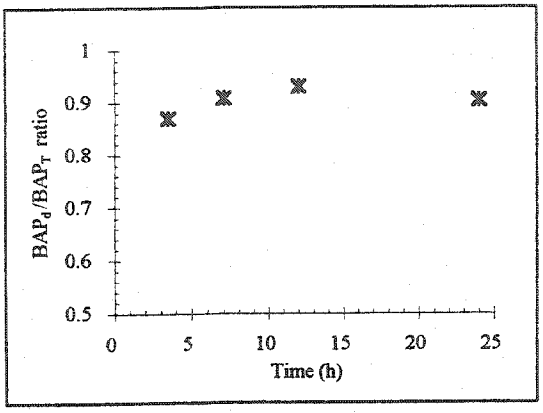


Fig-B-4-5. The ratio of BAP_d to BAP_T

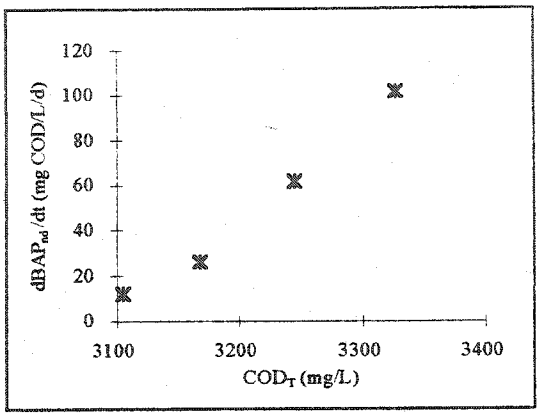


Fig-B-4-6. Linear relation between $dBAP_{nd}$ /dt and COD_T

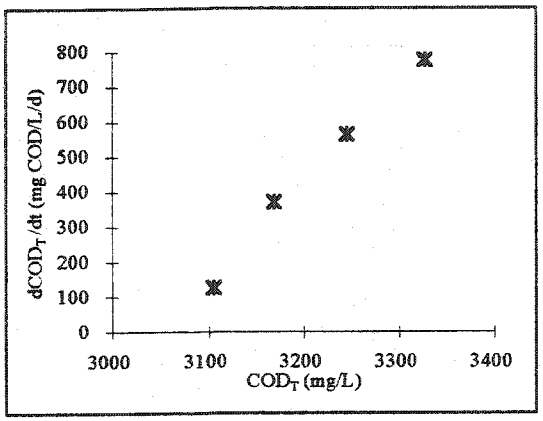


Fig-B-4-7. Linear relation between $dCOD_T/dt$ and COD_T

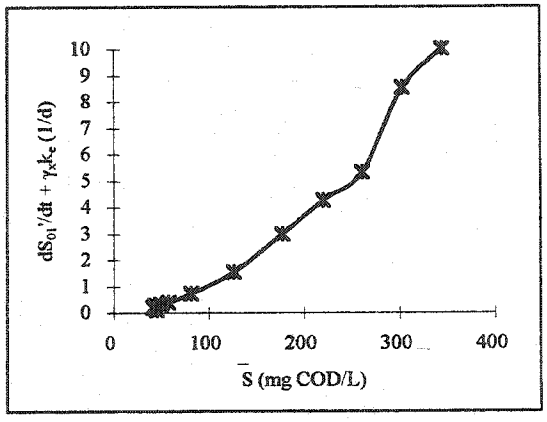


Fig-B-4-8. dS/dt vs S curve with S_0 = 367 mg/L

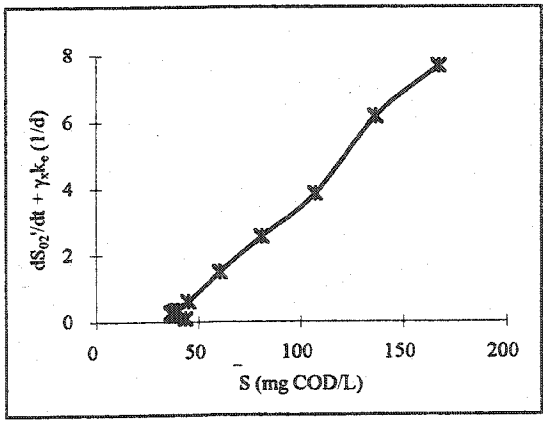


Fig-B-4-9. dS/dt vs S curve with S_0 = 184 mg/L

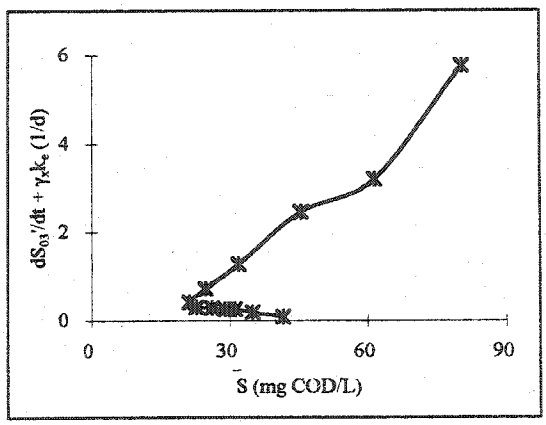


Fig-B-4-10. dS/dt vs S curve with S_0 = 93 mg/L

Batch Test 4. (Sludge from No. 3-500-10)					$\bar{X}_v$ =	2250	mg/L					
Time	S_{01}	S_{02}	S_{03}	$\bar{S}_{01}$	$\bar{S}_{02}$	$\bar{S}_{03}$	$dS_{01}'/dt+\gamma_x k_e$	$dS_{02}'/dt+\gamma_x k_e$	$dS_{03}'/dt+\gamma_x k_e$	BAP_{nd}	$*BAP_{nd}$	$dBAP_{nd}/dt$
h	mg/L	mg/L	mg/L	mg/L	mg/L	mg/L	d^{-1}	d^{-1}	d^{-1}	mg/L	mg/L	mg/L/d
0	367	184	93							6.2	6.2	
0.05	322	150	68	344.5	167	80.5	10.018	7.672	5.752		6.45	
0.1	284	123	55	303	136.5	61.5	8.521	6.174	3.187		6.72	
0.2	238	91	36	261	107	45.5	5.327	3.834	2.447		7.2	
0.3	202	71	28	220	81	32	4.258	2.552	1.272		7.7	
0.5	153	50	21.5	177.5	60.5	24.75	2.978	1.485	0.712		8.7	
1	100	40	21	126.5	45	21.25	1.534	0.617	0.414		10.9	
2	63	39.5	24.5	81.5	39.75	22.75	0.733	0.344	0.301		15.4	
3.5	52	38.4	27.8	57.5	38.95	26.15	0.391	0.320	0.289	22	20.8	100
5	46.5	37.2	30.2	49.25	37.8	29	0.311	0.280	0.255		25.9	
7	40	36	32	43.25	36.6	31.1	0.297	0.269	0.253	29	30.1	64
12	43	40	38	41.5	38	35	0.192	0.189	0.185	37	35.4	25
24	47.6	46.8	45.3	45.3	43.4	41.65	0.092	0.090	0.089	40.9	41.4	12
					$1/\bar{S}$	$1/(dS'/dt+\gamma_x k_e)$		Regression Output for k_1 and K_{S1}:				
f_1	0.297	0.354	0.369		0.0029	0.0998	k_1	Constant			0.080515	
f_2	0.667	0.609	0.620		0.0060	0.1303	12	Std Err of Y Est			0.005229	
f_3	0.036	0.037	0.012		0.0124	0.1739		R Squared			0.990127	
$f_1+f_2+f_3$	1	1	1				K_{s1}	No. of Observations			3	
							95	Degrees of Freedom			1	
								X Coefficient(s)			7.623606	
								Std Err of Coef.			0.761254	
* The data smoothened by the polynomial method (Gerald and Wheatley, 1989)												

Batch Test 4. (Cont.')

S_{01} -BAP_{nd}	S_{02} -BAP_{nd}	S_{03} -BAP_{nd}	COD_T	*COD_T	$dCOD_T/dt$	BAP_T	BAP_T	BAP_T at t	BAP_d/BAP_T	S_{01}'	S_{02}'	S_{03}'
S_{01} -BAP_{nd}	S_{02} -BAP_{nd}	S_{03} -BAP_{nd}	COD_T	*COD_T	$dCOD_T/dt$	BAP_T	BAP_T	BAP_T at t	BAP_d/BAP_T	S_{01} -BAP_d	S_{02} -BAP_d	S_{03} -BAP_d
mg/L	mg/L	mg/L	mg/L	mg/L	mg/L/d	mg/L	mg/L	mg/L	mg/L	mg/L	mg/L	mg/L
360.8	177.8	86.8	3439	3440		6.2	6.2			367	184	93
315.55	143.55	61.55		3438			8.2	2		320.25	148.25	66.25
277.28	116.28	48.28		3436			10.2	2		280.52	119.52	51.52
230.8	83.8	28.8		3432			14.2	4		231	84	29
194.3	63.3	20.3		3428			18.2	4		191.5	60.5	17.5
144.3	41.3	12.8		3421			25.2	7		136.5	33.5	5
89.1	29.1	10.1		3402			44.2	19		66.7	6.7	-12.3
47.6	24.1	9.1		3370			76.2	32		2.2	-21.3	-36.3
31.2	17.6	7	3345	3327	775	119	119.2	43	0.874	-46.4	-60	-70.6
20.6	11.3	4.3		3290			156.2	37		-83.8	-93.1	-100.1
9.9	5.9	1.9	3228	3245	562	201	201.2	45	0.907	-131.1	-135.1	-139.1
7.6	4.6	2.6	3182	3168	370	278	278.2	77	0.931	-199.8	-202.8	-204.8
6.2	5.4	3.9	3119	3105	126	341	341.2	63	0.905	-252.2	-253	-254.5
								AVG.	0.904			

Regression Output for k_2:	S_{01}	S_{02}	S_{03}
Constant	-0.99342	-1.67589	-1.30772
Std Err of Y Est	0.261994	0.038155	0.261028
R Squared	0.984906	0.999296	0.957417
No. of Observations	8	8	7
Degrees of Freedom	6	6	5
X Coefficient(s)	**0.0234**	**0.0517**	**0.0760**
Std Err of Coef.	0.001182	0.000561	0.007167

B-5. Batch Test 5 (S_0 = 367, 184 and 93 mg/L, respectively; acclimated sludge from SBR run No. 3-500 and θ_{xob} = 15 d)

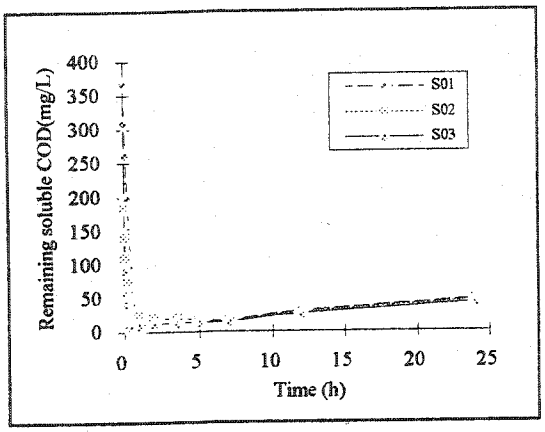


Fig.B-5-1. Soluble COD degradation vs time

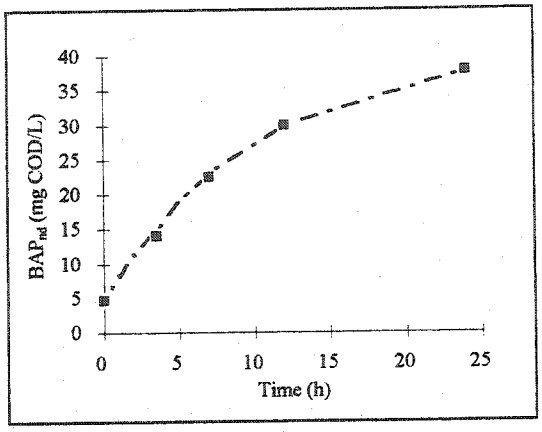


Fig-B-5-2. BAP_{nd} vs time

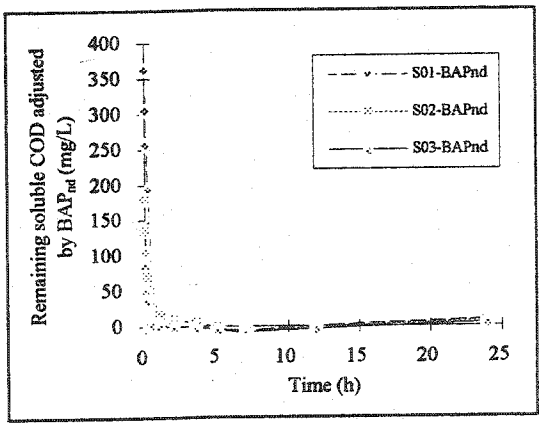


Fig-B-5-3. Soluble COD degradation vs time curves adjusted by BAP_{nd}

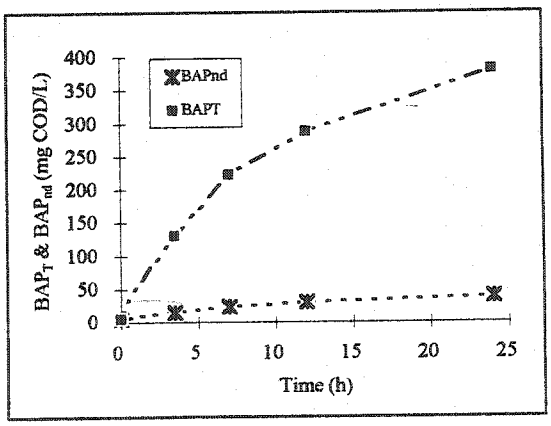


Fig-B-5-4. BAP_T compared to BAP_{nd} vs time

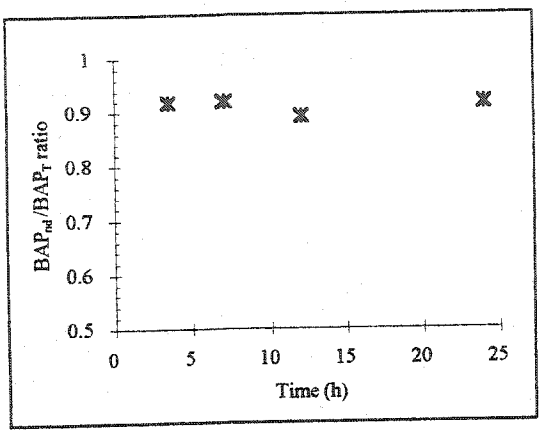


Fig-B-5-5. The ratio of BAP_d to BAP_T

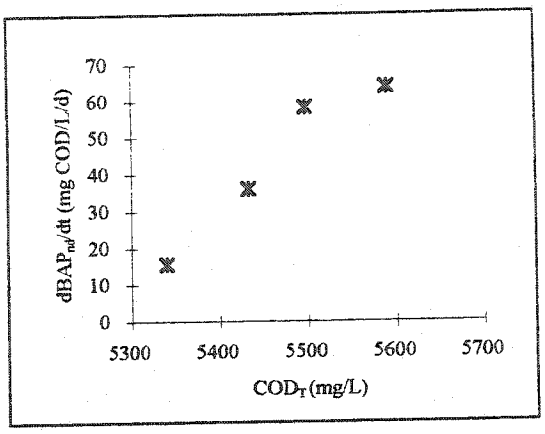


Fig-B-5-6. Linear relation between $dBAP_{nd}$ /dt and COD_T

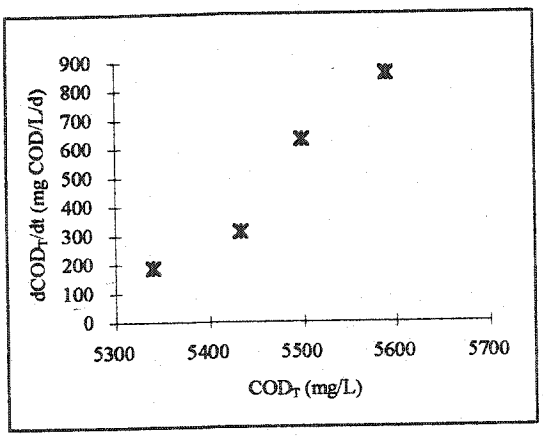


Fig-B-5-7. Linear relation between $dCOD_T/dt$ and COD_T

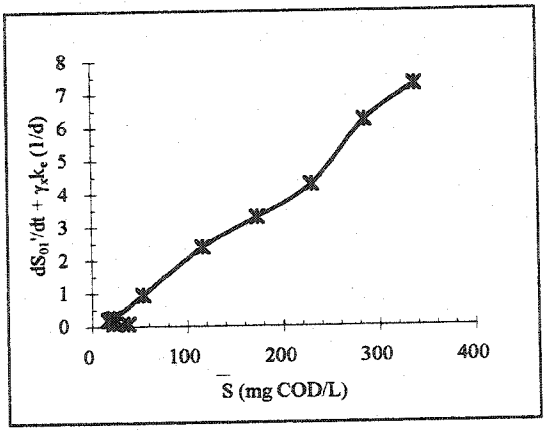


Fig-B-5-8. dS'/dt vs S curve with S_0 = 367

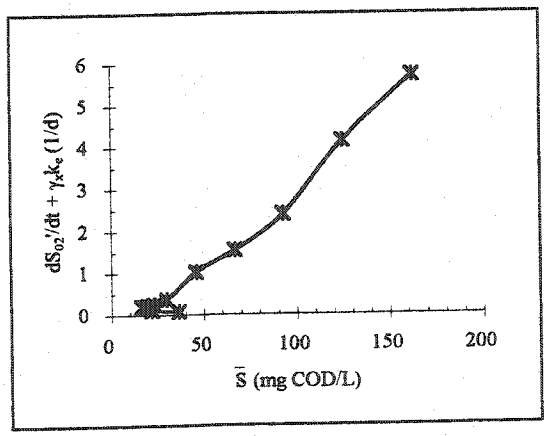


Fig-B-5-9. dS'/dt vs S curve with S_0 = 184 mg/L

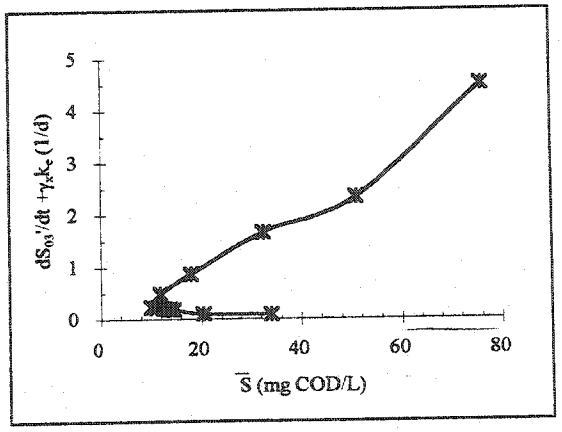


Fig-B-5-10. dS'/dt vs S curve with S_0 = 93 mg/L

Batch Test 5. (Sludge form No. 3-500-15)					$\overline{X}_v$ =	3960	mg/L					
Time	S_{01}	S_{02}	S_{03}	$\overline{S}_{01}$	$\overline{S}_{02}$	$\overline{S}_{03}$	$dS_{01}'/dt+\gamma_x k_e$	$dS_{02}'/dt+\gamma_x k_e$	$dS_{03}'/dt+\gamma_x k_e$	BAP_{nd}	* BAP_{nd}	$dBAP_{nd}/dt$
h	mg/L	mg/L	mg/L	mg/L	mg/L	mg/L	d^{-1}	d^{-1}	d^{-1}	mg/L	mg/L	mg/L/d
0	367	184	93							4.7	4.7	
0.05	310	140	59	338.5	162	76	7.293	5.718	4.506		4.9	
0.1	262	109	43	286	124.5	51	6.203	4.142	2.324		5.1	
0.2	198	76	22	230	92.5	32.5	4.263	2.384	1.657		5.5	
0.3	150	57	14	174	66.5	18	3.293	1.536	0.869		5.9	
0.5	83	35	9.8	116.5	46	11.9	2.387	1.024	0.484		6.6	
1	26	25	10.4	54.5	30	10.1	0.933	0.364	0.235		8.3	
2	21	21	11.9	23.5	23	11.15	0.257	0.251	0.218		11.3	
3.5	19.3	19.4	13.4	20.15	20.2	12.65	0.219	0.218	0.206	14	15	70.6
5	18.2	17.4	14.3	18.75	18.4	13.85	0.199	0.203	0.191		18.9	
7	17	15.5	14.9	17.6	16.45	14.6	0.191	0.193	0.185	22.5	23	54.9
12	30	28	26	23.5	21.75	20.45	0.100	0.100	0.102	32	30	33.6
24	47	44.8	41.9	38.5	36.4	33.95	0.079	0.080	0.080	38.5	37.8	15.6
					$1/\overline{S}$	$1/dS'/dt+\gamma_x k_e)$		Regression Output for k_1 and K_{S1}:				
f_1	0.303	0.334	0.337		0.0030	0.1371	k_1	Constant			0.118111	
f_2	0.683	0.637	0.642		0.0062	0.1749	8.5	Std Err of Y Est			0.008804	
f_3	0.014	0.029	0.020		0.0132	0.2219		R Squared			0.978545	
$f_1+f_2+f_3$	1	1	1				K_{S1}	No. of Observations			3	
							68	Degrees of Freedom			1	
								X Coefficient(s)			8.060012	
								Std Err of Coef.			1.19346	
* The data smoothened by the polynomial method (Gerald and Wheatley, 1989)												

Batch Test 5. (Cont.')										S_{01}'	S_{02}'	S_{03}'
S_{01} -BAP_{nd}	S_{02} -BAP_{nd}	S_{03} -BAP_{nd}	COD_T	*COD_T	$dCOD_T/dt$	BAP_T	BAP_T	BAP_T at t	BAP_d/BAP_T	S_{01} -BAP_d	S_{02} -BAP_d	S_{03} -BAP_d
mg/L	mg/L	mg/L	mg/L	mg/L	mg/L/d	mg/L	mg/L	mg/L	-	mg/L	mg/L	mg/L
362.3	179.3	88.3	5714	5715		4.7	4.7			367	184	93
305.1	135.1	54.1		5712			7.7	3		307.2	137.2	56.2
256.9	103.9	37.9		5709			10.7	3		256.4	103.4	37.4
192.5	70.5	16.5		5703			16.7	6		186.8	64.8	10.8
144.1	51.1	8.1		5697			22.7	6		133.2	40.2	-2.8
76.4	28.4	3.2		5686			33.7	11		55.9	7.9	-17.3
17.7	16.7	2.1		5668			51.7	18		-17.4	-18.4	-33
9.7	9.7	0.6		5635			84.7	33		-52.4	-52.4	-61.5
4.3	4.4	-1.6	5571	5590	857	130	129.7	45	0.918	-95.4	-95.3	-101.3
-0.7	-1.5	-4.6		5549			170.7	41		-133.6	-134.4	-137.5
-6	-7.5	-8.1	5522	5498	631	222	221.7	51	0.920	-181.7	-183.2	-183.8
0	-2	-4	5423	5433	312	287	286.7	65	0.892	-226.7	-228.7	-230.7
9.2	7	4.1	5350	5340	186	380	379.7	93	0.916	-294.9	-297.1	-300
								AVG.	0.911			

Regression Output for k_2:	S_{01}	S_{02}	S_{03}
Constant	-0.24809	-0.66878	-0.33081
Std Err of Y Est	0.257565	0.226274	0.258066
R Squared	0.988998	0.979414	0.978812
No. of Observations	7	7	6
Degrees of Freedom	5	5	4
X Coefficient(s)	**0.0213**	**0.0363**	**0.0605**
Std Err of Coef.	0.001006	0.002351	0.004447

B-6. Batch Test 6 (S_0 = 887, 445 and 221 mg/L, respectively; acclimated sludge from SBR run No. 2-250 and θ_{xob} = 10 d)

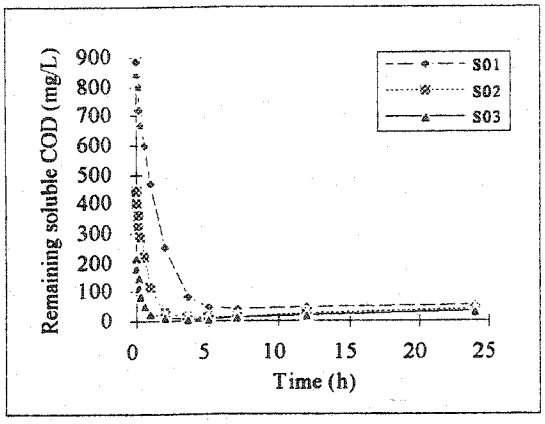


Fig. B-6-1. Soluble COD degradation vs time

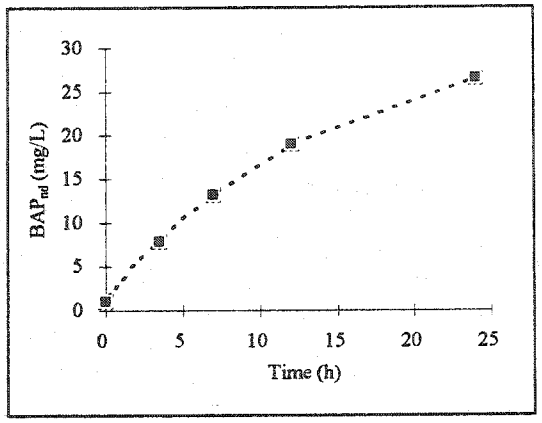


Fig. B-6-2. BAP_{nd} vs time

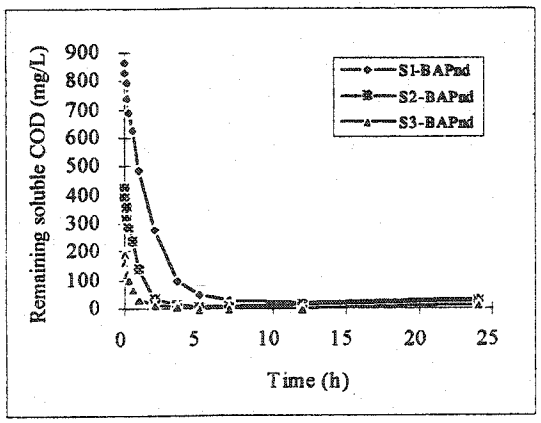


Fig. B-6-3. Soluble COD degradation vs time curves adjusted by BAP_{nd}

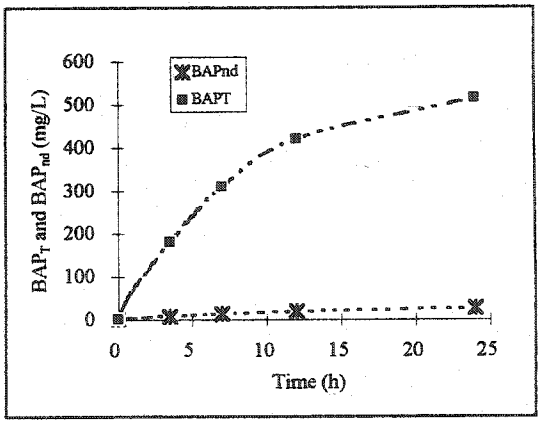


Fig. B-6-4. BAP_T compared to BAP_{nd} vs time

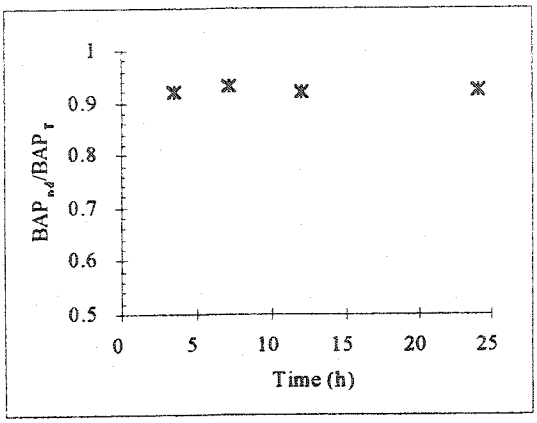


Fig. B-6-5. The ratio of BAP_d to BAP_T

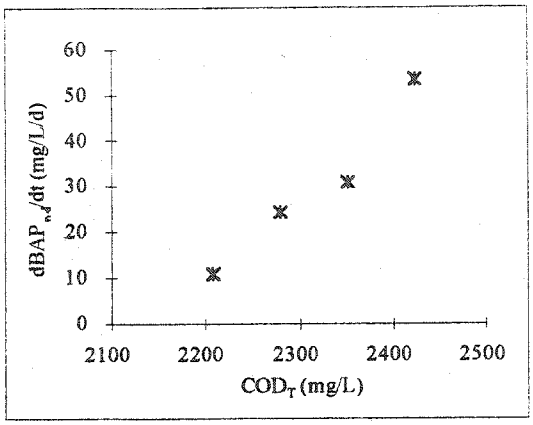


Fig. B-6-6. Linear relation between $dBAP_{nd}$ /dt and COD_T

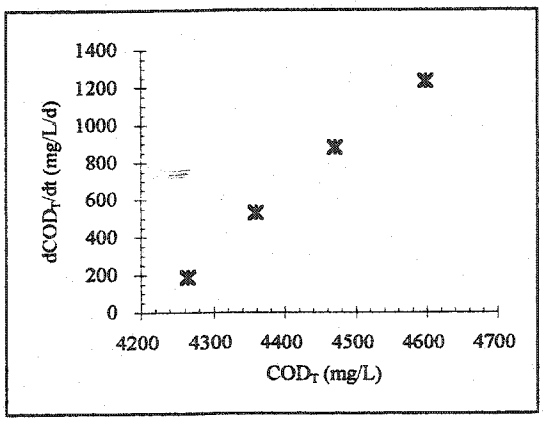


Fig. B-6-7. Linear relation between $dCOD_T/dt$ COD_T

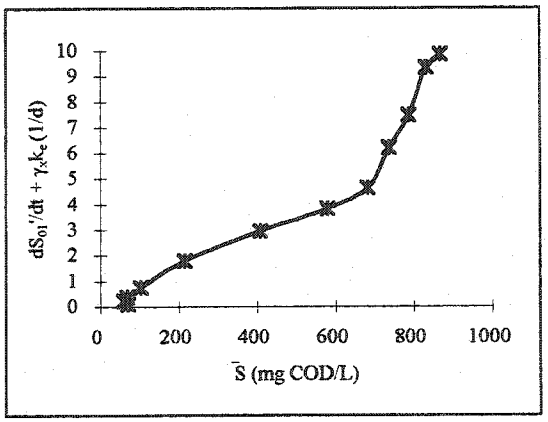


Fig. B-6-8. dS'/dt vs S curve with S_0 = 887 mg/L

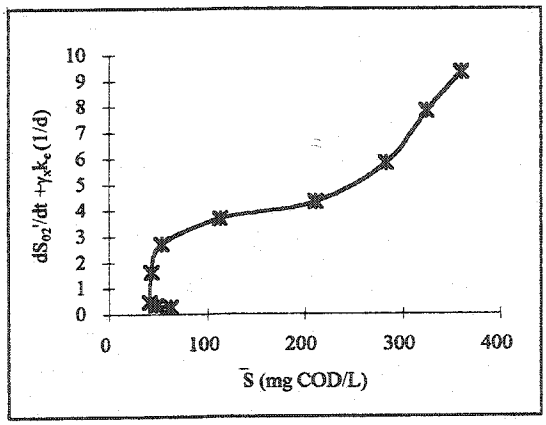


Fig. B-6-9. dS'/dt vs S curve with S_0 = 445 mg/L

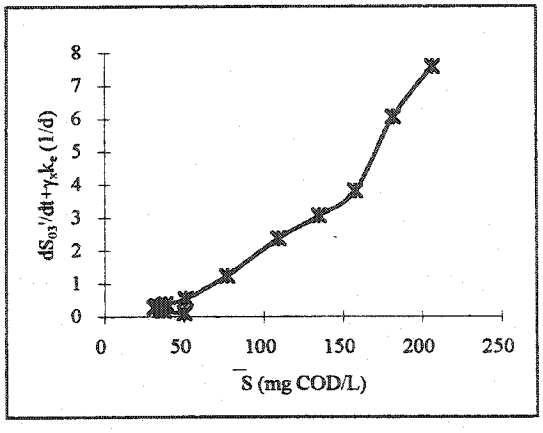


Fig. B-6-10. dS'/dt vs S curve with S_0 = 221 mg/L

Batch Test 6. (Sludge from No. 2-250-10)

$\overline{X}_v$ = 1900 mg/L

Time	S_{01}	S_{02}	S_{03}	$\overline{S}_{01}$	$\overline{S}_{02}$	$\overline{S}_{03}$	$dS_{01}'/dt+\gamma_x k_e$	$dS_{02}'/dt+\gamma_x k_e$	$dS_{03}'/dt+\gamma_x k_e$	BAP_{nd}	$*BAP_{nd}$	$dBAP_{nd}/dt$
h	mg/L	mg/L	mg/L	mg/L	mg/L	mg/L	d^{-1}	d^{-1}	d^{-1}	mg/L	mg/L	mg/L/d
0	887	445	221							22.2	22.2	
0.05	850	410	193	868.5	427.5	207	9.847	9.342	7.573		22.4	
0.1	815	381	171	832.5	395.5	182	9.342	7.826	6.058		22.6	
0.2	760	339	145	787.5	360	158	7.472	5.830	3.809		22.8	
0.3	715	309	125	737.5	324	135	6.209	4.314	3.051		23	
0.5	648	257	94	681.5	283	109.5	4.643	3.696	2.369		23.2	
1	512	165	60	580	211	77	3.809	2.698	1.232		24.2	
2	302	62	42	407	113.5	51	2.964	1.612	0.538		26.15	
3.5	128	45	34	215	53.5	38	1.789	0.467	0.392	30	29	53.5
5	78	41.8	31.8	103	43.4	32.9	0.732	0.338	0.330		31.4	
7	59.8	40.7	31.1	68.9	41.25	31.45	0.384	0.276	0.273	34.5	34	30.9
12	60	55	43	59.9	47.85	37.05	0.212	0.177	0.183	39.6	39.6	24.5
24	79	70.4	57.1	69.5	62.7	50.05	0.096	0.100	0.101	45	45	10.8

					$1/\overline{S}$	$1/(dS'/dt+\gamma_x k_e)$		Regression Output for k_1 and K_{S1}:		
f_1	0.239	0.288	0.320		0.001	0.102	k_1	Constant		0.089819
f_2	0.721	0.654	0.635		0.002	0.107	11	Std Err of Y Est		0.003479
f_3	0.040	0.058	0.045		0.005	0.132		R Squared		0.977083
$f_1+f_2+f_3$	1	1	1				K_{S1}	No. of Observations		3
							95	Degrees of Freedom		1
								X Coefficient(s)		8.553937
								Std Err of Coef.		1.310013

* The data smoothened by the polynomial method (Gerald and Wheatley, 1989)

Batch Test 6 (Cont.')

S_{01} -BAP_{nd}	S_{02} -BAP_{nd}	S_{03} -BAP_{nd}	COD_T	*COD_T	$dCOD_T/dt$	BAP_T	BAP_T	BAP_T at t	BAP_d/BAP_T	S_{01}'	S_{02}'	S_{03}'
										S_{01} -BAP_d	S_{02} -BAP_d	S_{03} -BAP_d
mg/L	mg/L	mg/L	mg/L	mg/L	mg/L/d	mg/L	mg/L	mg/L	-	mg/L	mg/L	mg/L
864.8	422.8	198.8		2515		22.2	22.2	2		887	445	221
827.6	387.6	170.6		2513			24.2	2		848.2	408.2	191.2
792.4	358.4	148.4		2511			26.2	4		811.4	377.4	167.4
737.2	316.2	122.2		2507			30.2	4		752.6	331.6	137.6
692	286	102		2503			34.2	6		703.8	297.8	113.8
624.8	233.8	70.8		2497			40.2	14		631	240	77
487.8	140.8	35.8		2483			54.2	23		482	135	30
275.85	35.85	15.85		2460			77.2	36		250.95	10.95	-9.05
99	16	5		2424	624	113.2	113.2	34	0.921	43.8	-39.2	-50.2
46.6	10.4	0.4		2390			147.2	38		-37.8	-74	-84
25.8	6.7	-2.9		2352	494	185.2	185.2	72	0.932	-91.4	-110.5	-120.1
20.4	15.4	3.4		2280	346	257.2	257.2	73	0.922	-157.6	-162.6	-174.6
34	25.4	12.1		2207	146	330.2	330.2	2207	0.926	-206.2	-214.8	-228.1
								Avg.	0.925			

Regression Output for k_2:	S_{01}	S_{02}	S_{03}
Constant	0.102328	-0.13865	-0.88018
Std Err of Y Est	0.191543	0.140665	0.119614
R Squared	0.989916	0.993858	0.99414
No. of Observations	6	5	6
Degrees of Freedom	4	3	4
X Coefficient(s)	*0.0067*	*0.0137*	*0.0293*
Std Err of Coef.	0.000337	0.000621	0.001126

B-7. Batch Test 7 (S_0 = 888, 443 and 220 mg/L, respectively; acclimated sludge from SBR run No. 2-250 and θ_{xob} = 15 d)

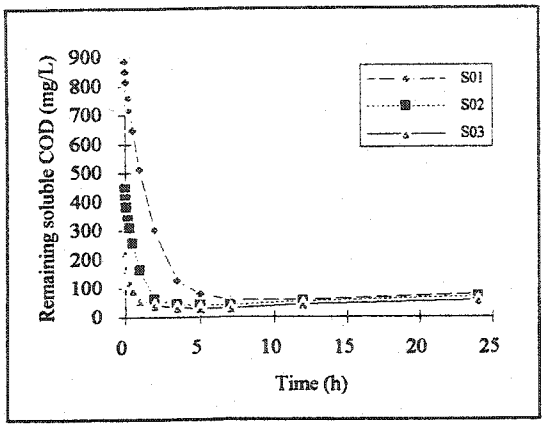


Fig. B-7-1. Soluble COD degradation vs time

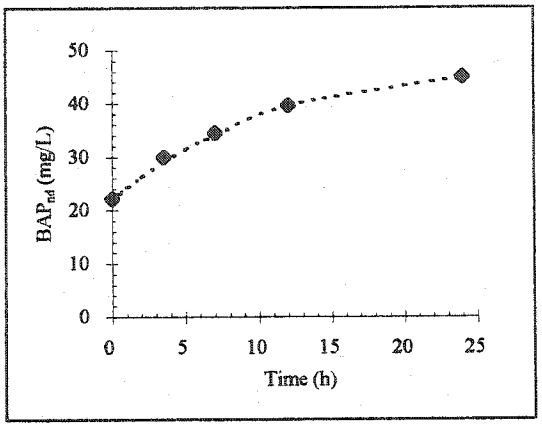


Fig. B-7-2. BAP_{nd} vs time

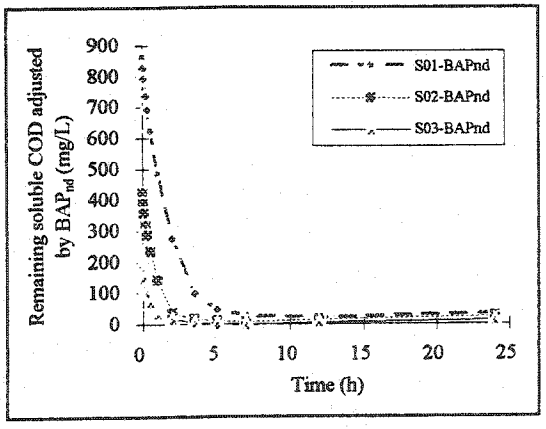


Fig. B-7-3. Soluble COD degradation vs time curves adjusted by BAP_{nd}

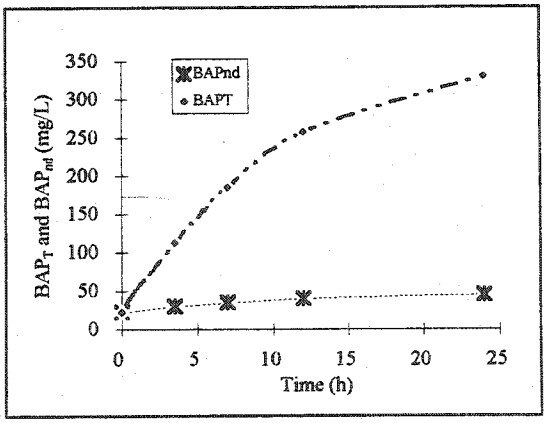


Fig. B-7-4. BAP_T compared to BAP_{nd} vs time

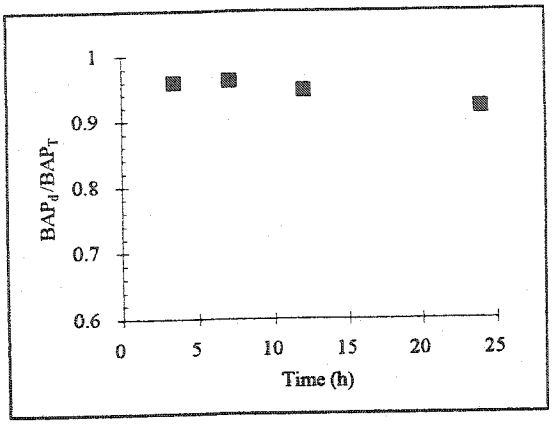


Fig. B-7-5. The ratio of BAP_d to BAP_T

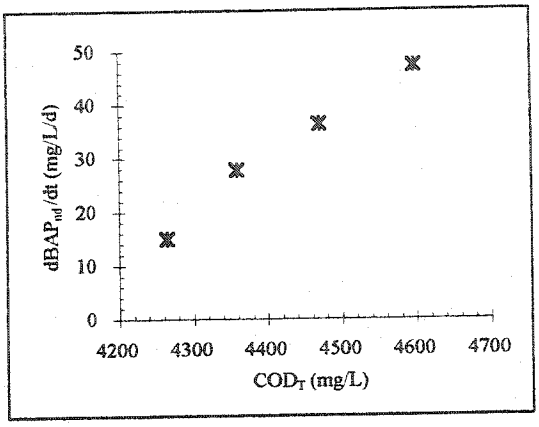


Fig. B-7-6. Linear relation between $dBAP_{nd}$ /dt and COD_T

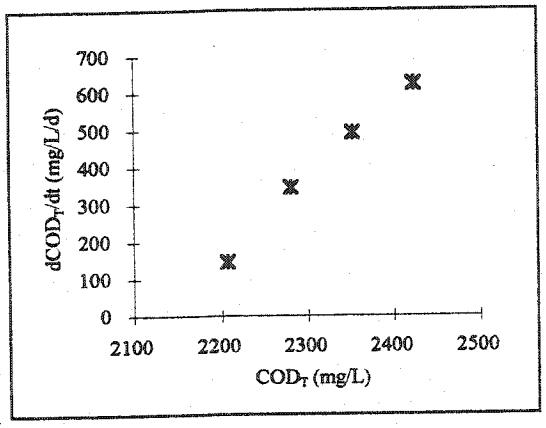


Fig. B-7-7. Linear relation between $dCOD_T/dt$ and COD_T

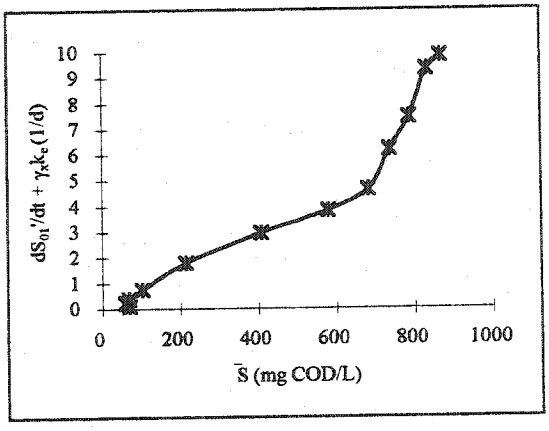


Fig. B-7-8. dS'/dt vs S curve with S_0 = 888 mg/L

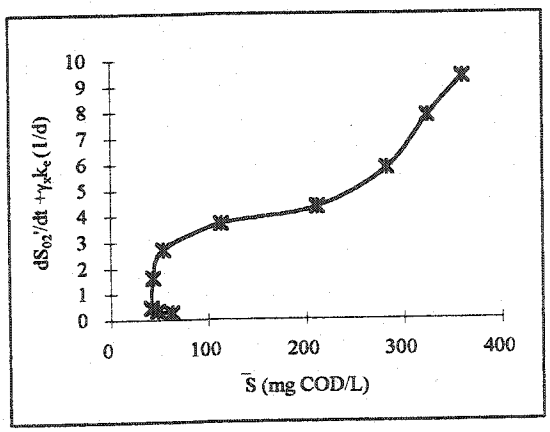


Fig. B-7-9. dS'/dt vs S curve with S_0 = 443 mg/L

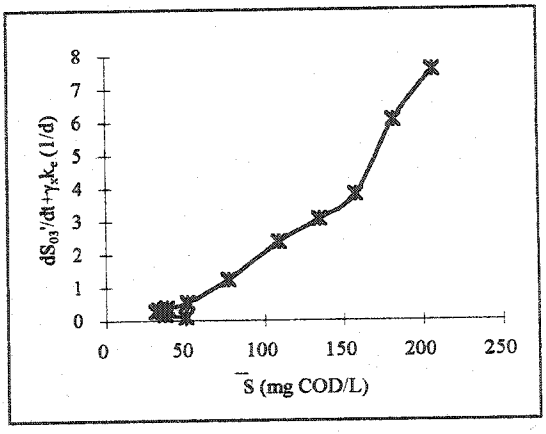


Fig. B-7-10. dS'/dt vs S curve with S_0 = 220 mg/L

Batch Test 7. (Sludge from 2-250-15)

					$\bar{X}_v$ =	3478	mg/L					
Time	S_{01}	S_{02}	S_{03}	$\bar{S}_{01}$	$\bar{S}_{02}$	$\bar{S}_{03}$	$dS_{01}'/dt+\gamma_x k_e$	$dS_{02}'/dt+\gamma_x k_e$	$dS_{03}'/dt+\gamma_x k_e$	BAP_{nd}	$*BAP_{nd}$	$dBAP_{nd}/dt$
h	mg/L	mg/L	mg/L	mg/L	mg/L	mg/L	d^{-1}	d^{-1}	d^{-1}	mg/L	mg/L	mg/L/d
0	888	443	220							1	1	
0.05	840	399	182	864	421	201	7.477	6.925	6.097		1.15	
0.1	795	364	152	817.5	381.5	167	6.925	5.545	4.855		1.3	
0.2	720	318	115	757.5	341	133.5	5.821	3.820	3.199		1.6	
0.3	670	284	89	695	301	102	4.030	2.926	2.374		1.85	
0.5	603	220	55	636.5	252	72	2.824	2.721	1.686		2.3	
1	470	113	25	536.5	166.5	40	2.250	1.892	0.829		3.5	
2	250	26	14	360	69.5	19.5	1.874	0.956	0.431		5.5	
3.5	79	16	8.8	164.5	21	11.4	1.110	0.369	0.347	7.9	8.1	49
5	45	11.5	9.8	62	13.75	9.3	0.466	0.331	0.305		10.5	
7	38.5	15	12	41.75	13.25	10.9	0.293	0.259	0.263	13.5	13.1	34
12	45	30	18.6	41.75	22.5	15.3	0.181	0.169	0.181	20.3	19	28
24	53.2	42	30.8	49.1	36	24.7	0.090	0.088	0.088	28	26.5	15

									Regression Output for k_1 and K_{S1}:			
									Constant			0.125074
								k_1	Std Err of Y Est			0.000802
f_1	0.285	0.323	0.321		1/$\bar{S}$	$1/(dS'/dt+\gamma_x k_e)$		8.0	R Squared			0.998635
f_2	0.683	0.648	0.664		0.001	0.134			No. of Observations			3
f_3	0.032	0.029	0.015		0.002	0.144		K_{S1}	Degrees of Freedom			1
$f_1+f_2+f_3$	1	1	1		0.005	0.164		62.9				
									X Coefficient(s)			7.869509
									Std Err of Coef.			0.29093

* The data smoothened by the polynomial method (Gerald and Wheatley, 1989)

Batch Test 7 (Cont.')										S_{01}'	S_{02}'	S_{03}'
S_{01} -BAP_{nd}	S_{02} -BAP_{nd}	S_{03} -BAP_{nd}	COD_T	*COD_T	$dCOD_T/dt$	BAP_T	BAP_T	BAP_T at t	BAP_d/BAP_T	S_{01} -BAP_d	S_{02} -BAP_d	S_{03} -BAP_d
mg/L	mg/L	mg/L	mg/L	mg/L	mg/L/d	mg/L	mg/L	mg/L	-	mg/L	mg/L	mg/L
887	442	219	4778	4778		1	1			888	443	220
838.85	397.85	180.85		4772			7	6		834.15	393.15	176.15
793.7	362.7	150.7		4767			12	5		784.3	353.3	141.3
718.4	316.4	113.4		4758			21	9		700.6	298.6	95.6
668.15	282.15	87.15		4750			29	8		642.85	256.85	61.85
600.7	217.7	52.7		4736			43	14		562.3	179.3	14.3
466.5	109.5	21.5		4708			71	28		402.5	45.5	-42.5
244.5	20.5	8.5		4661			118	47		137.5	-86.5	-98.5
70.9	7.9	0.7	4652	4598	1234	181	181	63	0.959	-93.9	-156.9	-164.1
34.5	1	-0.7		4538			241	60		-185.5	-219	-220.7
25.4	1.9	-1.1	4455	4470	878	309	309	68	0.962	-257.4	-280.9	-283.9
26	11	-0.4	4362	4359	533	420	420	111	0.947	-356	-371	-382.4
26.7	15.5	4.3	4254	4265	188	514	514	94	0.920	-434.3	-445.5	-456.7
								Avg.	0.947			
		Regression Output for k_2:			S_{01}	S_{02}	S_{03}					
		Constant			0.270357	0.266036	-0.020860					
		Std Err of Y Est			0.166263	0.126674	0.075350					
		R Squared			0.978438	0.990137	0.996560					
		No. of Observations			6	5	6					
		Degrees of Freedom			4	3	4					
		X Coefficient(s)			**0.0040**	**0.0093**	**0.0238**					
		Std Err of Coef.			0.000229	0.000536	0.000698					

B-8. Batch Test 8 (S_0 = 886, 665 and 443 mg/L, respectively; acclimated sludge from SBR run No. 7-500 and θ_{xob} = 10 d)

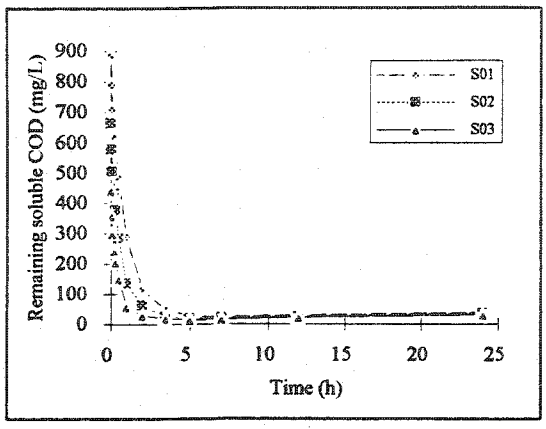


Fig.B-8-1. Soluble COD degradation vs time

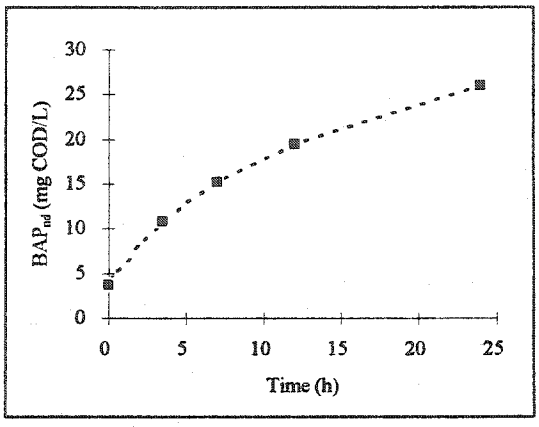


Fig. B-8-2. BAP_{nd} vs time

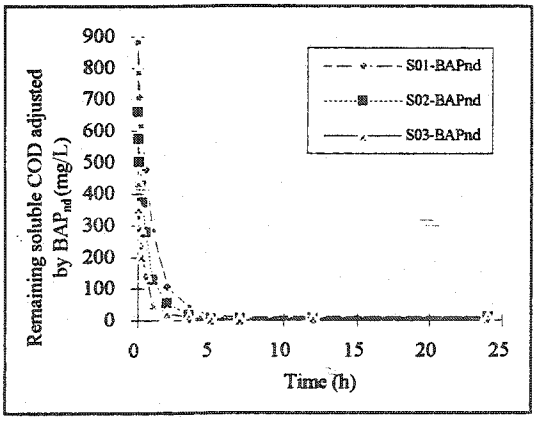


Fig. B-8-3. Soluble COD degradation vs time curves adjusted by BAP_{nd}

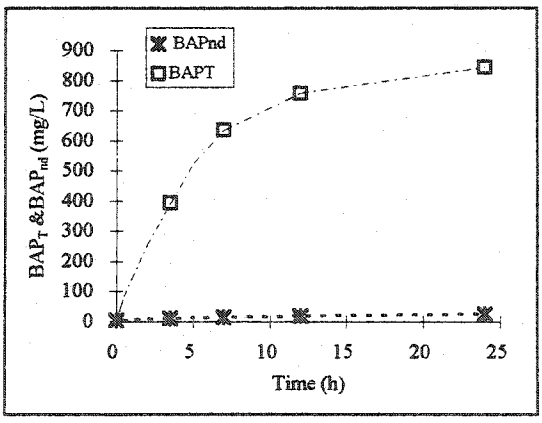


Fig. B-8-4. BAP_T compared to BAP_{nd} vs time

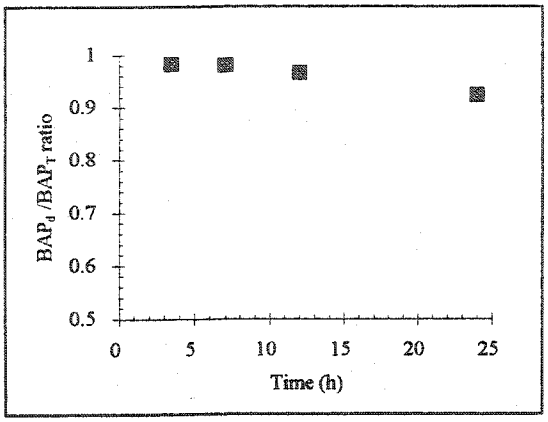


Fig. B-8-5. The ratio of BAP_d to BAP_T

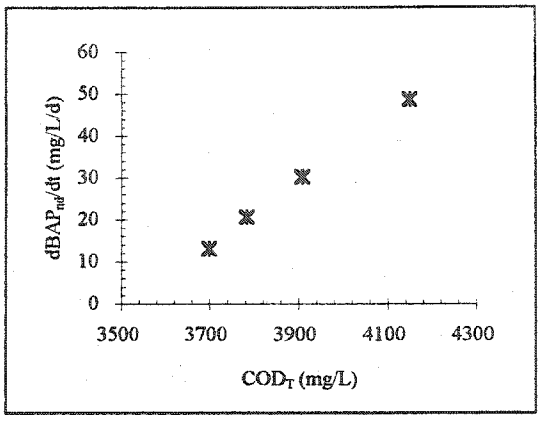


Fig. B-8-6. Linear relation between $dBAP_{nd}$ /dt and COD_T

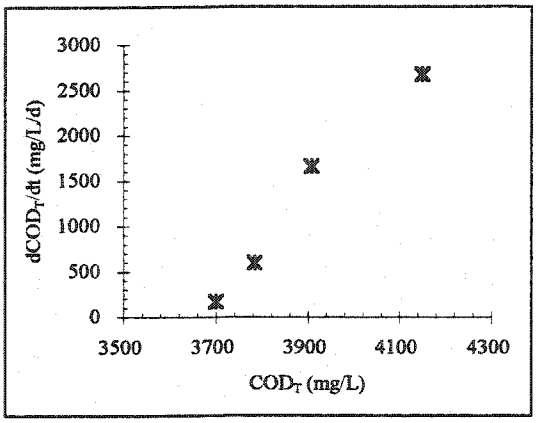


Fig. B-8-7. Linear relation between $dCOD_T/dt$ and COD_T

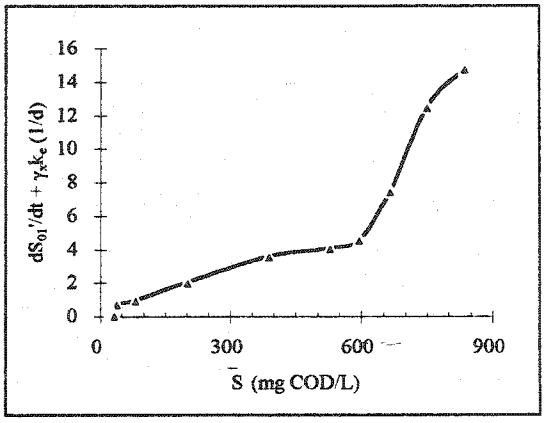


Fig. B-8-8. dS'/dt vs S curve with S_0 = 886 mg/L

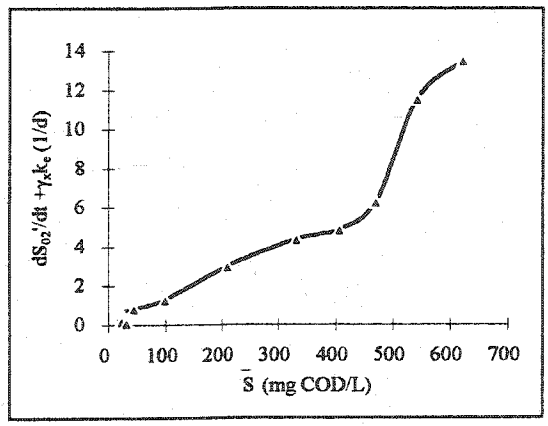


Fig. B-8-9. dS'/dt vs S curve with S_0 = 665 mg/L

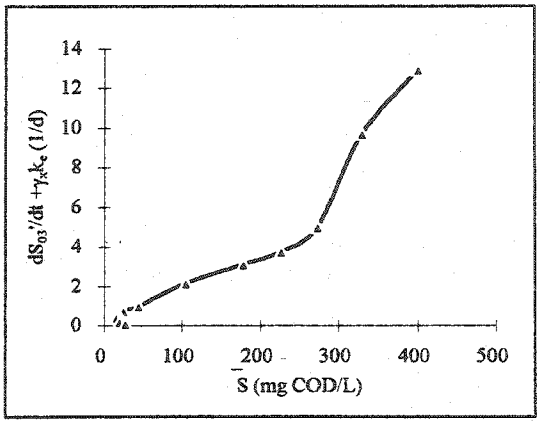


Fig. B-8-10. dS'/dt vs S curve with S_0 = 443 mg/L

Batch Test 8. (Sludge from 7-500-10)				$\bar{X}_v$ =	3418	mg/L						
Time	S_{01}	S_{02}	S_{03}	$\bar{S}_{01}$	$\bar{S}_{02}$	$\bar{S}_{03}$	$dS_{01}'/dt+\gamma_x k_e$	$dS_{02}'/dt+\gamma_x k_e$	$dS_{03}'/dt+\gamma_x k_e$	BAP_{nd}	* BAP_{nd}	$dBAP_{nd}/dt$
h	mg/L	mg/L	mg/L	mg/L	mg/L	mg/L	d^{-1}	d^{-1}	d^{-1}	mg/L	mg/L	mg/L/d
0	886	665	443							3.7	3.7	
0.05	790	578	360	838	621.5	401.5	14.768	13.504	12.942		3.86	
0.1	710	505	300	750	541.5	330	12.524	11.541	9.715		4	
0.2	620	432	245	665	468.5	272.5	7.467	6.273	5.009		4.3	
0.3	570	378	207	595	405	226	4.588	4.869	3.745		4.6	
0.5	485	285	150	527.5	331.5	178.5	4.100	4.381	3.117		5.1	
1	290	135	59	387.5	210	104.5	3.613	2.981	2.153		6	
2	114	62	30	202	98.5	44.5	2.038	1.315	1.006		8.2	
3.5	50	26	19	82	44	24.5	0.988	0.857	0.740	10.8	10.7	49
5	27	19.5	15.5	38.5	22.75	17.25	0.760	0.683	0.669		12.9	
7	24	20	16	25.5	19.75	15.75	0.434	0.421	0.421	15.2	15.2	30
12	29	26	23	26.5	23	19.5	0.206	0.205	0.203	19.5	19.5	21
24	36.6	35.2	31.5	32.8	30.6	27.25	0.086	0.085	0.085	26	26	13
					$1/\bar{S}$	$1/dS'/dt+\gamma_x k_e)$		Regression Output for k_1 and K_{S1}:				
f_1	0.331	0.298	0.324		0.0012	0.0677	k_1	Constant		0.061044		
f_2	0.657	0.687	0.666		0.0016	0.0741	16	Std Err of Y Est		0.003529		
f_3	0.012	0.015	0.010		0.0025	0.0773		R Squared		0.854702		
							K_{S1}	No. of Observations		3		
$f_1+f_2+f_3$	1	1	1				111	Degrees of Freedom		1		
								X Coefficient(s)		6.78256		
								Std Err of Coef.		3.70838		
* The data smoothened by the polynomial method (Gerald and Wheatley, 1989)												

Batch Test 8. (Cont.')

S_{01} -BAP_{nd}	S_{02}-BAP_{nd}	S_{03} -BAP_{nd}	COD_T	*COD_T	$dCOD_T/dt$	BAP_T	BAP_T	BAP_T at t	BAP_d/BAP_T	S_{01}'	S_{02}'	S_{03}'
										S_{01} -BAP_d	S_{02}-BAP_d	S_{03} -BAP_d
mg/L	mg/L	mg/L	mg/L	mg/L	mg/L/d	mg/L	mg/L	mg/L	-	mg/L	mg/L	mg/L
882	661	439	4540	4540		3.7				886	665	443
786	574	356		4531		12.7		9		781.16	569.16	351.16
706	501	296		4522		21.7		9		692.3	487.3	282.3
616	428	241		4506		37.7		16		586.6	398.6	211.6
565	373	202		4491		52.7		15		521.9	329.9	158.9
480	280	145		4460		83.7		31		406.4	206.4	71.4
284	129	53		4400		143.7		60		152.3	-2.7	-78.7
106	54	22		4290		253.7		110		-131.5	-183.5	-215.5
39.3	15	8.3	4142	4150	2674	393.7	394	140	0.982	-333	-357	-364
14.1	6.6	2.6		4018		525.7		132		-485.8	-493.3	-497.3
8.8	4.8	0.8	3928	3908	1659	635.7	636	110	0.979	-596.5	-600.5	-604.5
9.5	6.5	3.5	3765	3784	595	759.7	758	124	0.965	-711.2	-714.2	-717.2
10.6	9.2	5.5	3726	3700	168	843.7	844	84	0.923	-781.1	-782.5	-786.2
									0.962			

Regression Output for k_2:	S_{01}	S_{02}	S_{03}
Constant	0.448899	0.301254	0.336448
Std Err of Y Est	0.221005	0.231021	0.180768
R Squared	0.986294	0.990765	0.990316
No. of Observations	7	7	7
Degrees of Freedom	5	5	5
X Coefficient(s)	**0.0072**	**0.0122**	**0.0162**
Std Err of Coef.	0.00038	0.000526	0.000718

B-9. Batch Test 1 (S_0 = 884, 663 and 442 mg/L, respectively; acclimated sludge from SBR run No. 7-500 and θ_{xob} = 15 d)

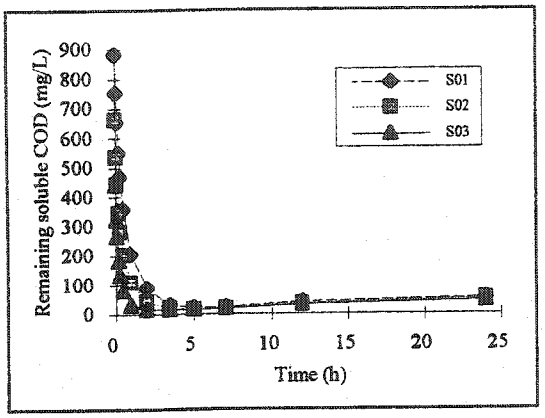


Fig. B-9-1. Soluble COD degradation vs time

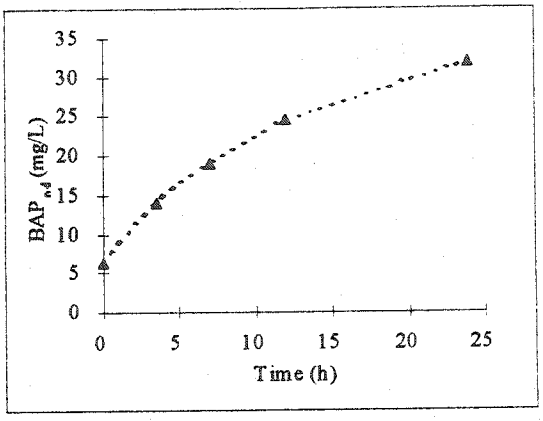


Fig. B-9-2. BAP_{nd} vs time

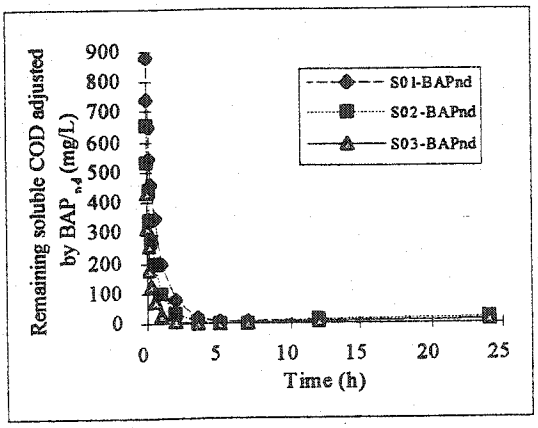


Fig. B-9-3. Soluble COD degradation vs time curves adjusted by BAP_{nd}

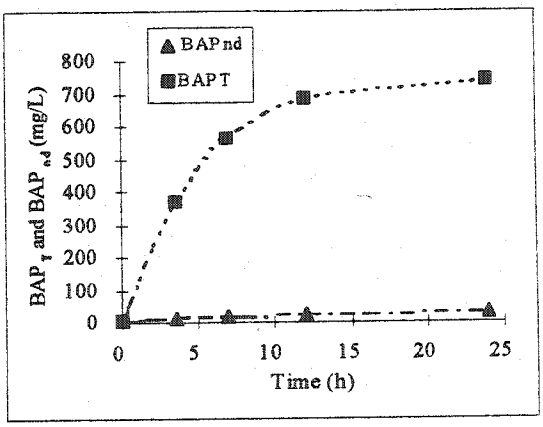


Fig. B-9-4. BAP_T compared to BAP_{nd} vs time

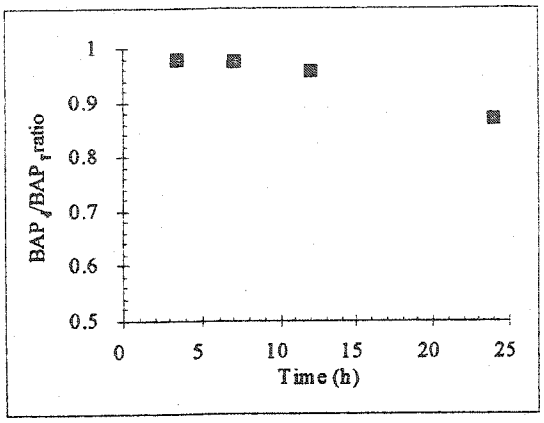


Fig. B-9-5. The ratio of BAP_d to BAP_T

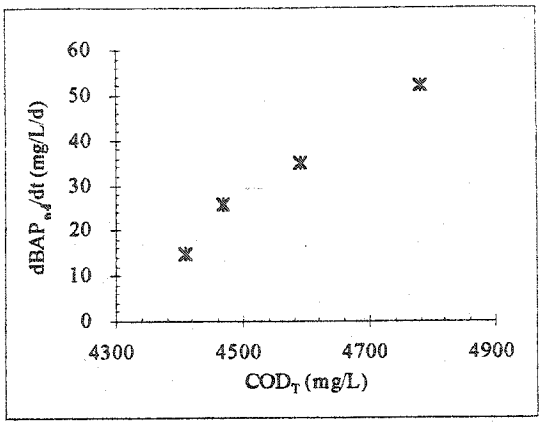


Fig. B-9-6. Linear relation between $dBAP_{nd}$ /dt and COD_T

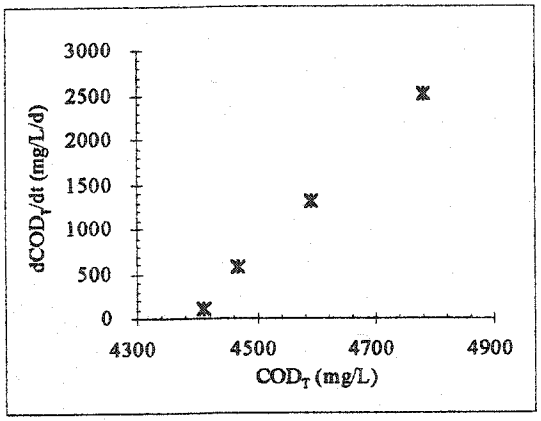


Fig. B-9-7. Linear relation between $dCOD_T/dt$ and COD_T

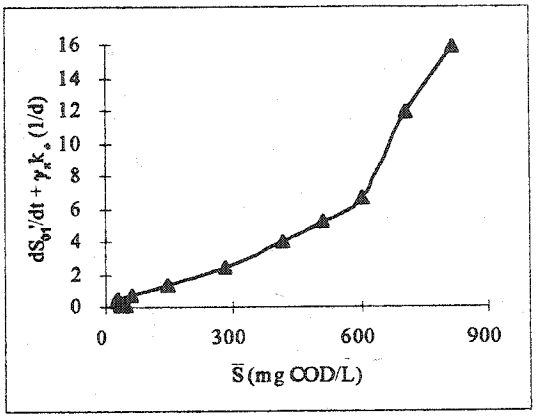


Fig. B-9-8. dS′/dt vs S curve with S_0 = 884 mg/L

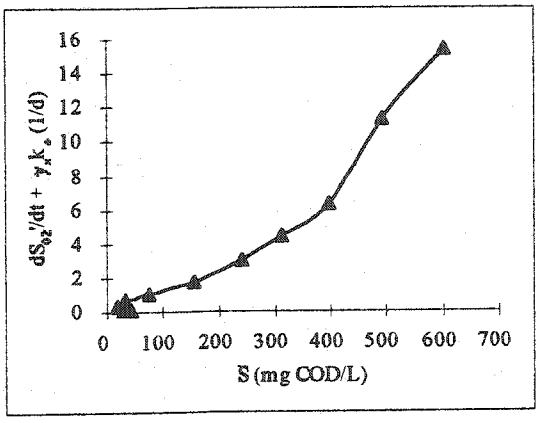


Fig. B-9-9. dS′/dt vs S curve with S_0 = 663 mg/L

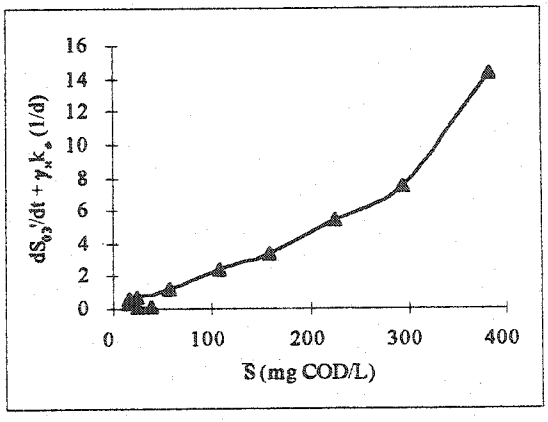


Fig. B-9-10. dS′/dt vs S curve with S_0 = 442 mg/L

Batch Test 9. (Sludge from 7-500-15)				$\bar{X}_v$ =	4195	mg/L						
Time	S_{01}	S_{02}	S_{03}	$\bar{S}_{01}$	$\bar{S}_{02}$	$\bar{S}_{03}$	$dS_{01}'/dt+\gamma_x k_e$	$dS_{02}'/dt+\gamma_x k_e$	$dS_{03}'/dt+\gamma_x k_e$	BAP_{nd}	*BAP_{nd}	$dBAP_{nd}/dt$
h	mg/L	mg/L	mg/L	mg/L	mg/L	mg/L	d^{-1}	d^{-1}	d^{-1}	mg/L	mg/L	mg/L/d
0	884	663	442							6.4	6.4	
0.05	752	536	324	818	599.5	383	15.932	15.360	14.331		6.55	
0.1	655	444	266	703.5	490	295	11.928	11.356	7.465		6.7	
0.2	551	346	183	603	395	224.5	6.607	6.264	5.406		7	
0.3	470	279	135	510.5	312.5	159	5.234	4.433	3.346		7.3	
0.5	359	203	81	414.5	241	108	3.981	2.980	2.351		7.7	
1	204	109	32	281.5	156	56.5	2.444	1.746	1.232		9	
2	89	42	16	146.5	75.5	24	1.304	1.029	0.737		11	
3.5	33	21	16.2	61	31.5	16.1	0.781	0.648	0.567	13.9	14	51
5	24.2	17.3	17.1	28.6	19.15	16.65	0.428	0.408	0.391		16.5	
7	24.5	19	18.3	24.35	18.15	17.7	0.311	0.307	0.309	19	19.1	35
12	40	35	31	32.25	27	24.65	0.161	0.160	0.164	25	24.5	29
24	54	51.3	44.7	47	43.15	37.85	0.062	0.061	0.063	32	32	14
					$1/\bar{S}$	$1/(dS'/dt+\gamma_x k_e)$		Regression Output for k_1 and K_{S1}:				
							k_1	Constant			0.056642	
f_1	0.321	0.337	0.338		0.001	0.063	18	Std Err of Y Est			6.9E-05	
f_2	0.665	0.659	0.657		0.002	0.065		R Squared			0.999814	
f_3	0.014	0.004	0.005		0.003	0.070	K_{S1}	No. of Observations			3	
$f_1+f_2+f_3$	1	1	1				89	Degrees of Freedom			1	
								X Coefficient(s)			5.038812	
								Std Err of Coef.			0.068811	
* The data smoothened by the polynomial method (Gerald and Wheatley, 1989)												

Batch Test 9. (Cont.')

S_{01}-BAP_{nd}	S_{02}-BAP_{nd}	S_{03}-BAP_{nd}	COD_T	*COD_T	$dCOD_T/dt$	BAP_T	BAP_T	BAP_T at t	BAP_d/BAP_T	S_{01}'	S_{02}'	S_{03}'
										S_{01}-BAP_d	S_{02}-BAP_d	S_{03}-BAP_d
mg/L	mg/L	mg/L	mg/L	mg/L	mg/L/d	mg/L	mg/L	mg/L	-	mg/L	mg/L	mg/L
877.6	656.6	435.6	5142	5145		6.4	6.4			884	663	442
745.45	529.45	317.45		5138			13.4	7		745.15	529.15	317.15
648.3	437.3	259.3		5131			20.4	7		641.3	430.3	252.3
544	339	176		5120			31.4	11		526.6	321.6	158.6
462.7	271.7	127.7		5110			41.4	10		435.9	244.9	100.9
351.3	195.3	73.3		5083			68.4	27		298.3	142.3	20.3
195	100	23		5027			124.4	56		88.6	-6.4	-83.4
78	31	5		4920			231.4	107		-131.4	-178.4	-204.4
19	7	2.2	4793	4780	2503	371	371.4	140	0.979	-324.4	-336.4	-341.2
7.7	0.8	0.6		4686			465.4	94		-424.7	-431.6	-431.8
5.4	-0.1	-0.8	4578	4590	1303	561	561.4	96	0.973	-517.8	-523.3	-524
15.5	10.5	6.5	4486	4468	586	683	683.4	122	0.956	-618.9	-623.9	-627.9
22	19.3	12.7	4409	4410	116	741	741.4	58	0.871	-655.4	-658.1	-664.7
								Avg.	0.944			

Regression Output for k_2:	S_{01}	S_{02}	S_{03}
	-0.08681	-0.10271	-0.06592
Std Err of Y Est	0.319845	0.414055	0.312699
R Squared	0.984815	0.970103	0.987909
No. of Observations	7	7	7
Degrees of Freedom	5	5	5
X Coefficient(s)	**0.0105**	**0.0148**	**0.0244**
Std Err of Coef.	0.000581	0.001163	0.001208

B-10. Batch Test 10 (S_0 = 936, 702 and 468 mg/L, respectively; acclimated sludge from SBR run No. 5-500 and θ_{xob} = 10 d)

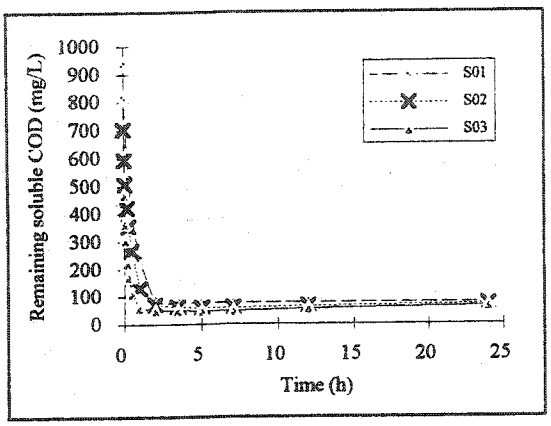


Fig.B-10-1. Soluble COD degradation vs time

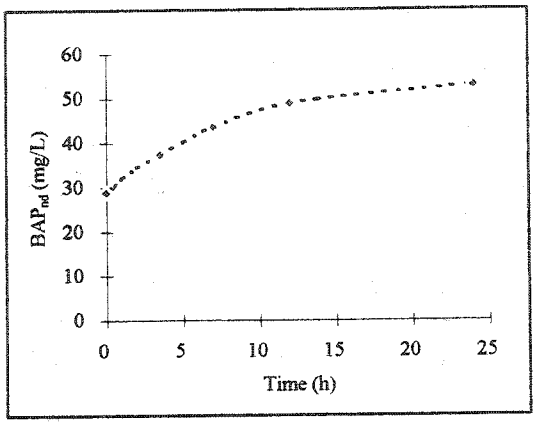


Fig. B-10-2. BAP$_{nd}$ vs time

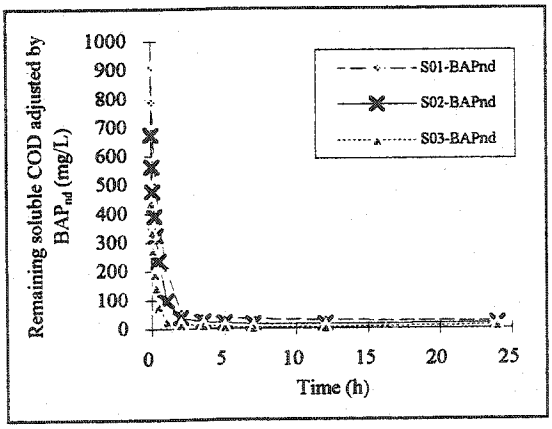


Fig. B-10-3. Soluble COD degradation vs time curves adjusted by BAP$_{nd}$

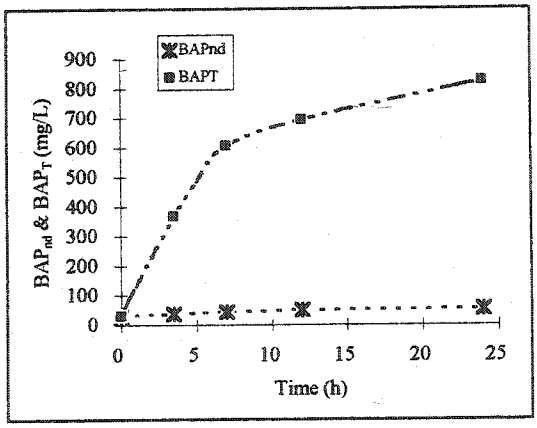


Fig. B-10-4. BAP$_T$ compared to BAP$_{nd}$ vs time

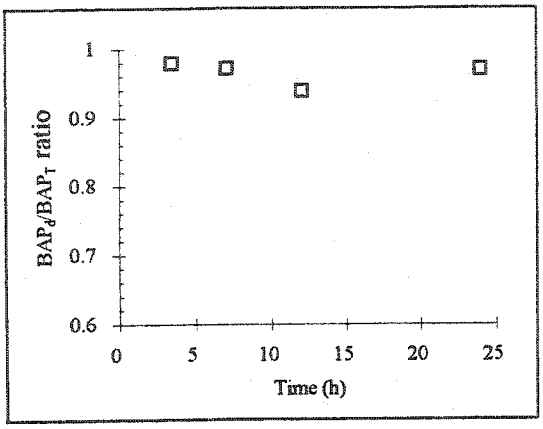


Fig. B-10-5. The ratio of BAP_d to BAP_T

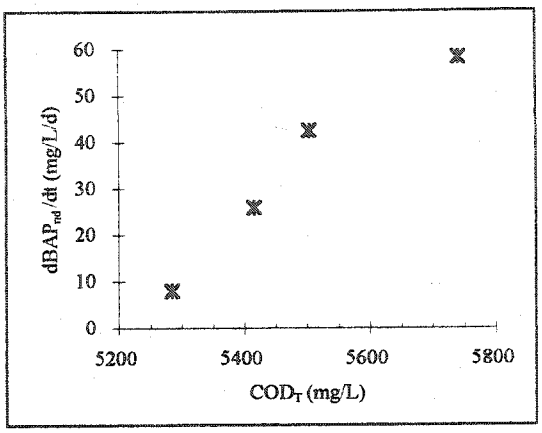


Fig. B-10-6. Linear relation between $dBAP_{nd}/dt$ and COD_T

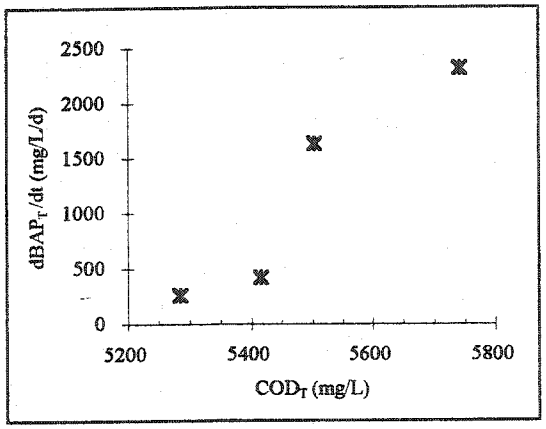


Fig. B-10-7. Linear relation between $dCOD_T/dt$ and COD_T

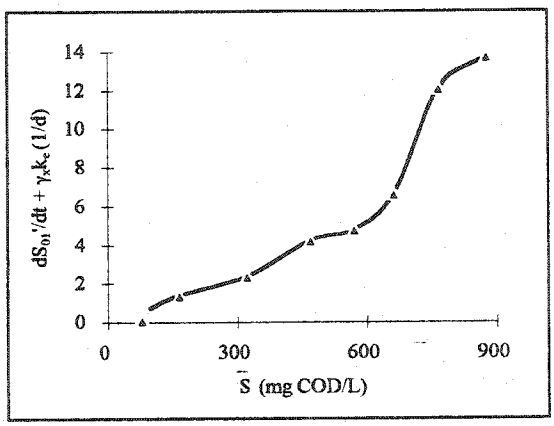


Fig. B-10-8. dS'/dt vs S curve with $S_0 = 936$

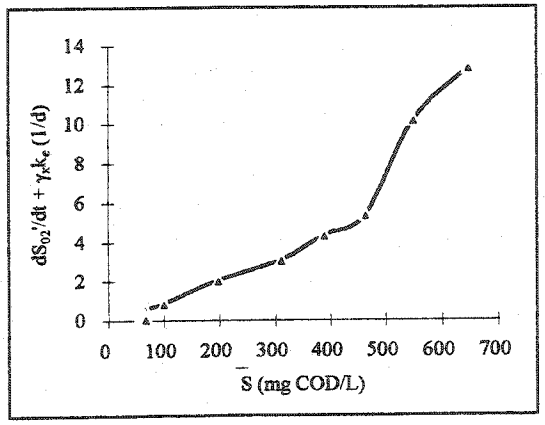


Fig. B-10-9. dS'/dt vs S curve with $S_0 = 702$ mg/L

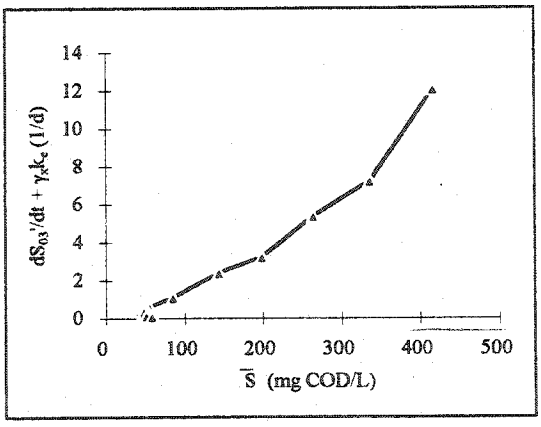


Fig. B-10-10. dS'/dt vs S curve with $S_0 = 468$ mg/L

Batch Test 10. (Sludge from 5-500-10)

$\overline{X}_v$ = 4340 mg/L

Time	S_{01}	S_{02}	S_{03}	$\overline{S}_{01}$	$\overline{S}_{02}$	$\overline{S}_{03}$	$dS_{01}'/dt+\gamma_x k_e$	$dS_{02}'/dt+\gamma_x k_e$	$dS_{03}'/dt+\gamma_x k_e$	BAP_{nd}	$*BAP_{nd}$	$dBAP_{nd}/dt$
h	mg/L	mg/L	mg/L	mg/L	mg/L	mg/L	d^{-1}	d^{-1}	d^{-1}	mg/L	mg/L	mg/L/d
0	936	702	468							28.9	28.9	
0.05	818	592	365	877	647	416.5	13.737	12.852	12.078		29.1	
0.1	715	506	306	766.5	549	335.5	12.080	10.200	7.214		29.28	
0.2	608	421	221	661.5	463.5	263.5	6.605	5.389	5.389		29.65	
0.3	534	355	175	571	388	198	4.787	4.345	3.239		29.9	
0.5	405	267	111	469.5	311	143	4.204	3.070	2.406		30.5	
1	240	130	59.1	322.5	198.5	85.05	2.362	2.052	1.111		32	
2	90	71	51	165	100.5	55.05	1.392	0.888	0.607		34.5	
3.5	79	61	49.8	84.5	66	50.4	0.584	0.580	0.547	39	37.4	58
5	77.8	59.8	47.6	78.4	60.4	48.7	0.474	0.474	0.478		40.2	
7	77	59.1	47.2	77.4	59.45	47.4	0.370	0.369	0.369	42.5	43.6	43
12	77.4	64	54	77.2	61.55	50.6	0.136	0.131	0.129	48	49	26
24	78	70	63.3	77.7	67	58.65	0.103	0.101	0.099	55	53	8

					$1/\overline{S}$	$1/(dS'/dt+\gamma_x k_e)$		Regression Output for k_1 and K_{S1}:		
f_1	0.303	0.292	0.303		0.0011	0.0728	k_1	Constant		0.068209
f_2	0.654	0.678	0.678		0.0015	0.0778	15	Std Err of Y Est		0.001639
f_3	0.042	0.030	0.019		0.0024	0.0828		R Squared		0.955708
$f_1+f_2+f_3$	1	1	1				K_{S1}	No. of Observations		3
							110	Degrees of Freedom		1
								X Coefficient(s)		7.510965
								Std Err of Coef.		1.61695

* The data smoothened by the polynomial method (Gerald and Wheatley, 1989)

Batch Test 10. (Cont.')										S_{01}'	S_{02}'	S_{03}'
S_{01} -BAP_{nd}	S_{02} -BAP_{nd}	S_{03} -BAP_{nd}	*COD_T	COD_T	$dCOD_T/dt$	BAP_T	BAP_T	BAP_T at t	BAP_d/BAP_T	S_{01} -BAP_d	S_{02} -BAP_d	S_{03} -BAP_d
mg/L	mg/L	mg/L	mg/L	mg/L	mg/L/d	mg/L	mg/L	mg/L	-	mg/L	mg/L	mg/L
907.1	673.1	439.1	6080	6080		29	29			935.9	701.9	467.9
788.9	562.9	335.9		6074			35	6		812.1	586.1	359.1
685.72	476.72	276.72		6068			41	6		703.28	494.28	294.28
578.35	391.35	191.35		6056			53	12		584.65	397.65	197.65
504.1	325.1	145.1		6044			65	12		498.9	319.9	139.9
374.5	236.5	80.5		6022			87	22		348.5	210.5	54.5
208	98	27.1		5976			133	46		139	29	-41.9
55.5	36.5	16.5		5880			229	96		-104.5	-123.5	-143.5
41.6	23.6	12.4	5778	5742	2318	367	367	138	0.979	-250.6	-268.6	-279.8
37.6	19.6	7.4		5624			485	118		-367	-385	-397.2
33.4	15.5	3.6	5489	5504	1632	605	605	120	0.972	-484.4	-502.3	-514.2
28.4	15	5	5432	5416	422	693	693	88	0.939	-566.6	-580	-590
25	17	10.3	5271	5285	262	824	824	131	0.969	-693	-701	-707.7
								Avg.	0.965			

Regression Output for k_2:	S_{01}	S_{02}	S_{03}
Constant	-0.23679	-0.26389	-0.55527
Std Err of Y Est	0.115075	0.158678	0.335585
R Squared	0.992597	0.992494	0.984901
No. of Observations	17	10	7
Degrees of Freedom	15	8	5
X Coefficient (s)	**0.0082**	**0.0111**	**0.0224**
Std Err of Coef.	0.000184	0.00034	0.00124

B-11. Batch Test 11 (S_0 = 936, 702 and 468 mg/L, respectively; acclimated sludge from SBR run No. 5-500 and θ_{xob} = 15 d)

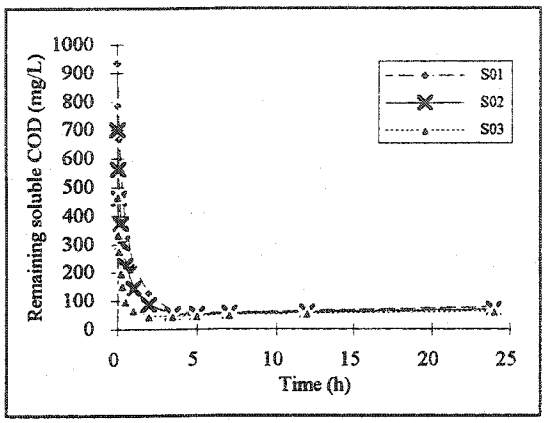


Fig.B-11-1. Soluble COD degradation vs time

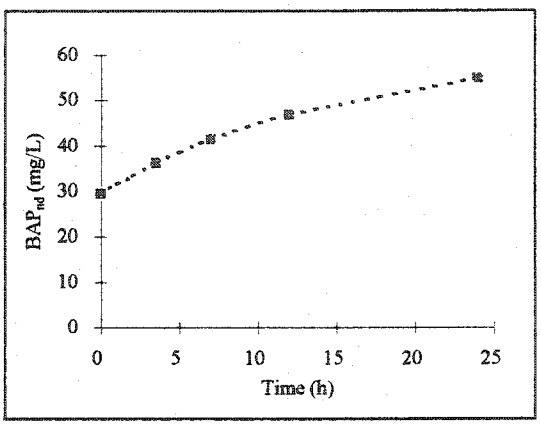


Fig. B-11-2. BAP_{nd} vs time

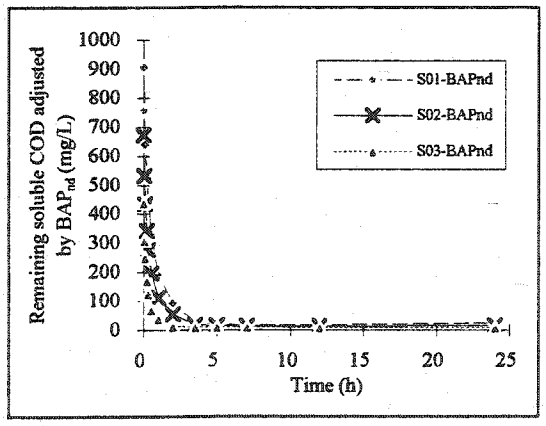


Fig. B-11-3. Soluble COD degradation vs time curves adjusted by BAP_{nd}

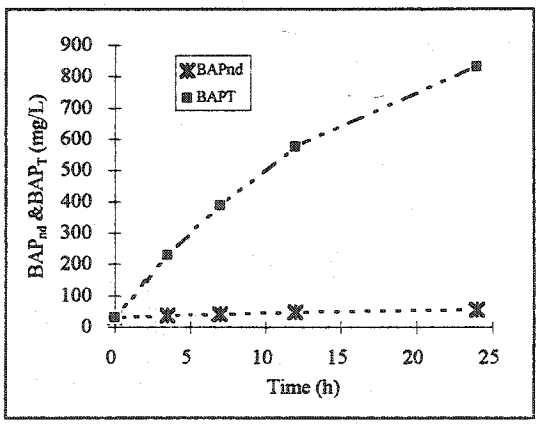


Fig. B-11-4. BAP_T compared to BAP_{nd} vs time

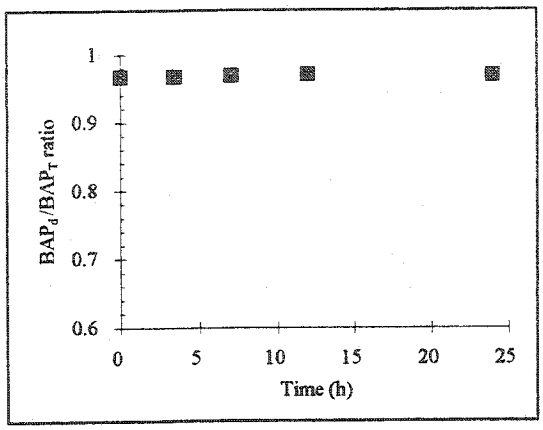


Fig. B-11-5. The ratio of BAP_d to BAP_T

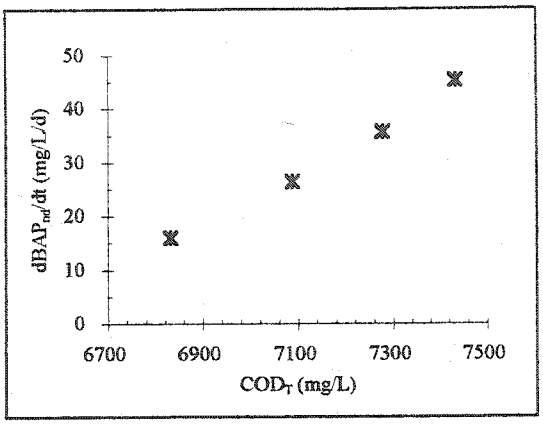


Fig. B-11-6. Linear relation between $dBAP_{nd}/dt$ and COD_T

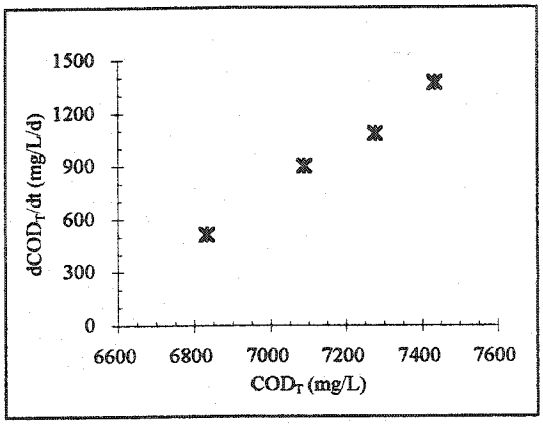


Fig. B-11-7. Linear relation between $dCOD_T/dt$ and COD_T

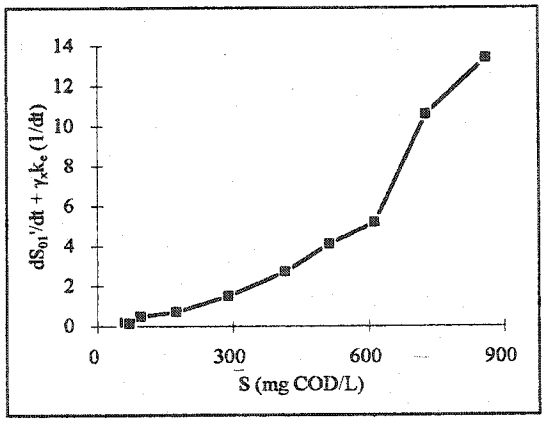


Fig. B-11-8. dS'/dt vs S curve with S_0 = 936 mg/L

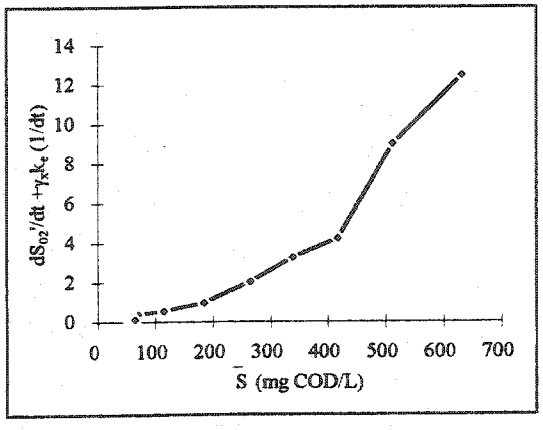


Fig. B-11-9. dS'/dt vs S curve with S_0 = 702 mg/L

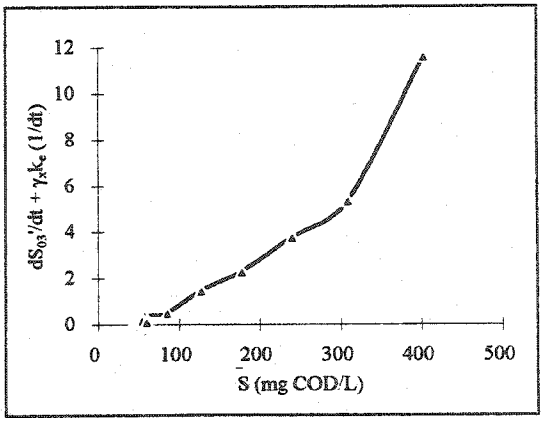


Fig. B-11-10. dS'/dt vs S curve with S_0 = 468 mg/L

Batch Test 11. (Sludge from 5-500-15)				$\bar{X}_v$ =	5513	mg/L						
Time	S_{01}	S_{02}	S_{03}	$\bar{S}_{01}$	$\bar{S}_{02}$	$\bar{S}_{03}$	$dS_{01}'/dt+\gamma_x k_e$	$dS_{02}'/dt+\gamma_x k_e$	$dS_{03}'/dt+\gamma_x k_e$	BAP_{nd}	* BAP_{nd}	$dBAP_{nd}/dt$
h	mg/L	mg/L	mg/L	mg/L	mg/L	mg/L	d^{-1}	d^{-1}	d^{-1}	mg/L	mg/L	mg/L/d
0	936	702	468							29.5	29.5	
0.05	786	562	338	861	632	403	13.358	12.487	11.616		29.6	
0.1	668	462	280	727	512	309	10.571	9.004	5.347		29.7	
0.2	556	372	200	612	417	240	5.173	4.216	3.780		29.9	
0.3	470	305	155	513	338.5	177.5	4.085	3.258	2.300		30.1	
0.5	360	225	100	415	265	127.5	2.692	2.039	1.495		30.5	
1	220	144	70	290	184.5	85	1.490	0.977	0.533		31.5	
2	128	87	46	174	115.5	58	0.695	0.542	0.398		33.3	
3.5	63	53	47	95.5	70	46.5	0.466	0.376	0.275	36.1	36.1	45.3
5	58.5	53	50	60.75	53	48.5	0.254	0.241	0.232		38.5	
7	58.5	55	52	58.5	54	51	0.230	0.226	0.226	41.3	41.3	35.7
12	65	60.7	56.3	61.75	57.85	54.15	0.198	0.199	0.200	46.8	46.8	26.4
24	78	70	63.3	71.5	65.35	59.8	0.131	0.132	0.133	54.8	54.8	16
					$1/\bar{S}$	$1/(dS'/dt+\gamma_x k_e)$		Regression Output for k_1 and K_{S1}:				
f_1	0.2943188	0.2828253	0.3630559		0.0011614	0.0748641	k_1	Constant		0.066038		
f_2	0.6811362	0.6956134	0.6132269		0.0015823	0.0800842	15	Std Err of Y Est		0.0013122		
f_3	0.024545	0.0215613	0.0237172		0.0024814	0.0860867		R Squared		0.9726998		
$f_1+f_2+f_3$	1	1	1				K_{S1}	No. of Observations		3		
							124	Degrees of Freedom		1		
								X Coefficient(s)		8.2143967		
								Std Err of Coef.		1.3761615		
* The data smoothened by the polynomial method (Gerald and Wheatley, 1989)												

Batch Test 11. (Cont.')

S_{01}-BAP_{nd}	S_{02}-BAP_{nd}	S_{03}-BAP_{nd}	COD_T	* COD_T	$dCOD_T/dt$	BAP_T	BAP_T	BAP_T at t	BAP_d/BAP_T	S_{01}'	S_{02}'	S_{03}'
S_{01}-BAP_d	S_{02}-BAP_d	S_{03}-BAP_d										
mg/L	mg/L	mg/L	mg/L	mg/L	mg/L/d	mg/L	mg/L	mg/L	-	mg/L	mg/L	mg/L
906.5	672.5	438.5	7635	7635		29.5	29.5			936	702	468
756.4	532.4	308.4		7632			32.5	3	0.967	783.1	559.1	335.1
638.3	432.3	250.3		7629			35.5	3		662.2	456.2	274.2
526.1	342.1	170.1		7623			41.5	6		544.4	360.4	188.4
439.9	274.9	124.9		7616			48.5	7		451.6	286.6	136.6
329.5	194.5	69.5		7604			60.5	12		330	195	70
188.5	112.5	38.5		7577			87.5	27		164	88	14
94.7	53.7	12.7		7518			146.5	59		14.8	-26.2	-67.2
26.9	16.9	10.9	7418	7435	1371	230	229.5	83	0.966	-130.4	-140.4	-146.4
20	14.5	11.5		7365			299.5	70		-202.5	-208	-211
17.2	13.7	10.7	7305	7277	1083	388	387.5	88	0.968	-287.7	-291.2	-294.2
18.2	13.9	9.5	7068	7089	902	576	575.5	188	0.971	-463.7	-468	-472.4
23.2	15.2	8.5	6842	6832	514	832	832.5	257	0.969	-699.7	-707.7	-714.4
								Avg.	0.968			

Regression Output for k_2:	S_{01}	S_{02}	S_{03}
Constant	-0.624568	-0.610487	-0.892967
Std Err of Y Est	0.3816959	0.3089119	0.2346974
R Squared	0.9671184	0.9673287	0.9877109
No. of Observations	7	7	7
Degrees of Freedom	5	5	5
X Coefficient(s)	**0.0089**	**0.0110**	**0.0195**
Std Err of Coef.	0.000734	0.0009065	0.0009742

B-12. Batch Test 12 (S_0 = 583, 350 and 117 mg/L, respectively; acclimated sludge from SBR run No. 5-250 and θ_{xob} = 10 d)

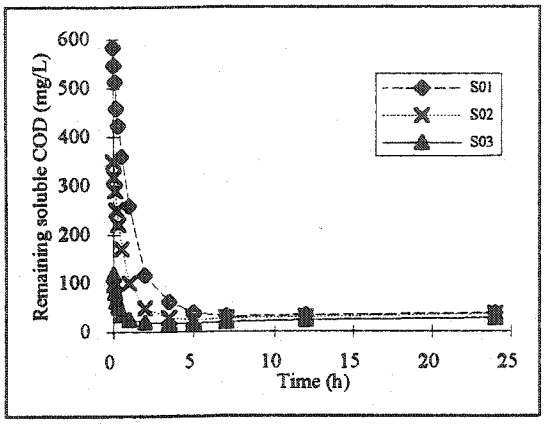


Fig. B-12-1. Soluble COD degradation vs time

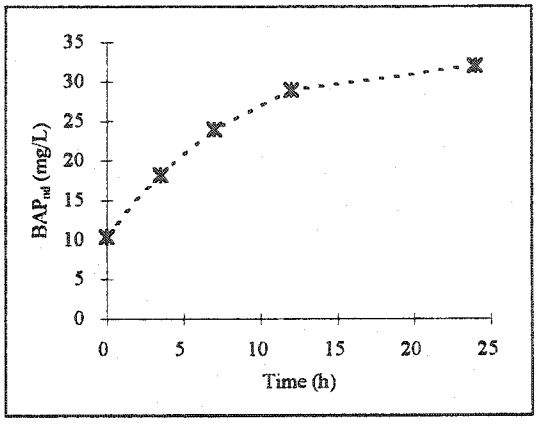


Fig. B-12-2. BAP_{nd} vs time

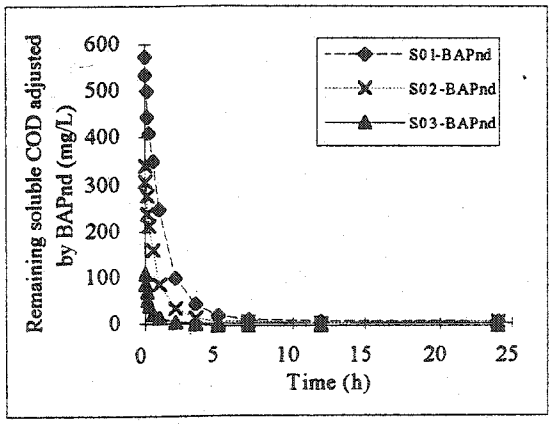


Fig. B-12-3. Soluble COD degradation vs time curves adjusted by BAP_{nd}

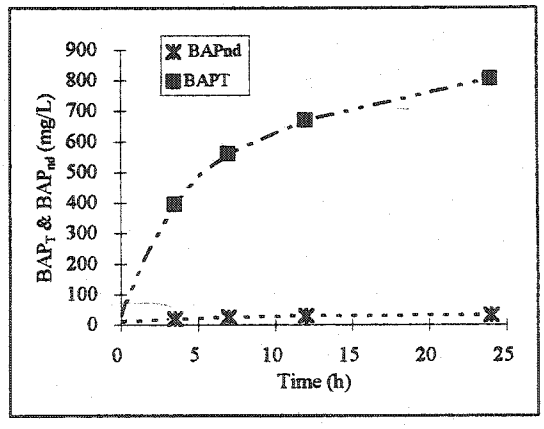


Fig. B-12-4. BAP_T compared to BAP_{nd} vs time

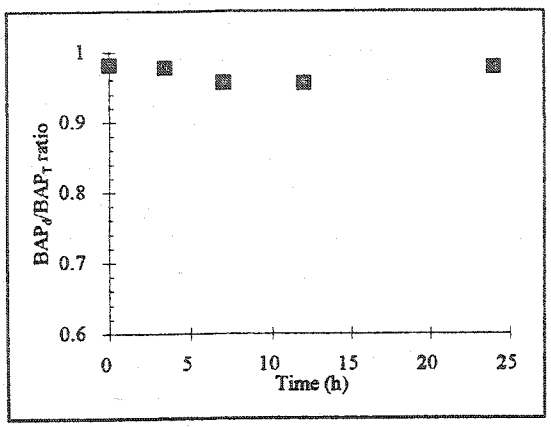


Fig. B-12-5. The ratio of BAP_d to BAP_T

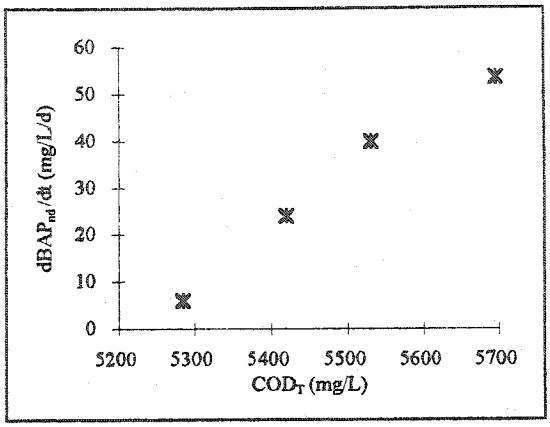


Fig. B-12-6. Linear relation between $dBAP_{nd}/dt$ and COD_T

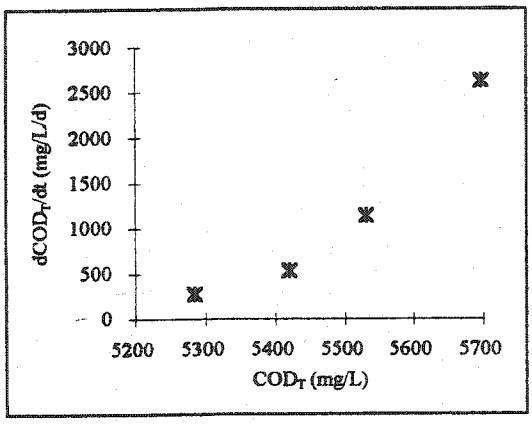


Fig. B-12-7. Linear relation between $dCOD_T/dt$ and COD_T

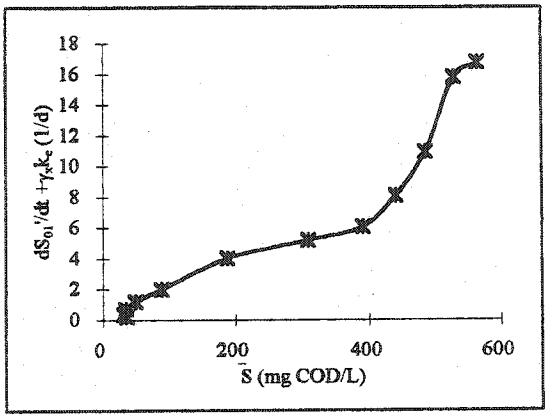


Fig. B-12-8. dS'/dt vs S curve with S_0 = 583 mg/L

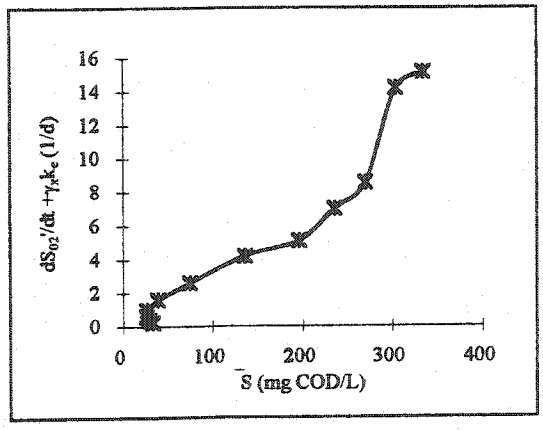


Fig. B-12-9. dS'/dt vs S curve with S_0 = 350 mg/L

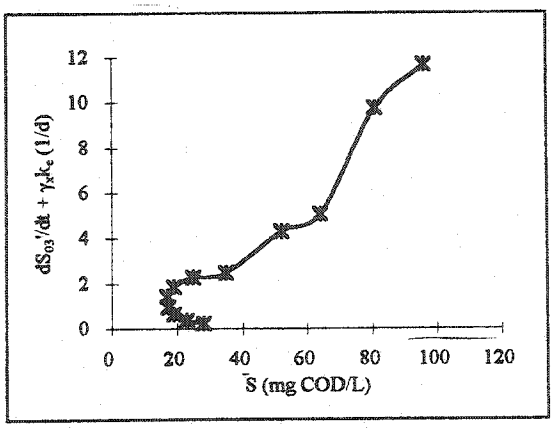


Fig. B-12-10. dS'/dt vs S curve with S_0 = 117 mg/L

Batch Test 12. (Sludge from No. 5-250-10)

					$\bar{X}_v$ =	1518	mg/L					
Time	S_{01}	S_{02}	S_{03}	$\bar{S}_{01}$	$\bar{S}_{02}$	$\bar{S}_{03}$	$dS_{01}'/dt+\gamma_x k_e$	$dS_{02}'/dt+\gamma_x k_e$	$dS_{03}'/dt+\gamma_x k_e$	BAP_{nd}	$*BAP_{nd}$	$dBAP_{nd}/dt$
h	mg/L	mg/L	mg/L	mg/L	mg/L	mg/L	d^{-1}	d^{-1}	d^{-1}	mg/L	mg/L	mg/L/d
0	583	350	117							10.4	10.4	
0.05	546	318	96	564.5	334	106.5	16.709	15.128	11.650		10.7	
0.1	512	289	81	529	303.5	88.5	15.760	14.179	9.753		11	
0.2	458	250	64	485	269.5	72.5	10.907	8.535	5.057		11.3	
0.3	422	221	52	440	235.5	58	8.077	6.970	4.282		11.5	
0.5	360	171	35	391	196	43.5	6.037	5.088	2.480		11.7	
1	258	101	25	309	136	30	5.183	4.171	2.274		12.9	
2	116	48	19	187	74.5	22	3.998	2.590	1.847		15.2	
3.5	61	29	17	88.5	38.5	18	1.989	1.609	1.430	17.0	18.2	53.5
5	39	24	17.3	50	26.5	17.15	1.181	1.002	0.946		20.8	
7	31	28	19	35	26	18.15	0.717	0.622	0.640	23.5	24	39.8
12	34	30	23	32.5	29	21	0.371	0.374	0.368	30.2	29	24.0
24	38	36	28	36	33	25.5	0.214	0.211	0.212	33.5	32	6
					$1/\bar{S}$	$1/(dS'/dt+\gamma_x k_e)$		Regression Output for k_1 and K_{S1}:				
f_1	0.294621	0.2900471	0.3494371		0.0017715	0.0598479	k_1	Constant			0.0733212	
f_2	0.6861684	0.6931684	0.652439		0.002994	0.0661026	14	Std Err of Y Est			0.0027306	
f_3	0.0192106	0.0167845	-0.001876		0.0093897	0.0858388		R Squared			0.9966325	
$f_1+f_2+f_3$	1	1	1				K_{S1}	No. of Observations			3	
							97	Degrees of Freedom			1	
								X Coefficient(s)			7.1459776	
								Std Err of Coef.			0.4153829	

* The data smoothened by the polynomial method (Gerald and Wheatley, 1989)

Batch Test 12. (Cont.')										S_{01}'	S_{02}'	S_{03}'
S_{01} -BAP_{nd}	S_{02} -BAP_{nd}	S_{03} -BAP_{nd}	COD_T	*COD_T	$dCOD_T/dt$	BAP_T	BAP_T	BAP_T at t	BAP_d/BAP_T	S_{01} -BAP_d	S_{02} -BAP_d	S_{03} -BAP_d
mg/L	mg/L	mg/L	mg/L	mg/L	mg/L/d	mg/L	mg/L	mg/L	-	mg/L	mg/L	mg/L
572.6	339.6	106.6	6080	6080		10.4	10.4			583	350	117
535.3	307.3	85.3		6064			26.4	16	0.981	530.3	302.3	80.3
501	278	70		6048			42.4	16		480.6	257.6	49.6
446.7	238.7	52.7		6033			57.4	15		411.9	203.9	17.9
410.5	209.5	40.5		6018			72.4	15		361.1	160.1	-8.9
348.3	159.3	23.3		6004			86.4	14		285.3	96.3	-39.7
245.1	88.1	12.1		5940			150.4	64		122.8	-34.2	-110.2
100.8	32.8	3.8		5829			261.4	111		-127.2	-195.2	-224.2
42.8	10.8	-1.2	5748	5697	2626	393	393.4	132	0.977	-311.6	-343.6	-355.6
18.2	3.2	-3.5		5603			487.4	94		-419.4	-434.4	-441.1
7	4	-5	5513	5531	1138	559	559.4	72	0.956	-504.4	-507.4	-516.4
5	1	-6	5436	5420	532.8	670	670.4	111	0.955	-607.4	-611.4	-618.4
6	4	-4	5267	5285	270	805	805.4	135	0.978	-735.4	-737.4	-745.4
								Avg.	0.969			

Regression Output for k_2:	S_{01}	S_{02}	S_{03}
Constant	-0.012285	-0.20184	0.0110616
Std Err of Y Est	0.2386863	0.1124848	0.1445941
R Squared	0.9775138	0.9968117	0.9834894
No. of Observations	11	7	8
Degrees of Freedom	9	5	6
X Coefficient(s)	**0.0121**	**0.0220**	**0.0433**
Std Err of Coef.	0.0006101	0.0005567	0.0022898

B-13. Batch Test 13 (S_0 = 583, 350 and 117 mg/L, respectively; acclimated sludge from SBR run No. 5-250 and θ_{xob} = 15 d)

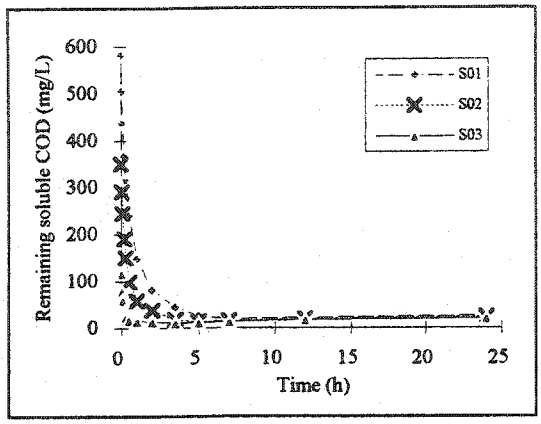


Fig.B-13-1. Soluble COD degradation vs time

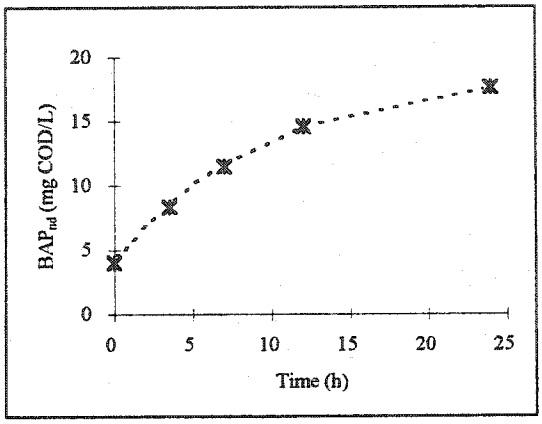


Fig. B-13-2. BAP_{nd} vs time

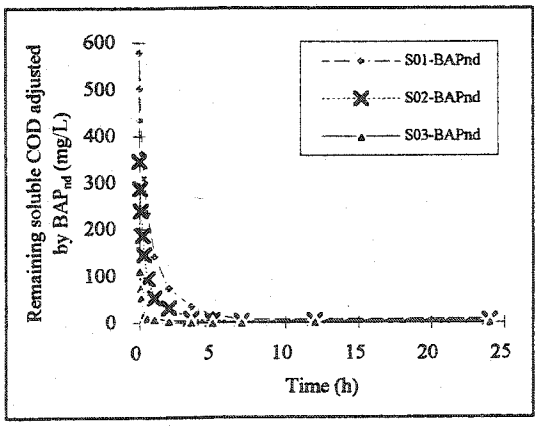


Fig. B-13-3. Soluble COD degradation vs time curves adjusted by BAP_{nd}

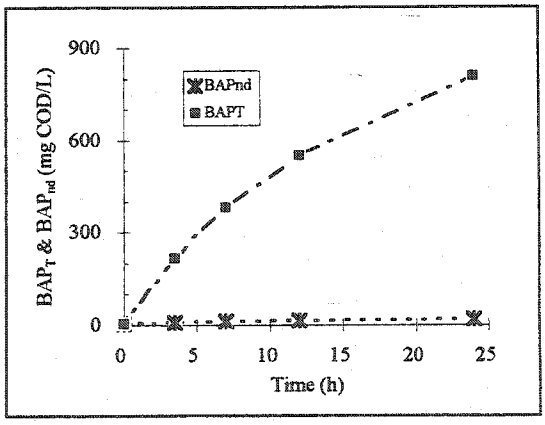


Fig. B-13-4. BAP_T compared to BAP_{nd} vs time

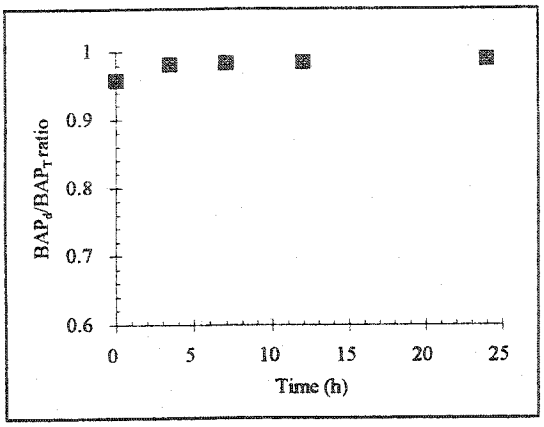


Fig. B-13-5. The ratio of BAP_d to BAP_T

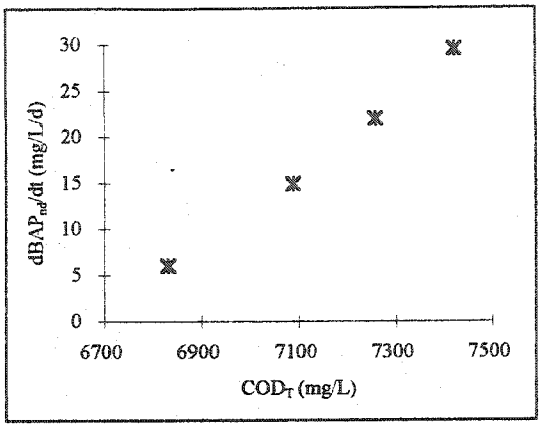


Fig. B-13-6. Linear relation between $dBAP_{nd}/dt$ and COD_T

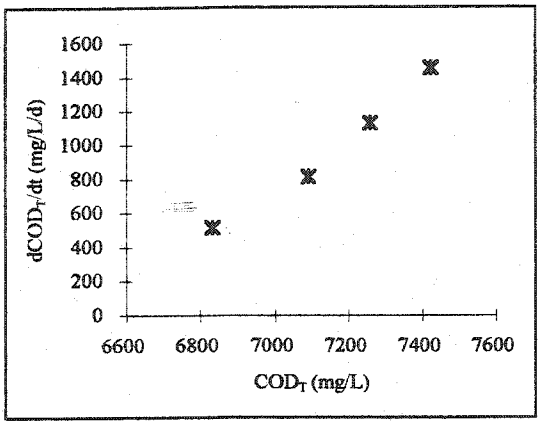


Fig. B-13-7. Linear relation between $dCOD_T/dt$ and COD_T

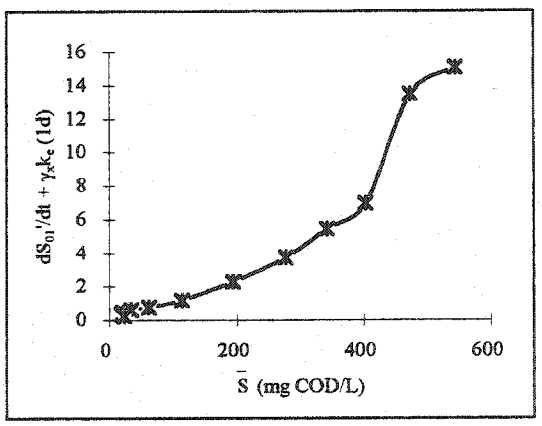


Fig. B-13-8. dS'/dt vs S curve with S_0 = 583 mg/L

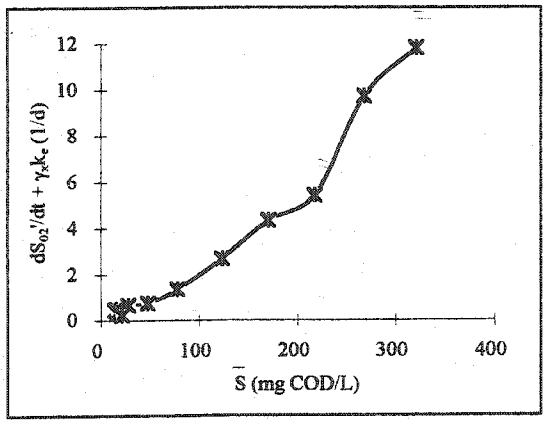


Fig. B-13-9. dS'/dt vs S curve with S_0 = 350 mg/L

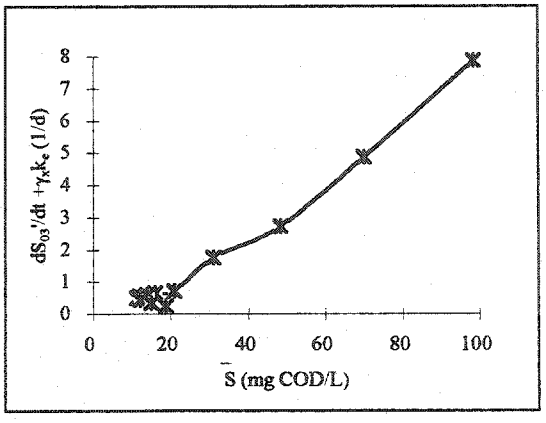


Fig. B-13-10. dS'/dt vs S curve with S_0 = 117 mg/L

Batch Test 13. (Sludge from No. 5-250-15)					$\overline{X}_v$ =	2680	mg/L					
Time	S_{01}	S_{02}	S_{03}	$\overline{S}_{01}$	$\overline{S}_{02}$	$\overline{S}_{03}$	$dS_{01}'/dt+\gamma_x k_e$	$dS_{02}'/dt+\gamma_x k_e$	$dS_{03}'/dt+\gamma_x k_e$	BAP_{nd}	BAP_{nd}	$dBAP_{nd}/dt$
h	mg/L	mg/L	mg/L	mg/L	mg/L	mg/L	d^{-1}	d^{-1}	d^{-1}	mg/L	mg/L	mg/L/d
0	583	350	117							4	4	
0.05	506	291	80	544.5	320.5	98.5	15.036	11.812	7.872		4.3	
0.1	438	244	60	472	267.5	70	13.460	9.699	4.863		4.4	
0.2	368	191	37	403	217.5	48.5	6.923	5.400	2.714		4.6	
0.3	315	150	25	341.5	170.5	31	5.418	4.344	1.746		4.6	
0.5	240	98	17	277.5	124	21	3.708	2.678	0.708		4.8	
1	148	58	15	194	78	16	2.269	1.338	0.658		5.6	
2	81	38	13	114.5	48	14	1.171	0.750	0.589		6.9	
3.5	44	17	11.2	62.5	27.5	12.1	0.758	0.662	0.548	8.9	8.5	30.9
5	26	13.8	11.5	35	15.4	11.35	0.597	0.508	0.487		10.1	
7	18.5	14.9	13	22.25	14.35	12.25	0.470	0.431	0.430	11	11.7	21.9
12	21.5	19	17	20	16.95	15	0.337	0.335	0.335	16	14.6	13.9
24	26	23	20.4	23.75	21	18.7	0.231	0.232	0.232	17.9	17.6	6
						$1/\overline{S}$	$1/(dS'/dt+\gamma_x k_e)$		Regression Output for k_1 and K_{S1}:			
f_1	0.311917	0.312139	0.419469			0.001837	0.066507	k_1	Constant			0.058196
f_2	0.669862	0.672543	0.569469			0.00312	0.084658	17	Std Err of Y Est			0.00668
f_3	0.018221	0.015318	0.011062			0.010152	0.127035		R Squared			0.976875
$f_1+f_2+f_3$	1	1	1					K_{S1}	No. of Observations			3
								118	Degrees of Freedom			1
									X Coefficient(s)			6.857602
									Std Err of Coef.			1.055102
* The data smoothened by the polynomial method (Gerald and Wheatley, 1989)												

Batch Test 13. (Cont.')

S_{01}-BAP_{nd}	S_{02}-BAP_{nd}	S_{03}-BAP_{nd}	COD_T	COD_T	$dCOD_T/dt$	BAP_T	BAP_T	BAP_T at t	BAP_d/BAP_T	S_{01}'	S_{02}'	S_{03}'
										S_{01}-BAP_d	S_{02}-BAP_d	S_{03}-BAP_d
mg/L	mg/L	mg/L	mg/L	mg/L	mg/L/d	mg/L	mg/L	-	mg/L	mg/L	mg/L	mg/L
579	346	113	7635	7635		4	4			583	350	117
501.7	286.7	75.7		7628			11	7	0.957	499.3	284.3	73.3
433.6	239.6	55.6		7621			18	7		424.4	230.4	46.4
363.4	186.4	32.4		7614			25	7		347.6	170.6	16.6
310.4	145.4	20.4		7607			32	7		287.6	122.6	-2.4
235.2	93.2	12.2		7600			39	7		205.8	63.8	-17.2
142.4	52.4	9.4		7567			72	33		81.6	-8.4	-51.4
74.1	31.1	6.1		7507			132	60		-44.1	-87.1	-112.1
35.5	8.5	2.7	7428	7423	1454	216	216	84	0.981	-163.5	-190.5	-196.3
15.9	3.7	1.4		7347			292	76		-255.9	-268.1	-270.4
6.8	3.2	1.3	7237	7258	1131	381	381	89	0.982	-350.8	-354.4	-356.3
6.9	4.4	2.4	7105	7089	811	550	550	169	0.983	-513.9	-516.4	-518.4
8.4	5.4	2.8	6792	6832	514	807	807	257	0.988	-763.4	-766.4	-769
									0.978			

Regression Output for k_2:	S_{01}	S_{02}	S_{03}
Constant	-0.31671	-0.23582	-0.56257
Std Err of Y Est	0.499005	0.954526	0.24469
R Squared	0.964358	0.923866	0.980892
No. of Observations	8	8	7
Degrees of Freedom	6	6	5
X Coefficient(s)	**0.0164**	**0.0332**	**0.0741**
Std Err of Coef.	0.001291	0.003889	0.004628

APPENDIX C NEW SBR MODEL SIMULATIONS

New SBR Model Simulation Results							
No. 2-250-5		S_0 =	232	mg/L	$\theta_{xob}\varphi$ =	3.33	d
				Model Predicted		**Experimental**	
Cycle time	S_1	S_2	S_3	S	VSS	S	VSS
min.	mg/L	mg/L	mg/L	mg/L	mg/L	mg/L	mg/L
0	0.48	0.04	20.25	20.77	4979	24.9	4706
10	4.84	17.79	19.26	41.89	3754	38	
40	4.85	19.02	19.07	42.95	2187	39.5	
60	4.8	18.82	19.04	42.66	1722	39.5	1588
70	1.36	6.98	19.67	28.02	1726	29.6	
95	0.5	0.5	20.09	21.08	1727	28.9	
120	0	0	0	20.7	1727	21.1	1535
			COD η	0.911		0.909	
			R_{tr}	0.979		1.099	
			L_{vtr}	2028		2025	
No. 2-250-10		S_0 =	232	mg/L	$\theta_{xob}\varphi$ =	6.67	d
				Model Predicted		**Experimental**	
Cycle time	S_1	S_2	S_3	S	VSS	S	VSS
min	mg/L	mg/L	mg/L	mg/L	mg/L	mg/L	mg/L
0	0.27	0	15.88	16.15	9213	19	8784
10	2.68	10.26	15.5	28.45	6931	26	
40	2.68	10.26	15.36	28.3	4002	25.1	
60	2.66	10.2	15.32	28.18	3134	29.6	3253
70	0.4	1.54	15.6	17.53	3136	16.7	
95	0.27	0.01	15.75	16.04	3134	19	
120	0	0	0	16.25	3133	15.2	3233
			COD η	0.930		0.934	
			R_{tr}	0.551		0.536	
			L_{vtr}	2071		2081	
No. 2-250-15		S_0 =	232	mg/L	$\theta_{xob}\varphi$ =	10	d
				Model Predicted		**Experimental**	
Cycle time	S_1	S_2	S_3	S	VSS	S	VSS
min	mg/L	mg/L	mg/L	mg/L	mg/L	mg/L	mg/L
0	0.19	0	14.08	14.27	10263	21.3	10502
10	2.33	9.23	13.84	25.4	7714	25.8	
40	2.36	9.21	13.74	25.31	4440	28.5	
60	2.35	9.17	13.71	25.23	3470	28.9	3725
70	0.27	1.11	13.89	15.27	3472	19	
95	0.19	0.01	13.99	14.18	3469	16.2	
120	0	0	0	14.5	3467	19	3665
			COD η	0.938		0.918	
			R_{tr}	0.502		0.465	
			L_{vtr}	2088		2045	

No. 3-500-5		S_0 =	528	mg/L	$\theta_x \varphi$ =	4.42	d
				Model predicted		**Experimental**	
Cycle time	S_1	S_2	S_3	S	VSS	S	VSS
min	mg/L	mg/L	mg/L	mg/L	mg/L	mg/L	mg/L
0	0.41	0	37.15	37.56	4835	42	5189
10	3.52	12.78	36.56	52.86	4363	52	
25	3.56	13.71	36.43	53.7	3815	47	4203
45	3.53	13.64	36.34	53.51	3273	57	
75	3.5	13.49	36.25	53.24	2707	58	
115	3.46	13.3	36.17	52.93	2210	56	2205
180	3.39	13	36.09	52.48	1716	51	1948
215	0.42	0.34	36.73	37.49	1719	47	2043
245	0.41	0.01	36.88	37.3	1718	44	
300	0.41	0	37.14	37.55	1716	44	2020
			COD η	0.929		0.917	
			R_{tr}	1.830		1.533	
			L_{vtr}	3622		3574	
No. 3-500-5		S_0 =	528	mg/L	$\theta_x \varphi$ =	8.08	d
				Model predicted		**Experimental**	
Cycle time	S_1	S_2	S_3	S	VSS	S	VSS
min	mg/L	mg/L	mg/L	mg/L	mg/L	mg/L	mg/L
0	0.22	0	29.73	29.95	8662	35	8621
10	1.96	7.42	29.51	38.89	7808	39	
25	1.98	7.46	29.42	38.86	6809	39.5	6958
45	1.97	7.43	29.35	38.75	5823	41	
75	1.96	7.39	29.27	38.62	4791	42	
115	1.95	7.34	29.2	38.48	3885	41	4008
180	1.93	7.25	29.13	38.3	2986	40.2	3285
195	0.25	0.47	29.32	30.04	2987	34	
215	0.22	0.01	29.41	29.64	2985	31	3192
245	0.22	0	29.52	29.74	2983	29	
300	0.22	0	29.72	29.94	2978	32	3214
			COD η	0.943		0.939	
			R_{tr}	1.070		0.988	
			L_{vtr}	3678		3663	

No. 5-500-5		$\theta_x\varphi$ =	3.33	d	S_0 =	434	479	mg/L	
				Model predicted		**Experimental results**			
Cycle time	S_1	S_2	S_3	S	VSS	S	S	VSS	VSS
min	mg/L	mg/L	mg/L	mg/L	mg/L	mg/L	mg/L	mg/L	mg/L
0	0.49	0.24	39.99	40.71	4384	32.4	33.4	4595	4665
15	3.96	14.83	39.22	58.02	3776	44.2	49.5	3913	4010
40	3.94	15.17	39.15	58.26	3081	49.1	56.8		
65	3.91	15.02	39.11	58.04	2610	49.1	55.3		
90	3.88	14.87	39.09	57.84	2269	49.7	53.7	2365	2360
105	0.62	1.95	39.8	42.38	2273	35.7	42.2		
120	0	0	0	40.71	2273	33.4	32.4	2336	2348
			COD η	0.837		0.923	0.932		
			R_{tr}	1.080		1.029	1.141		
			L_{vtr}	3070		3124	3132		
No. 5-500-10		$\theta_x\varphi$ =	6.67	d	S_0 =	434	479	mg/L	
				Model predicted		**Experimental results**			
Cycle time	S_1	S_2	S_3	S	VSS	S	S	VSS	VSS
min	mg/L	mg/L	mg/L	mg/L	mg/L	mg/L	mg/L	mg/L	mg/L
0	0.27	0.01	31.02	31.3	7512	29.7	31.2	7567	8198
15	2.3	8.65	30.79	41.74	6458	39.8	42.3	7250	7485
40	2.29	8.63	30.79	41.7	5246	40.7	47.7		
65	2.28	8.58	30.79	41.64	4424	38.3	45.3		
90	2.26	8.53	30.79	41.58	3831	42.9	44.1	3800	4153
105	0.28	0.25	31.09	31.62	3832	32.4	33.2		
120	0	0	0	31.4	3831	29.7	33.2	3796	4060
			COD η	0.874		0.932	0.931		
			R_{tr}	0.656		0.639	0.659		
			L_{vtr}	3139		3152	3126		
No. 5-500-15		$\theta_x\varphi$ =	10	d	S_0 =	434	479	mg/L	
				Model predicted		**Experimental results**			
Cycle time	S_1	S_2	S_3	S	VSS	S	S	VSS	VSS
min	mg/L	mg/L	mg/L	mg/L	mg/L	mg/L	mg/L	mg/L	mg/L
0	0.19	0	28.03	28.22	10120	23.5	29.7	10145	10287
15	1.68	6.36	27.88	35.93	8693	34.6	31.5	9593	10014
40	1.68	6.34	27.83	35.85	7049	33.3	36		
65	1.68	6.31	27.8	35.79	5936	34.2	32.4		
90	1.67	6.29	27.77	35.73	5131	38.7	36	5500	5695
105	0.19	0.06	27.96	28.21	5131	31.5	31.5		
120	0	0	0	28.22	5130	22.5	29.6	5502	5688
			COD η	0.887		0.948	0.938		
			R_{tr}	0.493		0.449	0.474		
			L_{vtr}	3163		3205	3152		

No. 5-250-5		$\theta_{xob}\varphi$ =	3.33	d	S_0 =	261	241	mg/L	
				Model predicted		**Experimental results**			
Cycle time	S_1	S_2	S_3	S	VSS	S	S	VSS	VSS
min	mg/L	mg/L	mg/L	mg/L	mg/L	mg/L	mg/L	mg/L	mg/L
0	0.58	1.41	19.92	21.91	2388	30.6	32.9	2108	2494
15	3.46	11.72	19.38	34.56	2057	31.5	31.2	1873	2205
40	3.56	13.2	19.29	36.06	1680	33.3	34.6	1485	1830
65	3.53	13.16	19.27	35.97	1425	34.2	29.5		
90	3.5	13.04	19.26	35.8	1241	36	29.5	1190	1345
105	1.02	4.36	19.74	25.11	1243	29.7	29.3		
120	0	0	0	22	1244	30	32.9	1146	1331
			COD η	0.912		0.885	0.863		
			R_{tr}	1.100		1.209	0.938		
			L_{vtr}	1691		1632	1611		
No. 5-250-10		$\theta_x\varphi$ =	6.67	d	S_0 =	261	241	mg/L	
				Model predicted		**Experimental results**			
Cycle time	S_1	S_2	S_3	S	VSS	S	S	VSS	VSS
min	mg/L	mg/L	mg/L	mg/L	mg/L	mg/L	mg/L	mg/L	mg/L
0	0.27	0.05	16.1	16.42	5156	21.2	17.1	3889	5287
15	1.72	6.07	15.88	23.67	4430	23.6	20.7	3457	4395
40	1.72	6.12	15.8	23.64	3596	22.8	21.6	2995	3416
65	1.71	6.09	15.75	23.55	3031	22.8	20.7		
90	1.71	6.06	15.71	23.48	2623	21.1	20.7	2229	2560
105	0.31	0.55	15.92	16.77	2624	21.1	18.9		
120	0	0	0	16.42	2623	21.1	17.1	2252	2459
			COD η	0.934		0.919	0.929		
			R_{tr}	0.534		0.639	0.546		
			L_{vtr}	1732		1698	1727		
No. 5-250-15		$\theta_x\varphi$ =	10	d	S_0 =	261	241	mg/L	
				Model predicted		**Experimental results**			
Cycle time	S_1	S_2	S_3	S	VSS	S	S	VSS	VSS
min	mg/L	mg/L	mg/L	mg/L	mg/L	mg/L	mg/L	mg/L	mg/L
0	0.19	0.02	14.11	14.32	6038	18.2	18.21	5876	5684
15	1.43	5.2	13.99	20.62	5186	21.6	25.8	5345	5230
40	1.43	5.21	13.96	20.6	4206	23.7	25.8	4407	4058
65	1.42	5.19	13.94	20.55	3542	23.7	23.1		
90	1.42	5.17	13.93	20.51	3063	25.5	22.2	3078	2878
105	0.21	0.31	14.06	14.57	3063	20.7	16.3		
120	0	0	0	14.34	3062	18.8	15.2	3054	2869
			COD η	0.943		0.928	0.937		
			R_{tr}	0.462		0.476	0.472		
			L_{vtr}	1748		1715	1741		

No. 6-250-5		$\theta_x\varphi$ =	3.33	d	S_0 =	265	mg/L
				Model predicted		**Experimental**	
Cycle time	S_1	S_2	S_3	S	VSS	S	VSS
min	mg/L	mg/L	mg/L	mg/L	mg/L	mg/L	mg/L
0	0.49	0.19	20.2	20.87	2464	19.1	2332
10	4.45	14.45	19.42	38.32	2122	35.6	
20	4.87	17.89	19.22	41.99	1868	39.8	
30	4.92	18.83	19.15	42.9	1671	35.6	1883
40	4.9	19.07	19.11	43.09	1513	43	
50	4.88	19.09	19.09	43.06	1385	45.1	
60	4.86	19.03	19.08	42.96	1277	52	1365
70	1.83	9.21	19.61	30.64	1281	38.2	
80	0.89	4.27	19.86	25.02	1282	35.2	
90	0.6	1.95	20	22.56	1283	26	
105	0.5	0.6	20.12	21.22	1283	26	
120	0	0	0	20.8	1282	19.1	1403
			COD η	0.922		0.928	
			R_{tr}	1.143		1.052	
			L_{vtr}	1675		1686	
No. 6-250-10		$\theta_x\varphi$ =	6.67	d	S_0 =	265	mg/L
				Model predicted		**Experimental**	
Cycle time	S_1	S_2	S_3	S	VSS	S	VSS
min	mg/L	mg/L	mg/L	mg/L	mg/L	mg/L	mg/L
0	0.27	0	15.86	16.14	4558	20.1	4208
10	2.68	9.64	15.54	27.86	3918	29.3	
20	2.72	10.36	15.48	28.56	3440	29.3	
30	2.71	10.41	15.45	28.57	3068	32.1	2882
40	2.7	10.38	15.42	28.51	2771	26.1	
50	2.7	10.35	15.4	28.44	2528	25.4	
60	2.69	10.32	15.38	28.38	2325	25.4	2067
70	0.54	2.55	15.62	18.72	2327	23	
80	0.3	0.61	15.7	16.61	2327	18.5	
90	0.28	0.14	15.75	16.17	2327	18.5	
105	0.27	0.02	15.81	16.1	2326	18.5	
120	0	0	0	16.2	2325	19.5	2194
			COD η	0.939		0.926	
			R_{tr}	0.642		0.671	
			L_{vtr}	1706		1683	

No. 6-250-15		$\theta_x\varphi$ =	10	d	S_0 =	265	mg/L
				Model predicted		**Experimental**	
Cycle time	S_1	S_2	S_3	S	VSS	S	VSS
min	mg/L	mg/L	mg/L	mg/L	mg/L	mg/L	mg/L
0	0.19	0	14.18	14.37	6288	16.5	5891
10	1.96	7.33	14	23.29	5401	25.9	
20	1.97	7.53	13.95	23.46	4737	23.2	
30	1.97	7.52	13.92	23.41	4221	26.4	3919
40	1.96	7.51	13.9	23.37	3808	28	
50	1.96	7.49	13.88	23.32	3471	25.1	
60	1.95	7.47	13.86	23.29	3189	25.1	2955
70	0.28	1.07	14.01	15.35	3190	19.1	
80	0.19	0.15	14.05	14.4	3190	16.5	
90	0.19	0.02	14.09	14.3	3189	14.5	
105	0.19	0	14.14	14.33	3187	16.5	
120	0	0	0	14.5	3186	17	3023
			COD η	0.945		0.936	
			R_{tr}	0.472		0.492	
			L_{vtr}	1718		1701	
No. 6-500-5		$\theta_x\varphi$ =	3.33	d	S_0 =	405	mg/L
				Model predicted		**Experimental**	
Cycle time	S_1	S_2	S_3	S	VSS	S	VSS
min	mg/L	mg/L	mg/L	mg/L	mg/L	mg/L	mg/L
0	0.48	0.01	37.39	37.89	3999	37	3756
10	5.64	20.76	36.28	62.69	3443	56.6	
20	5.8	23.31	36.14	65.25	3031	61.3	
30	5.78	23.6	36.1	65.48	2711	65.9	
40	5.75	23.54	36.09	65.37	2455	56.8	
50	5.72	23.41	36.08	65.2	2246	60.6	
60	5.69	23.27	36.07	65.03	2071	60.6	1831
70	1.25	7.1	36.91	45.27	2076	46.6	
80	0.59	2.01	37.19	39.79	2078	44.7	
90	0.5	0.56	37.32	38.38	2078	40.1	
105	0.49	0.08	37.45	38.01	2077	34.5	
120	0	0	0	38.05	2076	37.3	1700
			COD η	0.906		0.908	
			R_{tr}	1.061		1.298	
			L_{vtr}	2516		2521	

No. 6-500-10		$\theta_x\varphi$ =	6.67	d	S_0 =	405	mg/L
				Model predicted		**Experimental**	
Cycle time	S_1	S_2	S_3	S	VSS	S	VSS
min	mg/L	mg/L	mg/L	mg/L	mg/L	mg/L	mg/L
0	0.27	0	29.37	29.64	7124	33.2	6568
10	3.24	12.64	28.93	44.81	6124	46.5	
20	3.25	12.89	28.86	44.99	5377	38.9	
30	3.24	12.85	28.81	44.9	4796	45.8	
40	3.23	12.81	28.76	44.8	4331	55	
50	3.22	12.77	28.73	44.71	3951	48.1	
60	3.21	12.72	28.7	44.63	3634	46.5	3009
70	0.37	1.42	29.05	30.84	3637	35.3	
80	0.28	0.15	29.13	29.56	3637	34.4	
90	0.27	0.02	29.19	29.48	3636	32.4	
105	0.27	0	29.28	29.55	3634	30.5	
120	0	0	0	29.8	3633	33.2	2799
			COD η	0.926		0.918	
			R_{tr}	0.620		0.797	
			L_{vtr}	2573		2549	
No. 6-500-15		$\theta_x\varphi$ =	10	d	S_0 =	405	mg/L
				Model predicted		**Experimental**	
Cycle time	S_1	S_2	S_3	S	VSS	S	VSS
min	mg/L	mg/L	mg/L	mg/L	mg/L	mg/L	mg/L
0	0.19	0	26.22	26.41	9827	29	9396
10	2.31	9.19	25.97	37.47	8441	38.1	
20	2.34	9.22	25.91	37.46	7404	33.8	
30	2.34	9.19	25.86	37.39	6598	35.2	
40	2.33	9.17	25.82	37.32	5952	33.8	
50	2.33	9.15	25.79	37.26	5424	36.8	
60	2.32	9.13	25.76	37.21	4984	35.6	4562
70	0.21	0.44	25.96	26.61	4986	28.4	
80	0.19	0.02	26.02	26.23	4984	29.1	
90	0.19	0	26.07	26.26	4983	23.7	
105	0.19	0	26.14	26.33	4981	29.1	
120	0	0	0	26.4	4979	29.1	4495
			COD η	0.935		0.928	
			R_{tr}	0.456		0.502	
			L_{vtr}	2596		2578	

No. 7-250-5		$\theta_{xob}\varphi$ =	4.17	d	S_0 =	253	241	mg/L	
				Model predicted		Experimental results			
Cycle time	S_1	S_2	S_3	S	VSS	S	S	VSS	VSS
min	mg/L	mg/L	mg/L	mg/L	mg/L	mg/L	mg/L	mg/L	mg/L
0	0.41	0.02	18.72	19.14	1530	24.3	20.5	1409	1467
30	2.79	9.59	18.26	30.65	1322	29.2	33.6		
60	2.81	10.24	18.19	31.23	1169	28.5	31.8		
105	2.78	10.17	18.13	31.08	1000	36.1	33.8	815	852
180	2.72	9.93	18.07	30.72	812	32.4	25.9	724	732
210	0.64	2.3	18.43	21.38	814	23.5	22.8		
255	0.41	0.24	18.6	19.26	813	21.1	25		
300	0.41	0.03	18.71	19.14	813	21.1	19	709	720
			COD η	0.924		0.917	0.925		
			R_{tr}	0.676		0.785	0.740		
			L_{vtr}	1287		1276	1288		
No. 7-250-10		$\theta_{xob}\varphi$ =	8.33	d	S_0 =	253	241	mg/L	
				Model predicted		Experimental results			
Cycle time	S_1	S_2	S_3	S	VSS	S	S	VSS	VSS
min	mg/L	mg/L	mg/L	mg/L	mg/L	mg/L	mg/L	mg/L	mg/L
0	0.22	0	15.01	15.23	2632	18.3	20.1	2563	2530
30	1.64	5.93	14.82	22.39	2267	25	21.5		
60	1.64	5.96	14.78	22.38	1995	21.4	26		
105	1.62	5.92	14.73	22.27	1695	24.2	23.5	1615	1697
150	1.61	5.87	14.7	22.18	1476	19.8	24.6		
180	1.61	5.83	14.68	22.12	1361	23.1	25.3	1189	1190
210	0.25	0.48	14.84	15.57	1361	17.9	14.1		
255	0.22	0.01	14.93	15.16	1360	15.9	16		
300	0.22	0	15	15.23	1358	18.5	19.2	1203	1088
			COD η	0.940		0.927	0.924		
			R_{tr}	0.409		0.468	0.489		
			L_{vtr}	1309		1290	1286		
No. 7-250-15		$\theta_{xob}\varphi$ =	12.50	d	S_0 =	253	241	mg/L	
				Model predicted		Experimental results			
Cycle time	S_1	S_2	S_3	S	VSS	S	S	VSS	VSS
min	mg/L	mg/L	mg/L	mg/L	mg/L	mg/L	mg/L	mg/L	mg/L
0	0.15	0	13.46	13.61	3600	16	17.1	3410	3502
30	1.2	4.36	13.37	18.92	3097	19.2	20.1		
60	1.19	4.35	13.34	18.89	2720	21.5	22.5		
105	1.19	4.33	13.32	18.83	2304	16.8	20.1	2119	2257
150	1.18	4.3	13.3	18.79	2002	20.8	20.1		
180	1.18	4.29	13.3	18.76	1842	21.2	22.3	1654	1782
210	0.16	0.14	13.4	13.7	1842	18.3	15.8		
255	0.15	0	13.46	13.62	1839	16.2	14.2		
300	0.15	0	13.53	13.68	1837	15.3	17.1	1626	1703
			COD η	0.946		0.940	0.932		
			R_{tr}	0.307		0.351	0.316		
			L_{vtr}	1318		1308	1298		

No. 7-500-5		$\theta_{xob}\varphi$ =	4.17	d	S_0 =	499	540	mg/L	
				Model predicted		Experimental results			
Cycle time	S_1	S_2	S_3	S	VSS	S	S	VSS	VSS
min	mg/L	mg/L	mg/L	mg/L	mg/L	mg/L	mg/L	mg/L	mg/L
0	0.41	0	37.17	37.57	2474	37.7	40.5	2543	2556
30	3.48	13.15	36.52	53.15	2140	54.2	57.8	2228	2242
60	3.45	13.27	36.43	53.15	1892	57.8	57.8		
105	3.4	13.07	36.34	52.81	1618	49.8	50.6	1685	1740
150	3.36	12.86	36.28	52.5	1419	49	49.8		
180	3.33	12.73	36.25	52.31	1314	49.7	48.2	1333	1403
210	0.48	1.18	36.79	38.45	1317	40.1	41.4		
255	0.41	0.03	36.99	37.43	1316	38.5	40.1	1293	1388
300	0.41	0	37.16	37.56	1315	37.7	36.5	1295	1388
			COD η	0.925		0.924	0.927		
			R_{tr}	0.844		0.855	0.871		
			L_{vtr}	2722		2721	2728		
No. 7-500-10		$\theta_{xob}\varphi$ =	8.33	d	S_0 =	499	540	mg/L	
				Model predicted		**Experimental results**			
Cycle time	S_1	S_2	S_3	S	VSS	S	S	VSS	VSS
min	mg/L	mg/L	mg/L	mg/L	mg/L	mg/L	mg/L	mg/L	mg/L
0	0.22	0	29.72	29.94	4317	34.5	33.5	4284	4330
30	1.98	7.48	29.47	38.93	3720	47	43.8	3663	3736
60	1.97	7.44	29.4	38.81	3273	41	48.2		
105	1.96	7.38	29.32	38.65	2780	44.1	46	2678	2797
150	1.94	7.32	29.26	38.52	2421	44.2	41.7		
180	1.93	7.27	29.23	38.44	2232	44.1	40.9	2180	2223
210	0.23	0.12	29.46	29.81	2232	36.9	40.1		
255	0.22	0	29.59	29.81	2230	36.9	33.7	2163	2235
300	0.22	0	29.71	29.94	2227	34.5	38.5	2120	2280
			COD η	0.940		0.931	0.923		
			R_{tr}	0.502		0.526	0.528		
			L_{vtr}	2765		2739	2716		
No. 7-500-15		$\theta_{xob}\varphi$ =	12.50	d	S_0 =	499	540	mg/L	
				Model predicted		**Experimental results**			
Cycle time	S_1	S_2	S_3	S	VSS	S	S	VSS	VSS
min	mg/L	mg/L	mg/L	mg/L	mg/L	mg/L	mg/L	mg/L	mg/L
0	0.15	0	26.9	27.06	5765	32.9	26.9	5865	5830
30	1.47	5.55	26.74	33.76	4960	35.8	35.8	5055	5000
60	1.46	5.53	26.68	33.67	4357	36.6	38.2		
105	1.45	5.5	26.61	33.57	3692	33.7	40.1	3785	3781
150	1.45	5.46	26.57	33.48	3207	29.7	35.3		
180	1.44	5.44	26.54	33.43	2952	28.1	36.9	3076	3090
210	0.16	0.02	26.69	26.87	2951	25.3	26.9		
255	0.15	0	26.79	26.95	2947	25.7	31.7	3094	3058
300	0.15	0	26.9	27.05	2943	29.9	36.9	3110	3071
			COD η	0.946		0.940	0.926		
			R_{tr}	0.383		0.362	0.393		
			L_{vtr}	2781		2765	2725		

No. 8-250-5		$\theta_{xob}\varphi$ =	4.17	d	S_0 =	238	mg/L
				Model predicted		Experimental	
Cycle time	S_1	S_2	S_3	S	VSS	S	VSS
min	mg/L	mg/L	mg/L	mg/L	mg/L	mg/L	mg/L
0	0.41	0	18.87	19.28	1521	21.5	1358
30	3.96	14.31	18.14	36.41	1233	33.5	
60	3.99	15.33	18.01	37.33	1043	39.6	865
90	3.94	15.27	17.95	37.16	908	38.2	
120	3.89	15.08	17.91	36.87	807	38.2	657
135	1.54	7.49	18.25	27.27	809	30.5	
180	0.44	0.81	18.58	19.83	811	23.8	
240	0.41	0.04	18.73	19.18	810	22.8	
300	0.41	0	18.87	19.28	808	23	672
			COD η	0.919		0.903	
			R_{tr}	0.638		0.768	
			L_{vtr}	1167		1147	

No. 8-250-10		$\theta_{xob}\varphi$ =	8.33	d	S_0 =	238	mg/L
				Model predicted		Experimental	
Cycle time	S_1	S_2	S_3	S	VSS	S	VSS
min	mg/L	mg/L	mg/L	mg/L	mg/L	mg/L	mg/L
0	0.22	0	15.1	15.32	2729	18.4	2324
30	2.27	8.59	14.79	25.65	2200	24.6	
60	2.25	8.62	14.71	25.58	1849	24.6	1455
90	2.24	8.55	14.65	25.44	1598	28.1	
120	2.22	8.48	14.61	25.31	1410	24.6	1018
135	0.5	2.37	14.76	17.63	1412	18	
180	0.22	0.05	14.89	15.16	1411	22.1	
240	0.22	0	14.99	15.22	1408	15.6	
300	0.22	0	15.1	15.32	1406	18.6	1020
			COD η	0.936		0.922	
			R_{tr}	0.375		0.516	
			L_{vtr}	1188		1170	

No. 8-250-15		$\theta_{xob}\varphi$ =	12.5	d	S_0 =	238	mg/L
				Model predicted		Experimental	
Cycle time	S_1	S_2	S_3	S	VSS	S	VSS
min	mg/L	mg/L	mg/L	mg/L	mg/L	mg/L	mg/L
0	0.15	0	13.65	13.8	3647	19	3346
30	1.69	6.46	13.45	21.6	2934	22.8	
60	1.68	6.44	13.38	21.5	2461	25.2	2151
90	1.67	6.4	13.33	21.4	2122	19	
120	1.66	6.36	13.29	21.32	1868	19.5	1580
135	0.26	1.15	13.39	14.8	1869	16.6	
180	0.15	0.01	13.47	13.63	1867	15.3	
240	0.15	0	13.56	13.71	1864	15.6	
300	0.15	0	13.64	13.8	1860	15.6	1615
			COD η	0.942		0.934	
			R_{tr}	0.287		0.331	
			L_{vtr}	1196		1186	

No. 8-500-5		$\theta_{xob}\varphi$ =	4.17	d	S_0 =	461	405	mg/L	
				Model predicted		Experimental results			
Cycle time	S_1	S_2	S_3	S	VSS	S	S	VSS	VSS
min	mg/L	mg/L	mg/L	mg/L	mg/L	mg/L	mg/L	mg/L	mg/L
0	0.41	0	37.62	38.02	2463	46	43.2	2304	2229
15	4.88	17.71	36.74	59.33	2202	55.6	50		
30	5.04	20.11	36.55	61.7	1997	54.8	58.4		
60	4.98	20.3	36.39	61.67	1691	64.6	62.4	1530	1476
120	4.84	19.69	36.22	60.75	1308	63.8	60.8	1153	1108
135	1.12	6.32	36.81	44.25	1313	48.6			
150	0.52	1.9	37.01	39.43	1314	44.6	37.6		
180	0.41	0.17	37.17	37.75	1313	44.4	36.8		
240	0.41	0	37.39	37.8	1311	43.7	37.7	1145	1054
300	0.41	0	37.61	38.01	1309	45	43.2	1142	1049
			COD η	0.918		0.902	0.906		
			R_{tr}	0.715		0.874	0.828		
			L_{vtr}	2231		2191	2201		
No. 8-500-10		$\theta_{xob}\varphi$ =	8.33	d	S_0 =	461	405	mg/L	
				Model predicted		Experimental results			
Cycle time	S_1	S_2	S_3	S	VSS	S	S	VSS	VSS
min	mg/L	mg/L	mg/L	mg/L	mg/L	mg/L	mg/L	mg/L	mg/L
0	0.22	0	29.91	30.13	4417	37.2	30.4	4242	3996
15	2.8	10.86	29.56	43.22	3940	44.5	39.2		
30	2.8	11.1	29.47	43.37	3561	48.8	41.6		
60	2.78	11.02	29.33	43.13	2994	40.4	45.2	2866	2601
120	2.73	10.83	29.17	42.73	2284	39.2	40.6	2168	1905
135	0.32	1.36	29.41	31.09	2286	35.2			
150	0.23	0.16	29.47	29.86	2286	32	32.8		
185	0.22	0	29.58	29.8	2284	28.4	31.2		
240	0.22	0	29.73	29.95	2280	34	30.4		
300	0.22	0	29.9	30.12	2276	37.2	30.4	2160	1867
			COD η	0.935		0.919	0.934		
			R_{tr}	0.419		0.471	0.482		
			L_{vtr}	2275		2235	2274		
No. 8-500-15		$\theta_{xob}\varphi$ =	8.33	d	S_0 =	461	405	mg/L	
				Model predicted		Experimental results			
Cycle time	S_1	S_2	S_3	S	VSS	S	S	VSS	VSS
min	mg/L	mg/L	mg/L	mg/L	mg/L	mg/L	mg/L	mg/L	mg/L
0	0.15	0	27.01	27.17	5902	32	24	5603	5192
15	2.08	8.18	26.8	37.06	5260	32.8	36		
30	2.08	8.21	26.72	37.02	4749	43.8	33.6		
60	2.07	8.16	26.61	36.84	3983	37.2	35.6	3701	3388
90	2.05	8.11	26.53	36.7	3435		36.8		
120	2.04	8.06	26.47	36.57	3024	37.2	36	2725	2480
135	0.18	0.5	26.61	27.29	3026	32.6			
150	0.16	0.03	26.65	26.84	3024	29.8	26.4		
180	0.15	0	26.72	26.88	3022	28.6	26.4		
240	0.15	0	26.87	27.02	3016	30.4	24.8		
300	0.15	0	27.01	27.16	3011	32	26.4	2720	2356
			COD η	0.941		0.931	0.943		
			R_{tr}	0.321		0.379	0.386		
			L_{vtr}	2292		2264	2296		

APPENDIX D RESULTS OF AMINO ACID ANALYSIS

Analytical Results of Amino-acids

			Dissolving											
		20 g protein	80 g in 200L											
		containing	water as feed	Tested feed		Batch 3.5 h		Batch 7 h		Batch 12 h		Batch 24 h		
Protein	MW	mg	mg/L	*μmol/L*	mg/L	*μmol/L*	mg/L	*μmol/L*	mg/L	*μmol/L*	mg/L	*μmol/L*	mg/L	
Glutamic acid	147	3405	68.0	*631*	**80.4**	*8.09*	**3.2**							
Aspartic acid	133	2059	41.1	*416*	**47.9**			*1.5*	**0.5**	*1.1*	**0.5**	*3.1*	**0.9**	
Leucine	131	1470	29.4	*308*	**35.0**	*12.35*	**4.4**							
Arginie	174	1347	26.9	*202*	**30.5**									
Lysine	146	1128	22.5	*211*	**26.7**	*7.42*	**2.9**							
Serine	105	932	18.6	*232*	**21.1**	*51.19*	**14.6**	*5.2*	**1.3**	*3.5*	**1.2**	*3.9*	**0.9**	
Phenylalanine	165	929	18.6	*153*	**21.9**									
Proline	115	919	18.4	*217*	**21.6**									
Valine	117	901	18.0	*206*	**20.9**	*8.54*	**2.7**							
Isoleucine	131	878	17.5	*184*	**20.9**	*8.2*	**2.9**							
Alanine	89	768	15.3	*239*	**18.4**	*22.82*	**5.5**	*3.0*	**0.6**					
Tyrosine *(Norleucine Std)*	181	683	13.6	*4617*	*N/A*	*980*		1138		*798.3*		*1221.2*		
Threonine	119	682	13.6	*168*	**17.3**	*15.77*	**5.1**			*1.5*	**0.9**			
Glycine	75	745	14.9	*272*	**17.7**	*38.96*	**8.0**	*9.8*	**1.7**	*2.6*	**1.0**	*6.8*	**1.1**	
Histidine	155	465	9.3	*78*	**10.5**	*11.49*	**4.8**							
Methionine	149	239	4.8	*15*	**1.9**									
Cysteine	121	233	4.7	*5*	**0.5**			*1.9*	**0.5**	*2.3*	**0.9**	*3.6*	**1.0**	
Tryptophan	204	233	4.7	*missing*	**0**									
Total Aminoacid		**18016**	**360.0**		**393.1**		**54.3**		**4.6**		**4.5**		**3.9**	

$$\text{Aminoacid Concentration (mg / L)} = \left[\frac{\text{Tested } (\mu\,\text{mol / L})}{\text{Standard}} \times \text{Molar Weight}\right] \times \text{(Dilution Times)}$$

Dilution time is 4 (5 mL sample into 20 mL) for the feed and 2.67 (75 mL sample into 200 mL) for the other samples.

APPENDIX D RESULTS OF AMINO ACID ANALYSIS

Analytical Results of Amino-acids (cont.')

	Batch blnk 0 h		Batch blnk 7 h		Batch blnk 24 h		SBR2 Eff.		CFSTR1 Eff.		CFSTR2 Eff.		CFSTR3 Eff.	
Protein	*µmol/L*	mg/L	*µmol/L*	mg/L	*µmol/L*	mg/L	*µmol/L*	mg/L	*µmol/L*	mg/L	*µmol/L*	mg/L	*µmol/L*	mg/L
Glutamic acid														
Aspartic acid	*0.9*	**0.3**	*1.1*	**0.3**	*2.3*	**0.7**	*3*	**0.4**	*3.5*	**1.0**	*3.5*	**1.1**	*2.7*	**0.8**
Leucine														
Arginie														
Lysine														
Serine	*3.9*	**1.0**	*1.7*	**0.4**	*5.3*	**1.3**	*5*	**0.5**	*5.7*	**1.3**	*5.7*	**1.4**	*4.4*	**1.1**
Phenylalanine														
Proline														
Valine			*4.2*	**1.0**	*0.4*	**0.1**								
Isoleucine														
Alanine														
Tyrosine *(Norleucine Std)*	*1097*		*1306.1*		*1112.4*		*4486*		*1210*		*1107.6*		*1152.1*	
Threonine											*2.7*	**0.8**		
Glycine	*3.2*	**0.6**			*2.6*	**0.5**	*9*	**0.6**	*7.2*	**1.2**	*8.1*	**1.5**	*1.3*	**0.2**
Histidine														
Methionine														
Cysteine	*1.8*	**0.5**	*1.8*	**0.4**	*1.7*	**0.5**	*3*	**0.3**	*3.4*	**0.9**	*3.2*	**0.9**	*3.2*	**0.9**
Tryptophan														
Total Aminoacid		**2.4**		**2.1**		**3.1**		**1.7**		**4.4**		**5.7**		**3.0**

Analytical Results of Amino-acids (cont.')

	SG batch 0 h		SG batch 3.5 h		SG batch 8 h		SG batch 24 h		SG-blnk 0 h		SG-blnk 3.5 h		SG-blnk 8 h		SG-blnk 24 h	
Protein	*µmol/L*	mg/L	*µmol/L*	mg/L	*µmol/L*	mg/L	*µmol/L*	mg/L	*µmol/L*	mg/L	*µmol/L*	mg/L	*µmol/L*	mg/L	*µmol/L*	mg/L
Glutamic acid																
Aspartic acid			*3.2*	**1.0**			*3.4*	**1.0**					*3.9*	**1.2**	*3.4*	**1.0**
Leucine							*5.3*	**1.6**					*1.1*	**0.3**	*17.4*	**5.2**
Arginie																
Lysine																
Serine			*4.8*	**1.2**	*6.3*	**1.5**	*5.3*	**1.3**			*5.5*	**1.3**	*9.1*	**2.2**	*4.6*	**1.1**
Phenylalanine																
Proline																
Valine					*6.3*	**1.6**	*13.3*	**3.6**					*8.3*	**2.2**	*24*	**6.4**
Isoleucine					*5*	**1.4**	*9.4*	**2.9**					*6.2*	**1.9**	*19.8*	**5.9**
Alanine													*9.1*	**1.9**		
Tyrosine *(Norleucine Std)*	*1028*		*1127.4*		*1212.5*		*1150*		*1165*		*1183.2*		*1155.4*		*1176.8*	
Threonine					*3*	**0.8**	*3.5*	**1.0**					*3.5*	**1.0**	*5.3*	**1.4**
Glycine			*1.1*	**0.2**	*6.3*	**1.0**					*5.8*	**1.0**	*7*	**1.2**		
Histidine																
Methionine																
Cysteine			*3.3*	**0.9**	*3.3*	**0.9**	*3.3*	**0.9**			*3.6*	**1.0**	*3.3*	**0.9**	*3.5*	**1.0**
Tryptophan																
Total Aminoacid		**0.0**		**3.3**		**7.2**		**12.3**		**0.0**		**3.3**		**12.8**		**21.9**

SG is the system using only sugar as its feed

APPENDIX E EXPERIMENTAL RESULTS OF THE CFSTR SYSTEM

CFSTR system, S_0 = 250 mg/L

CFSTR, t_{dc} = 3.5 h

	TSS (mg/L)			VSS (mg/L)			S_0	S_e (mg/L)			COD η			R (d^{-1})			L_v (mg/L^{-2}/d)		
	CFSTR1	CFSTR2	CFSTR3	CFSTR1	CFSTR2	CFSTR3	(mg/L)	CFSTR1	CFSTR2	CFSTR3	CFSTR1	CFSTR2	CFSTR3	CFSTR1	CFSTR2	CFSTR3	CFSTR1	CFSTR2	CFSTR3
	1805	2948	4620	1697	2745	4241	212	25.2	21.7	20.7	0.881	0.898	0.902	0.755	0.475	0.309	1281	1305	1312
	1902	2913	4748	1788	2712	4359	237	25.1	22.2	13.8	0.894	0.906	0.942	0.813	0.543	0.351	1453	1473	1531
	2063	3045	4409	1939	2835	4047	237	21.4	21.9	19.9	0.91	0.908	0.916	0.762	0.52	0.368	1478	1475	1489
Avg.	**1923**	**2969**	**4592**	**1808**	**2764**	**4216**	**229**	**23.9**	**21.9**	**18.1**	**0.895**	**0.904**	**0.92**	**0.777**	**0.513**	**0.343**	**1404**	**1418**	**1444**

CFSTR, t_{dc} = 5 h

	TSS (mg/L)			VSS (mg/L)			S_0	S_e (mg/L)			COD η			R (d^{-1})			L_v (mg/L^{-2}/d)		
	CFSTR1	CFSTR2	CFSTR3	CFSTR1	CFSTR2	CFSTR3	(mg/L)	CFSTR1	CFSTR2	CFSTR3	CFSTR1	CFSTR2	CFSTR3	CFSTR1	CFSTR2	CFSTR3	CFSTR1	CFSTR2	CFSTR3
	1285	2249	3008	1188	2094	2761	248	22.3	25.5	15.5	0.91	0.897	0.938	0.912	0.51	0.404	1083	1068	1116
	1328	2215	3146	1248	2062	2888	264	25.2	17.5	18.7	0.905	0.934	0.929	0.918	0.574	0.408	1146	1183	1177
	1208	2197	2891	1202	2045	2654	224	20.6	19.2	22.2	0.908	0.914	0.901	0.812	0.481	0.365	976	983	969
Avg.	**1274**	**2220**	**3015**	**1213**	**2067**	**2768**	**245**	**22.7**	**20.7**	**18.8**	**0.908**	**0.915**	**0.923**	**0.881**	**0.521**	**0.392**	**1069**	**1078**	**1087**

CFSTR, t_{dc} = 8 h

	TSS (mg/L)			VSS (mg/L)			S_0	S_e (mg/L)			COD η			R (d^{-1})			L_v (mg/L^{-2}/d)		
	CFSTR1	CFSTR2	CFSTR3	CFSTR1	CFSTR2	CFSTR3	(mg/L)	CFSTR1	CFSTR2	CFSTR3	CFSTR1	CFSTR2	CFSTR3	CFSTR1	CFSTR2	CFSTR3	CFSTR1	CFSTR2	CFSTR3
	905	1428	2224	792	1329	2042	251	23.1	22	21.3	0.908	0.912	0.915	0.863	0.517	0.338	684	687	689
	1001	1532	2156	941	1426	1979	262	24.8	19.4	18.2	0.905	0.926	0.931	0.756	0.51	0.37	712	728	731
	923	1424	2198	830	1326	2018	245	27.1	18.9	18.8	0.889	0.923	0.923	0.788	0.512	0.336	654	678	679
Avg.	**943**	**1461**	**2193**	**854**	**1361**	**2013**	**253**	**25.0**	**20.1**	**19.4**	**0.901**	**0.92**	**0.923**	**0.802**	**0.513**	**0.348**	**683**	**698**	**700**

CFSTR, t_{dc} = 11 h

	TSS (mg/L)			VSS (mg/L)			S_0	S_e (mg/L)			COD η			R (d^{-1})			L_v (mg/L^{-2}/d)		
	CFSTR1	CFSTR2	CFSTR3	CFSTR1	CFSTR2	CFSTR3	(mg/L)	CFSTR1	CFSTR2	CFSTR3	CFSTR1	CFSTR2	CFSTR3	CFSTR1	CFSTR2	CFSTR3	CFSTR1	CFSTR2	CFSTR3
	672	995	1475	619	926	1354	240	19.9	15.8	19.2	0.917	0.934	0.92	0.776	0.528	0.356	480	489	482
	728	907	1389	653	825	1275	255	18.5	20.6	21.9	0.927	0.919	0.914	0.79	0.62	0.399	516	511	509
	696	1036	1456	645	958	1337	256	23.7	23	18.1	0.907	0.91	0.929	0.786	0.531	0.388	507	508	519
Avg.	**699**	**979**	**1440**	**639**	**903**	**1322**	**250**	**20.7**	**19.8**	**19.7**	**0.917**	**0.921**	**0.921**	**0.784**	**0.56**	**0.381**	**501**	**503**	**503**

APPENDIX E EXPERIMENTAL RESULTS OF THE CFSTR SYSTEM

CFSTR system, S_0 = 250 mg/L (Cont.')

CFSTR, t_{dc} = 3.5 h

Regression Output:

$1/\theta_x$	R		
0.2	0.777	Constant	-0.04838
0.1	0.513	Std Err of Y Est	0.028355
0.066667	0.343	R Squared	0.975666
		No. of Observations	3
		Degrees of Freedom	1
k_e (d^{-1})	Y		
0.048	0.31	X Coefficient(s)	0.313408
		Std Err of Coef.	0.049496

CFSTR, t_{dc} = 5 h

Regression Output:

$1/\theta_x$	R		
0.2	0.881	Constant	-0.04787
0.1	0.521	Std Err of Y Est	0.007197
0.066667	0.392	R Squared	0.998391
		No. of Observations	3
		Degrees of Freedom	1
k_e (d^{-1})	Y		
0.048	0.29	X Coefficient(s)	0.286513
		Std Err of Coef.	0.011503

CFSTR, t_{dc} = 8 h

Regression Output:

$1/\theta_x$	R		
0.2	0.811	Constant	-0.04146
0.1	0.513	Std Err of Y Est	0.020288
0.066667	0.348	R Squared	0.986446
		No. of Observations	3
		Degrees of Freedom	1
k_e (d^{-1})	Y		
0.041	0.29	X Coefficient(s)	0.293686
		Std Err of Coef.	0.034425

CFSTR, t_{dc} = 11 h

Regression Output:

$1/\theta_x$	R		
0.2	0.784	Constant	-0.07076
0.1	0.56	Std Err of Y Est	0.044188
0.066667	0.381	R Squared	0.953789
		No. of Observations	3
		Degrees of Freedom	1
k_e (d^{-1})	Y		
0.071	0.34	X Coefficient(s)	0.335614
		Std Err of Coef.	0.073873

CFSTR system, S_0 = 500 mg/L

CFSTR, t_d = 3.5 h

	TSS (mg/L)			VSS (mg/L)			S_0	S_e (mg/L)			COD η			R (d^{-1})		
	CFSTR1	CFSTR2	CFSTR3	CFSTR1	CFSTR2	CFSTR3	(mg/L)	CFSTR1	CFSTR2	CFSTR3	CFSTR1	CFSTR2	CFSTR3	CFSTR1	CFSTR2	CFSTR3
	5035	7538	11540	4593	7050	10708	484	52	35.6	36.1	0.893	0.926	0.925	0.645	0.436	0.287
	4805	7473	11620	4388	6988	10818	487	43.6	46.9	39.5	0.910	0.904	0.919	0.693	0.432	0.284
	4628	7583	11730	4243	6983	10790	497	47.6	42.9	47.3	0.904	0.914	0.905	0.726	0.446	0.286
	4778	7668	10955	4358	7130	10125	488	55.4	54	41.3	0.886	0.889	0.915	0.681	0.417	0.303
	4650	7704	10940	4264	7235	10118	490	41.2	44.3	35.1	0.916	0.910	0.928	0.722	0.422	0.308
Avg.	**4812**	**7566**	**11461**	**4396**	**7038**	**10610**	**489**	**49.7**	**44.9**	**41.1**	**0.898**	**0.908**	**0.916**	**0.686**	**0.433**	**0.290**

CFSTR, t_d = 11 h

	TSS (mg/L)			VSS (mg/L)			S_0	S_e (mg/L)			COD η			R (d^{-1})		
	CFSTR1	CFSTR2	CFSTR3	CFSTR1	CFSTR2	CFSTR3	(mg/L)	CFSTR1	CFSTR2	CFSTR3	CFSTR1	CFSTR2	CFSTR3	CFSTR1	CFSTR2	CFSTR3
	1180	1603	2038	1040	1413	1752	444	31.2	44.8	37.8	0.930	0.899	0.915	0.866	0.616	0.506
	1330	1628	1673	1186	1453	1465	531	43	43.3	34.2	0.919	0.918	0.936	0.898	0.732	0.740
	1447	1375	1968	1259	1220	1708	436	38.9	38.9	40.7	0.911	0.911	0.907	0.688	0.710	0.505
	1373	2733	3553	1198	2525	3280	617	45.6	42.4	44	0.926	0.931	0.929	1.041	0.497	0.381
	1263	2325	4358	1073	2123	4005	460	34	36	36.5	0.926	0.922	0.921	0.866	0.436	0.231
	1460	2210	3950	1242	2015	3658	436	36.8	39.4	41.2	0.916	0.910	0.906	0.701	0.429	0.235
	1311	2652	3203	1126	2418	2980	461	64	35.2	37.8	0.861	0.924	0.918	0.769	0.384	0.310
	1389	2428	3075	1205	2262	2868	505	39.6	40.5	35.8	0.922	0.920	0.929	0.843	0.448	0.357
	1538	2270	2518	1383	2105	2350	512	38.1	29.7	36.5	0.926	0.942	0.929	0.748	0.500	0.441
Avg.	**1366**	**2136**	**2926**	**1190**	**1948**	**2674**	**489**	**41.2**	**38.9**	**38.3**	**0.915**	**0.920**	**0.921**	**0.824**	**0.528**	**0.412**

CFSTR system, S_0 = 500 mg/L (Cont.')

CFSTR, t_d = 5 h

	TSS (mg/L)			VSS (mg/L)			S_0 (mg/L)		S_e (mg/L)			COD η			R (d^{-1})		
	CFSTR1	CFSTR2	CFSTR3	CFSTR1	CFSTR2	CFSTR3	CFSTR1	2 & 3	CFSTR1	CFSTR2	CFSTR3	CFSTR1	CFSTR2	CFSTR3	CFSTR1	CFSTR2	CFSTR3
	3315	4745	6543	3065	4325	5945	472	407	47	34	37	0.900	0.916	0.909	0.666	0.414	0.299
	3363	5173	6305	3130	4718	5698		460		51	42		0.889	0.909		0.416	0.352
	3145	4848	5850	2896	4333	5265	489	408	31	40	38	0.937	0.902	0.907	0.759	0.408	0.337
	3140	5129	5568	2815	4578	4910	466	453	37	43	31	0.921	0.905	0.932	0.732	0.430	0.413
	3295	5333	5908	3039	4883	5313	469	390	40	24	20	0.915	0.938	0.949	0.678	0.360	0.334
	3412			3167			478		43			0.910			0.659		
	3460	5129	6023	3202	4578	5385	501	424	33	47	37	0.934	0.889	0.913	0.702	0.395	0.345
	3487	5269	6124	3197	4845	5553	520	429	50	38	35	0.904	0.911	0.918	0.706	0.387	0.341
	3266	5225	6026	3027	4733	5375	449	532	31	51	53	0.931	0.904	0.900	0.663	0.488	0.428
	3238	5385	5668	2984	4992	5068	524	424	51	40	40	0.903	0.906	0.906	0.761	0.369	0.364
	3396	5583	6018	3125	5118	5378		425		33	36		0.922	0.915		0.368	0.347
	3522	5408	5993	3279	4915	5369	476	490	35	29	48	0.926	0.941	0.902	0.646	0.450	0.395
	3079	5227	6428	2842	4773	5885	504	534	40	35	48	0.921	0.934	0.910	0.784	0.502	0.396
	2800	5093	6205	2635	4550	5655		479		35	38		0.927	0.921		0.468	0.374
	2695	5170		2496	4613		545	456	59	42	43	0.892	0.908	0.906	0.935	0.431	
	2730	5208	6068	2500	4735	5538		489		38	38		0.922	0.922		0.457	0.391
	2488	5025	6075	2296	4683	5540	499	485	34	24	44	0.932	0.951	0.909	0.972	0.473	0.382
	3267	5308	6445	3000	4755	5885		403		31	27		0.923	0.933		0.376	0.307
	3370	5305	5418	3108	4840	4940	480		40			0.917			0.680		
	3783	5189	7003	3486	4723	6380	510		37			0.927			0.651		
	3443	5503	7820	3178	4955	7195		430		35	50		0.919	0.884		0.383	0.254
	3248	5655	7990	2983	5185	7503	459	489	37	37	44	0.919	0.924	0.910	0.679	0.418	0.285
	2908	5288	8013	2678	4763	7343	483		36			0.925			0.801		
			7525			6943		530		48	56		0.909	0.894			0.328
		4918	7518		4535	6868		514		51	33		0.901	0.936		0.490	0.336
Avg.	**3211**	**5222**	**6458**	**2962**	**4745**	**5867**	**490**	**460**	**40.1**	**38.4**	**39.9**	**0.918**	**0.916**	**0.914**	**0.734**	**0.424**	**0.350**

CFSTR system, S_0 = 500 mg/L (Cont.')

CFSTR, t_d = 8 h

	TSS (mg/L)			VSS (mg/L)			S_0	S_e (mg/L)			COD η			R (d^{-1})		
	CFSTR1	CFSTR2	CFSTR3	CFSTR1	CFSTR2	CFSTR3	(mg/L)	CFSTR1	CFSTR2	CFSTR3	CFSTR1	CFSTR2	CFSTR3	CFSTR1	CFSTR2	CFSTR3
	1560	2358	3778	1425	2153	3428	451	41	31.2	30	0.909	0.931	0.933	0.863	0.585	0.368
	1488	2585	4033	1388	2355	3673	437	41.9	35.7	42.8	0.904	0.918	0.902	0.854	0.511	0.322
	1603	2593	4005	1443	2368	3650	433	39.1	40.1	34.8	0.910	0.907	0.920	0.819	0.498	0.327
	1598	2435	4105	1368	2240	3745	493	52	38.8	38.8	0.895	0.921	0.921	0.967	0.608	0.364
	1540	2395	3995	1318	2108	3668	470	54.3	36.1	24.9	0.884	0.923	0.947	0.946	0.618	0.364
	1581	2158	3663	1352	1968	3353	489	39.3	27.9	43.6	0.920	0.943	0.911	0.998	0.703	0.399
	1660	2380	3348	1463	2180	3050	479	48.5	30.5	44.5	0.899	0.936	0.907	0.883	0.617	0.427
	1690	2675	3613	1472	2425	3338	438	31.5	52.7	35.8	0.928	0.880	0.918	0.828	0.477	0.361
	1569	2873	3458	1358	2643	3203	462		37.6	28.2		0.919	0.939		0.482	0.406
	1525	2750	3643	1296	2540	3418	428		30.5	41.5		0.929	0.903		0.469	0.339
	1530	2498	3785	1300	2305	3298	474	37.1	49	31.3	0.922	0.897	0.934	1.008	0.553	0.403
	1563	2638	3685	1345	2423	3393	415	31.9	28.1	28.6	0.923	0.932	0.931	0.854	0.479	0.342
	1610	2825	3485	1403	2588	3255	515	32.2	43.6	35.6	0.937	0.915	0.931	1.032	0.546	0.442
	1613		3688	1458		3325	470	29		45	0.938		0.904	0.907		0.383
	1670	2560	3370	1518	2305	2995	437	38	53	35	0.913	0.879	0.920	0.789	0.500	0.403
	1938	2268	3590	1758	2120	3285	487	48	38		0.901	0.922		0.749	0.635	
	1872	2548		1625	2330		461	49	43		0.894	0.907		0.761	0.538	
	1723	2613		1576	2453		515	42.9	33.3		0.917	0.935		0.899	0.589	
	1858	2858		1688	2528		492	41.9	35.2		0.915	0.928		0.800	0.542	
	1810	2608		1653	2298		501	43	28		0.914	0.944		0.831	0.617	
	1933	2823		1730	2500		583	49	39		0.916	0.933		0.926	0.653	
Avg.	**1664**	**2572**	**3703**	**1473**	**2342**	**3380**	**473**	**41.6**	**37.6**	**36.0**	**0.913**	**0.920**	**0.921**	**0.880**	**0.561**	**0.377**

CFSTR system, S_0 = 500 mg/L (Cont.')

CFSTR, t_d = 3.5 h

L_v (mg/L^{-2}/d)				
CFSTR1	CFSTR2	CFSTR3	R	$1/\theta_x$
2962	3075	3071	0.69	0.2
3040	3018	3069	0.43	0.1
3082	3114	3084	0.29	0.0667
2966	2976	3063		
3077	3056	3119	k_e (d^{-1})	Y
3013	**3046**	**3072**	0.038	0.34

CFSTR, t_d = 11 h

L_v (mg/L^{-2}/d)				
CFSTR1	CFSTR2	CFSTR3	R	$1/\theta_x$
901	871	886	0.82	0.2
1065	1064	1084	0.53	0.1
866	866	862	0.41	0.0667
1247	1254	1250		
929	925	924	k_e (d^{-1})	Y
871	865	861	0.071	0.33
866	929	923		
1015	1013	1024		
1034	1052	1037		
977	**982**	**984**		

CFSTR, t_d = 5 h

L_v (mg/L^{-2}/d)				
CFSTR1	CFSTR2	CFSTR3	R	$1/\theta_x$
2040	1790	1776	0.73	0.2
	1963	2006	0.43	0.1
2198	1766	1776	0.35	0.0667
2059	1968	2026		
2059	1757	1776	k_e (d^{-1})	Y
2088			0.049	0.34
2246	1810	1858		
2256	1877	1891		
2006	2309	2299		
2270	1843	1843		
	1882	1867		
2117	2213	2122		
2227	2395	2333		
	2131	2117		
2333	1987	1982		
	2165	2165		
2232	2213	2117		
	1786	1805		
2112				
2270				
	1896	1824		
2026	2170	2136		
2146				
	2314	2275		
	2222	2309		
2158	**2022**	**2014**		

CFSTR, t_d = 8 h

L_v (mg/L^{-2}/d)				
CFSTR1	CFSTR2	CFSTR3	R	$1/\theta_x$
1230	1259	1263	0.88	0.2
1185	1204	1183	0.56	0.1
1182	1179	1195	0.38	0.0667
1323	1363	1363		
1247	1302	1335	k_e (d^{-1})	Y
1349	1383	1336	0.042	0.27
1292	1346	1304		
1220	1156	1207		
	1273	1301		
	1193	1160		
1311	1275	1328		
1149	1161	1159		
1448	1414	1438		
1323		1275		
1197	1152	1206		
1317	1347			
1236	1254			
1416	1445			
1350	1370			
1374	1419			
1602	1632			
1303	**1306**	**1270**		

APPENDIX F SLUDGE SETTLING DATA

Sludge Settling Data

	SBR system			CFSTR system	
$\theta_{xob}\varphi$	R_{tr}	SVI	θ_x	R	SVI
d	d^{-1}	mL/g	d	d^{-1}	mL/g
3.3	1.44	183	15	0.51	191
8	0.98	148	5	0.76	306
6	1.03	163	15	0.38	104
2.4	1.41	273	10	0.47	124
4.6	1.1	161	10	0.46	137
1.46	2.6	546	5	0.8	198
2.44	1.38	307	15	0.35	69
1.59	2.3	515	5	0.75	96
1.95	1.54	335	10	0.5	88
1.06	2.68	663	15	0.44	44
1.67	1.83	479	10	0.48	98
1.23	2.53	571	15	0.37	82
1.25	2.82	749	10	0.52	156
8.33	0.67	152	5	0.76	224
12.5	0.45	79	10	0.52	286
12.5	0.39	78	5	0.76	103
4.17	0.56	177	10	0.48	80
8.33	0.38	127	15	0.31	57
12.5	0.38	92	5	0.65	64
4.17	0.67	176	10	0.44	85
8.33	0.61	150	15	0.29	62
12.5	0.42	86			
2.5	1.5	413			
5	0.85	119			
7.5	0.54	90			
3.33	1.06	153			
6.67	0.77	83			
10	0.46	55			
3.75	0.67	107			
7.5	0.42	60			
11.25	0.4	37			
3.75	0.76	335			
7.5	0.48	50			
11.25	0.3	45			
3.33	0.85	169			
6.67	0.58	115			
10	0.4	32			
3.33	1.03	368			
6.67	0.64	24			
10	0.45	31			
3.33	1.12	398			
6.67	0.56	19			
10	0.41	28			
3.33	1.03	137			
6.67	0.7	176			
10	0.48	29			

APPENDIX G ANALYSIS OF NEW DEFINED DESIGN PARAMETERS OF AN SBR SYSTEM

(Three examples for Figs. A1, B1 and C1 on page 144, S_0 = 500 mg/L)

V_b	V_i	α	Q	n	t_{ed}	t_c	t_f	t_r	φ	V_{ef}	t_{tr}	L_{vtr}
(L)	(L)	-	(L/h)	-	(h)	(h)	(h)	(h)	-	(L)	(h)	(mg/L/d)
8	2	0.25	600	300	4	3	0.01	1.99	0.667	5.323	2.662	1503
8	2	0.25	30	15	4	3	0.2	1.8	0.667	5.133	2.567	1558
8	2	0.25	15	8	4	3	0.4	1.6	0.667	4.933	2.467	1622
8	2	0.25	10	5	4	3	0.6	1.4	0.667	4.733	2.367	1690
8	2	0.25	7.5	4	4	3	0.8	1.2	0.667	4.533	2.267	1765
8	2	0.25	6.0	3	4	3	1	1	0.667	4.333	2.167	1846
8	2	0.25	5.0	3	4	3	1.2	0.8	0.667	4.133	2.067	1935
8	2	0.25	4.3	2	4	3	1.4	0.6	0.667	3.933	1.967	2034
8	2	0.25	3.8	2	4	3	1.6	0.4	0.667	3.733	1.867	2143
8	2	0.25	3.3	2	4	3	1.8	0.2	0.667	3.533	1.767	2264
8	2	0.25	3.0	2	4	3	2	0	0.667	3.333	1.667	2400

V_b	V_i	α	Q	n	t_{ed}	t_c	t_f	t_r	φ	V_{ef}	t_{tr}	L_{vtr}
(L)	(L)	-	(L/h)	-	(h)	(h)	(h)	(h)	-	(L)	(h)	(mg/L/d)
8	4	0.5	400	300	6	3	0.01	1.99	0.667	5.33	4.00	1001
8	4	0.5	20.0	15	6	3	0.2	1.8	0.667	5.20	3.90	1026
8	4	0.5	10.0	8	6	3	0.4	1.6	0.667	5.07	3.80	1053
8	4	0.5	6.7	5	6	3	0.6	1.4	0.667	4.93	3.70	1081
8	4	0.5	5.0	4	6	3	0.8	1.2	0.667	4.80	3.60	1111
8	4	0.5	4.0	3	6	3	1	1	0.667	4.67	3.50	1143
8	4	0.5	3.3	3	6	3	1.2	0.8	0.667	4.53	3.40	1176
8	4	0.5	2.9	2	6	3	1.4	0.6	0.667	4.40	3.30	1212
8	4	0.5	2.5	2	6	3	1.6	0.4	0.667	4.27	3.20	1250
8	4	0.5	2.2	2	6	3	1.8	0.2	0.667	4.13	3.10	1290
8	4	0.5	2.0	2	6	3	2	0	0.667	4.00	3.00	1333

V_b	V_i	α	Q	n	t_{ed}	t_c	t_f	t_r	φ	V_{ef}	t_{tr}	L_{vtr}
(L)	(L)	-	(L/h)	-	(h)	(h)	(h)	(h)	-	(L)	(h)	(mg/L/d)
8	6	0.75	200	300	12	3	0.01	1.99	0.667	5.33	8.00	500
8	6	0.75	10.0	15	12	3	0.2	1.8	0.667	5.27	7.90	506
8	6	0.75	5.0	8	12	3	0.4	1.6	0.667	5.20	7.80	513
8	6	0.75	3.3	5	12	3	0.6	1.4	0.667	5.13	7.70	519
8	6	0.75	2.5	4	12	3	0.8	1.2	0.667	5.07	7.60	526
8	6	0.75	2.0	3	12	3	1	1	0.667	5.00	7.50	533
8	6	0.75	1.7	3	12	3	1.2	0.8	0.667	4.93	7.40	541
8	6	0.75	1.4	2	12	3	1.4	0.6	0.667	4.87	7.30	548
8	6	0.75	1.3	2	12	3	1.6	0.4	0.667	4.80	7.20	556
8	6	0.75	1.1	2	12	3	1.8	0.2	0.667	4.73	7.10	563
8	6	0.75	1.0	2	12	3	2	0	0.667	4.67	7.00	571

APPENDIX H DATA FOR STATISTICAL ANALYSIS OF MODEL FIT

				Pred'd					Pred'd					Pred'd
u	y	η	ε	S	u	y	η	ε	S	u	y	η	ε	S
1	24.9	20.8	3.76	21.14	45	33.3	36.1	-3.40	36.70	89	29.5	35.8	-6.94	36.44
2	38	41.9	-4.63	42.63	46	34.2	36.0	-2.41	36.61	90	29.3	25.1	3.74	25.56
3	39.5	43.0	-4.21	43.71	47	36	35.8	-0.44	36.44	91	32.9	22.0	10.51	22.39
4	39.5	42.7	-3.92	43.42	48	29.7	25.1	4.14	25.56	92	17.1	16.4	0.39	16.71
5	29.6	28.0	1.08	28.52	49	30	22.0	7.61	22.39	93	20.7	23.7	-3.39	24.09
6	28.9	21.1	7.45	21.45	50	21.2	16.4	4.49	16.71	94	21.6	23.6	-2.46	24.06
7	21.1	20.7	0.03	21.07	51	23.6	23.7	-0.49	24.09	95	20.7	23.6	-3.27	23.97
8	19	16.2	2.56	16.44	52	22.8	23.6	-1.26	24.06	96	20.7	23.5	-3.20	23.90
9	26	28.5	-2.96	28.96	53	22.8	23.6	-1.17	23.97	97	18.9	16.8	1.83	17.07
10	25.1	28.3	-3.70	28.80	54	21.1	23.5	-2.80	23.90	98	17.1	16.4	0.39	16.71
11	29.6	28.2	0.92	28.68	55	21.1	16.8	4.03	17.07	99	18.21	14.3	3.64	14.57
12	16.7	17.5	-1.14	17.84	56	21.1	16.4	4.39	16.71	100	25.8	20.6	4.81	20.99
13	19	16.0	2.68	16.32	57	18.2	14.3	3.63	14.57	101	25.8	20.6	4.83	20.97
14	15.2	16.3	-1.34	16.54	58	21.6	20.6	0.61	20.99	102	23.1	20.6	2.19	20.91
15	21.3	14.3	6.78	14.52	59	23.7	20.6	2.73	20.97	103	22.2	20.5	1.33	20.87
16	25.8	25.4	-0.05	25.85	60	23.7	20.6	2.79	20.91	104	16.3	14.6	1.47	14.83
17	28.5	25.3	2.74	25.76	61	25.5	20.5	4.63	20.87	105	15.2	14.3	0.61	14.59
18	28.9	25.2	3.22	25.68	62	20.7	14.6	5.87	14.83	106	33.4	40.7	-8.03	41.43
19	19	15.3	3.46	15.54	63	18.8	14.3	4.21	14.59	107	49.5	58.0	-9.55	59.05
20	16.2	14.2	1.77	14.43	64	32.4	40.7	-9.03	41.43	108	56.8	58.3	-2.49	59.29
21	19	14.5	4.24	14.76	65	44.2	58.0	-14.85	59.05	109	55.3	58.0	-3.77	59.07
22	42	37.6	3.77	38.23	66	49.1	58.3	-10.19	59.29	110	53.7	57.8	-5.17	58.87
23	52	52.9	-1.80	53.80	67	49.1	58.0	-9.97	59.07	111	42.2	42.4	-0.93	43.13
24	47	53.7	-7.65	54.65	68	49.7	57.8	-9.17	58.87	112	32.4	40.7	-9.03	41.43
25	57	53.5	2.54	54.46	69	35.7	42.4	-7.43	43.13	113	31.2	31.3	-0.66	31.86
26	58	53.2	3.81	54.19	70	33.4	40.7	-8.03	41.43	114	42.3	41.7	-0.18	42.48
27	56	52.9	2.13	53.87	71	29.7	31.3	-2.16	31.86	115	47.7	41.7	5.26	42.44
28	51	52.5	-2.41	53.41	72	39.8	41.7	-2.68	42.48	116	45.3	41.6	2.92	42.38
29	47	37.5	8.84	38.16	73	40.7	41.7	-1.74	42.44	117	44.1	41.6	1.78	42.32
30	44	37.3	6.04	37.96	74	38.3	41.6	-4.08	42.38	118	33.2	31.6	1.02	32.18
31	44	37.6	5.78	38.22	75	42.9	41.6	0.58	42.32	119	33.2	31.4	1.24	31.96
32	35	30.0	4.52	30.48	76	32.4	31.6	0.22	32.18	120	29.7	28.2	0.98	28.72
33	39	38.9	-0.58	39.58	77	29.7	31.4	-2.26	31.96	121	31.5	35.9	-5.07	36.57
34	39.5	38.9	-0.05	39.55	78	23.5	28.2	-5.22	28.72	122	36	35.9	-0.49	36.49
35	41	38.8	1.56	39.44	79	34.6	35.9	-1.97	36.57	123	32.4	35.8	-4.03	36.43
36	42	38.6	2.69	39.31	80	33.3	35.9	-3.19	36.49	124	36	35.7	-0.36	36.36
37	41	38.5	1.84	39.16	81	34.2	35.8	-2.23	36.43	125	31.5	28.2	2.79	28.71
38	40.2	38.3	1.22	38.98	82	38.7	35.7	2.34	36.36	126	29.6	28.2	0.88	28.72
39	34	30.0	3.43	30.57	83	31.5	28.2	2.79	28.71	127	19.1	20.9	-2.14	21.24
40	31	29.6	0.83	30.17	84	22.5	28.2	-6.22	28.72	128	35.6	38.3	-3.40	39.00
41	29	29.7	-1.27	30.27	85	32.9	21.9	10.60	22.30	129	39.8	42.0	-2.94	42.74
42	32	29.9	1.53	30.47	86	31.2	34.6	-3.97	35.17	130	35.6	42.9	-8.06	43.66
43	30.6	21.9	8.30	22.30	87	34.6	36.1	-2.10	36.70	131	43	43.1	-0.86	43.86
44	31.5	34.6	-3.67	35.17	88	29.5	36.0	-7.11	36.61	132	45.1	43.1	1.28	43.82

APPENDIX H DATA FOR STATISTICAL ANALYSIS OF MODEL FIT

				Pred'd					Pred'd					Pred'd
u	y	η	ε	S	u	y	η	ε	S	u	y	η	ε	S
133	52	43.0	8.28	43.72	177	38.9	45.0	-6.89	45.79	221	21.2	18.8	2.11	19.09
134	38.2	30.6	7.02	31.18	178	45.8	44.9	0.10	45.70	222	18.3	13.7	4.36	13.94
135	35.2	25.0	9.74	25.46	179	55	44.8	9.40	45.60	223	16.2	13.6	2.34	13.86
136	26	22.6	3.04	22.96	180	48.1	44.7	2.60	45.50	224	15.3	13.7	1.38	13.92
137	26	21.2	4.40	21.60	181	46.5	44.6	1.08	45.42	225	37.7	37.6	-0.54	38.24
138	19.1	20.8	-2.07	21.17	182	35.3	30.8	3.91	31.39	226	54.2	53.2	0.11	54.09
139	20.1	16.1	3.67	16.43	183	34.4	29.6	4.32	30.08	227	57.8	53.2	3.71	54.09
140	29.3	27.9	0.95	28.35	184	32.4	29.5	2.40	30.00	228	49.8	52.8	-3.95	53.75
141	29.3	28.6	0.23	29.07	185	30.5	29.6	0.43	30.07	229	49	52.5	-4.43	53.43
142	32.1	28.6	3.02	29.08	186	33.2	29.8	2.87	30.33	230	49.7	52.3	-3.54	53.24
143	26.1	28.5	-2.92	29.02	187	29	26.4	2.12	26.88	231	40.1	38.5	0.97	39.13
144	25.4	28.4	-3.55	28.95	188	38.1	37.5	-0.04	38.14	232	38.5	37.4	0.41	38.09
145	25.4	28.4	-3.48	28.88	189	33.8	37.5	-4.33	38.13	233	37.7	37.6	-0.53	38.23
146	23	18.7	3.95	19.05	190	35.2	37.4	-2.85	38.05	234	34.5	29.9	4.03	30.47
147	18.5	16.6	1.60	16.90	191	33.8	37.3	-4.18	37.98	235	47	38.9	7.38	39.62
148	18.5	16.2	2.04	16.46	192	36.8	37.3	-1.12	37.92	236	41	38.8	1.50	39.50
149	18.5	16.1	2.11	16.39	193	35.6	37.2	-2.27	37.87	237	44.1	38.7	4.76	39.34
150	19.5	16.2	3.01	16.49	194	28.4	26.6	1.32	27.08	238	44.2	38.5	5.00	39.20
151	16.5	14.4	1.87	14.63	195	29.1	26.2	2.40	26.70	239	44.1	38.4	4.98	39.12
152	25.9	23.3	2.20	23.70	196	23.7	26.3	-3.03	26.73	240	36.9	29.8	6.56	30.34
153	23.2	23.5	-0.68	23.88	197	29.1	26.3	2.30	26.80	241	36.9	29.8	6.56	30.34
154	26.4	23.4	2.57	23.83	198	29.1	26.4	2.23	26.87	242	34.5	29.9	4.03	30.47
155	28	23.4	4.21	23.79	199	24.3	19.1	4.82	19.48	243	32.9	27.1	5.36	27.54
156	25.1	23.3	1.37	23.73	200	29.2	30.7	-1.99	31.19	244	35.8	33.8	1.44	34.36
157	25.1	23.3	1.40	23.70	201	28.5	31.2	-3.28	31.78	245	36.6	33.7	2.33	34.27
158	19.1	15.4	3.48	15.62	202	36.1	31.1	4.47	31.63	246	33.7	33.6	-0.47	34.17
159	16.5	14.4	1.84	14.66	203	32.4	30.7	1.13	31.27	247	29.7	33.5	-4.37	34.07
160	14.5	14.3	-0.05	14.55	204	23.5	21.4	1.74	21.76	248	28.1	33.4	-5.92	34.02
161	16.5	14.3	1.92	14.58	205	21.1	19.3	1.50	19.60	249	25.3	26.9	-2.05	27.35
162	17	14.5	2.24	14.76	206	21.1	19.1	1.62	19.48	250	25.7	27.0	-1.73	27.43
163	37	37.9	-1.56	38.56	207	18.3	15.2	2.80	15.50	251	29.9	27.1	2.37	27.53
164	56.6	62.7	-7.20	63.80	208	25	22.4	2.21	22.79	252	20.5	19.1	1.02	19.48
165	61.3	65.3	-5.11	66.41	209	21.4	22.4	-1.38	22.78	253	33.6	30.7	2.41	31.19
166	65.9	65.5	-0.74	66.64	210	24.2	22.3	1.53	22.67	254	31.8	31.2	0.02	31.78
167	56.8	65.4	-9.73	66.53	211	19.8	22.2	-2.77	22.57	255	33.8	31.1	2.17	31.63
168	60.6	65.2	-5.76	66.36	212	23.1	22.1	0.59	22.51	256	25.9	30.7	-5.37	31.27
169	60.6	65.0	-5.58	66.18	213	17.9	15.6	2.05	15.85	257	22.8	21.4	1.04	21.76
170	46.6	45.3	0.53	46.07	214	15.9	15.2	0.47	15.43	258	25	19.3	5.40	19.60
171	44.7	39.8	4.20	40.50	215	18.5	15.2	3.00	15.50	259	19	19.1	-0.48	19.48
172	40.1	38.4	1.04	39.06	216	16	13.6	2.15	13.85	260	20.1	15.2	4.60	15.50
173	34.5	38.0	-4.19	38.69	217	19.2	18.9	-0.06	19.26	261	21.5	22.4	-1.29	22.79
174	37.3	38.1	-1.43	38.73	218	21.5	18.9	2.27	19.23	262	26	22.4	3.22	22.78
175	33.2	29.6	3.03	30.17	219	16.8	18.8	-2.36	19.16	263	23.5	22.3	0.83	22.67
176	46.5	44.8	0.89	45.61	220	20.8	18.8	1.68	19.12	264	24.6	22.2	2.03	22.57

APPENDIX H DATA FOR STATISTICAL ANALYSIS OF MODEL FIT

				Pred'd					Pred'd					Pred'd
u	y	η	ε	S	u	y	η	ε	S	u	y	η	ε	S
265	25.3	22.1	2.79	22.51	309	38.2	36.9	0.68	37.52	353	32.8	37.1	-4.92	37.72
266	14.1	15.6	-1.75	15.85	310	30.5	27.3	2.75	27.75	354	43.8	37.0	6.12	37.68
267	16	15.2	0.57	15.43	311	23.8	19.8	3.62	20.18	355	37.2	36.8	-0.29	37.49
268	19.2	15.2	3.70	15.50	312	22.8	19.2	3.28	19.52	356	37.2	36.6	-0.02	37.22
269	17.1	13.6	3.25	13.85	313	23	19.3	3.38	19.62	357	32.6	27.3	4.83	27.77
270	20.1	18.9	0.84	19.26	314	18.4	15.3	2.81	15.59	358	29.8	26.8	2.48	27.32
271	22.5	18.9	3.27	19.23	315	24.6	25.7	-1.51	26.11	359	28.6	26.9	1.24	27.36
272	20.1	18.8	0.94	19.16	316	24.6	25.6	-1.43	26.03	360	30.4	27.0	2.90	27.50
273	20.1	18.8	0.98	19.12	317	28.1	25.4	2.21	25.89	361	32	27.2	4.36	27.64
274	22.3	18.8	3.21	19.09	318	24.6	25.3	-1.16	25.76	362	43.2	38.0	4.50	38.70
275	15.8	13.7	1.86	13.94	319	18	17.6	0.06	17.94	363	50	59.3	-10.38	60.38
276	14.2	13.6	0.34	13.86	320	22.1	15.2	6.67	15.43	364	58.4	61.7	-4.40	62.80
277	17.1	13.7	3.18	13.92	321	15.6	15.2	0.11	15.49	365	62.4	61.7	-0.37	62.77
278	40.5	37.6	2.26	38.24	322	18.6	15.3	3.01	15.59	366	60.8	60.8	-1.03	61.83
279	57.8	53.2	3.71	54.09	323	19	13.8	4.95	14.05	367	37.6	39.4	-2.53	40.13
280	57.8	53.2	3.71	54.09	324	22.8	21.6	0.82	21.98	368	36.8	37.8	-1.62	38.42
281	50.6	52.8	-3.15	53.75	325	25.2	21.5	3.32	21.88	369	37.7	37.8	-0.77	38.47
282	49.8	52.5	-3.63	53.43	326	19	21.4	-2.78	21.78	370	43.2	38.0	4.51	38.69
283	48.2	52.3	-5.04	53.24	327	19.5	21.3	-2.20	21.70	371	30.4	30.1	-0.27	30.67
284	41.4	38.5	2.27	39.13	328	16.6	14.8	1.54	15.06	372	39.2	43.2	-4.79	43.99
285	40.1	37.4	2.01	38.09	329	15.3	13.6	1.43	13.87	373	41.6	43.4	-2.54	44.14
286	36.5	37.6	-1.73	38.23	330	15.6	13.7	1.65	13.95	374	45.2	43.1	1.30	43.90
287	33.5	29.9	3.03	30.47	331	15.6	13.8	1.55	14.05	375	40.6	42.7	-2.89	43.49
288	43.8	38.9	4.18	39.62	332	46	38.0	7.30	38.70	376	32.8	29.9	2.41	30.39
289	48.2	38.8	8.70	39.50	333	55.6	59.3	-4.78	60.38	377	31.2	29.8	0.87	30.33
290	46	38.7	6.66	39.34	334	54.8	61.7	-8.00	62.80	378	30.4	30.0	-0.08	30.48
291	41.7	38.5	2.50	39.20	335	64.6	61.7	1.83	62.77	379	30.4	30.1	-0.25	30.65
292	40.9	38.4	1.78	39.12	336	63.8	60.8	1.97	61.83	380	24	27.2	-3.65	27.65
293	40.1	29.8	9.76	30.34	337	48.6	44.3	3.56	45.04	381	36	37.1	-1.72	37.72
294	33.7	29.8	3.36	30.34	338	44.6	39.4	4.47	40.13	382	33.6	37.0	-4.08	37.68
295	38.5	29.9	8.03	30.47	339	44.4	37.8	5.98	38.42	383	35.6	36.8	-1.89	37.49
296	26.9	27.1	-0.64	27.54	340	43.7	37.8	5.23	38.47	384	36.8	36.7	-0.55	37.35
297	35.8	33.8	1.44	34.36	341	45	38.0	6.31	38.69	385	36	36.6	-1.22	37.22
298	38.2	33.7	3.93	34.27	342	37.2	30.1	6.53	30.67	386	26.4	26.8	-0.92	27.32
299	40.1	33.6	5.93	34.17	343	44.5	43.2	0.51	43.99	387	26.4	26.9	-0.96	27.36
300	35.3	33.5	1.23	34.07	344	48.8	43.4	4.66	44.14	388	24.8	27.0	-2.70	27.50
301	36.9	33.4	2.88	34.02	345	40.4	43.1	-3.50	43.90	389	26.4	27.2	-1.24	27.64
302	26.9	26.9	-0.45	27.35	346	39.2	42.7	-4.29	43.49					
303	31.7	27.0	4.27	27.43	347	35.2	31.1	3.56	31.64		*Regression Statistics*			
304	36.9	27.1	9.37	27.53	348	32	29.9	1.61	30.39		Multiple R			0.9382
305	21.5	19.3	1.88	19.62	349	28.4	29.8	-1.93	30.33		R Square			0.8801
306	33.5	36.4	-3.56	37.06	350	34	30.0	3.52	30.48		Adjusted R Square			0.8776
307	39.6	37.3	1.61	37.99	351	37.2	30.1	6.55	30.65		Standard Error			3.9506
308	38.2	37.2	0.38	37.82	352	32	27.2	4.35	27.65		Observations			389